8-1-1977

VIMS-BLM Wave Climate Model of the Baltimore Canyon Trough Shelf and Shoreline

Victor Goldsmith
Virginia Institute of Marine Science

106

VIMS-BLM WAVE CLIMATE MODEL OF THE BALTIMORE CANYON TROUGH SHELF AND SHORELINE

Victor Goldsmith

Special Report in Applied Marine Science
and Ocean Engineering No. 106
of the
Virginia Institute of Marine Science
Gloucester Point, Virginia 23062

This report was extracted from "Middle Atlantic Outer Continental Shelf Environmental Studies: Volume II. Chemical and Biological Benchmark Studies", the final report to the Bureau of Land Management, U. S. Department of Interior, prepared by the Virginia Institute of Marine Science under Contract No. 08550-CT-5-42. References to other chapters and appendices of the complete report have been left intact in this extract.

August 1977

VIMS-BLM WAVE CLIMATE MODEL OF THE BALTIMORE CANYON TROUGH SHELF AND SHORELINE

Victor Goldsmith

Special Report in Applied Marine Science
and Ocean Engineering No. 106
of the
Virginia Institute of Marine Science
Gloucester Point, Virginia 23062

This report was extracted from "Middle Atlantic Outer Continental Shelf Environmental Studies: Volume II. Chemical and Biological Benchmark Studies", the final report to the Bureau of Land Management, U. S. Department of Interior, prepared by the Virginia Institute of Marine Science under Contract No. 08550-CT-5-42. References to other chapters and appendices of the complete report have been left intact in this extract.

August 1977

CHAPTER 12

TABLE OF CONTENTS

CHAPTER 12

VIMS-BLM WAVE CLIMATE MODEL OF THE BALTIMORE CANYON TROUGH SHELF AND SHORELINE-

METHODOLOGY AND DATA FOR:

Shelf Wave Height and Bottom Orbital Velocity
Shoreline Wave Height and Energy

V. Goldsmith

INTRODUCTION

A Wave Climate Model of the Baltimore Canyon Trough Shelf area encompassing the designated lease blocks, was developed as part of this year's contract. This rapidly produced regional Climate Model (after Goldsmith et al. 1974), completed in December 1975, along with a suite of computer-generated graphics, is primarily aimed at assisting present investigators in evaluating baseline environmental considerations and in selecting smaller areas for intensive field studies within the lease block area. Therefore, as explained within this text, this initial model provides regional, not site-specific, analyses. Definitive statements will require a more exhaustive treatment of these data and compatible conclusions via feedback from investigators in other disciplines engaged in parallel lines of inquiry.

Similarly, the wave data computed for these 12 conditions have not been specifically weighted by frequency of occurrence (which will be done in the next phase of this study), though they encompass the important wave conditions.

These data for 12 wave conditions, which are displayed in a page-size format in order to facilitate their use, include Shelf Diagrams of Wave Rays (Appendix 12-A), Wave Ray Density (Appendix 12-B), Computer-Contoured Wave Heights (Appendix 12-C), and Wave Bottom Orbital Velocities (Appendix 12-D); Hand-Contoured Wave Heights (Appendix 12-E), and Wave Bottom Orbital Velocities (Appendix 12-F); Shoreline Histograms of Wave Ray Density (Appendix 12-G), Wave Heights (Appendix 12-H), and Wave Energy (Appendix 12-I).

WAVE MODEL THEORY

Wave Theory

Standard linear wave theory modified for friction effects was employed in the computation of the 19 wave parameters. Wave refraction was based on the application of the principles of geometric optics (i.e., Snell's Law).

Applicability of this theory in such wave climate models is discussed in Goldsmith et al. (1974), Goldsmith et al. (1977), Colonell et al. (1975), and in standard texts. A friction coefficient of .02 was used, and its justification is discussed in Goldsmith (1976).

In general, much confidence exists in the accuracy of the diagrams because of the excellent correspondence with aerial photographs in a number of comparisons at other locations (e.g., Goldsmith et al. 1974). Less confidence exists in the computations of wave height and related parameters in the Virginian Sea Wave Climate Model (VSWCM) and all other similar wave refraction models, due to a lack of comparison of waves measured in the field with those in the model computations. Because of this, the following analyses were undertaken.

Singularities

A major cause of uncertainity in wave height computations is the presence of occasional calculations of unusually high wave heights, referred to here as singularities. A singularity is a point where a function is not differentiable or analytic. Classical wave refraction theory for water waves (discussed below), which closely parallels the theory of geometrical optics, fails to quantitatively describe wave behavior (i.e., a singularity) in the vicinity of caustics. A caustic is defined as the envelope of a family of wave rays produced by refraction over various sea floor configurations. This is a real physical phenomenon, which occurs in areas of crossed wave fronts, and which is presumed to be correctly displayed on refraction diagrams, in the form of crossed wave rays. However, not all areas of crossed wave rays on refraction diagrams have corresponding mathematical singularities. Thus, the relationship between the mathematical "failure", referred to here as a singularity, and the real physical phenomenon, referred to here as a wave caustic, is quite subtle. It is the purpose of this section to address this subject, notable by the surprising absence of discussions in the literature[1], which results from a basic failing within linear wave theory. First, the cause of these singularities will be explained, and then their effect on the BCTWCM data will be assessed. The shelf wave heights and maximum bottom wave orbital velocities (Umb) are presented in the form of computer contour diagrams. Partly because of the format chosen for the presentation of the data, the effect of singularities, as will be shown, was insignificant.

The effects of shoaling and refraction can be estimated by linear wave theory. For example, the propagation of surface waves into shallow water is analyzed by consideration of the wave energy between two vertical

[1] As will be shown, such singularities result from any computer program incorporating the Munk & Arthur (1951) wave intensity method, such as Dobson (1967) (which is the basis for the BCTWCM), Lepetit (1964), Jen (1969), Orr & Herbich (1969), Mogel & Street (1975), Smith & Camfield (1972), Thrall (1973), Mogel & Street (1974), May (1974), Coleman & Wright (1971), Skovgaard et al. (1975), U.S. Army Eng. District, Wilmington (1973) as well as those employing other methods such as Abernathy & Gilbert (1975).

planes which are orthogonal to the wave crests and which intersect with the surface to produce wave rays. Energy is assumed not to be transmitted along the wave crest; thus, it is not transmitted across wave rays. If it is also assumed that the wave period is constant and that there is no loss or gain of energy from reflection or percolation, then linear wave theory provides the well-known result,

$$\frac{H}{H_o} = K_r K_s K_f \tag{1}$$

Where:

H is modified wave height

H_o is initial deep water wave height

K_r is coefficient of refraction

K_s is coefficient of shoaling

K_f is the wave height reduction factor due to friction and is proportional to 1/f where f is the friction coefficient

The coefficient of refraction is given by

$$K_r = \left(\frac{b_o}{b}\right)^{\frac{1}{2}} \tag{2}$$

Where:

b_o is initial distance between adjacent rays in deep water

b is distance between adjacent rays

With the advent and application of high-speed computers, there was one change in the theory employed in most of the computer-drawn wave refraction diagrams which is often overlooked by those interpreting these diagrams. This relates to the variation in the spacing (b) between the wave rays, which is used to compute the wave heights along the wave front. In the older, manually drawn diagrams, a simple ratio of the perpendicular distance between adjacent rays in deep water relative to shallow waters was used to calculate the shallow water wave heights, wave energy, and other parameters. In the computer-drawn diagrams a method suggested by Munk and Arthur (1951) has been adopted. This method assumes that a second ray is spaced an infinitesimal distance from the first ray. The mathematical expressions relating to "wave intensity" proposed by Munk and Arthur (1951) are used to calculate the ray spacing, and consequently, the wave height. Thus, in the wave refraction diagrams employing this technique, wave heights and other related wave parameters are calculated along each wave ray, and each ray is "unaware" of the presence of rays other than its neighbor, an infinitesimal distance away. Thus, from a practical point, wave ray diagrams can be produced without crossed rays merely by limiting the number of rays input into the refraction analysis (i.e., increase the spacing between input ray to the point where no rays cross).

Partly for this reason, Chao (1974) suggested reverting back to a variation of the manual method, for the proper interpretation of crossed waves, even for computer-drawn diagrams. However, in a more recent paper, Chao returned to the Munk and Arthur (1951) wave intensity method, with some modification within the wave caustic area (Chao et al. 1975).

The Munk and Arthur (1951) approach, which has become standard in nearly all wave height computations within such computer wave models, (as well as within the VSWCM based on Dobson 1967), employs a finite-difference scheme to compute b:

$$\frac{d^2b}{dt^2} + p\,\frac{db}{dt} + qb = 0 \qquad (3)$$

Where:

$$p\ (t) = -2\left(\frac{\partial C}{\partial x}\cos\alpha + \frac{\partial C}{\partial y}\sin\alpha\right) \qquad (4)$$

$$q\ (t) = C\left(\frac{\partial^2 C}{\partial x^2}\sin^2\alpha - \frac{\partial^2 C}{\partial x \partial y}\sin\alpha\cos\alpha + \frac{\partial^2 C}{\partial y^2}\cos^2\alpha\right) \qquad (5)$$

This equation is developed in detail in Skovgaard et al. (1975, p. 5.)[1]

It can be seen in Equation 2 that in the calculation of wave refraction coefficient (K_r), as b approaches 0, when the wave rays cross, the resulting wave height will approach infinity, at least according to linear wave theory and Snell's Law. Wave observations and subsequent theoretical work prove that this is certainly not the case; wave heights do not become infinitely high (Figure 12-1). However, since energy is assumed conserved between two rays, and assumed to be nontransferable across adjacent rays, there is a theoretical problem when trying to describe the situation where the rays get very close to each other, or even cross. This results in computations of unusually large wave heights, and thus poses practical problems in computer computations such as these. This problem was recognized and stated explicitly in Munk and Arthur (1951, p. 104), but has rarely been discussed in subsequent literature, most notably in the widespread application of Munk and Arthur's techniques in nearly all computer wave models.

Munk and Arthur's theoretical wave intensity relationships (Equations 3, 4, & 5) have been transposed by Dobson (1967) in his computer program (subroutine HEIGHT), via several manipulations, to the following relationships:

$$b = ((p - 2) * B1 + (4 - q) * B2)/(p + 2) \qquad (6)$$

[1] There is some confusion over the correct form in the literature since there is a mistaken form given in LePetit (1964, p. 7) and there is a typographical error in the text of Dobson (1967), but not in the listing of the computer program. Since then several sources have commented on these mistakes (Skovgaard et al. 1975; Whalin 1971; and Abernathy & Gilbert 1975).

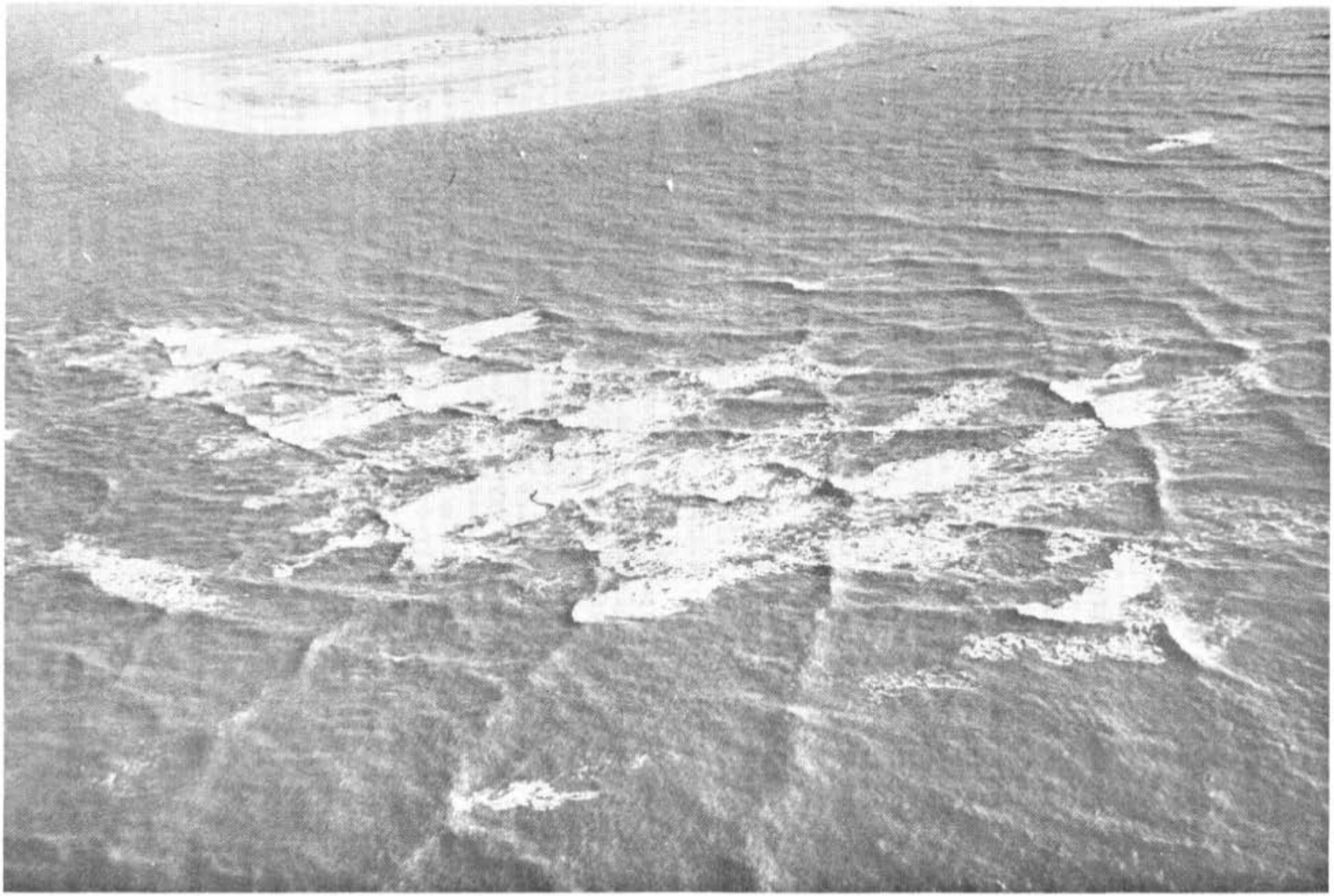

Figure 12-1. Photograph illustrating a caustic region.

Where:

p = Equation 4

q = Equation 5

B1 = b computed in previous iteration

B2 = B computed in two previous iterations

The program was modified to print out the values of these parameters, which were then plotted for a number of wave rays. Plots of pertinent parameters along two of these wave rays, exemplifying a singularity and a non-singularity case, are shown in Figure 12-2. From these and other plots and Equations 1 and 2 it can be seen that: (1) for a singularity to occur both (p - 2) B1 and (4 - q) B2 must simultaneously approach 0; (2) the closer that both of these parameters approach to 0, the larger the wave height singularity; and (3) the location of the singularity appears to show very little relation to the computed depth changes. (These depths along the wave ray are computed from 12 surrounding depths using a second order trend surface.) In Munk and Arthur's scheme, b is calculated for two wave rays located only an infinitesimal distance apart. It is important to remember that these two adjacent 'mathematical' ray crossings (described in Equation 3) resulting in wave height singularities, do not directly relate to the ray crossings shown by the wave ray diagrams.

A test was made to delineate the relationships between the wave ray diagrams and the wave height computations for the same shelf area and wave input conditions. In this test, the VSWCM was used to compute wave heights in an area of complex bathymetry, resulting from shoals and linear ridges, south of Chincoteague, Virginia. A 0.5 NM depth grid (Goldsmith et al. 1974) was employed. The one major difference from previous calculations was that in this test a large number of wave rays were input at a spacing of 0.25 NM (four times as many rays as usual density). The input wave condition was a 10 second wave from the east with an initial deep water wave height of 1.8 m. The areas of mathematically-computed wave height singularities were indicated on the resulting wave ray diagram (Figure 12-3a). The ray diagram with a greater number of input rays and resulting ray crossings is shown to correlate with more of the locations of the mathematical singularities than are observed with normal ray density. From this comparison, it may be assumed that if a sufficient density of wave rays are input, the mathematically computed wave height singularities will also be shown on the wave ray diagrams as areas of intense wave ray crossing (Figure 12-3a). Of course, the cost for such extensive computations over large regions makes this approach prohibitive in most cases.

The resulting wave ray diagram was also precisely compared at the same scale (using a Zoom-Transfer Scope) with the depth configuration as depicted on the original 1.8 m long mylar stable base depth grid (Goldsmith et al. 1974). From this comparison it was learned that:

(1) Some, but by no means all or even most, areas of complex bathymetry result in wave height singularities; i.e., many areas of crossed-wave ray patterns resulting from complex bathymetry do not have corresponding wave height singularity computations.

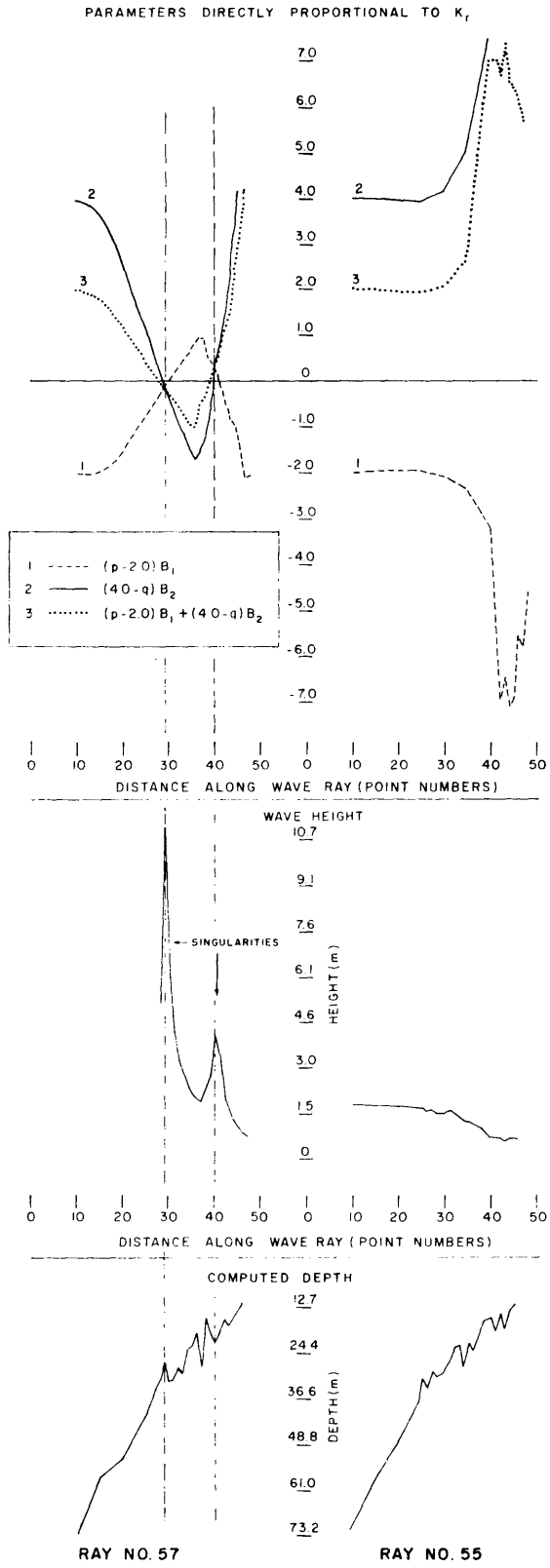

Influence of p and q on Computation of Wave Height Singularities
From: VSWCM Az = 90° T = 10 sec. Tide = 0.0 Step Size = 3.0

Figure 12-2. Plots illustrating computation of singularities.

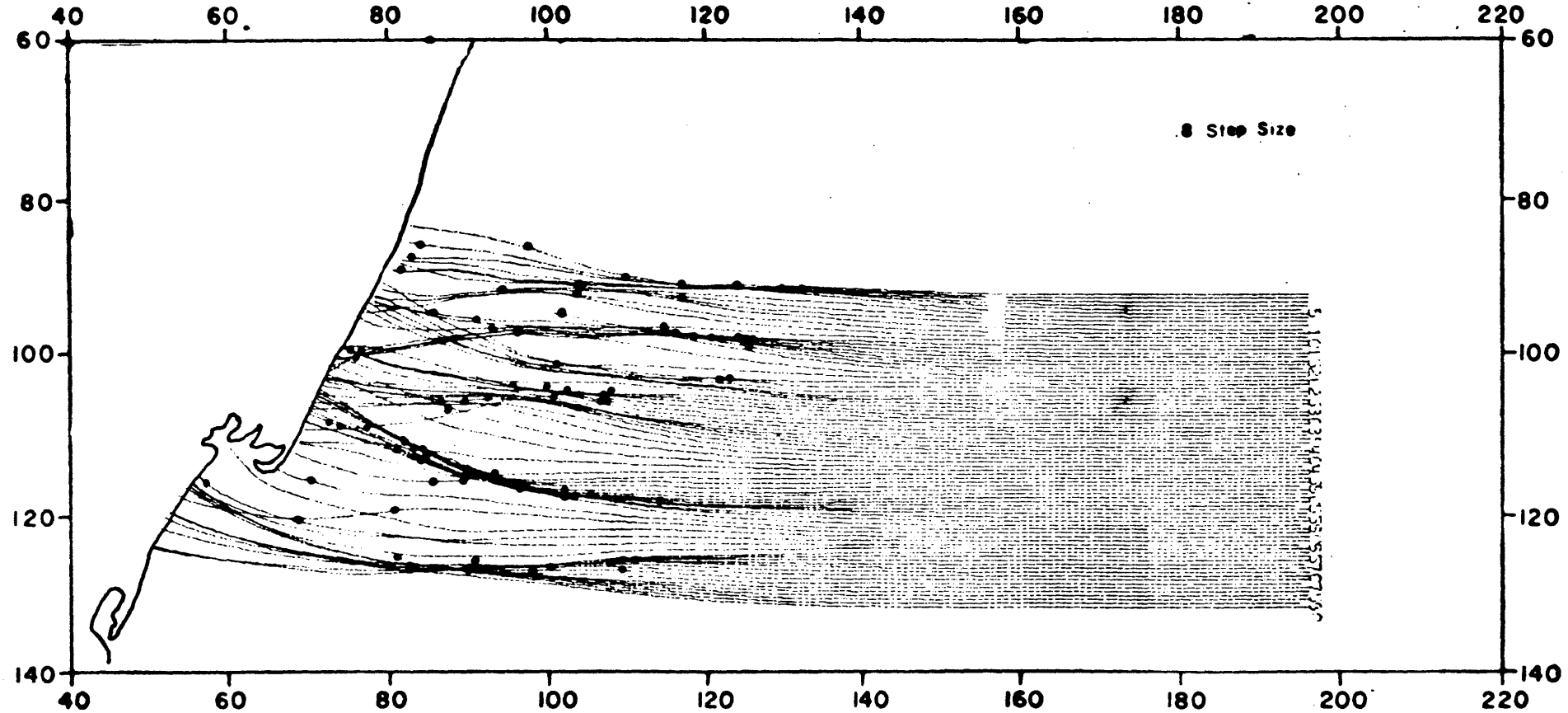

Figure 12-3a. Comparison of crossed wave rays with mathematically computed singularities (VSWCM) for step size 0.8.

(2) Although most wave height singularities occur over complex bathymetry and in the nearshore, they also occur in areas of relatively gently sloping bathymetry where the depth contours and resulting wave patterns, are concave-shaped and landward-facing (i.e., open towards direction of wave propagation) over a large distance. In this situation, the two wave rays, which are an infinitesimal distance apart, tend to approach each other over a long distance.

An additional test was made in this area. The input step size was reduced in order to further delineate the relationship between the computed mathematical singularities at the areas of wave ray crossings in wave ray diagrams (Figures 12-3a and 12-3b). (The step size is the interval at which all wave calculations are made along each wave ray in the model; calculations are made at discrete intervals.) The step size intervals are quite closely spaced; the criterion used was that they should be close enough so that at the scale of presentation, the wave rays should appear as continuously drawn smooth lines. These steps, for practical purposes, are determined by time intervals and not distance, so that they vary with different wave periods, and vary with decreasing distance with decreasing depths for the same wave periods. In general, the distances are 0.5, 0.48, and 0.45 NM in the lease block areas (BCTWCM) for wave periods of 8, 10, and 12 sec., respectively (Table 12-1).

Table 12-1. BCTWCM step size for 8, 10, and 12 second waves. Time Step = 1.0 sec; Azimuth = 90^{o}; Tide = 0.0

Wave Period	Deep Water	Lease Block	Shallow Water
8	0.5 NM	0.5 NM	0.4 NM
10	0.5 NM	0.48 NM	0.25 NM
12	0.5 NM	0.45 NM	0.15 NM

As a result of varying the step size while keeping all other parameters the same, it was determined that, in general, singularities occur in different locations with different step sizes (Figures 12-3a and 12-3b and Table 12-2. The total number of singularities decreased (79 to 64 with time steps of 0.8 and 3.0, respectively), although the increased number of singularities (15) occurred in the nearshore with the slower time step (Table 12-3). This is because with a larger step size, less calculations are made along each ray and less areas of singularities are hit. Also, the rays are most vulnerable in shallow water where they move slower, and with a smaller time step will have more encounters with the complex bathymetry of this area. Thus, if calculations were made quasicontinuously along each ray, all areas of crossed-rays in the wave ray diagrams would have concomitant mathematical singularities. Moreover, this implies that the presence or absence of singularities in the BCTWCM calculations, as well as the exact heights calculated at these singularities, is pretty much serendipitous. That is, if the time step caused the wave height calculations to be made exactly at the singularity (Figure 12-2), the wave height would be infinite (which has never occurred). Instead, the maximum wave heights calculated are only ten's of meters (rarely).

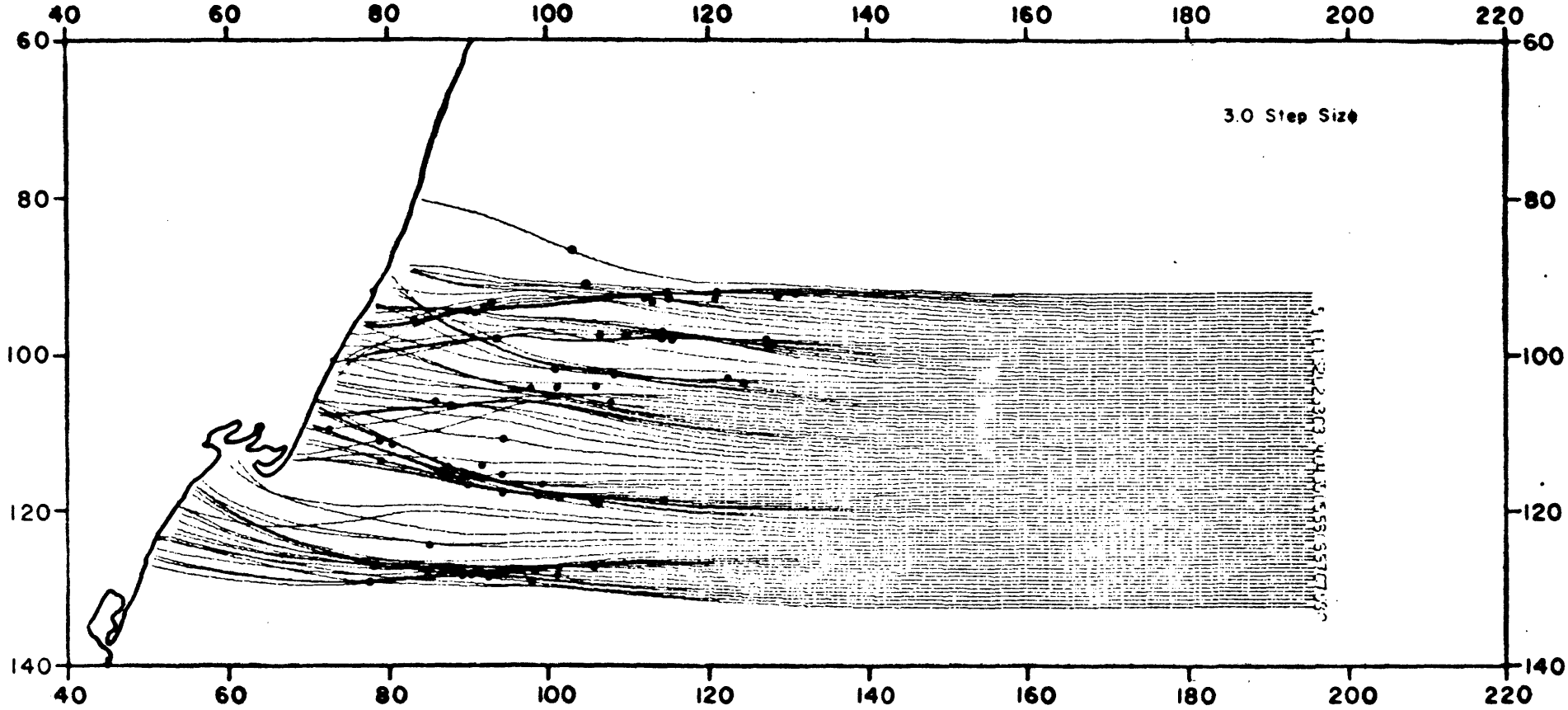

Figure 12-3b. Comparison of crossed wave rays with mathematically computed singularities (VSWCM) for step size 3.0.

Table 12-2. Summary of time step comparisons.

Step Size (sec)	Distance (NM) Between Computations		Number of Singularities	Percent of Total Singularities	Number of Singularities Located in Shallow Water d < 15 m	Total Number of Wave Rays	Number of Wave Rays with One or More Singularities
	Deep	Shallow					
0.8	0.4	0.2	79	100	15	81	68
3.0	0.75	0.5	64	81	2	81	60

Table 12-3. Contour comparisons between computer drawn, hand drawn, and wave orthogonal density for a selected shelf area in 16 numbered squares (22 kilometers on a side; see Figures 12-6 and 12-7 for location of squares listed in various columns).

Area	Tide	Similar contour patterns for wave height in both computer-drawn and hand-contoured diagrams	Total	Wave heights shown in computer diagrams at the 1 meter level missing in hand contour diagrams	Wave heights shown in computer diagrams at the 2 & 3 meter level missing in hand contour diagrams	Wave heights in hand contour at the 1 meter level missing in computer diagrams	Wave heights in hand contour at the 2 & 3 meter level missing in computer diagrams	Wave ray density similar to computer contour	Wave ray density similar to hand contour
45° 8'	0	1,2,5,6,9	5	13	3,10,13	0	0	4,7,8, 11,14	3,4,7,8,11, 13,14
45°10'	0	1,2,3,5,6,7,8, 9,10,12,13,16	12	15	4,11,14, 15	0	0	2,3,6, 7,13	2,3,4,6,7,8, 10,11,13,15
45°10'	5	1,2,3,5,6,7,8, 9,10,12,13,15,16	13	11	4,14	0	0	2,3,6, 8,13	All
45°12'	0	1,2,3,5,6,7,9, 10,12,13,15,16	13	11	11	0	4,8	13,14	2,3,4,6,7, 8,11,13,14
90° 8'	0	1,4,7,8,11,12 14,15,16	9	3,10	2,5,6,9, 13	0	10,3	4,7,8, 11,14	All
90°10'	0	1,2,4,5,9,12, 15,16	8	8,14	3,6,7,10, 11,13	0	0	2,4,15	3,6,7,8, 11,13,14
90°10'	5	1,2,5,8,9,11, 12,15,16	9	10	3,4,6,7, 10,13,14	0	0	2	3,4,6,7,11, 13

Table 12-3 (concluded)

Area	Tide	Similar contour patterns for wave height in both computer-drawn and hand-contoured diagrams	Total	Wave heights shown in computer diagrams at the 1 meter level missing in hand contour diagrams	Wave heights shown in computer diagrams at the 2 & 3 meter level missing in hand contour diagrams	Wave heights in hand contour at the 1 meter level missing in computer diagrams	Wave heights in hand contour at the 2 & 3 meter level missing in computer diagrams	Wave ray density similar to computer contour	Wave ray density similar to hand contour
90°12'	0	1,2,3,5,6,7,9, 10,12,13,15,16	12	4,8	11,14	0	0	2,3,6, 13	4,7,8,11,14
135° 8'	0	1,3,4,7,8,11, 12,14,15,16	10	0	2,5,6,9, 10,13	0	5	3,4,7,8, 11,14	2,6,13
135°10'	0	1,2,5,8,9,12, 15,16	8	0	3,4,5,7, 10,11,13	0	0	4,8	2,3,6,7,11, 13,14
135°10	5	1,2,3,4,5,9, 12,15,16	9	13	6,7,8,10, 11,13,14	0	0	0	2,3,6,7,8, 11,13,14
135°12'	0	1,2,5,6,7,9,10, 11,12,13,15,16	12	1	3,4,8,14	0	0	2,11	3,4,6,7,8, 13,14

Most importantly, plots of wave height made along all of the 1800 wave rays in the 12 wave conditions show that the areas of wave height singularities are quite small. These plots of wave heights made along each ray of the BCTWCM output indicate that in every case, these singularities are expressed by narrow, steep, symmetrical curves, which are easily discerned on such plots (Figure 12-4). Thus, from the plots of the parameters in Munk & Arthur's wave intensity method (Figure 12-2) and the wave ray diagram comparison with the wave heights singularities (Figure 12-3a and 12-3b), the cause of the computations of unusually large wave heights within the BCTWCM is clearly established.

It is also necessary to define a 'singularity' as precisely as possible in order to evaluate the effect of such singularities on the BCTWCM wave height computations. These heights are being presented in the form of computer-contoured diagrams (discussed in a later section) of shelf wave height distribution. The proper definition and interpretation of these singularities (or crossed-rays, i.e., caustics) does not appear to be the problem it was once thought to be. Chao has undertaken a thorough series of theoretical (Chao 1970, 1971), wave tank (Chao & Pierson 1970, 1972) and continental shelf (Chao 1972, 1974; Chao et al. 1975) refraction studies of this singularity phenomena. The results can be summarized within the context of two shelf areas: at the singularity, and down wave from the singularity region.

At the singularity, where unusually high wave heights are computed according to linear wave theory, numerous wave observations in the nearshore (Figure 12-1) and the above-mentioned theoretical wave tank work of Chao and Pierson indicate that instead, at the point of wave crossing, maximum wave heights of 1.8 to 2.0 times the incoming wave height occur (Figure 12-5a, 12-5b, 12-5c). These efforts have been further substantiated by Whalin's (1971) wave tanks studies, where the maximum observed wave height at the region of wave front crossings (depicted as wave ray crossings) was 1.7 times the incoming wave height (Whalin 1971, Figure 21).

Downwave from the singularity (i.e., caustic), the question of possible wave alterations has been summarized by Chao (1974, p. 32). "The rays, after escaping from the caustic regions, eventually follow the continued ray path and the wave conditions are determined by the b factor just as if no caustic had occurred except that there has been a phase shift, which is unobservable because of the randomness of waves in nature. These conditions eliminate the necessity of the evaluations of the waves near a caustic. . ." Although some wave height changes may occur in the waves that pass through a caustic region, theoretical and wave tank studies (Chao and Pierson 1972) suggest that such changes seaward of the zone of breaking waves may be minimal and well within the accuracy bounds set by other limiting factors, such as accuracy of depth information.

In summary, singularities may be identified by plotting wave height calculations made along each ray, and appear as narrow, symmetrical, steep curves, considerably above the 'regional' wave ray height distribution. More precisely, the singularity is defined here as where the wave heights become abruptly greater than two times the wave heights entering the singularity region. For these data, with an input deep water wave height of 1.8 m, the singularity is defined as being greater than 4 m, and less if

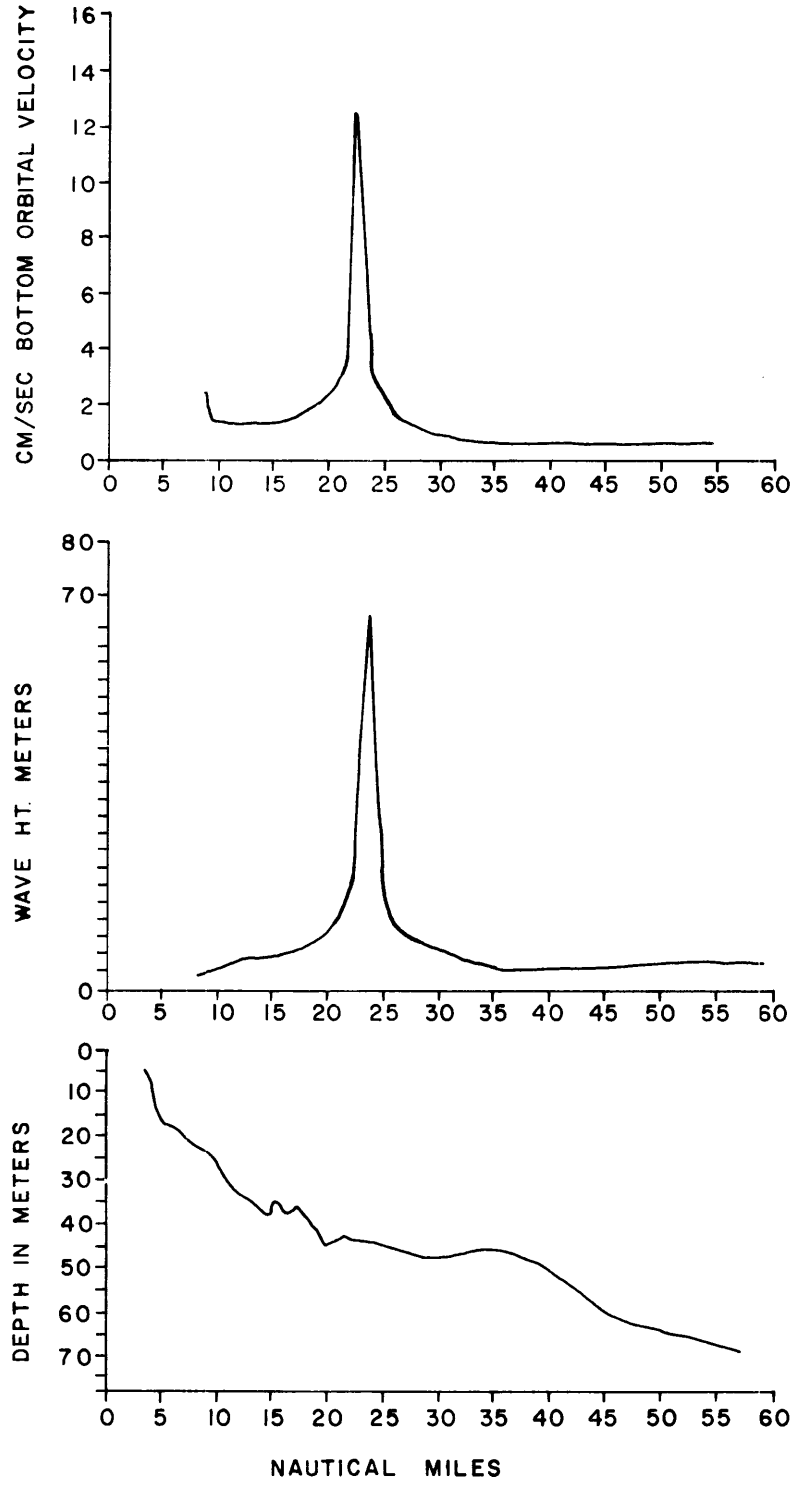

Figure 12-4. Graph of wave height, bottom orbital velocity and depth along wave ray #7 (BCTWCM); Outer continental shelf to Jones Beach, Long Island.

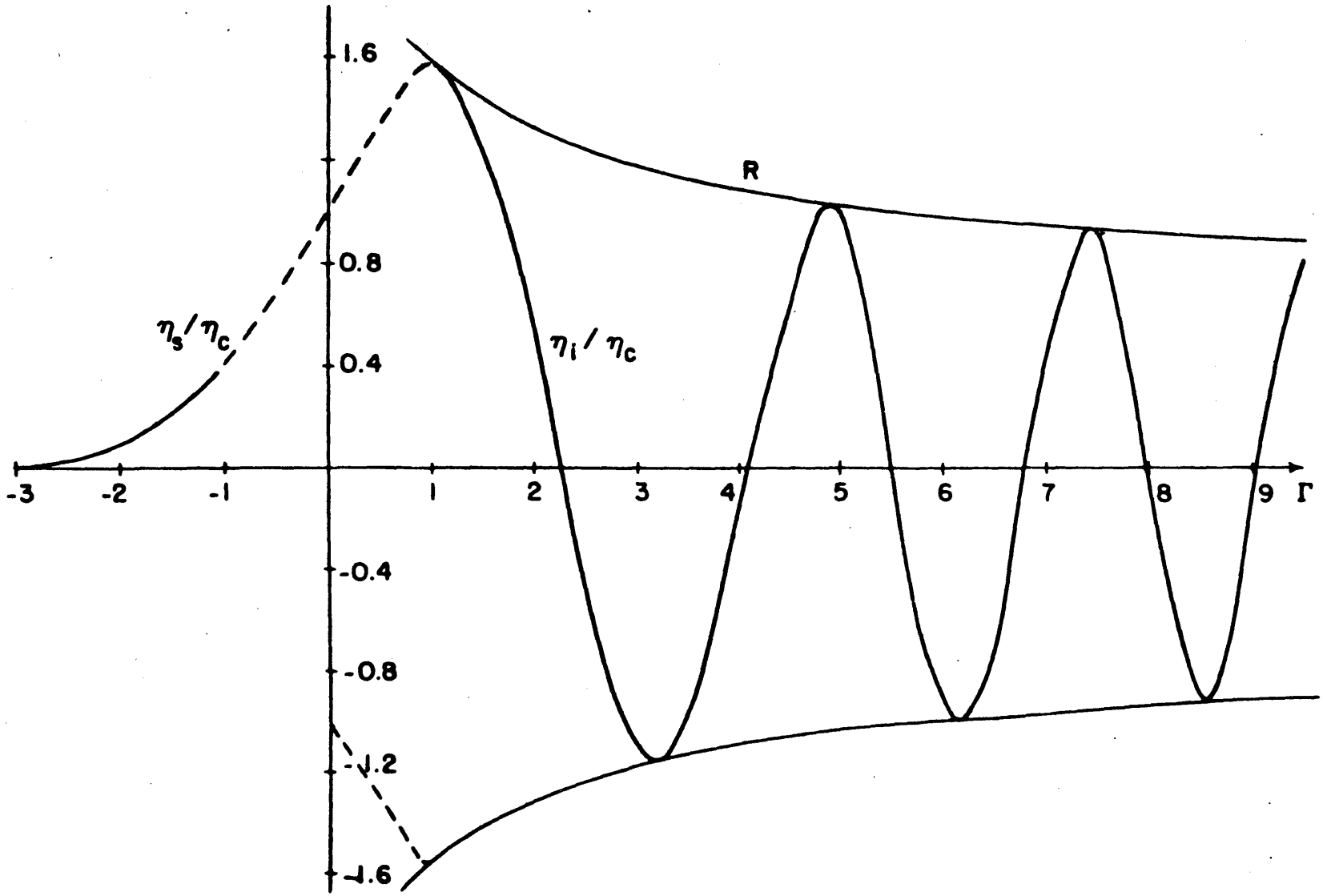

Figure 12-5a. Theoretical water surface elevations in the vicinity of a caustic (Y. Y. Chao 1970).

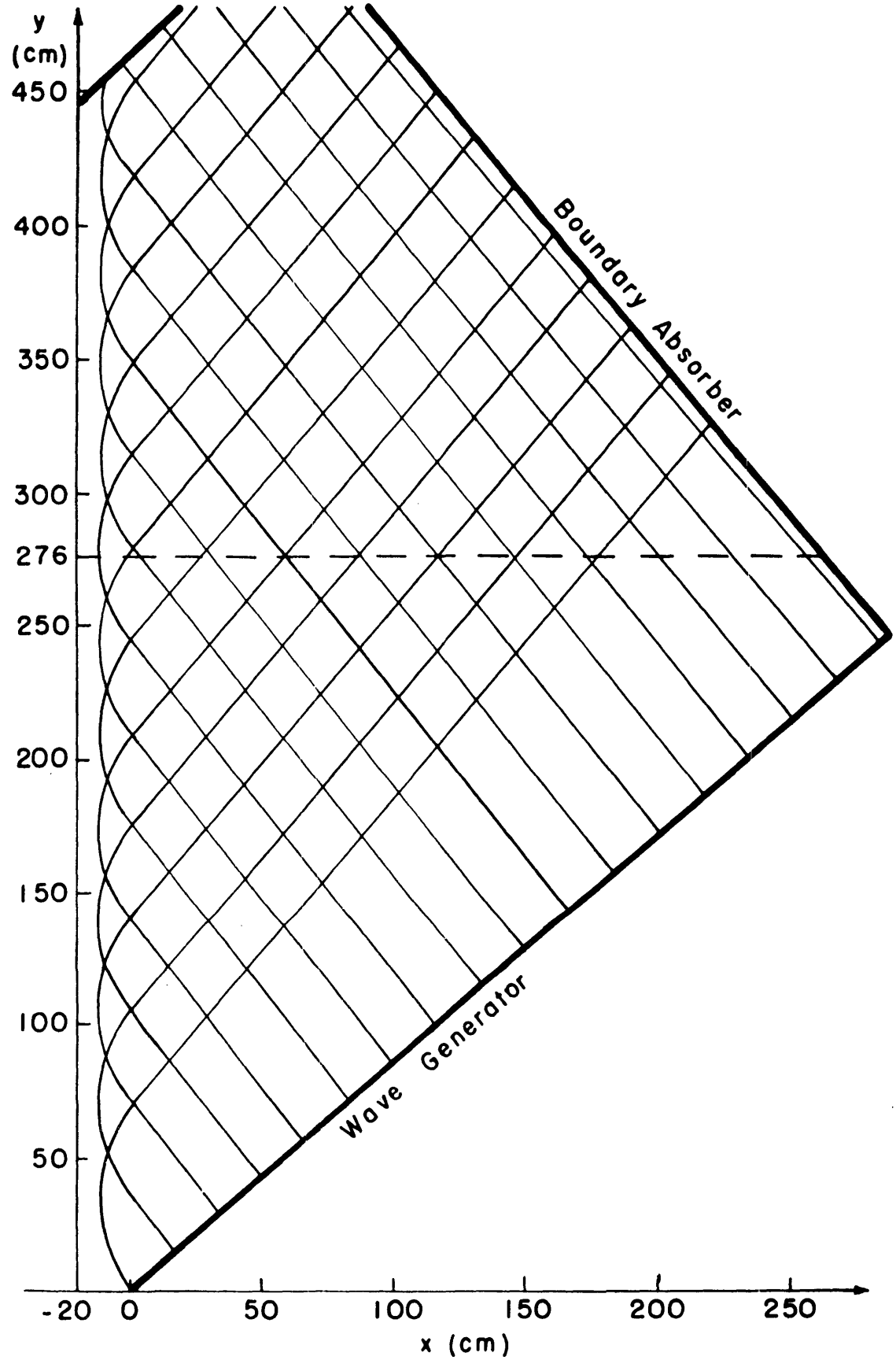

Figure 12-5b. Plane view of wave tank layout and wave pattern for a wave period of 0.73 sec. The wave heights measured along y = 276 are given in Figure 12-5c (Chao and Pierson 1970).

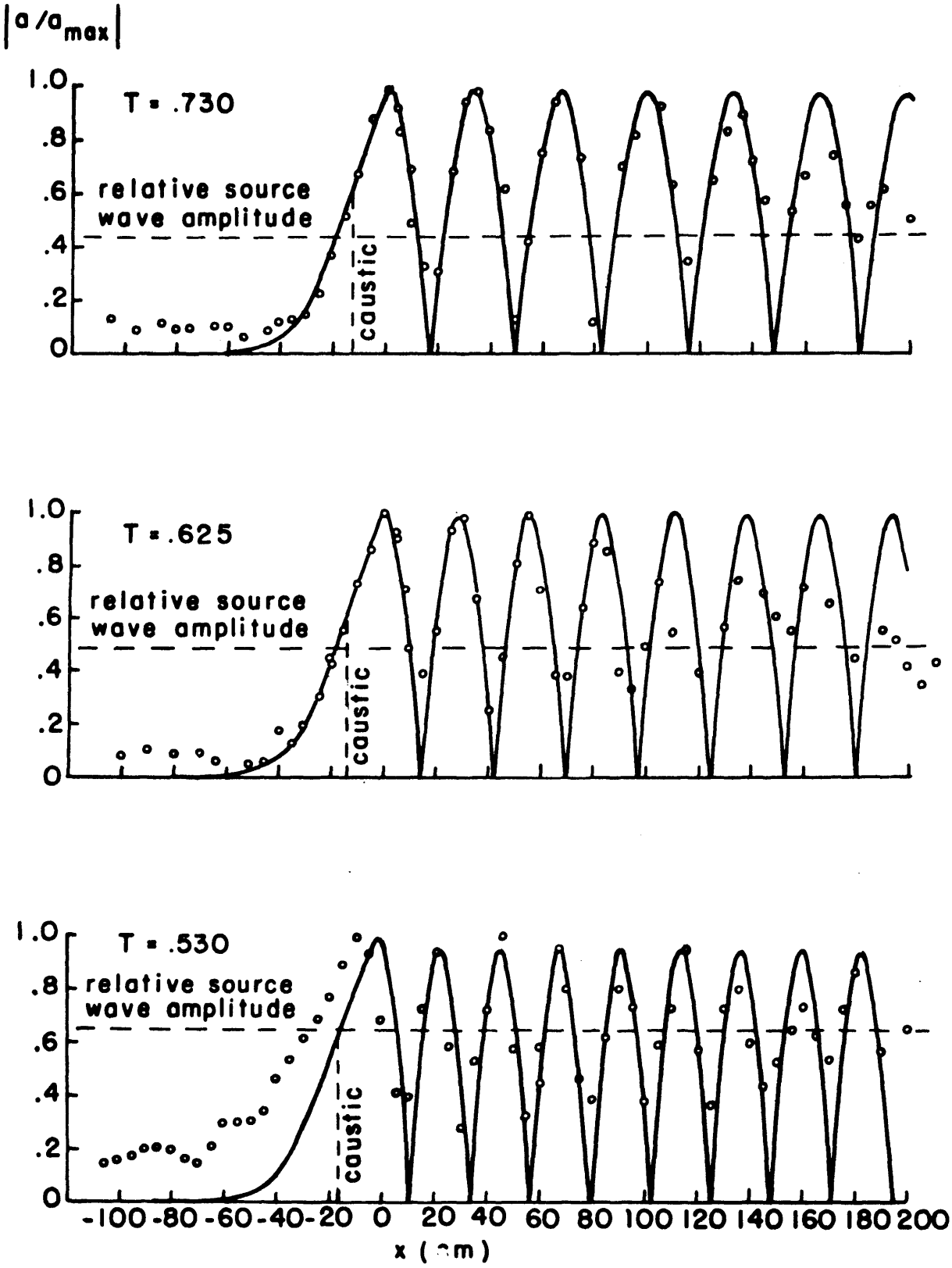

Figure 12-5c. Comparison between theoretical (solid line) and wave tank measurements (small circles) of water surface elevations in the vicinity of a caustic, measured perpendicular to depth contours (@ y = 276 in Figure 12-5b). The ratio of the source wave height (a, and the dashed line) is compared to the maximum caustic wave height (a_{max}) generated in several experiments for each specific wave period. (from Chao and Pierson 1970).

the refracted wave height just before the singularity is less than 1.8 m. The exact heights achieved within the singularity, and even the occurrence of the singularity itself, are serendipitous in that they are completely dependent on the time step which determines where the calculations are made. With respect to these VIMS-BLM BCTWCM computations, in every case studied, abrupt increases in height occurred as the clearly visible symmetrical perturbation just discussed (Figure 12-4). Furthermore, the time step within the model computations was such that the singularity was commonly defined by 3 to 8 wave height computations (i.e., 3 to 8 time steps) along a wave ray.

Having quantitatively defined the singularity, it is now possible to assess the effect of these singularities on the wave height data output in the form of computer-contoured diagrams. A plot of the singularities of wave height against the depth in terms of the depth/wave length ratio ($^{d}/L$), for 8, 10, and 12 sec. conditions for waves from the east revealed that nearly all the singularities occurred between $0.1 < {}^{d}/L < 0.3$ for 10 to 12 sec. and most occurred between $0.15 < {}^{d}/L < 0.35$ for 8 sec. For 10 and 12 sec. waves, this area encompasses a portion of the mid-shelf region. This smaller area, encompassing all the lease blocks, was chosen for intensive study (Figure 12-6, 12-7). In this mid-shelf area, all of the wave height computations (i.e., the actual wave height values) along each wave ray and the computations for each of the 12 wave conditions were plotted on a planimetric surface at a scale approximately five times that shown in the final form (Appendix 12-E). The total number of wave height singularity computations (defined as $H < 4.0$ m) averaged 0.5% of the total height computations. The singularities were then located and shown to occupy an average of 40% for the 12 wave conditions of the surface shelf area bounded by the 3 m wave height contour (summarized in Table 12-4). That is, most of the shelf areas indicated by the 3 m wave height contour (an indication of high wave energy) in the computer-generated diagrams appear to be "real". Although the extent of the area encompassed by the 3 m contour is thus biased to some extent, when all the singularities are removed from the data, the same areas of high wave energy are still indicated for the shelf.

With respect to the effect of the singularities on the maximum bottom wave orbital velocity (Umb) calculations, this can be determined simply by overlaying the Umb diagrams over the wave height contour diagrams, and then discarding all Umb contoured values that were based on wave height singularities. Umb computations are complexly related to wave height, depth, and wave period. Thus Umb calculations involving singularities are not all necessarily > 60 cm/sec.

WAVE MODEL INPUT

Depth Information

Depth input data consisted of 97,650 depths on magnetic tape in a two-dimensional array (315 x 310) transcribed from NOS original sounding data, and transposed into a Tranverse Mercator Projection (Figures 12-8, 12-9, 12-10; Tables 12-5 and 12-6). These techniques and the background philosophy are extensively described in Goldsmith et al. (1974, p. 13-19) and Goldsmith et al. (1977). The accuracy of the depth information and

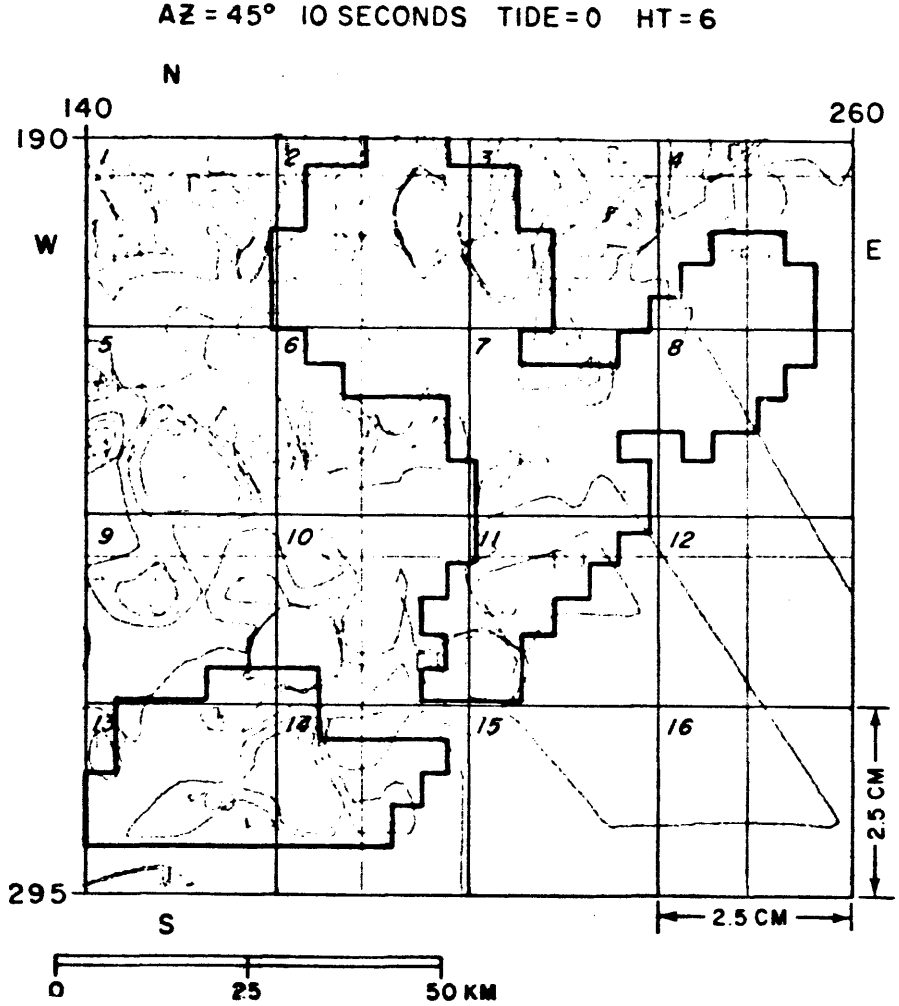

Figure 12-6. Location of 16 square overlay for comparing computer contours with hand contours in selected shelf area encompassing lease blocks.

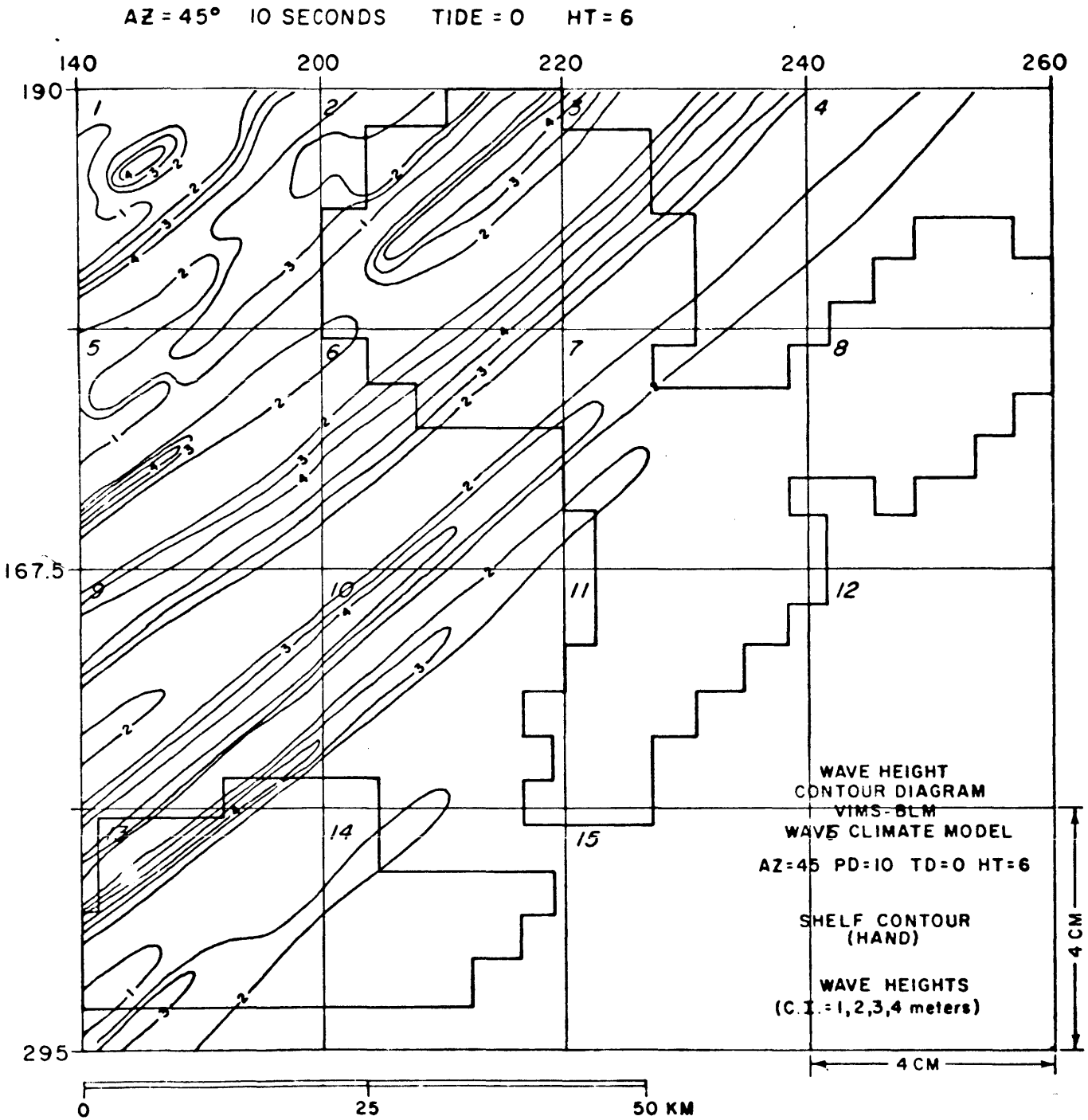

Figure 12-7. Location of same 16 squares shown in Figure 12-6, for use with hand contours.

Table 12-4. Effects of singularities on hand contouring of wave heights for selected shelf areas encompassing lease blocks.

Area	Tide	Total points available	% of data > 3 meter contour	% of data > 4 meter contour	% of 3 meter contour represented by singularities	% of data > 60 cm/sec contour
45° 8 sec	0	6,897	0.01	0.26	55	0.159
45°10 sec	0	6,897	1.95	0.97	49	1.360
45°10 sec	5	6,897	3.40	1.62	47	2.230
45°12 sec	0	6,897	2.94	1.24	42	5.190
90° 8 sec	0	11,595	0.05	0.02	50	0.034
90°10 sec	0	11,595	0.49	0.15	31	1.344
90°10 sec	5	11,595	0.56	0.25	45	0.913
90°12 sec	0	11,595	1.17	0.57	48	4.320
135° 8 sec	0	16,075	0.00	0.00	0	0
135°10 sec	0	16,075	0.29	0.11	38	1.500
135°10 sec	5	16,075	0.25	0.11	36	0.913
135°12 sec	0	16,075	2.05	0.72	35	5.210
			1.10	0.50	40	1.93

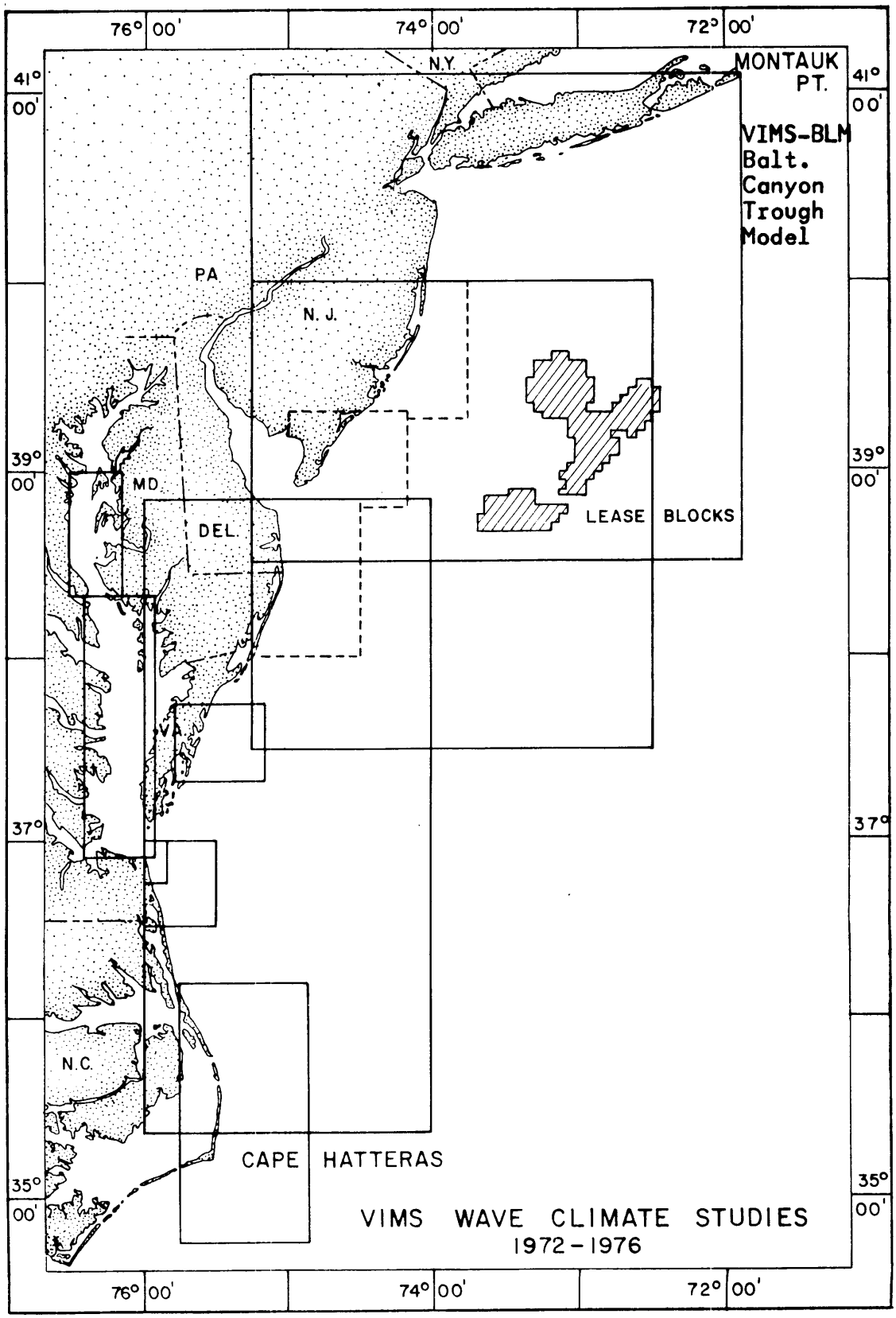

Figure 12-8. Location map of VIMS-BLM wave model and designated lease blocks, with respect to other VIMS studies.

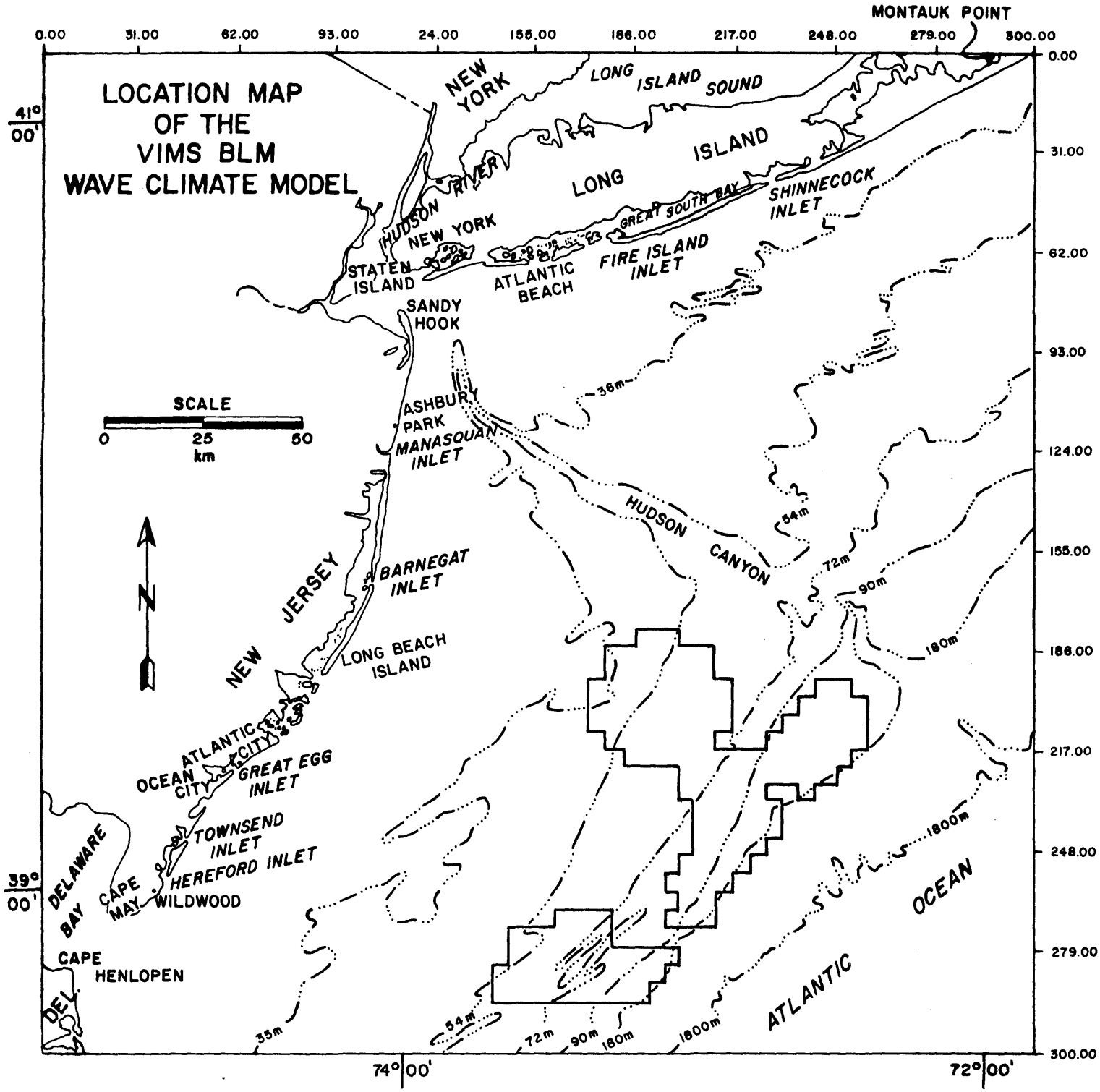

Figure 12-9. Detailed map of VIMS-BLM Model area including geographic names, bathymetry, and grid.

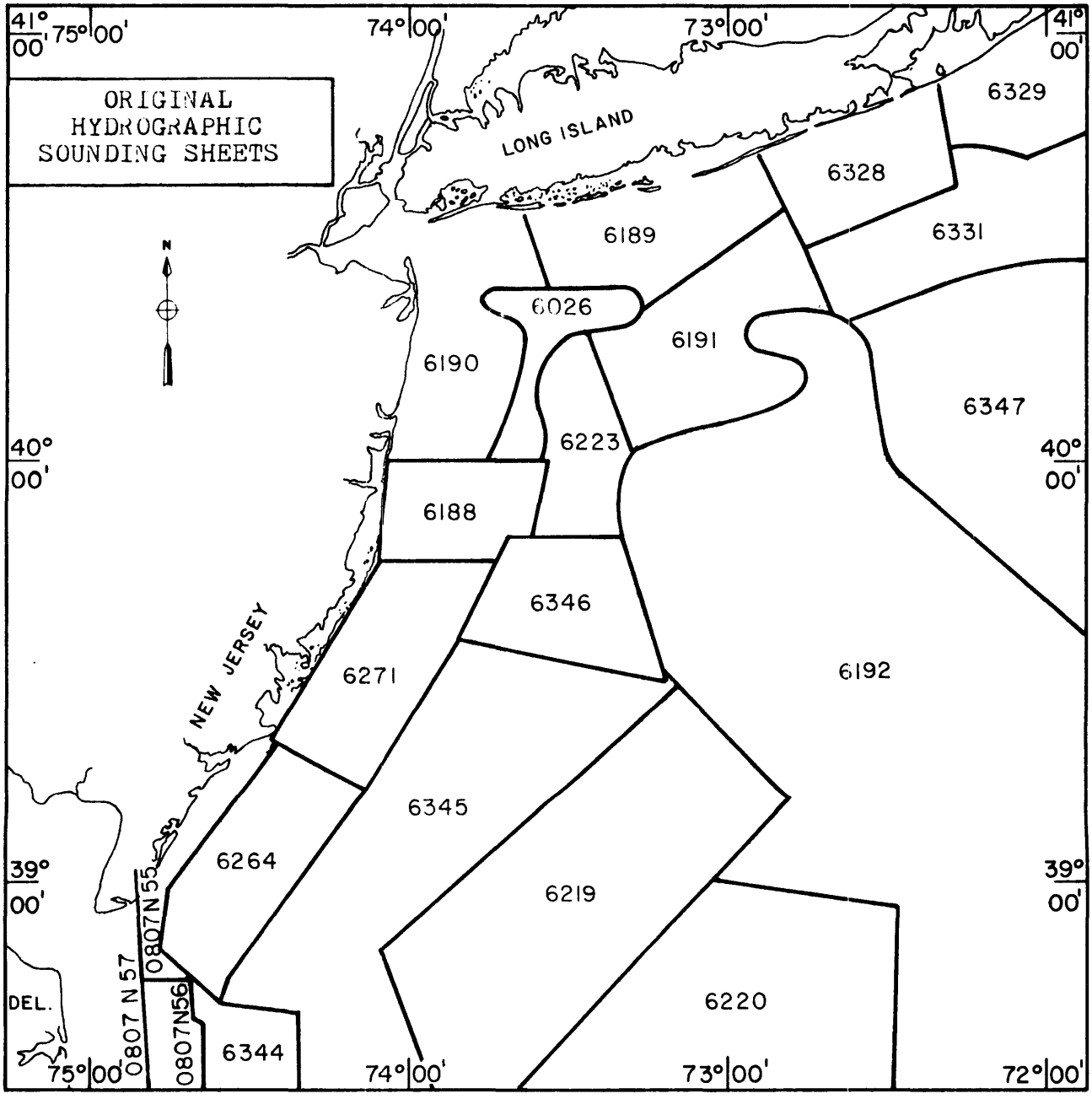

Figure 12-10. Source of depth information. Refer to numbers of original hydrographic sounding sheets, Table 12-6 which provides information on date, scale, and sounding units.

Table 12-5. VIMS Wave Climate Model Studies, 1972-1976.

Area	X (N-S)	Y (W-E)	Total Depths	(Grid Corner Coord. (lat. & Long.) NW	SW	SE	NE	Order	Grid Den. (NM)
Virginian Sea	420	201	84,000	38°48 76°03	35°21' 76°00'30"	35°21' 73°59'05"	38°48' 73°57'	1st	0.50
Wachapreague	100	99	9,900	37°45' 75°43'	37°20' 75°43'	37°20' 75°10'	37°45' 75°10'	2nd	0.25
Southeastern Virginia	120	102	12,240	37°00' 76°04'30"	36°30' 76°01'30"	36°30' 75°30'	37°00' 75°30'	2nd	0.25
Virginia Beach	140	99	14,000	36°59'30" 76°01'30"	36°45' 76°01'30"	36°45' 75°59'18"	36°59'48" 75°59'30"	3rd	0.10
New Jersey	300	254	75,900	40°00' 75°15'	37°30' 75°15'	37°30' 72°30'	40°00' 72°30'	1st	0.50
Lower Chesapeake Bay	360	94	33,840	38°23' 76°25'	36°55' 76°25'	36°55' 75°55'	38°23' 75°55'	1st	0.25
Upper Chesapeake Bay	155	69	10,695	39°00' 76°32'	38°20' 76°32'	38°20' 76°10'	39°00' 76°10'	1st	0.25
New Jersey upper	165	158	26,070	39°58'45" 74°34'	39°18' 74°34'30"	39°17'45" 73°44'	39°58'15" 73°43'	2nd	0.25
middle	120	135	16,200	39°18' 74°54'30"	38°48'30" 74°53'30"	38°48'15" 74°11'	39°18' 74°11'	2nd	0.25
lower	180	100	18,000	38°49' 75°12'	38°04' 75°12'	38°04' 74°41'	38°49' 74°41'	2nd	0.25
Baltimore Canyon Trough Grid	315	310	97,650	45°05' 75°15'	38°30' 75°15'	38°30' 71°50'	45°05' 71°50'	1st	0.50
Hatteras Grid	345	170	58,650	36°12' 75°45'	34°45' 75°45'	34°45' 74°50'	36°12' 74°50'	2nd	0.25

Table 12-6. Original hydrographic sounding sheets (NOS) used in supplying depth information (see Figure 12-10 for location).

Map No.	Date	Scale	Soundings in:
6026	1936	40,000	feet
6188	1936	40,000	feet
6189	1936	40,000	feet
6190	1936	40,000	feet
6191	1936	40,000	feet
6192	1936	120,000	fathoms
6219	1937	120,000	feet
6220	1937	120,000	fathoms
6223	1937	40,000	feet
6264	1937	40,000	feet
6271	1937	40,000	feet
6328	1938	40,000	feet
6329	1938	40,000	feet
6331	1938	80,000	feet
6344	1938	40,000	feet
6345	1938	80,000	fathoms
6346	1938	40,000	fathoms
6347	1938	120,000	fathoms
0807N-55	1967	250,000	fathoms
0807N-56	1967	250,000	fathoms
0807-N57	1967	250,000	fathoms

depth transposition techniques employed here are discussed in Sallenger et al. (1975).

Wave Input Conditions

The philosophy used in choosing these particular wave conditions and the problems relating to an adequate base of shelf wave information are discussed in Goldsmith et al. (1974, p. 20-27). An evaluation of data output from the Virginian Sea Wave Climate Model (VSWCM) (Figure 12-8) was made to assist in choosing these wave input conditions.

The twelve representative wave conditions are given in Table 12-7.

Table 12-7

NE	8, 10, and 12 second periods	0 ft. Tide
NE	10 second period	+1.5 m Tide
E	8, 10, and 12 second periods	0 ft. Tide
E	10 second period	+1.5 m Tide
SE	8, 10, and 12 second periods	0 ft. Tide
SE	10 second period	+1.5 m Tide

These wave input conditions encompass much of the ship wave observations in the area (Marsden Squares 116-55 and 152-05) as well as the Saville Wave Hindcast Data (using the SMB significant wave method) computed for the area adjacent to New York Harbor (Saville 1954).

Wave heights were set at 6 feet (1.8 m) in all cases in order to be consistent with the VSWCM data. It should be also noted that in using linear wave theory modified for friction, varying the input wave heights do not change the refraction diagrams or the resulting relative spatial distribution of wave energy concentrations and diminutions.

WAVE OUTPUT DATA

Computations were made on an IBM 370 computer. The most significant wave data listed in the computer printouts were portrayed graphically in the form of wave ray diagrams, shelf contour plots, and shoreline histograms. The computer program for contouring used here is described by Hamm et al. (1975) and was tested at the NASA-Langley Computer Center. Whereas the computer generated values are in English units, all diagrams are in metric units. These diagrams and figure numbers are listed in the Appendix.

Wave Ray Diagrams (Appendix 12-A)

Several comments concerning the preparation of the graphic CALCOMP plots are in order. All diagrams were plotted close to page size in order to promote accessibility and ease of handling. Thus far more detail went into their preparation than might appear at first glance. For example, the 12 wave ray diagrams were computed using a total of 97,650 depths on a 0.5 NM grid. Some indication can be obtained from the ray diagrams by noting the large number of input wave rays, with 102 wave rays (east diagrams) to 210 wave rays (southeast) input at one NM intervals.

Wave Ray Density Analysis (Appendix 12-B)

The twelve wave conditions simulated by wave refraction of the Baltimore Canyon Trough Lease Block Area were analyzed for variations in density of orthogonals. Using the relationship $K_r = (\frac{b_o}{b})^{\frac{1}{2}}$, where b is the distance between wave rays, the variations in ray spacing due to wave refraction should be a measure of local variations of wave energy.

The lease block area wave orthogonal diagrams for the twelve wave conditions were photographically enlarged to about 1.5x greater than the original page size. These were then scaled, and a two nautical mile square grid was superimposed. The orthogonals in each two nautical mile square were counted and recorded on the grid.

Both the northeast (45^o) and southeast (135^o) wave conditions had an initial .707 NM orthogonal spacing due to an oblique orientation to the grid squares. This resulted in an initial orthogonal density of 4 orthogonals per 2 NM grid square for unrefracted waves. The east (90^o) wave conditions had an initial deep water orthogonal spacing of 1.0 NM oriented normal to the grid squares, with an initial orthogonal density of 2 orthogonals per

2 NM grid square. The orthogonal densities of the east (90°) wave conditions were "normalized" to those of the northeast (45°) and southeast (135°) wave conditions which had an initial density of 3.4 rays (i.e., K_r = 1.0) for purposes of comparison.

The normalized orthogonal densities were contoured in five intervals indicating degree of convergence and divergence--0 orthogonals/2NM square, extreme divergence; 1-2 orthogonals/2NM square, divergence; 3-4 orthogonals/2 NM square, no convergence or divergence; 5-6 orthogonals/2 NM square, convergence; 7-8 orthogonals/2NM square, extreme convergence--as shown in diagrams (Appendix 12-B). The values of the refraction coefficients for each orthogonal density level were determined and are also shown in these diagrams.

By comparing the results from 12 wave conditions, only two areas of the lease block areas show significant wave convergence activity, the northwest section of the northern area and western 1/3 of the southern lease block area. Eight second waves from northeast, east or southeast show no variations in energy in the lease block areas. The ten second wave conditions with 0 and 1.2 m tides all show a slight convergence of wave energy in the NW lease block area, but none exceed a calculated refraction coefficient of 1 (D). All areas of convergence are flanked by areas of divergence, indicating that these are areas of complex wave activity.

The twelve second wave conditions from the east and southeast each show a complex wave condition in the northwest lease block area, and to a lesser extent, at the western 1/3 of the southern area. No calculated K_r values, however, exceed "divergence". The northeast 12 second wave condition is the most extreme case of wave convergence in the lease block areas in this investigation. For this condition, calculated K_r values exceed "extreme convergence". The western half of the southern lease area show areas of convergence and divergence. The northeast area of the northern lease block show a highly complex wave situation, with extreme convergences flanked by divergences of wave energy.

Based on the results of this phase of the investigation, it is obvious that the northwest area of the northern lease block is an area where the variations in wave activity are a primary concern. The second most complex area lies in the western third of the southern area.

Contour Diagrams (Appendices 12-C and 12-D)

The shelf height diagrams were contoured at 1, 2, and 3 meters corresponding to 55%, 90%, and 167% of the input height of 1.8 meters. The maximum bottom orbital velocity was contoured at 15, 27, and 60 cm/sec corresponding (very approximately) to the minimum velocity required to: (1) erode and (2) transport medium sand, and (3) the initiation of oscillation ripples (CERC 1973, Figure 4-22). The original computations were made at intervals of 0.5 NM in "deep" water, and lesser intervals in shallow water (Table 12-8), so that more detailed information was available in shallower areas where greater refraction occurs (i.e., in deep water, depth (D) > 1/2 wave length (1), every tenth point along each wave ray used; in areas of slight refraction (1/2 L $\geq$ D > 1/4 L), every

fifth point was used; and in depths where significant wave refraction could occur (D < 1/4 L), every point was used.) Wave height and bottom velocities were only contoured over those shelf areas in which wave refraction occurred.

Table 12-8. Number of points used in preparation of contour diagrams.

Wave Condition			Number of Points		
Condition From	T (sec)	Tide (ft)	Available	Used	ISKIP
NE	8	0	3,182	1138	2
NE	10	0	6,056	1255	4
NE	12	0	9,528	1059	8
E	8	0	5,916	1151	4
E	10	0	11,078	1211	8
E	12	0	17,781	1037	16
SE	8	0	8,491	943	8
SE	10	0	16,068	945	16
SE	12	0	25,000	1359	16
NE	10	+5	6,056	1188	4
E	10	+5	11,078	1147	8
SE	10	+5	16,068	945	16

Table 12-8 presents the number of points generated over the shelf which were available for contouring and the number of points actually used. Because of the wide variation in data points available and the very high cost of computer contouring, three different interval skip factors (ISKIP) were used. This reduction procedure results in approximately the same data density throughout the contour plot (about 25 data points/sq. inch or 3.8 points cm^2 of graph, corresponding to one point/9 mi^2 of shelf area). This is a continuous reduction process from ray to ray so that the points chosen for contouring are staggered along the wave rays of each diagram.

Despite the high density of input wave rays and contoured data, there is a tendency in some shelf areas for the contouring to follow individual wave rays due to very extensive wave refraction. Comparison of the contours and wave ray diagrams for each condition will indicate these areas, alleviating over-reliance on output from a single wave ray in this regional approach.

Comparison of Computer Contouring with Hand Contouring of Wave Heights, and with Hand Contouring of Orthogonal Density

The weighing of all data points by the Computer Contour Program was tested through the use of a 60 x 60 test array. The input data for this grid approximated a bull's-eye with three contours at intervals of 1 meter from 3 to 12 feet (the original height computations were in feet). The program used was most effective in contouring the bull's-eye diagram (Figure 12-11) using a simple data pattern.

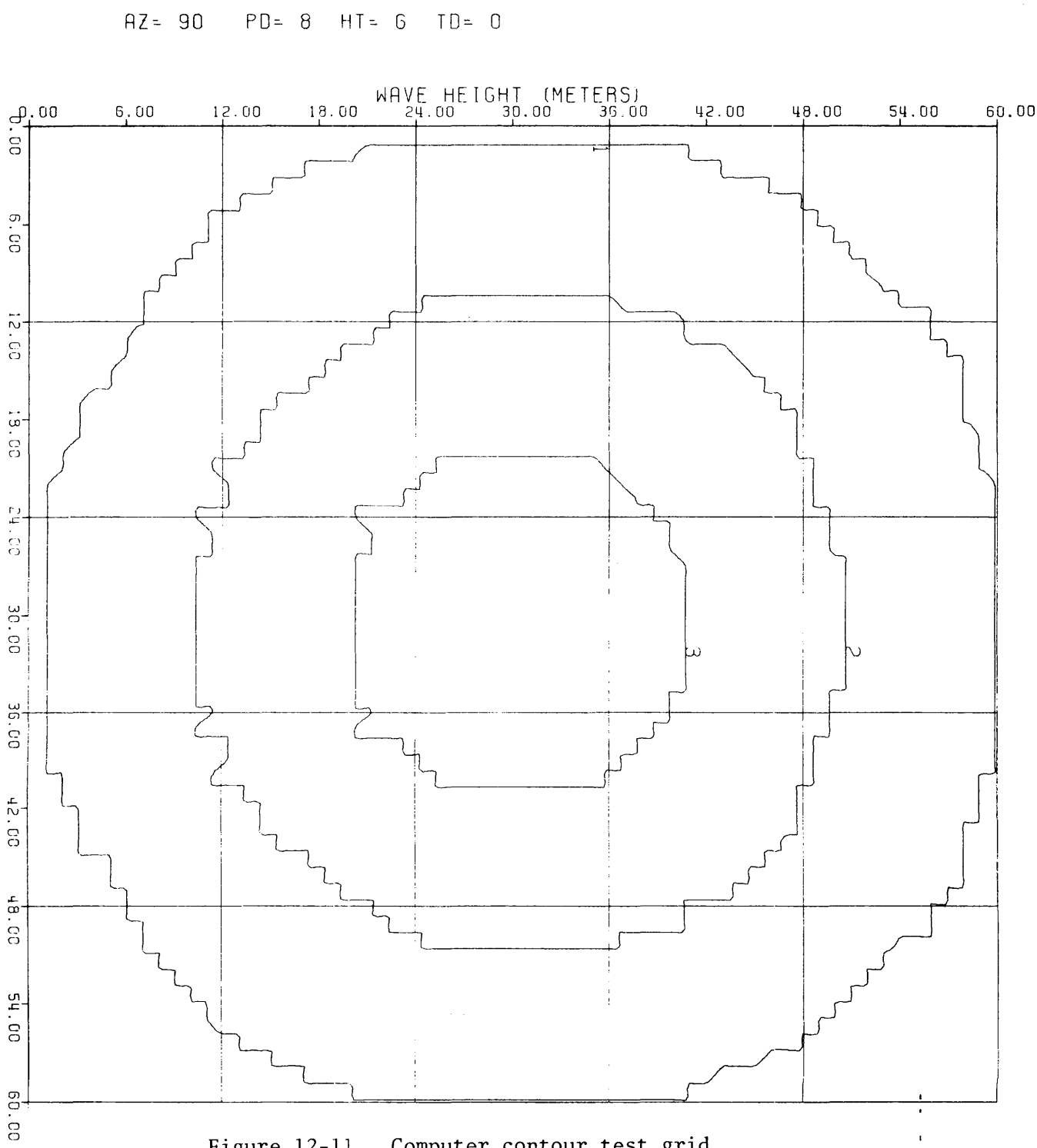

Figure 12-11. Computer contour test grid.

In order to check the validity of the Computer Contouring Program under complex conditions, the data was hand contoured within an area encompassing the designated lease block area. First, the value of every computed wave height (in meters) was plotted along each wave ray in order to also evaluate the ISKIP factor on the computer plotting. The shelf wave height diagrams were hand contoured at 1, 2, 3 and > 4 meters corresponding to 55%, 90%, 167%, and > 180% of the input height of 1.8 meters. This also made it possible to delineate and assess the singularities (see Singularity section). The maximum bottom orbital velocity was hand contoured at 15, 27, and > 60 cm/sec corresponding to the computed contours.

The plotting utilized a CALCOMP plotter at a scale of 50 x 50 cm. This size was large enough to print each number legibly, allowing sufficient distance between points for hand contouring, while still maintaining a format that could be easily reduced to page size.

The hand contour diagrams revealed a concentration of data points in the northwest sector of the lease block grid due to extensive wave refraction into this area by the nonuniform bathymetry (Figure 12-12). In addition, this portion of the study area also has very complex bathymetry and also showed a concentration of data in the computer contour diagrams.

The exhaustive comparison of the data generated by the computer, hand, and orthogonal density contours is summarized in Table 12-2. Table 12-2 was generated by using a 16 square overlay with each square about 22 km on a side, in order to correlate common sectors of the lease block area in both the computer and hand-drawn contours. These numbers represent comparisons of contours within the 16 squares in the selected study area, as well as, in the case of computer contours, those points outside the block that could conceivably influence contours within a square. Table 12-4 represents percent of the data indicating high wave heights (> 3 m) and bottom orbital velocities in excess of 60 cm/sec. The bottom velocities are influenced by the singularities about the same percentage as the wave heights (Table 12-3) (see earlier Singularity section).

The hand contour diagrams should have an advantage over the other methods, due to the utilization of all data points. This appears to be substantiated by the closer comparison of the hand contours with the hand drawn orthogonal density diagrams, than with the computer contours (Table 12-4). Another important aspect of the printing of every point along the ray is the delineation of the location of each singularity along the wave ray.

The major limitation of the hand contoured diagrams is that countless man hours are spent in the preparation of the diagrams and the tedious task of hand contouring thousands of data points, even for this smaller selected area. Because of the abundant data points and complex ray crossings, the hand contours also have a tendency to follow the wave rays across the lease block grid, which is another major limitation. This bias cannot be significantly alleviated due to the inability of the contourer to weigh the numerous points within a small region.

The computer contour diagrams are easily generated (though expensive) and have the ability to handle large quantities of data. It is for this

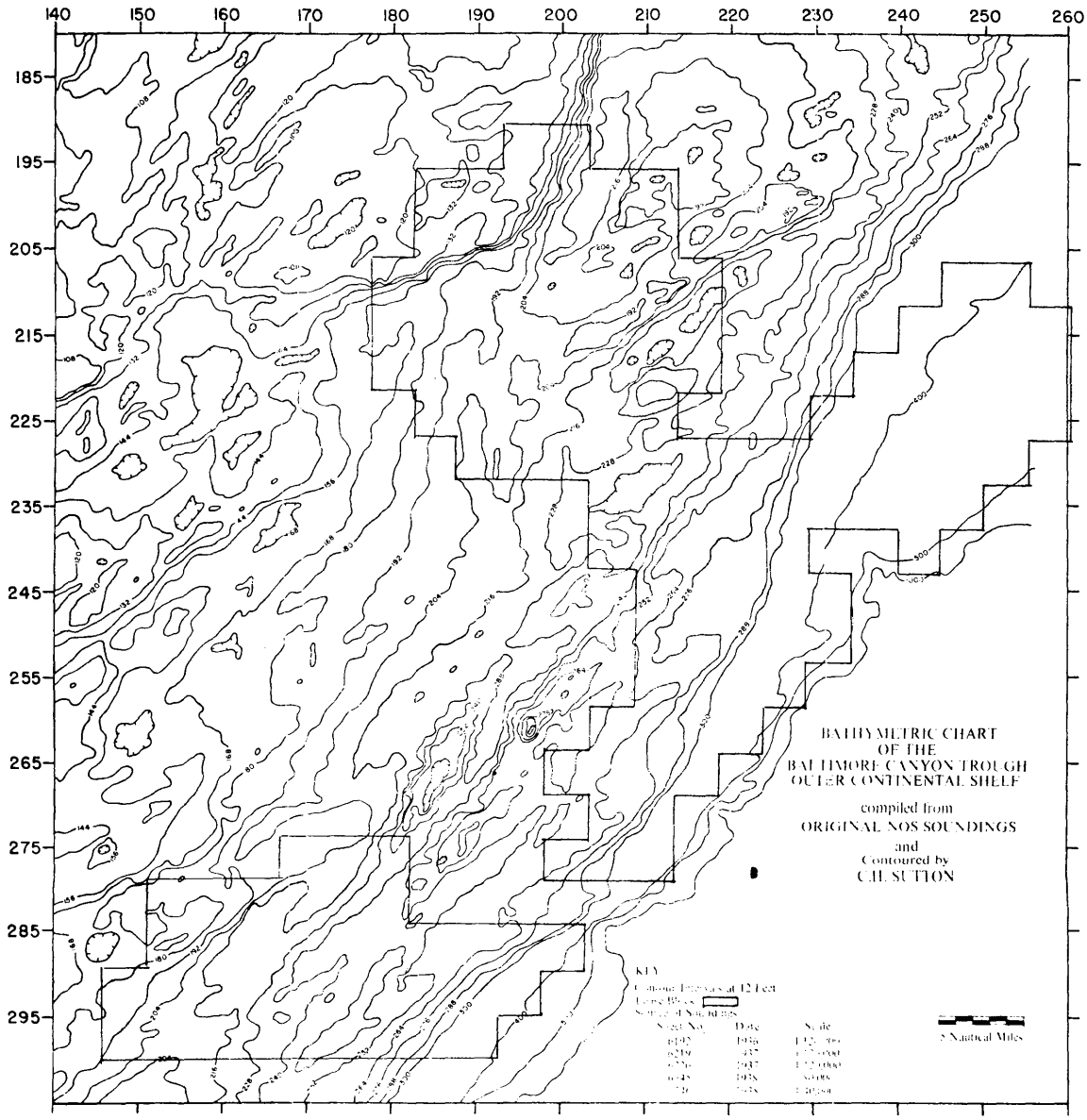

Figure 12-12. Bathymetric map of the lease block area.

reason they were adopted for the regional wave studies on this extensive area of the continental shelf. The Computer Contour Program has the ability to evaluate and weigh the values at all points within an area and draw a smooth contour. This, in theory, is far superior to hand contouring with associated human biases. Computer contouring, however, is quite complex and involves very complicated equations which "weight" the different values. (The equations, of course, may also have human biases though they are more subtle.) The summary comparison table indicates that although the program uses an ISKIP factor in some areas, it generates more contours than the hand method (Table 12-4). This is explainable in some of the blocks around the perimeter of the 16 square grid. If a value at a point outside the grid was large enough, it could result in the drawing of an additional contour line within the square. The problem, however, is consistent throughout the 16 squares indicating there is another factor influencing the program. When compared to the orthogonal density diagrams (which most closely resemble the hand contours), the same phenomenon is also encountered. There is an increase in areas of high wave heights in the computer contouring where ray density remains unchanged (see Table 12-2). The total effect, if any, of the singularities on the program is not fully understood and could be a factor in the production of the extra contours.

Orthogonal density contour diagrams proved very useful in the analysis of the wave ray data. Since the only data needed to produce the diagrams is wave orthogonal diagrams, the final product can be produced rapidly, yielding abundant regional information on shelf wave energy distribution. When compared to the hand and the computer generated diagrams, they prove not only accurate but free from the influence of singularities.

However, it is felt that greater site-specific detail can be delineated by the computer contouring. The orthogonal density diagrams depict areas of converging and diverging wave rays. The areas of convergence represent an increase in wave height, while divergence represents a decrease in wave heights. Wave heights contours reflect these regions by a change in the contour interval. While the two sets of contours (hand and computer) are comparable to specific areas in the orthogonal density diagrams, they do not necessarily contour the areas exactly alike. The contour diagrams treat the data in a more sophisticated manner revealing subtle differences that do not appear in the density diagrams. It is, therefore, possible for both types of contour diagrams to compare favorably to the density diagrams, yet (because of greater detail) not compare sufficiently to each other. (See Table 12-2.)

In summary, the comparison between computer-contoured and hand-contoured wave height computations and with wave orthogonal density diagrams indicates that: (1) most areas are similar (average of 10/16 squares for all conditions and average of 13/16 squares for 12 sec. waves, which have the most complex distributions in this area); (2) most of the differences in the remaining squares are due to extra 2 and 3 m contours in the computer contour diagrams; (3) the wave orthogonal density resembles most closely the hand contouring, in that both of these types lack site-specific detail; (4) no apparent loss in information in this regional overview occurs due to the use of the ISKIP factor (to save computer costs), in that nearly all areas of high wave energy indicated in the hand-contoured diagrams are shown in the computer-contoured diagrams (only

2/16 squares in only 3/12 wave conditions in the computer contour diagrams do not show comparable areas of high wave energy due to the use of the ISKIP factor); (5) the computer contours avoid human biases and the tendency of hand contours to follow distinct wave rays.

Shoreline Histograms (Appendices 12-F, 12-H, and 12-I)

The histograms depicting variations in wave parameters along the shoreline show wave heights (Appendix 12-H), wave energy (Appendix 12-I), and shoreline orthogonal density (Appendix 12-G). Shoreline histograms are presented on two separate plots corresponding to the New Jersey/ Delaware (approximately north-south) and Long Island (east-west) shoreline segments. (There are no Long Island shoreline histograms for northeast wave conditions.)

The histogram class interval is one nautical mile (or two grid points). This is the same interval as the input wave rays and twice the density of the depth grid. These histograms include only the data from waves reaching the shore. Waves breaking further offshore are not included. Where two wave rays reach shore within the same histogram class interval, the graphs display the sum of the two wave heights or energies (i.e., not the average). This arbitrary procedure was used because of the difficulty in deciding when two wave rays occur exactly together in view of the limitations of scale and density of the input depth grid (i.e., if two rays occur exactly together, the heights at the end of the rays should be added). Another reason for this summation involves the manner in which the wave parameter computations are made in the Munk-Arthur wave intensity method, adopted in this, and most other such studies. The histograms class intervals which involve such summing of two or more wave rays can be determined by comparing the histograms with the wave ray diagrams.

Orthogonal density is a measure of wave energy concentration along the shoreline. The parameter plotted is the number of wave orthogonals per nautical mile of shoreline. A totally uniform distribution has a value of one, as this is the input wave ray density.

Data Availability and Storage

All computer generated output data is stored on microfiche and is available on request. In addition, all of the data is stored on magnetic tape at VIMS. These tapes will be retained to the end of the contract period (approximately February 1978). The shoreline wave data is available on punch cards. Since these data are generated data, not environmental data, it is not planned to deposit copies of tapes with the Environmental Data Service with the other VIMS-BLM data.

DISCUSSION

Although definitive conclusions should not be made on the basis of this regional Wave Climate Model without further analysis of substantiating data from other studies, these computations clearly indicate shelf and shoreline

areas of nonuniform wave energy distribution that require further investigation. There is much of interest revealed in this first regional Wave Model of this area, but this brief discussion is limited to the continental shelf area encompassed within the designated lease block areas, and portions of the shoreline downwave from these lease block areas. The most prominent shelf morphological feature is the Hudson Canyon and Shelf Valley, which strongly affects both the shelf and shoreline wave energy distribution.

Continental Shelf

The most significant result of this study is the indication in the northwest and southwest portions of the designated lease block area of several specific areas of wave energy concentration for waves from the northeast with periods of 10 and 12 seconds at low tide (Figure 12-A2 & 12-A3). This effect is enhanced somewhat for Tide = +5 ft. (1.52 m) (Figure 12-A10). This area involves the northwest portion of the designated Lease Blocks in the New Jersey 18-3 lease area. Less wave energy concentrations occur in this and the southwest portions of the designated lease blocks for east 12 seconds and southeast 12 second waves. In general, wave refraction by southeast waves along the axis of the Hudson Canyon and Channel results in areas of lower wave energy in the more landward portions of the designated lease blocks. These areas are clearly indicated in the shelf contour diagrams. Figures 12-13 and 12-14 show composites of the areas of high shelf wave heights and high bottom orbital velocities, respectively, for the 12 computed wave conditions within the designated lease blocks.

Shoreline Areas Downwave From Designated Lease Blocks

In general shoreline wave energy is less concentrated under high tide conditions than low tide because there is less refraction due to greater depths. In both situations, however, distinct areas of shoreline wave energy concentration occur. Similarly, larger shoreline wave energy concentrations occur for the longer period waves because they start refracting in deeper water further from shore.

The shoreline expression of the shelf wave energy concentrations for the important northeast, 12 second wave condition, is in the area from Cape May, New Jersey, to the south. Delaware Bay entrance is a notable area of wave energy concentration for this and all other northeast and east wave conditions.

East 12 second waves have three strong shoreline indications of wave energy concentrations, caused partially by refraction over lease block areas, on Long Beach, north of Wildwood, New Jersey, and less concentration south of Atlantic City (Figure 12-9, 12-A6, 12-G6a, 12-H6, 12-I6a). The Long Beach Island area and the shoreline south of Manasquan Inlet exhibit a wave energy concentration for east 10 second waves (Figures 12-9, 12-A5, 12-G5a, 12-H5, and 12-I5a).

Shoreline effects from refraction over the Hudson Canyon and Channel are most dramatically shown for the Asbury Park, New Jersey area and south, and the Barnagat Inlet, New Jersey shoreline area for southeast 10 and 12

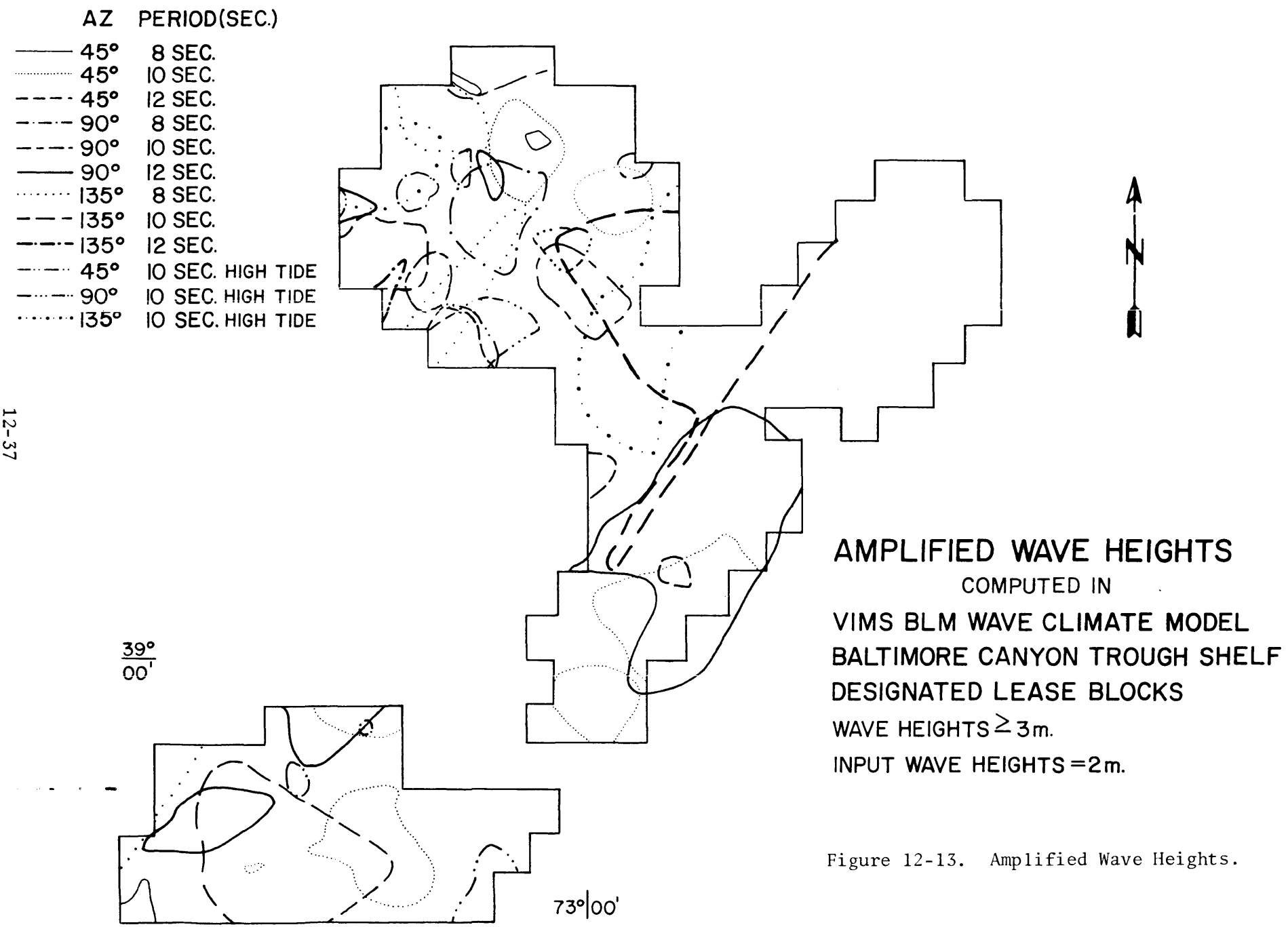

Figure 12-13. Amplified Wave Heights.

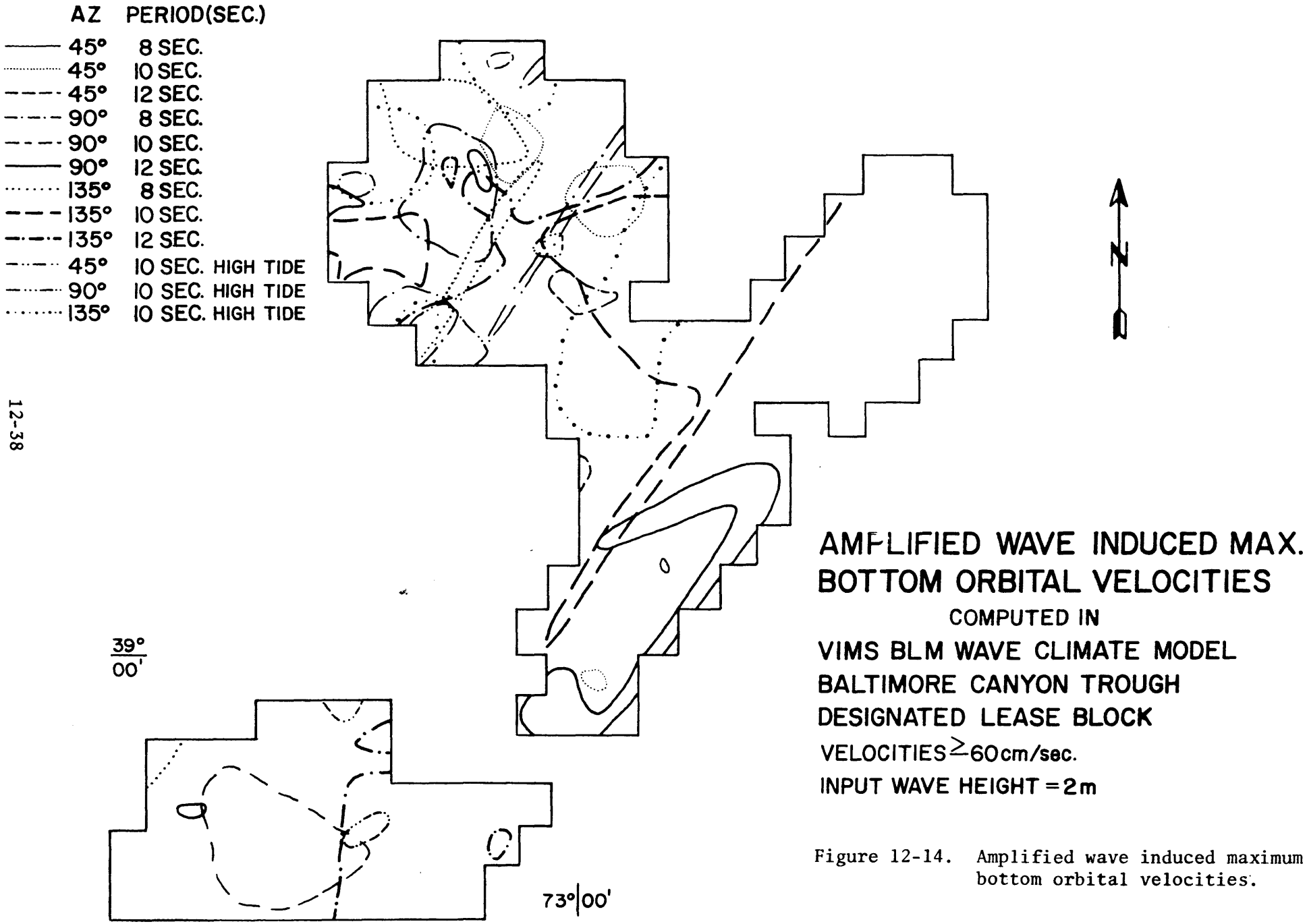

Figure 12-14. Amplified wave induced maximum bottom orbital velocities.

second waves (Figures 12-A8, 12-A9, 12-H8a, 12-H9a, and 12-I8a). Lesser, but still significant, shoreline concentrations for these wave conditions also occur south of Little Egg Inlet, and south of Atlantic City, New Jersey. Significant areas of wave energy concentration on Long Island revealed in studies are at Atlantic Beach and east, and at Fire Island (Figures 12-9, 12-A8, 12-G7b, 12-G8b, 12-H7a, 12-H8b, 12-I7b, 12-I8b).

At this time a cautionary note must be injected. These are regional, not site-specific, analyses. Definitive conclusions will require more exhaustive treatment of data in site-specific areas of concern.

Interaction with Other Disciplines

This regional wave climate model with computer generated graphs is assisting other investigators in interpretation of their findings and will aid in the selection of areas for intensive field studies.

An example of this fruitful interchange between disciplines is the use of the patterns of computed bottom orbital velocities in understanding the distribution of benthic organisms. Biological zonation patterns across the shelf are affected by many factors, but a factor of particular importance to benthic infauna is the extent and frequency of wave disturbance of bottom sediments. D. F. Boesch and his colleagues at VIMS find that the wave activity seems to have great biological relevance (both directly and via influence on sediment type) in that increase in bottom orbital velocity shoreward corresponds well with major changes in infaunal communities. Furthermore, on the inner and mid-shelf, bottom orbital velocity contours seem to correspond with the presence of ridge and swale topography, which strongly affects the distribution of infauna. Ridge and flank sediments are inhabited by small interstitial animals, rapid burrowers, and a few tube dwelling animals which feed on surface deposits. The indigenous species are obviously adapted for a precarious existence in the dynamic sand. Swales are generally covered by finer sediments but often also include a lag of shell, pebbles, and clay lumps. The benthic organisms in the swales are much more numerous and diverse, and include deposit feeders, which feed on organics in the sub-surface sediments, filter feeders, and epifauna living on shell and pebbles. In addition, this area has a much higher biomass than the ridges.

It is hoped that feedback from the investigators in other disciplines will provide the necessary information to further refine this first-order model.

Alleviation of Singularity Problem

Based on the intensive analyses of the abundant wave data generated by the BCTWCM, the singularities have been clearly defined, their areal extent delineated, and their effect on the wave data shown to be negligible. Nevertheless, they occur in all present wave refraction computation schemes. Until such time as a theoretical basis is developed, making this aspect of the mathematical computations correspond better to reality, we have adopted within the BCTWCM a practical solution to the singularity problem, as

outlined below:

1. A test is made to determine when a singularity region is being entered into by the wave ray, by testing each subsequent new wave height (H_T) calculation made as the wave propagates across to determine if it is greater than two times any of the 12 previous wave height computations ($H_{1 \text{ to } 12}$).

2. If $H_T > 2H_1$, for example, then the ray is allowed to continue, without recording the data until the singularity region is passed (i.e., the new $H_T < 2H_1$, the wave height which "tripped" the bypass steps).

3. Then, a new wave ray is formally restarted landward of the singularity region, with the new input wave height set at the last wave height value to pass the singularity test (i.e., before encountering the singularity region). The reason that the new ray is formally restarted is that many steps in the computations incorporate values previously computed along the wave ray, and thus all values computed within the singularity region are ignored.

4. The newly started ray will be given as input the same starting coordinates (X,Y) and input angle (AZ) that the ray had just after passing through the singularity region. This is because great confidence exists in the ability of the wave ray diagrams to accurately portray complex wave-crossing situations, as determined from comparisons with aerial photographs. Thus, continuity can be maintained in the ray diagrams, as the waves pass over the shelf.

5. Singularity regions are indicated as such in the (a) computations (i.e., printouts) by a statement in place of the computations within the singularity, and (b) in the wave ray diagrams by a dashed, instead of a solid line.

The shoreline computations of rays passing through such singularity regions should thus be a better representation of real wave conditions since the mathematically questionable regions are effectively bypassed. These wave heights will be slightly more conservative (from a design point of view) since the loss to bottom friction was not computed as the waves passed through the relatively narrow singularity region. However, based on the exhaustive analyses reported herein, this effect is considered quite small.

Summary of Significant Findings

1. Wave computations produced by the VIMS-BLM Baltimore Canyon Trough Wave Climate Model (BCTWCM) encompassing 97,650 depths on a 0.5 NM grid, indicate that the northwest portion of the Mid-Atlantic OCS lease block area contains relatively larger wave heights and areas

of intense bottom scour under large northeast and east waves, than other shelf areas.

2. Shoreline wave patterns are quite complex, and it would be difficult to discern changes in wave patterns along the shore caused by bathymetric changes in the lease block areas due to oil rig or pipeline activities.

3. The presence of singularities in standard linear wave theory, related to areas of crossed wave fronts, has been thoroughly described and their effects on these calculations has been evaluated and found to be negligible. A practical solution is suggested to reduce the impact of singularities on wave computations through a proposed test for singularities, in order to bypass them.

4. Preliminary qualitative comparisons indicate relationships between the computed areas of high bottom scour, and the distribution of shelf sediments and benthic invertebrates. More detailed wave computations (using a second order 0.25 NM depth grid) are needed to evaluate these qualitative relationships.

ACKNOWLEDGEMENTS

This report is the result of work by myself and my coworkers P. S. Rosen, R. A. Gammisch, C. H. Sutton, E. F. Hogge, and M. J. Carron.

The conscientious assistance of Anita W. Haywood in assembling the depth information is acknowledged. The art and photographic work resulted from the talented efforts of M. Williams, K. Stubblefield, and P. Peoples, and K. Thornberry and W. Jenkins, respectively. L. Zellmer, C. Diggs, and N. Blake assisted in assembling this report. The manuscript was critically reviewed by R. J. Byrne and J. Jacobson.

NASA-Langley Research Center allowed VIMS to use depth information accumulated by VIMS under contract to NASA, as well as the contour and histogram computer programs developed in a previous joint VIMS-NASA study. Their cooperation made possible the speedy development of this model.

These two computer programs were adapted to the IBM 370 computer by G. H. Shaw and F. K. Degges, of the VIMS Computer Department. We should also like to formally acknowledge the excellent cooperation furnished by the William and Mary Computer Center (notably P. Hoyle and V. Colbert) in preparing for, and during, our massive computations.

LITERATURE CITED

Abernathy, C.L., and Gilbert, G., 1975. Refraction of Wave Spectra. Hydraulics Research Station, Wallingford, Oxfordshire, England. Report No. INT 117.

Chao, Yung-Yao, 1970. The Theory of Wave Refraction in Shoaling Water, Including the Effects of Caustics and the Spherical Earth. Geophys. Sci. Lab. TR-70-17 (Contracts N62306-67-C-0124 and N62306-70-A-0075), Dep. Meteorol. and Oceanogr., New York Univ. (Available from DDC as AD 711 304).

Chao, Yung-Yao, 1971. An Asymptotic Evaluation of the Wave Field Near a Smooth Caustic. J. Geophys. Res., Vol. 76, No. 30, pp. 7401-7408.

Chao, Yung-Yao, 1972. Refraction of Ocean Surface Waves on the Continental Shelf. Fourth Annual Offshore Technology Conference-Preprints, Volume I, Paper No. OTC 1616, pp. I-965-I-976.

Chao, Yung-Yao, 1974. Wave Refraction Phenomena Over the Continental Shelf Near the Chesapeake Bay Entrance. U.S. Army CERC Tech. Memo. No. 47, 53 p.

Chao, Yung-Yao, and Pierson, W.J., Jr., 1970. An Experimental Study of Gravity Wave Behavior Near a Straight Caustic. Geophys. Sci. Lab. TR-70-71 (Contract N00014-67-A0467-001), Dep. Meteorol. and Oceanogr., New York Univ. (Available from DDC as AD 721 437).

Chao, Yung-Yao, and Pierson, W.J., 1972. Experimental Studies of the Refraction of Uniform Wave Trains and Transient Wave Groups near a Straight Caustic. J. Geophys. Research, Vol. 77, No. 24, pp. 4545-4554.

Chao, Yung-Yao, Jones, A.M., and Roney, J.R., 1975. Wave environment prediction in the Coastal Zone: Proc. Del., A.S.C.E.

Coleman, J.M., and Wright, L.D., 1971. Analysis of Major River Systems and Their Deltas: Procedures and Rationale, with Two Examples. Tech. Rep. No. 95 (Contract N00014-69-A-0211-0003), Coastal Studies Institute, Louisiana State University (Available from DDC as AD 723-575).

Colonell, J.M., Farrell, S. and Goldsmith, V., 1973. Wave refraction analysis: aid to interpretation of coastal hydraulics. A.S.C.E. Hydraulics Div. Conf.: Hydraulic Engineering and the Environment, Montana State University, Bozeman.

C.E.R.C., 1973. Shore Protection Manual: U.S. Army Corps of Engineers, U.S. Gov't. Printing Office, 3 vols.

Dobson, R.S., 1967. Some Applications of a digital computer to hydraulic engineering problems: Tech. Rep. No. 80 (Contract Nonr 225 (85)), Dept. Civil Eng., Stanford Univ.

Goldsmith, V., Morris, W.D., Byrne, R.J. and Whitlock, C.H., 1974. Wave Climate Model of the Mid-Atlantic Shelf and Shoreline (Virginian Sea): Model Development, Shelf Geomorphology, and Preliminary Results. VIMS SRAMSOE No. 48.

Goldsmith V., 1976. Continental shelf wave climate models: a critical link between shelf hydraulics and shoreline processes: AAPG An. Meeting, Dallas and SEPM Spec. Publ., Nearshore Processes - Physical Biological; VIMS Contrib. No. 708, in R.A. Davis, Jr. (ed.) SEPM Special Publication No. 23, Beach and Nearshore Sedimentation, p. 39-60.

Goldsmith, V., Morris, W.D., Sutton, C.H., and Poole, L.R., 1977. Wave Climate Model of the Middle Atlantic Shelf and Shoreline (Virginian Sea) II-Distribution of Wave Heights, Bottom Orbital Velocities and Wave Energy over the Shelf and Along the Shoreline. VIMS SRAMSOE No. 48, 28 p. plus 5 app.

Hamm, R.W., Kibler, J.F. and Morris, W.D., 1975. A program for contouring randomly spaced data. NASA Langley Research Center Tech. Memo, Hampton, Virginia, 27 p. and 10 figures.

Jen, Y., 1969. Wave Refraction Near San Pedro Bay, California, J. Waterways and Harbors Div., American Soc. Civil Eng., Vol. 95, No. WW3, p. 379-393.

Lepetit, J.P., 1964. Etude De la Refraction de la Houle Monocramatique par le Calcul Numerique. Bull. Centre Recher. and Essais de Chatou, No. 9, pp. 3-25.

May, J.P., 1974. A Computer Program to Determine the Distribution of Energy Dissipation in Shoaling Water Waves with Examples from Coastal Florida. In : Sediment Transport in the Near Shore Zone, Proceedings of a Symposium Published Jointly by Coastal Research Notes, and the Department of Geology, Florida State University, Tallahassee, Fla.

Mogel, T.R., and Street, R.L., 1974. Computation of Alongshore Energy and Littoral Transport. Proceedings of the Twelfth Coastal Engineering Conference, Volume 2, pages 899-918.

Mogel, T.R., and Street, R.L., 1975. Computer Evaluation of Littoral Transport. 14th Coastal Engineering Proc. A.S.C.E., N.Y., p. 715-725.

Munk, W.H. and Arthur, R.S., 1951. Wave Intensity along a Refracted Ray. Symposium on Gravity Waves, Circ. 521 National Bureau of Standards, Washington, D.C.

Orr, T.E., and Herbuch, J.B., 1969. Numerical Calculation of Wave Refraction by Digital Computer. C.O.E. Rep. No. 114 (Sea Grant Publ. No. 209), Texas A & M University.

Sallenger, A.H., Goldsmith, V., and Sutton, C.H., 1975. Bathymetric Comparisons: A manual of methodology, error criteria and techniques. VIMS SRAMSOE No. 66, 36 p. plus 12 figures.

Saville, T., Jr., 1954. North Atlantic Coast Wave Statistics Hindcast by Bretschneider-Revised Sverdrup-Munk Method. Tech Mem. No. 55, Beach Erosion Board, U.S. Army, Corps of Eng.

Skovgaard, O., Jonsson, I.G., and Bertelsen, J.A., 1975. Computation of Wave Heights Due to Refraction and Friction Journal of the Waterways, Harbors, and Coastal Engineering Division. Proceedings of the American Society of Engineers, Vol. 101, No. WW1.

Smith, B.S.L., and Camfield, F.L., 1972. A Refraction Study and Program for Periodic Waves Approaching a Shoreline, and Extending Beyond the Breaking Point. Tech. Rep. No. 16 (Contract No. N00014-69-A0407), Coll. Mar. Stud., Univ. of Delaware.

Thrall, D.E., 1973. Development of a Computer Program to Stimulate Wind Wave Generation, Refraction, and Shoaling in the Gulf of Maine. EDAL Rep. No. 113 (Rep. No. UNH-SG-106), Univ. of New Hampshire.

U.S. Army Engineer District, Wilmington, 1973. General Design memorandum-Phase I-Hurricane-Wave Protection-Beach Erosion Control, Brunswick County, N.C., Beach Projects Yanpon Beach and Long Beach Segments: Wilmington, N.C., 125 p. and 9 app.

Whalin, R.W., 1971. The Limit of Applicability of Linear Wave Refraction Theory in a Convergence Zone. U.S. Army Engineer Waterways Experiment Station, Vicksburg, Mississippi. Research Report H-71-3. 66 p. plus Appendix.

APPENDIX

List of Figures

Appendix	(Figure No.)	Wave Conditions Direction (from)	T (sec)	Tide (ft)	Diagram Type	Wave Parameter
A	1	NE (45°)	8	0	Wave Ray Diagrams	
	2	NE	10	0		
	3	NE	12	0		
	4	E (90°)	8	0		
	5	E	10	0		
	6	E	12	0		
	7	SE (135°)	8	0		
	8	SE	10	0		
	9	SE	12	0		
	10	NE	10	+5		
	11	E	10	+5		
	12	SE	10	+5		
B	1	NE	8	0	Wave Ray Density	
	2	NE	10	0		
	3	NE	12	0		
	4	E	8	0		
	5	E	10	0		
	6	E	12	0		
	7	SE	8	0		
	8	SE	10	0		
	9	SE	12	0		
	10	NE	10	+5		
	11	E	10	+5		
	12	SE	10	+5		
C	1	NE	8	0	Shelf Contour (Computer)	Wave Heights (Contour Interval= 1,2,3 meters)
	2	NE	10	0		
	3	NE	12	0		
	4	E	8	0		
	5	E	10	0		
	6	E	12	0		
	7	SE	8	0		
	8	SE	10	0		
	9	SE	12	0		
	10	NE	10	+5		
	11	E	10	+5		
	12	SE	10	+5		

List of Figures (continued)

Appendix	(Figure No.)	Wave Conditions Direction (from)	T (sec)	Tide (ft)	Diagram Type	Wave Parameter
D	1	NE	8	0	Maximum Bottom Horizontal	
	2	NE	10	0	Wave Orbital Velocity	
	3	NE	12	0	(Computer)	
	4	E	8	0		
	5	E	10	0		
	6	E	12	0		(Contour Interval=
	7	SE	8	0		15,27,60 cm/sec)
	8	SE	10	0		
	9	SE	12	0		
	10	NE	10	+5		
	11	E	10	+5		
	12	SE	10	+5		
E	1	NE	8	0	Shelf Contour	Wave Heights
	2	NE	10	0	(Hand)	(Contour Interval=
	3	NE	12	0		1,2,3,4 meters)
	4	E	8	0		
	5	E	10	0		
	6	E	12	0		
	7	SE	8	0		
	8	SE	10	0		
	9	SE	12	0		
	10	NE	10	+5		
	11	E	10	+5		
	12	SE	10	+5		
F	1	NE	8	0	Maximum Bottom Horizontal	
	2	NE	10	0	Wave Orbital Velocity	
	3	NE	12	0	(Hand)	
	4	E	8	0		
	5	E	10	0		
	6	E	12	0		
	7	SE	8	0		(Contour Interval=
	8	SE	10	0		15,27,60 cm/sec)
	9	SE	12	0		
	10	NE	10	+5		
	11	E	10	+5		
	12	SE	10	+5		

List of Figures (concluded)

Appendix	(Figure No.)	Wave Conditions Direction (from)	T (sec)	Tide (ft)	Diagram Type	Wave Parameter
G	1 a	NE	8	0	Shoreline Histograms	Orthogonal Density (Wave Orthogonals per nautical mile)
	2 a	NE	10	0		
	3 a	NE	12	0		
	4 a & b	E	8	0		
	5 a & b	E	10	0		
	6 a & b	E	12	0		
	7 a & b	SE	8	0		
	8 a & b	SE	10	0		
	9 a & b	SE	12	0		
	10 a	NE	10	+5		
	11 a & b	E	10	+5		
	12 a & b	SE	10	+5		
H	1 a	NE	8	0	Shoreline Histograms; a & b correspond to New Jersey & Long Island	Wave Height (meters)
	2 a	NE	10	0		
	3 a	NE	12	0		
	4 a & b	E	8	0		
	5 a & b	E	10	0		
	6 a & b	E	12	0		
	7 a & b	SE	8	0		
	8 a & b	SE	10	0		
	9 a & b	SE	12	0		
	10 a	NE	10	+5		
	11 a & b	E	10	+5		
	12 a & b	SE	10	+5		
I	1 a	NE	8	0	Shoreline Histograms	Wave Energy (joules)
	2 a	NE	10	0		
	3 a	NE	12	0		
	4 a & b	E	8	0		
	5 a & b	E	10	0		
	6 a & b	E	12	0		
	7 a & b	SE	8	0		
	8 a & b	SE	10	0		
	9 a & b	SE	12	0		
	10 a & b	NE	10	+5		
	11 a & b	E	10	+5		
	12 a & b	SE	10	+5		

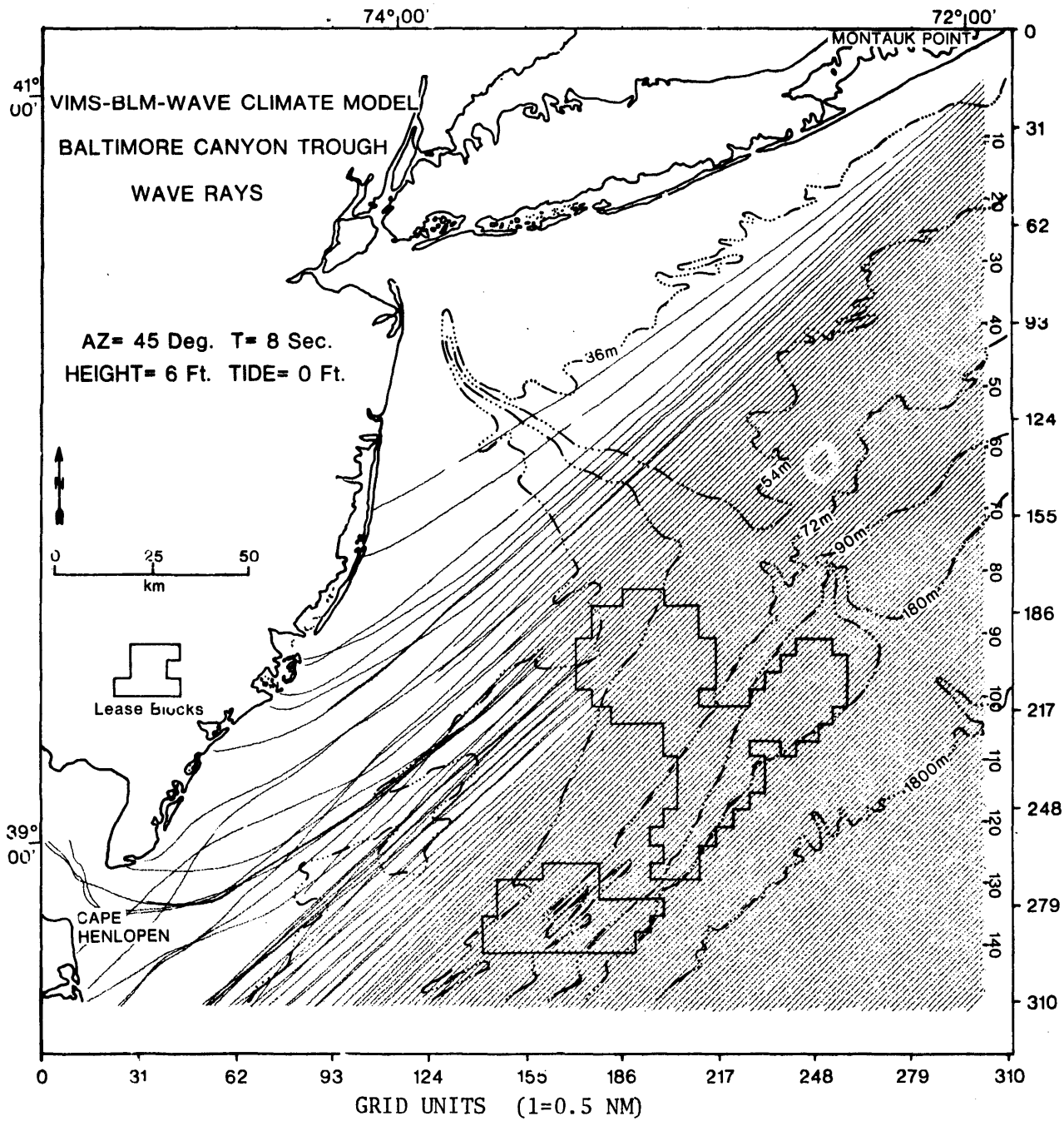
74°00'
72°00'
MONTAUK POINT
41° 00'
VIMS-BLM-WAVE CLIMATE MODEL
BALTIMORE CANYON TROUGH
WAVE RAYS
AZ= 45 Deg. T= 8 Sec.
HEIGHT= 6 Ft. TIDE= 0 Ft.
36m
54m
72m
90m
180m
1800m
0 25 50
km
Lease Blocks
39° 00'
CAPE HENLOPEN
0 31 62 93 124 155 186 217 248 279 310
GRID UNITS (1=0.5 NM)
0 31 62 93 124 155 186 217 248 279 310
10 20 30 40 50 60 70 80 90 100 110 120 130 140

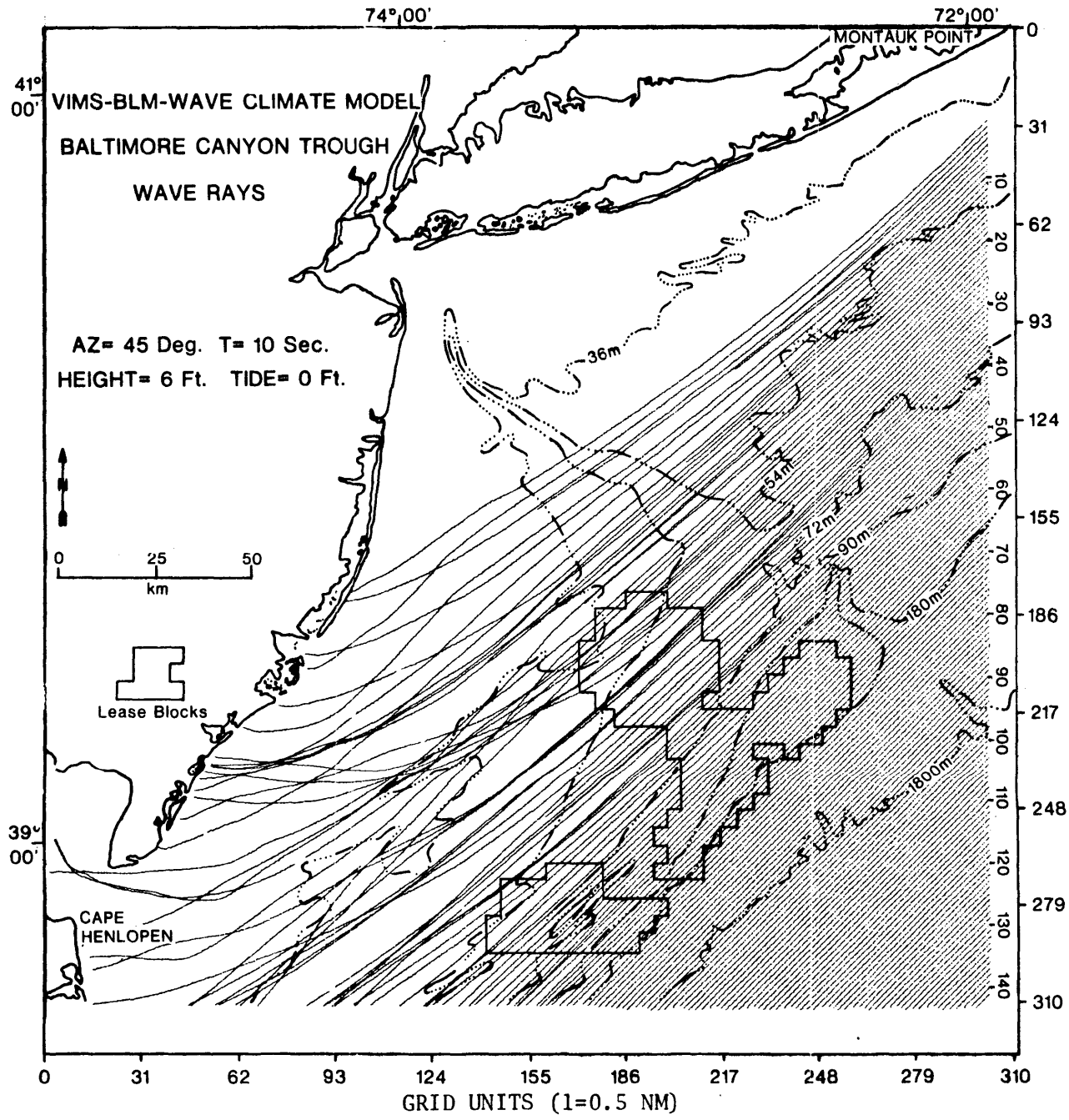
74°00'
72°00'
MONTAUK POINT
41° 00'
VIMS-BLM-WAVE CLIMATE MODEL
BALTIMORE CANYON TROUGH
WAVE RAYS
AZ= 45 Deg. T= 10 Sec.
HEIGHT= 6 Ft. TIDE= 0 Ft.
0 25 50
km
Lease Blocks
36m
54m
72m
90m
180m
1800m
39° 00'
CAPE HENLOPEN
0 31 62 93 124 155 186 217 248 279 310
GRID UNITS (1=0.5 NM)
10 20 30 40 50 60 70 80 90 100 110 120 130 140
0 31 62 93 124 155 186 217 248 279 310

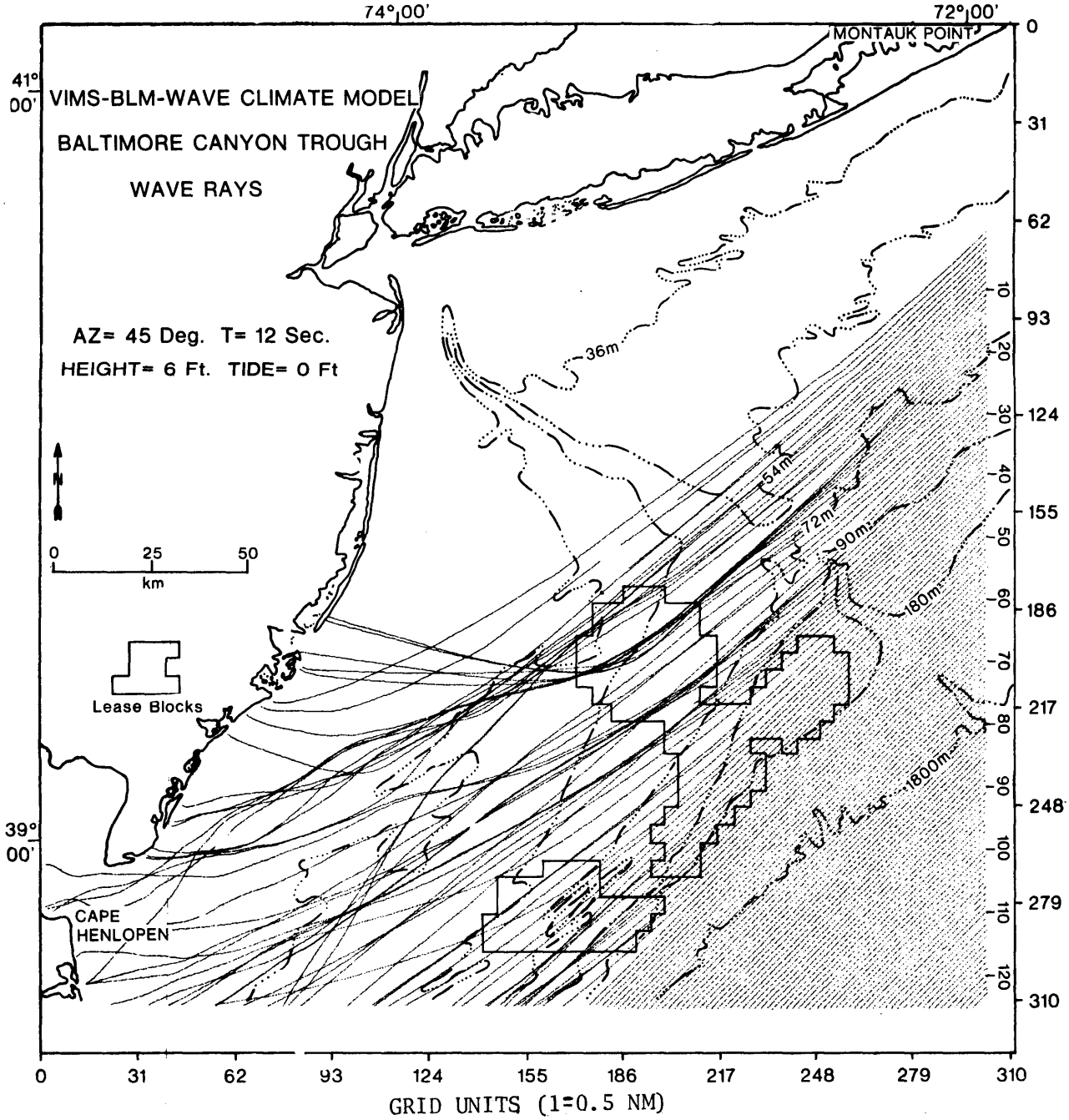
74°00'
72°00'
MONTAUK POINT
41° 00'
VIMS-BLM-WAVE CLIMATE MODEL
BALTIMORE CANYON TROUGH
WAVE RAYS
AZ= 45 Deg. T= 12 Sec.
HEIGHT= 6 Ft. TIDE= 0 Ft
N
0 25 50
km
Lease Blocks
36m
54m
72m
90m
180m
1800m
39° 00'
CAPE HENLOPEN
0 31 62 93 124 155 186 217 248 279 310
GRID UNITS (1=0.5 NM)
0 31 62 93 124 155 186 217 248 279 310
10 20 30 40 50 60 70 80 90 100 110 120

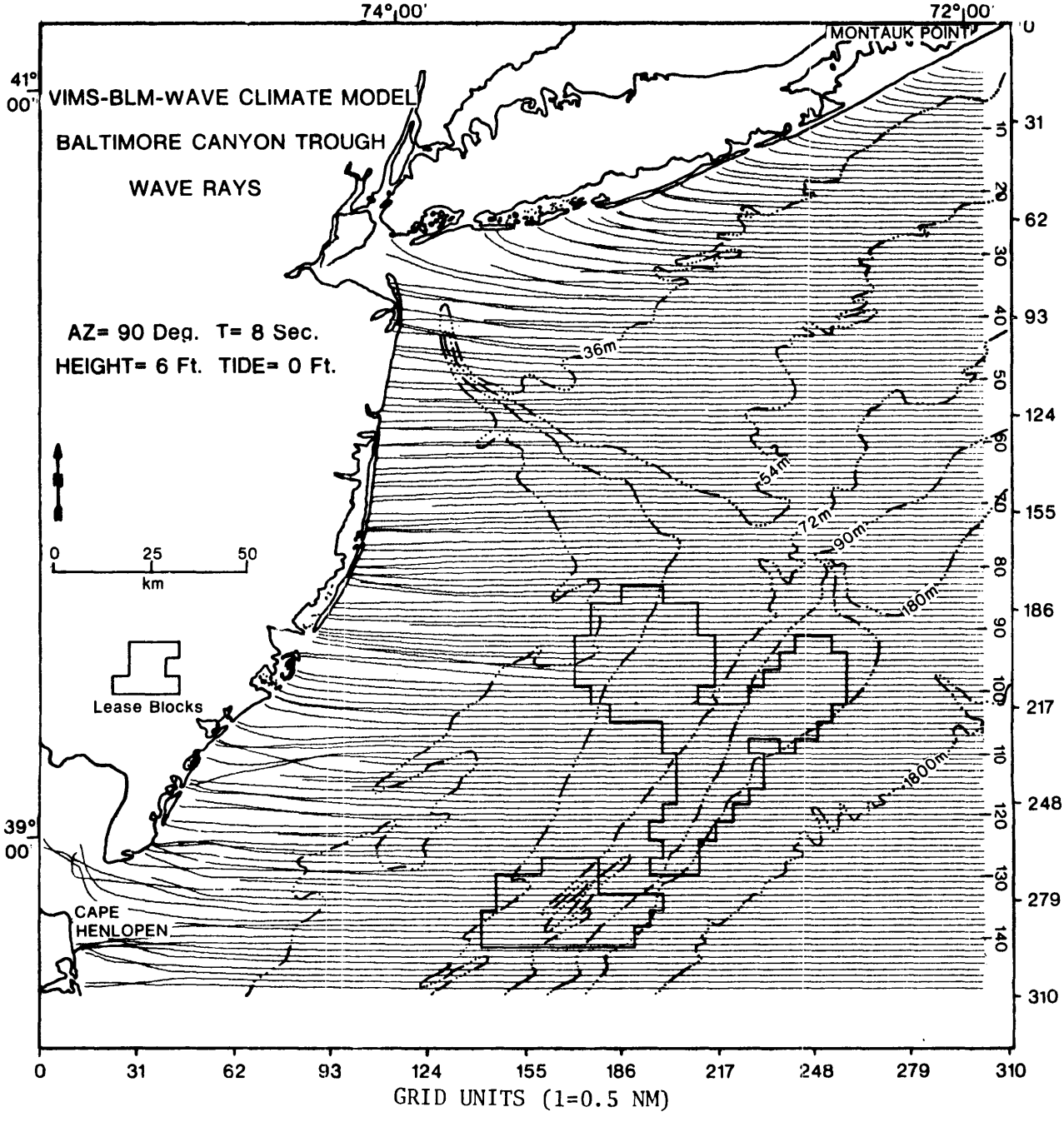
74°00'
72°00'
MONTAUK POINT
41° 00'
VIMS-BLM-WAVE CLIMATE MODEL
BALTIMORE CANYON TROUGH
WAVE RAYS
AZ= 90 Deg. T= 8 Sec.
HEIGHT= 6 Ft. TIDE= 0 Ft.
0 25 50
km
Lease Blocks
36m
54m
72m
90m
180m
1800m
39° 00'
CAPE HENLOPEN
0 31 62 93 124 155 186 217 248 279 310
GRID UNITS (1=0.5 NM)
0 31 62 93 124 155 186 217 248 279 310
10 20 30 40 50 60 70 80 90 100 110 120 130 140

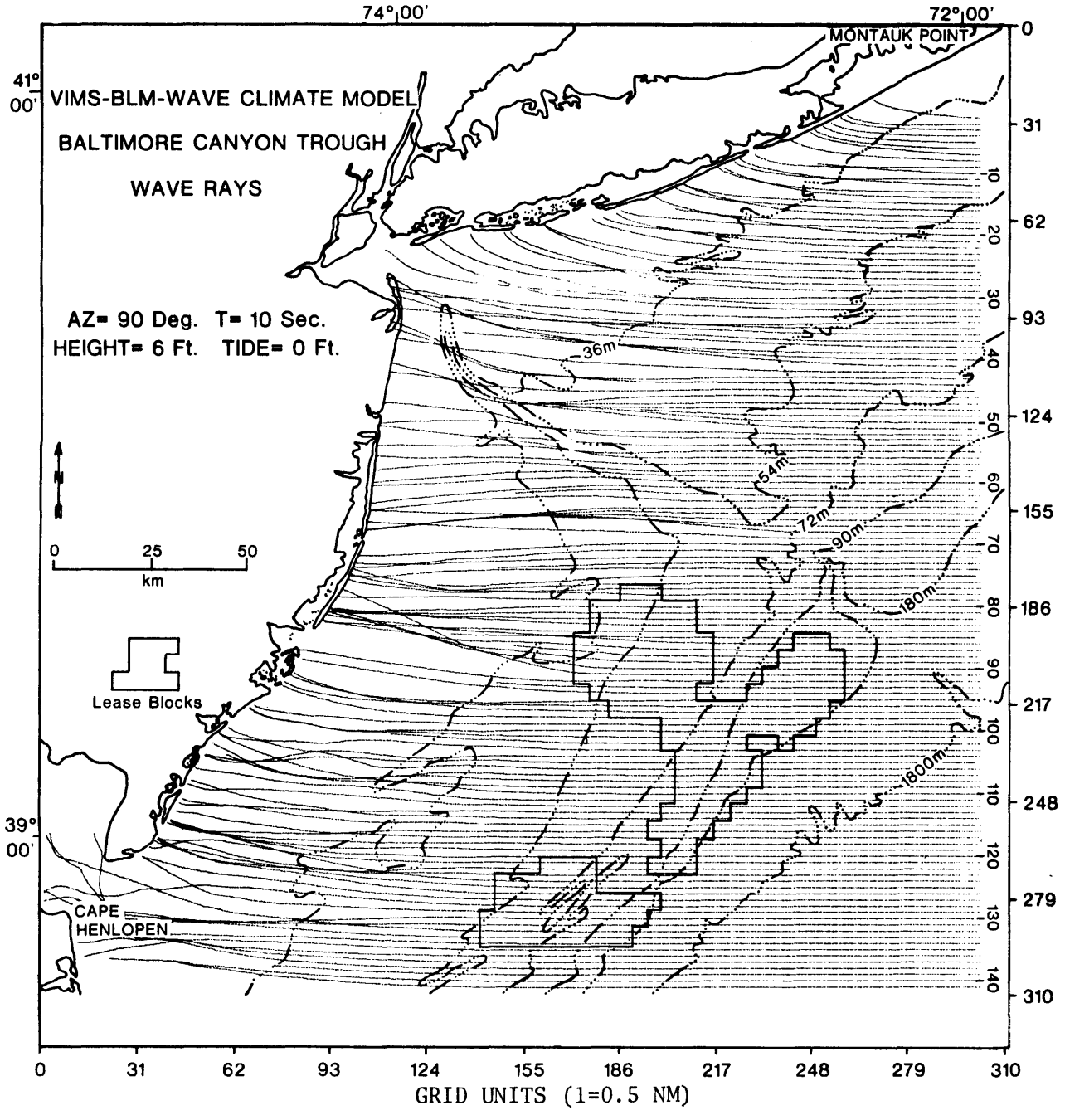
74°00'
72°00'
MONTAUK POINT
41° 00'
VIMS-BLM-WAVE CLIMATE MODEL
BALTIMORE CANYON TROUGH
WAVE RAYS
AZ= 90 Deg. T= 10 Sec.
HEIGHT= 6 Ft. TIDE= 0 Ft.
36m
54m
72m
90m
180m
1800m
N
0 25 50
km
Lease Blocks
39° 00'
CAPE HENLOPEN
0 31 62 93 124 155 186 217 248 279 310
GRID UNITS (1=0.5 NM)
0 31 62 93 124 155 186 217 248 279 310
10 20 30 40 50 60 70 80 90 100 110 120 130 140

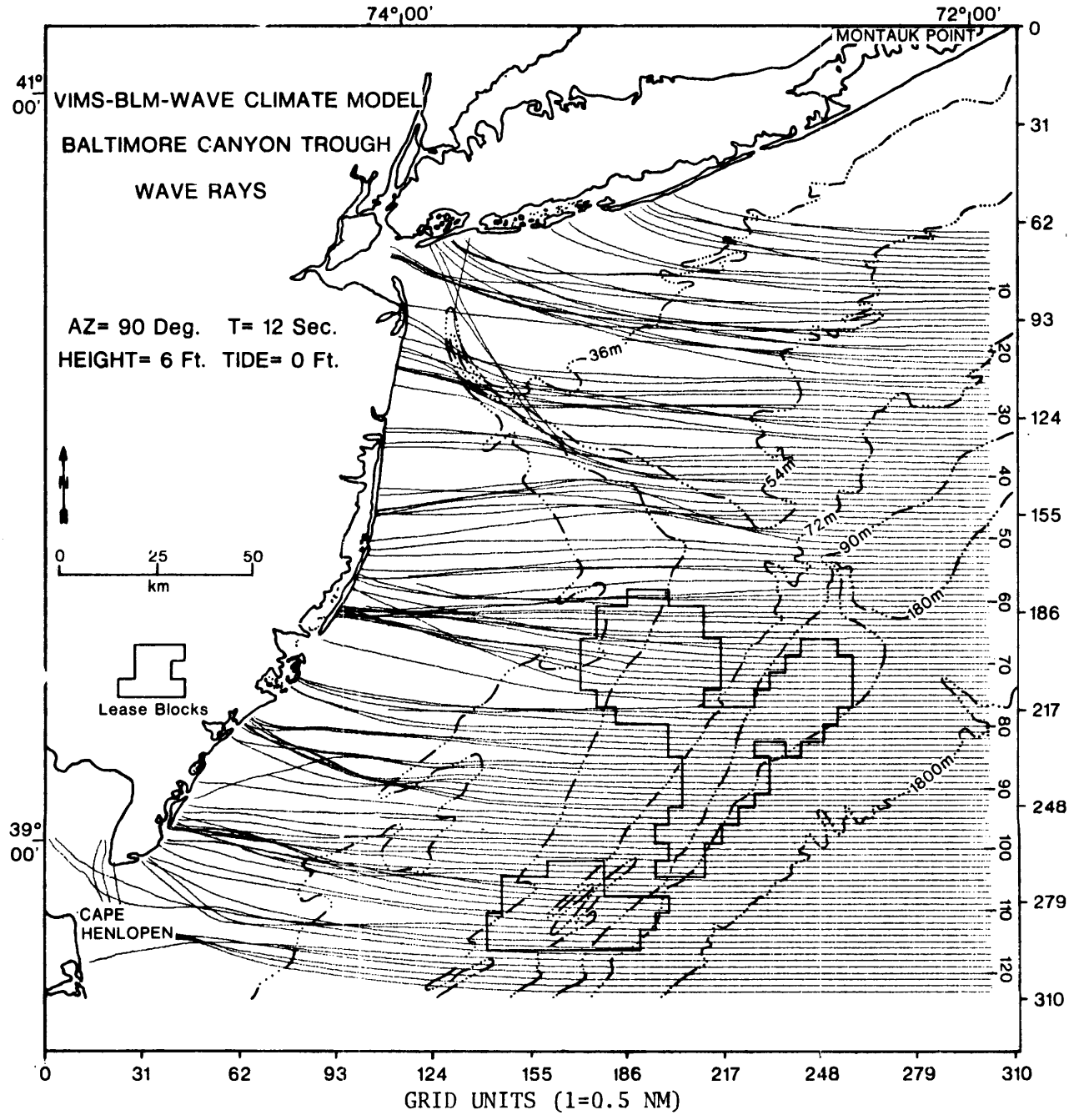
74°00'
72°00'
MONTAUK POINT
41° 00'
VIMS-BLM-WAVE CLIMATE MODEL
BALTIMORE CANYON TROUGH
WAVE RAYS
AZ= 90 Deg. T= 12 Sec.
HEIGHT= 6 Ft. TIDE= 0 Ft.
N
0 25 50
km
Lease Blocks
36m
54m
72m
90m
180m
1800m
39° 00'
CAPE HENLOPEN
0 31 62 93 124 155 186 217 248 279 310
GRID UNITS (1=0.5 NM)
0 31 62 93 124 155 186 217 248 279 310
10 20 30 40 50 60 70 80 90 100 110 120

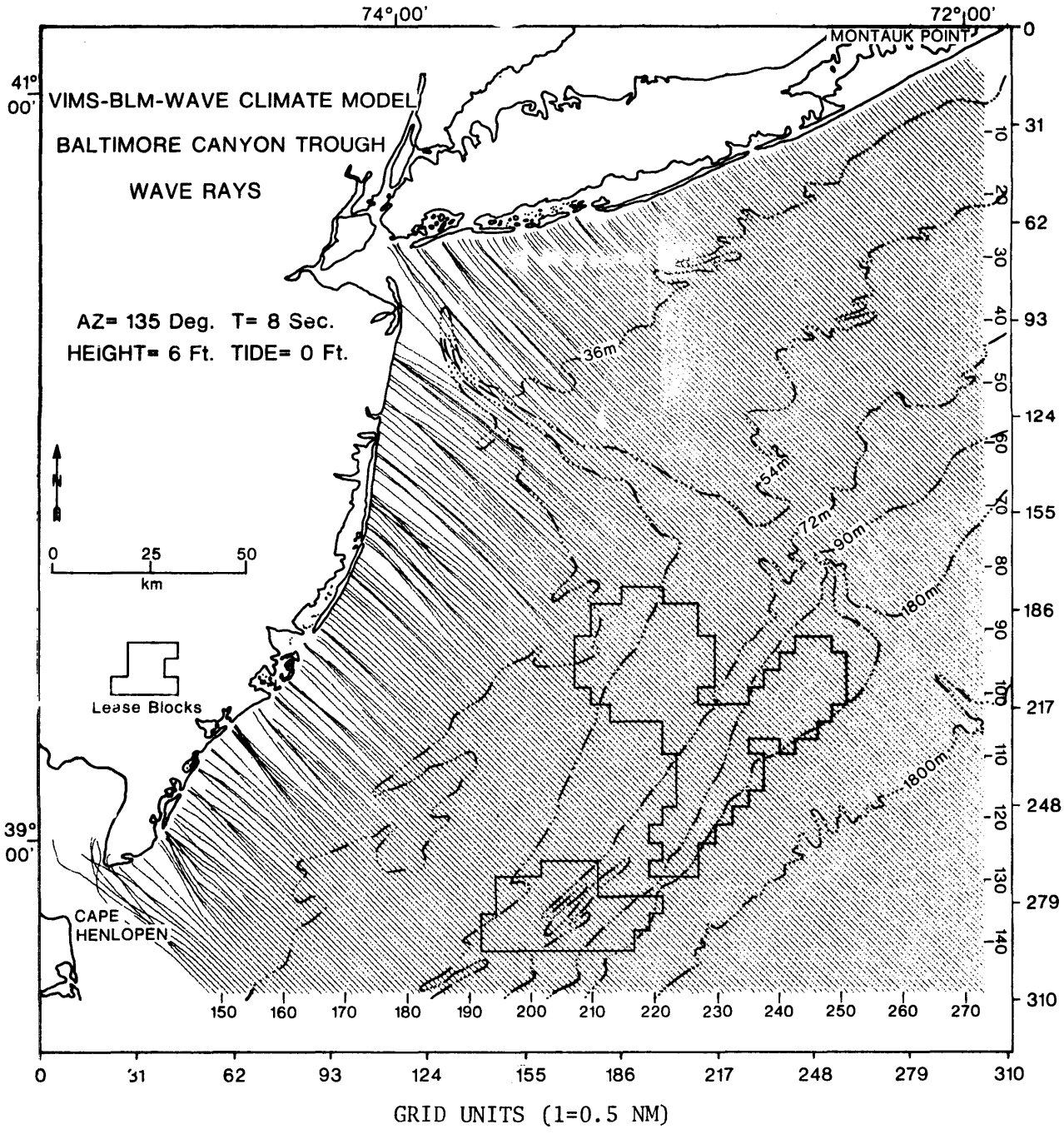
74°00'
72°00'
MONTAUK POINT
41° 00'
VIMS-BLM-WAVE CLIMATE MODEL
BALTIMORE CANYON TROUGH
WAVE RAYS
AZ= 135 Deg. T= 8 Sec.
HEIGHT= 6 Ft. TIDE= 0 Ft.
36m
54m
72m
90m
180m
1800m
0 25 50
km
Lease Blocks
39° 00'
CAPE HENLOPEN
150 160 170 180 190 200 210 220 230 240 250 260 270
0 31 62 93 124 155 186 217 248 279 310
0 10 20 30 40 50 60 70 80 90 100 110 120 130 140
0 31 62 93 124 155 186 217 248 279 310
GRID UNITS (1=0.5 NM)

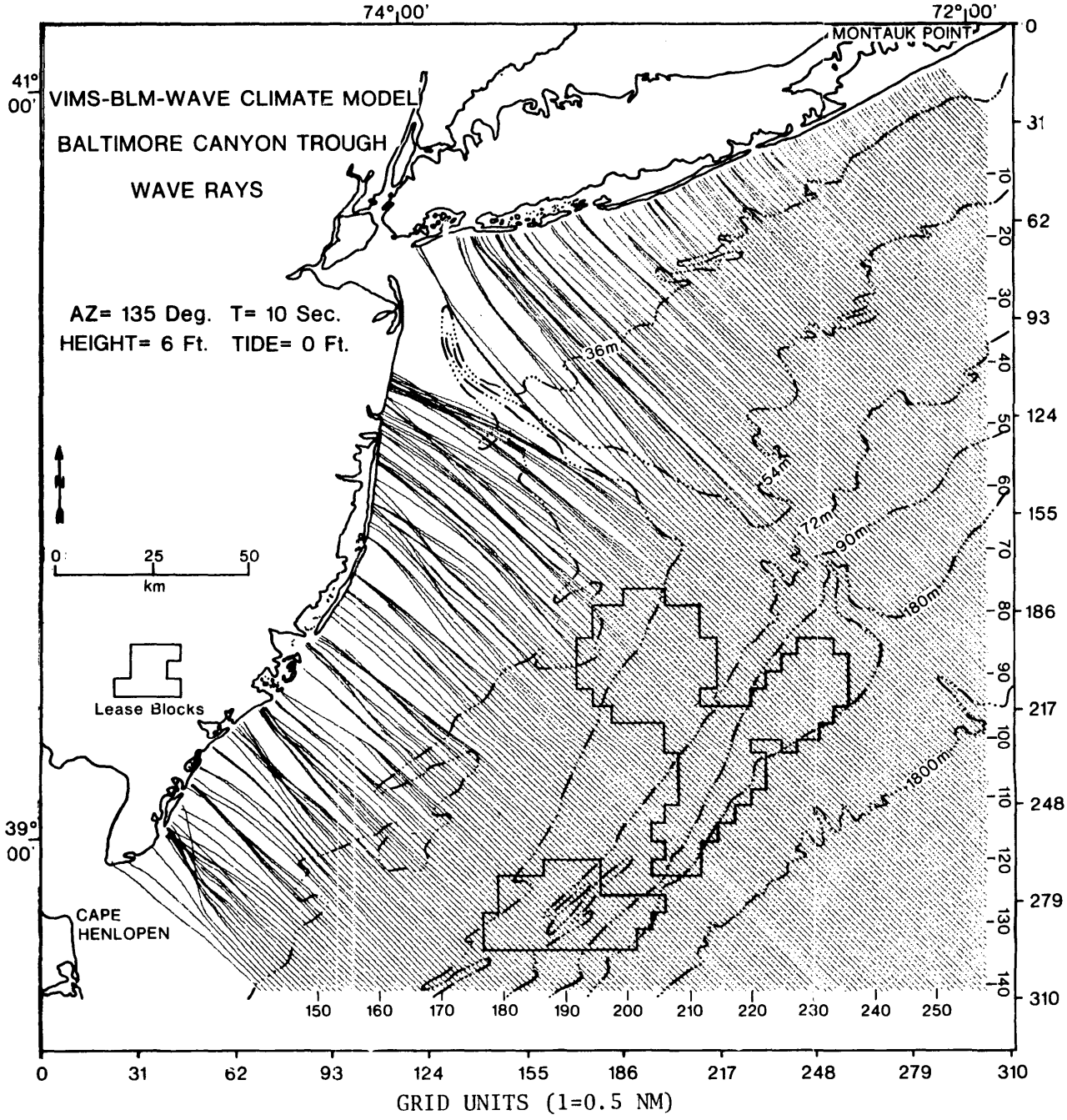
74°00'
72°00'
MONTAUK POINT
41° 00'
VIMS-BLM-WAVE CLIMATE MODEL
BALTIMORE CANYON TROUGH
WAVE RAYS
AZ= 135 Deg. T= 10 Sec.
HEIGHT= 6 Ft. TIDE= 0 Ft.
36m
54m
72m
90m
180m
1800m
0 25 50
km
Lease Blocks
39° 00'
CAPE HENLOPEN
0 31 62 93 124 155 186 217 248 279 310
GRID UNITS (1=0.5 NM)
0 31 62 93 124 155 186 217 248 279 310
10 20 30 40 50 60 70 80 90 100 110 120 130 140
150 160 170 180 190 200 210 220 230 240 250

A8

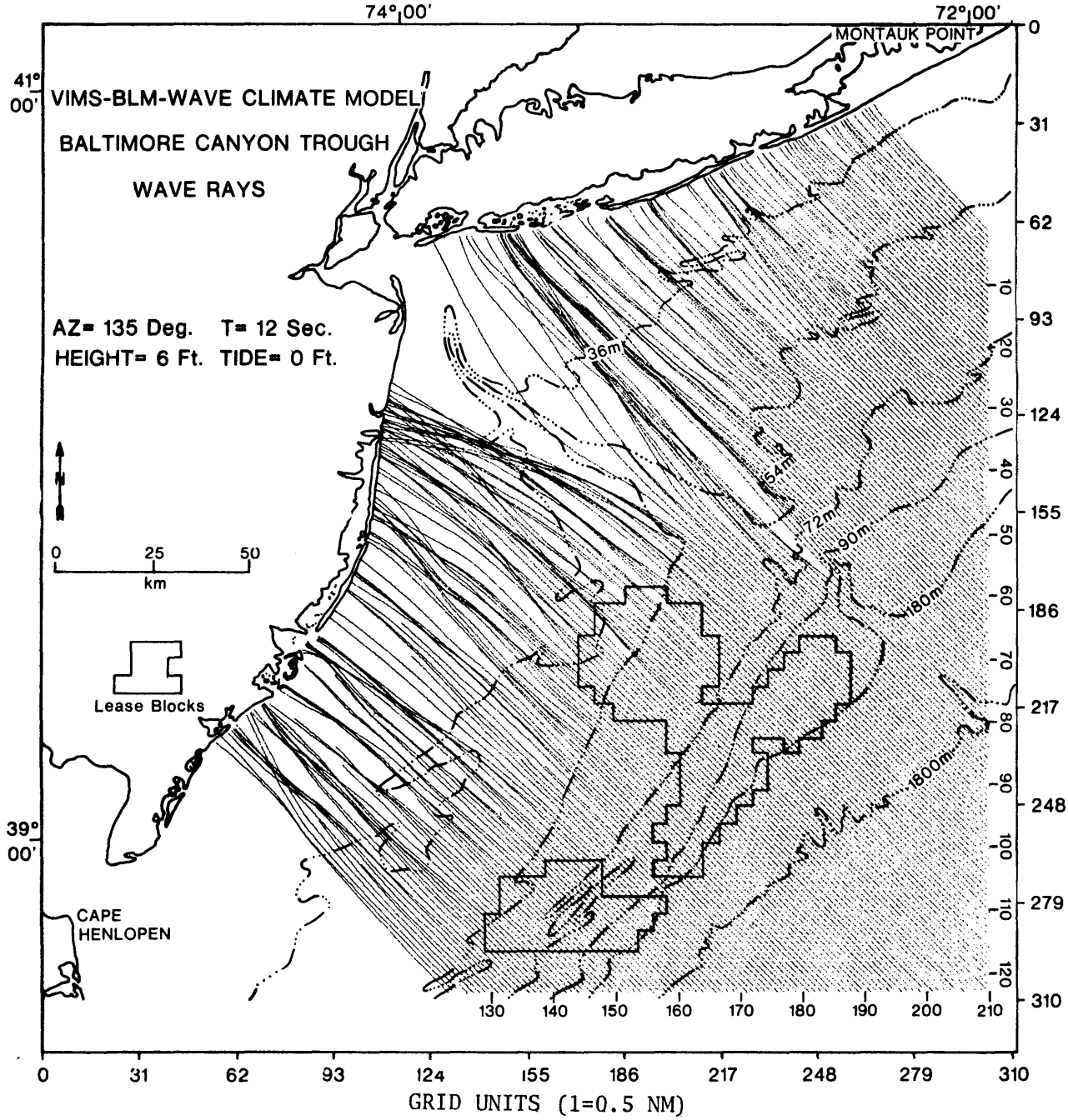
74°00'
72°00'
MONTAUK POINT
41° 00'
VIMS-BLM-WAVE CLIMATE MODEL
BALTIMORE CANYON TROUGH
WAVE RAYS
AZ= 135 Deg. T= 12 Sec.
HEIGHT= 6 Ft. TIDE= 0 Ft.
36m
54m
72m
90m
180m
1800m
0 25 50
km
Lease Blocks
39° 00'
CAPE HENLOPEN
0 31 62 93 124 155 186 217 248 279 310
130 140 150 160 170 180 190 200 210
GRID UNITS (1=0.5 NM)

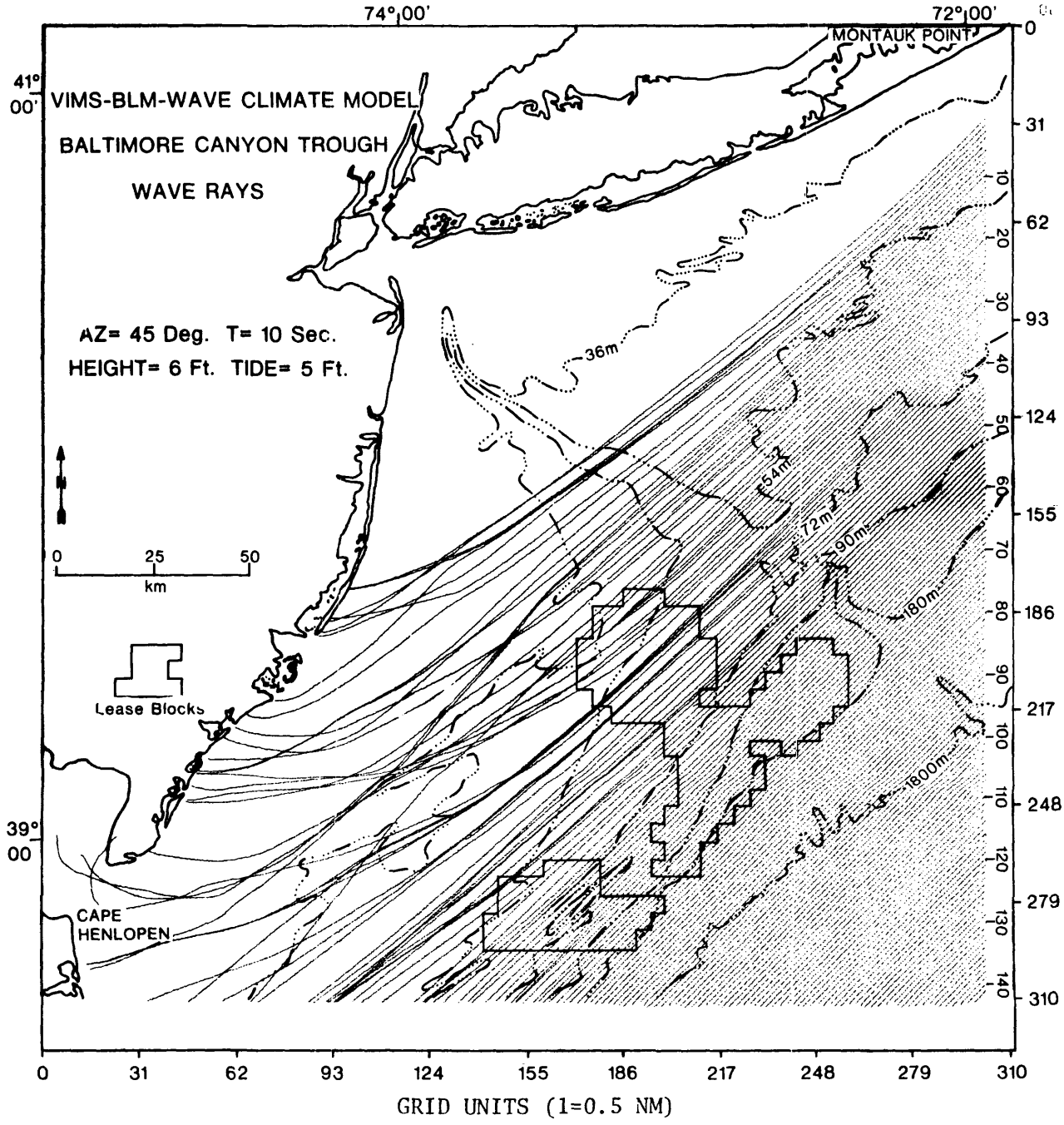
74°00'
72°00'
MONTAUK POINT
41° 00'
VIMS-BLM-WAVE CLIMATE MODEL
BALTIMORE CANYON TROUGH
WAVE RAYS
AZ= 45 Deg. T= 10 Sec.
HEIGHT= 6 Ft. TIDE= 5 Ft.
36m
54m
72m
90m
180m
1800m
0 25 50
km
Lease Blocks
39° 00'
CAPE HENLOPEN
0 31 62 93 124 155 186 217 248 279 310
GRID UNITS (1=0.5 NM)
0 31 62 93 124 155 186 217 248 279 310
10 20 30 40 50 60 70 80 90 100 110 120 130 140

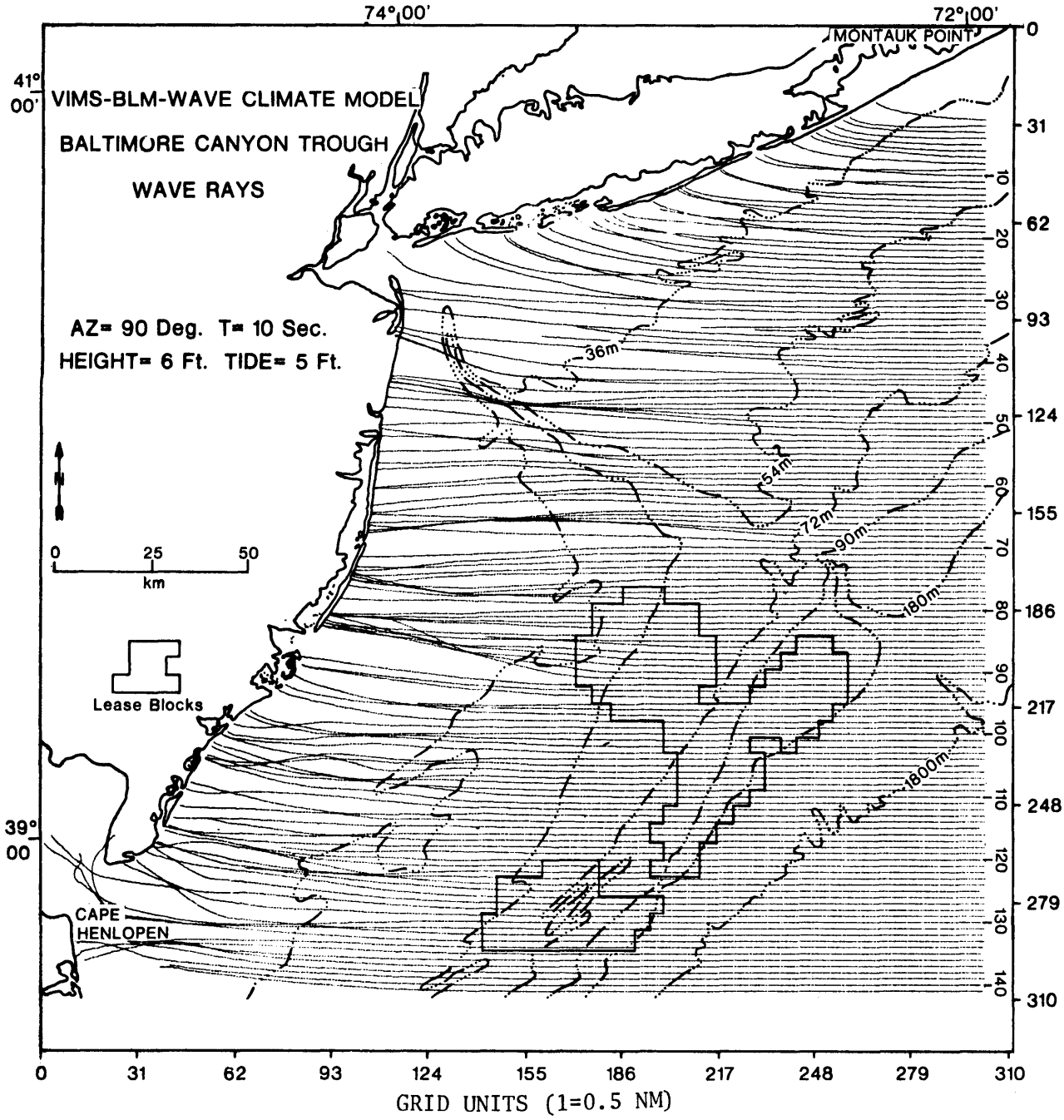
74°00'
72°00'
MONTAUK POINT
41° 00'
VIMS-BLM-WAVE CLIMATE MODEL
BALTIMORE CANYON TROUGH
WAVE RAYS
AZ= 90 Deg. T= 10 Sec.
HEIGHT= 6 Ft. TIDE= 5 Ft.
36m
54m
72m
90m
180m
1800m
0 25 50
km
Lease Blocks
39° 00
CAPE HENLOPEN
0 31 62 93 124 155 186 217 248 279 310
GRID UNITS (1=0.5 NM)
0 31 62 93 124 155 186 217 248 279 310
10 20 30 40 50 60 70 80 90 100 110 120 130 140

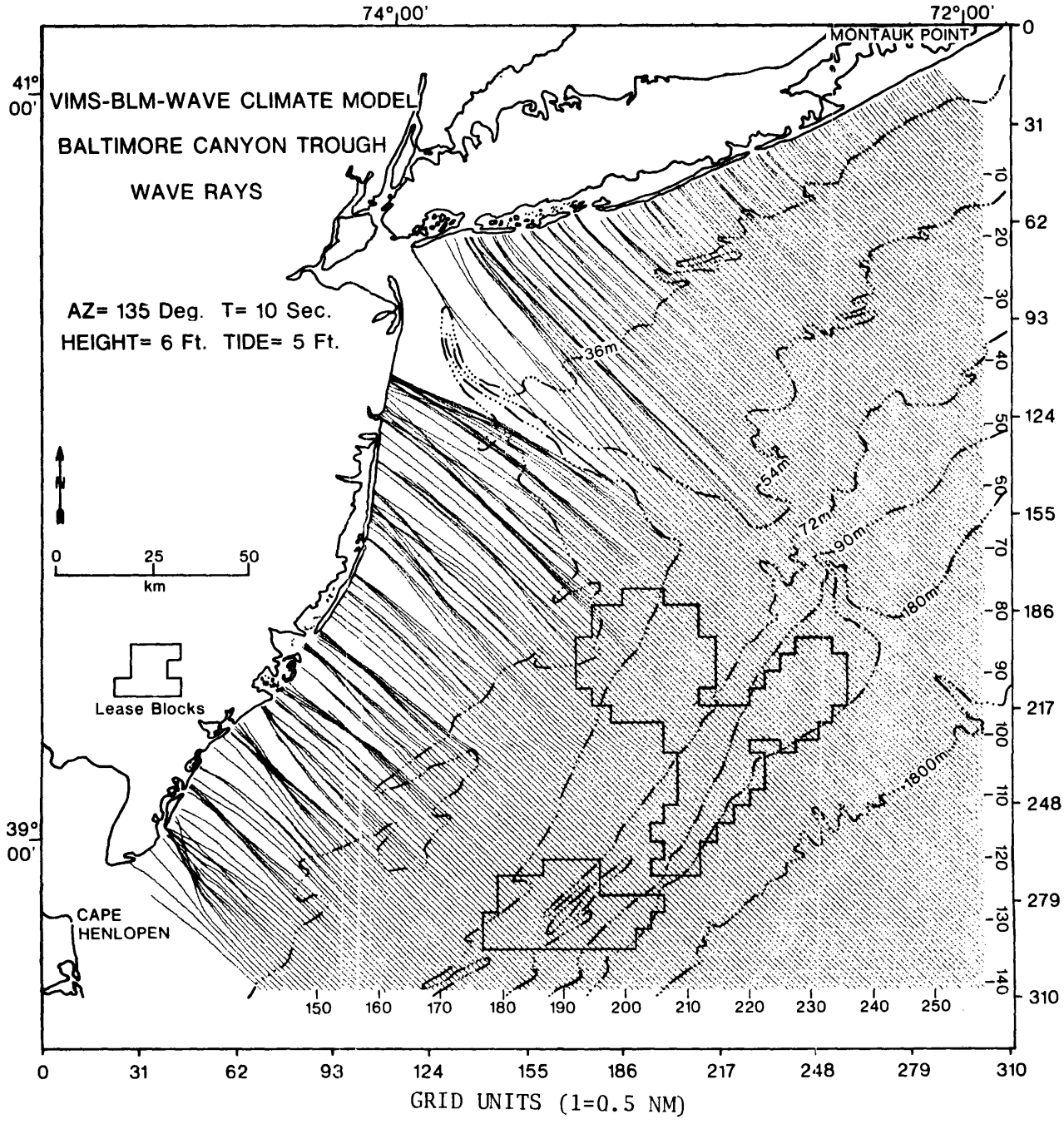
74°00'
72°00'
MONTAUK POINT
41° 00'
VIMS-BLM-WAVE CLIMATE MODEL
BALTIMORE CANYON TROUGH
WAVE RAYS
AZ= 135 Deg. T= 10 Sec.
HEIGHT= 6 Ft. TIDE= 5 Ft.
36m
54m
72m
90m
180m
1800m
0 25 50
km
Lease Blocks
39° 00'
CAPE HENLOPEN
0 31 62 93 124 155 186 217 248 279 310
150 160 170 180 190 200 210 220 230 240 250
10 20 30 40 50 60 70 80 90 100 110 120 130 140
GRID UNITS (1=0.5 NM)

VIMS-BLM BALTIMORE CANYON TROUGH
LEASE BLOCK AREA ORTHOGONAL DENSITY

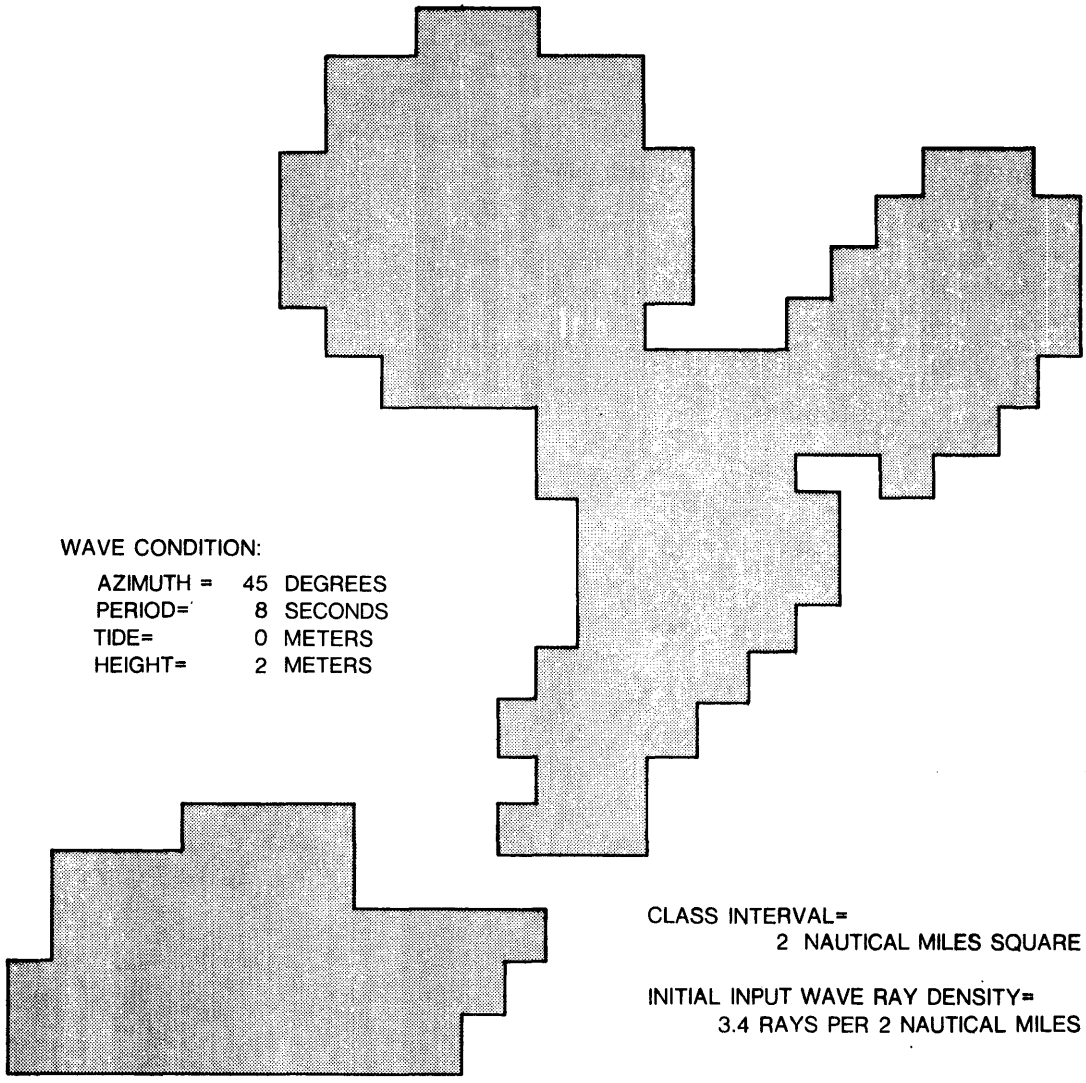

WAVE CONDITION:

AZIMUTH =	45	DEGREES
PERIOD=	8	SECONDS
TIDE=	0	METERS
HEIGHT=	2	METERS

CLASS INTERVAL=
2 NAUTICAL MILES SQUARE

INITIAL INPUT WAVE RAY DENSITY=
3.4 RAYS PER 2 NAUTICAL MILES

LEGEND

	RAY DENSITY (rays per 2 n.m. square)	$(Kr=(\frac{bo}{b})^{1/2})$
HIGH DIVERGENCE	< 1	< .559
DIVERGENCE	1-2	.559-.791
NO CHANGE	3-4	.968-1.118
CONVERGENCE	5-6	1.249-1.370
HIGH CONVERGENCE	7-8	1.478-1.581

VIMS-BLM BALTIMORE CANYON TROUGH
LEASE BLOCK AREA ORTHOGONAL DENSITY

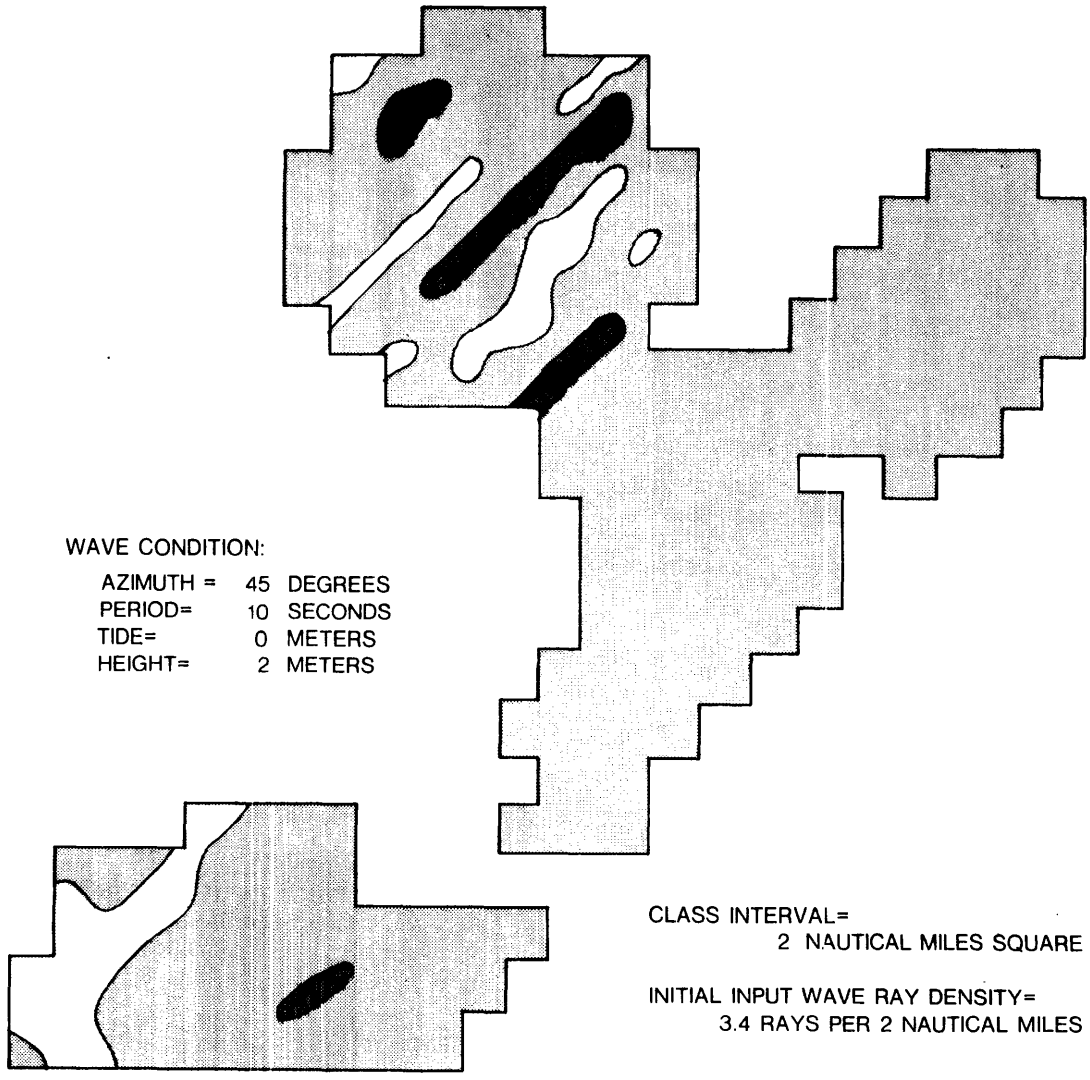

WAVE CONDITION:

AZIMUTH =	45	DEGREES
PERIOD=	10	SECONDS
TIDE=	0	METERS
HEIGHT=	2	METERS

CLASS INTERVAL=
2 NAUTICAL MILES SQUARE

INITIAL INPUT WAVE RAY DENSITY=
3.4 RAYS PER 2 NAUTICAL MILES

LEGEND

	RAY DENSITY (rays per 2 n.m. square)	($Kr=(\frac{bo}{b})^{1/2}$)
HIGH DIVERGENCE	< 1	< .559
DIVERGENCE	1-2	.559-.791
NO CHANGE	3-4	.968-1.118
CONVERGENCE	5-6	1.249-1.370
HIGH CONVERGENCE	7-8	1.478-1.581

VIMS-BLM BALTIMORE CANYON TROUGH
LEASE BLOCK AREA ORTHOGONAL DENSITY

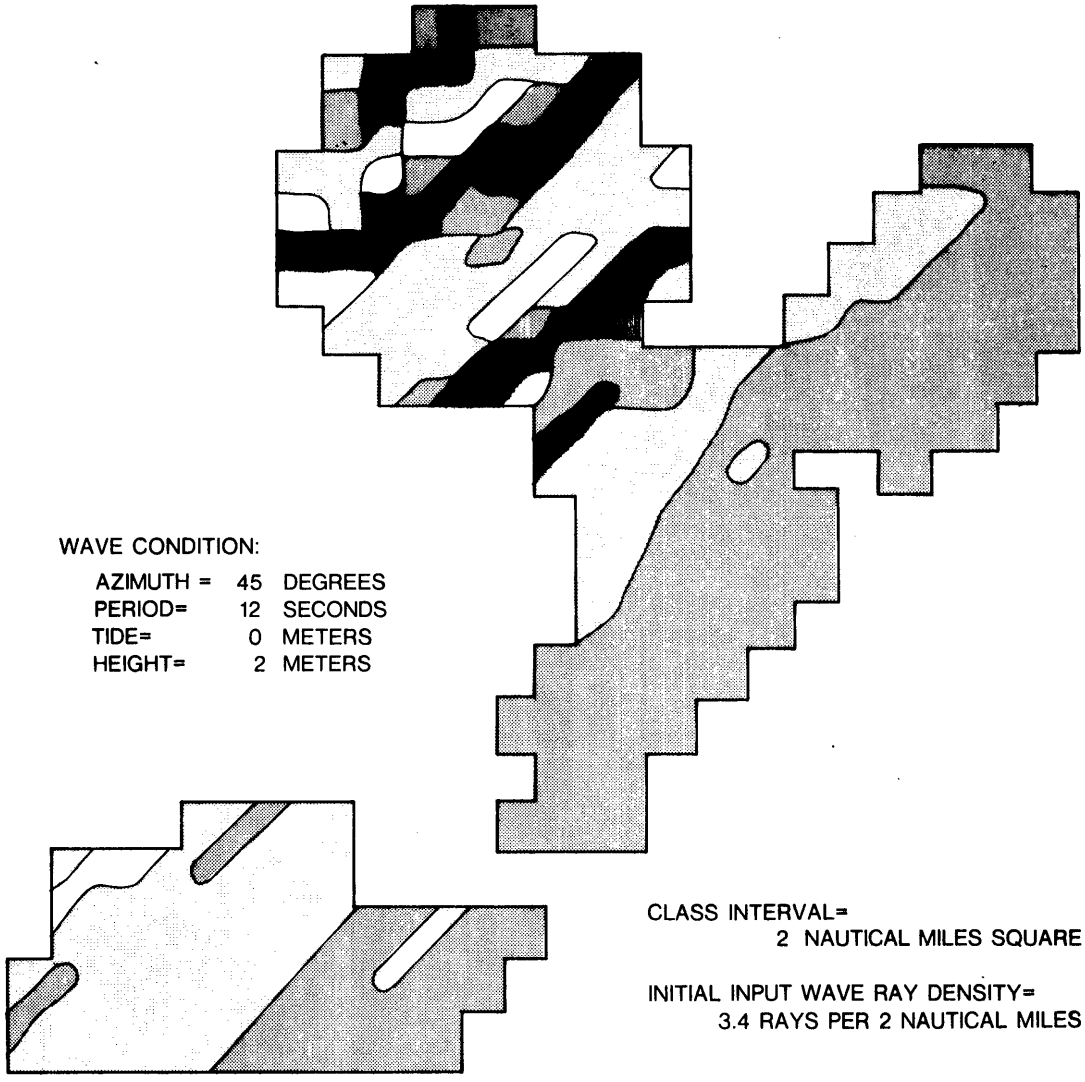

WAVE CONDITION:

AZIMUTH =	45	DEGREES
PERIOD=	12	SECONDS
TIDE=	0	METERS
HEIGHT=	2	METERS

CLASS INTERVAL=
2 NAUTICAL MILES SQUARE

INITIAL INPUT WAVE RAY DENSITY=
3.4 RAYS PER 2 NAUTICAL MILES

LEGEND

	RAY DENSITY (rays per 2 n.m. square)	($Kr=(\frac{bo}{b})^{1/2}$)
HIGH DIVERGENCE	< 1	< .559
DIVERGENCE	1-2	.559-.791
NO CHANGE	3-4	.968-1.118
CONVERGENCE	5-6	1.249-1.370
HIGH CONVERGENCE	7-8	1.478-1.581

VIMS-BLM BALTIMORE CANYON TROUGH
LEASE BLOCK AREA ORTHOGONAL DENSITY

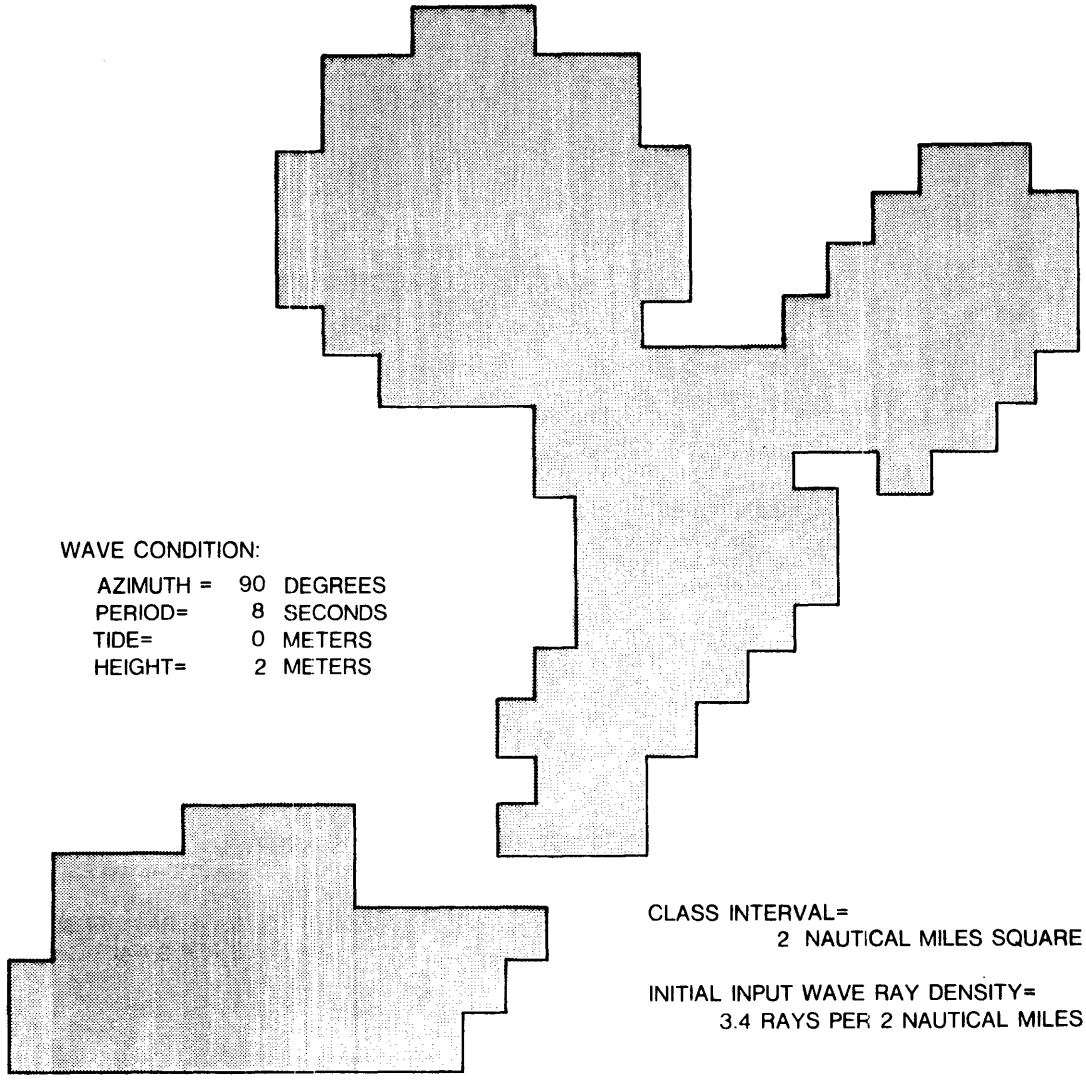

WAVE CONDITION:

AZIMUTH =	90	DEGREES
PERIOD=	8	SECONDS
TIDE=	0	METERS
HEIGHT=	2	METERS

CLASS INTERVAL=
2 NAUTICAL MILES SQUARE

INITIAL INPUT WAVE RAY DENSITY=
3.4 RAYS PER 2 NAUTICAL MILES

LEGEND

	RAY DENSITY (rays per 2 n.m. square)	($Kr=(\frac{bo}{b})^{1/2}$)
HIGH DIVERGENCE	< 1	< .559
DIVERGENCE	1-2	.559-.791
NO CHANGE	3-4	.968-1.118
CONVERGENCE	5-6	1.249-1.370
HIGH CONVERGENCE	7-8	1.478-1.581

VIMS-BLM BALTIMORE CANYON TROUGH
LEASE BLOCK AREA ORTHOGONAL DENSITY

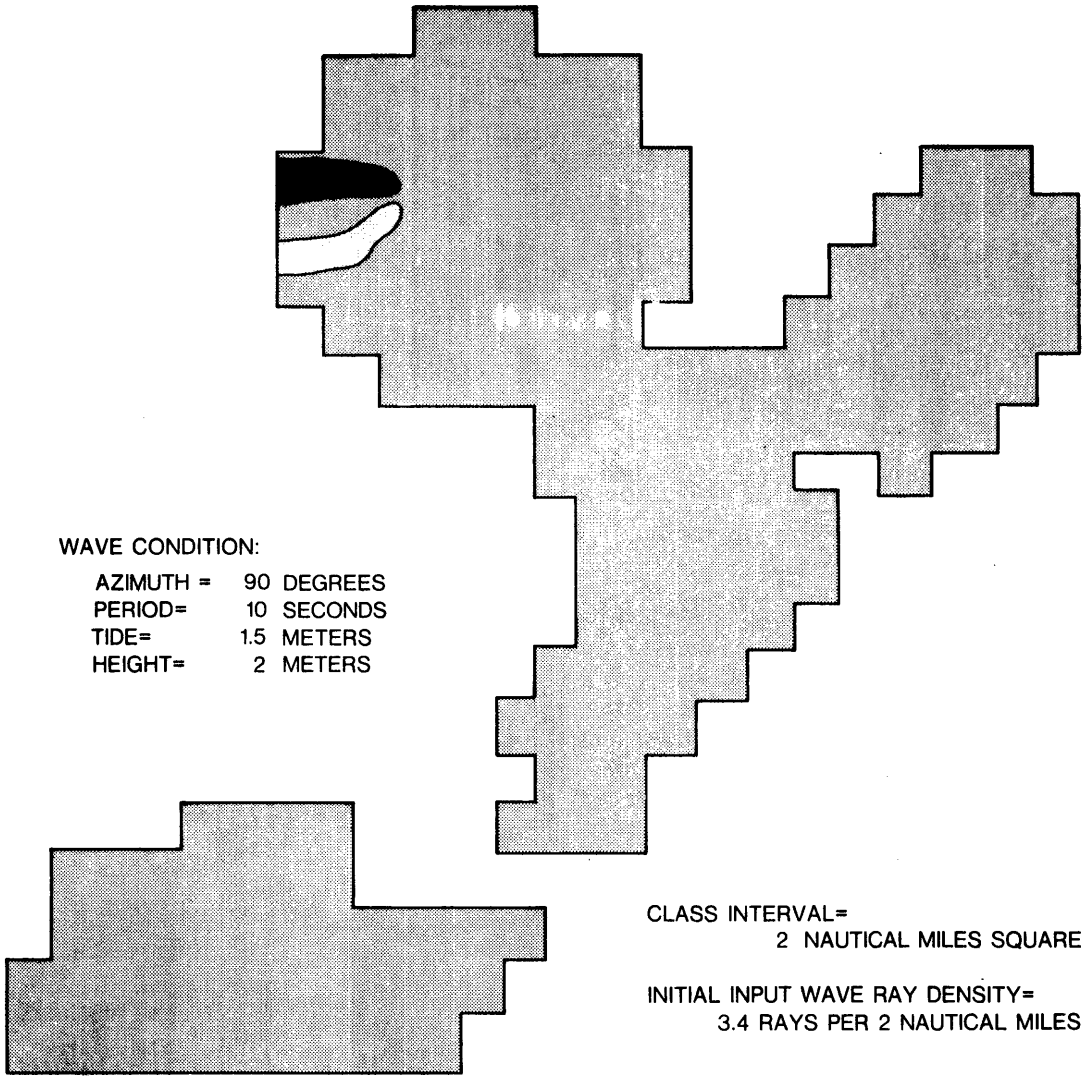

WAVE CONDITION:

AZIMUTH =	90	DEGREES
PERIOD=	10	SECONDS
TIDE=	1.5	METERS
HEIGHT=	2	METERS

CLASS INTERVAL=
2 NAUTICAL MILES SQUARE

INITIAL INPUT WAVE RAY DENSITY=
3.4 RAYS PER 2 NAUTICAL MILES

LEGEND

	RAY DENSITY (rays per 2 n.m. square)	($Kr=(\frac{bo}{b})^{1/2}$)
HIGH DIVERGENCE	< 1	< .559
DIVERGENCE	1-2	.559-.791
NO CHANGE	3-4	.968-1.118
CONVERGENCE	5-6	1.249-1.370
HIGH CONVERGENCE	7-8	1.478-1.581

VIMS-BLM BALTIMORE CANYON TROUGH
LEASE BLOCK AREA ORTHOGONAL DENSITY

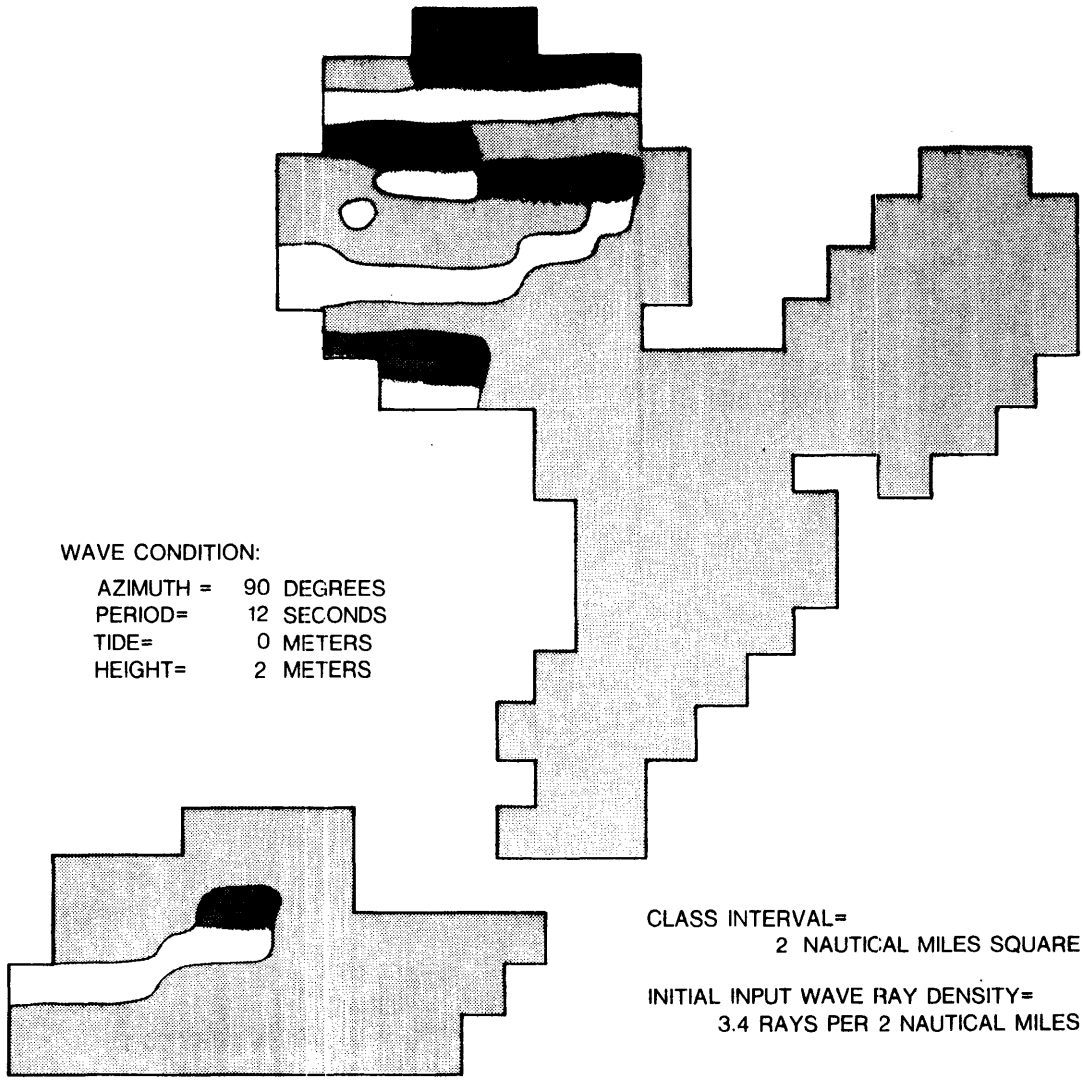

WAVE CONDITION:

AZIMUTH =	90	DEGREES
PERIOD=	12	SECONDS
TIDE=	0	METERS
HEIGHT=	2	METERS

CLASS INTERVAL=
2 NAUTICAL MILES SQUARE

INITIAL INPUT WAVE RAY DENSITY=
3.4 RAYS PER 2 NAUTICAL MILES

LEGEND

	RAY DENSITY (rays per 2 n.m. square)	($Kr=(\frac{bo}{b})^{1/2}$)
HIGH DIVERGENCE	< 1	< .559
DIVERGENCE	1-2	.559-.791
NO CHANGE	3-4	.968-1.118
CONVERGENCE	5-6	1.249-1.370
HIGH CONVERGENCE	7-8	1.478-1.581

VIMS-BLM BALTIMORE CANYON TROUGH
LEASE BLOCK AREA ORTHOGONAL DENSITY

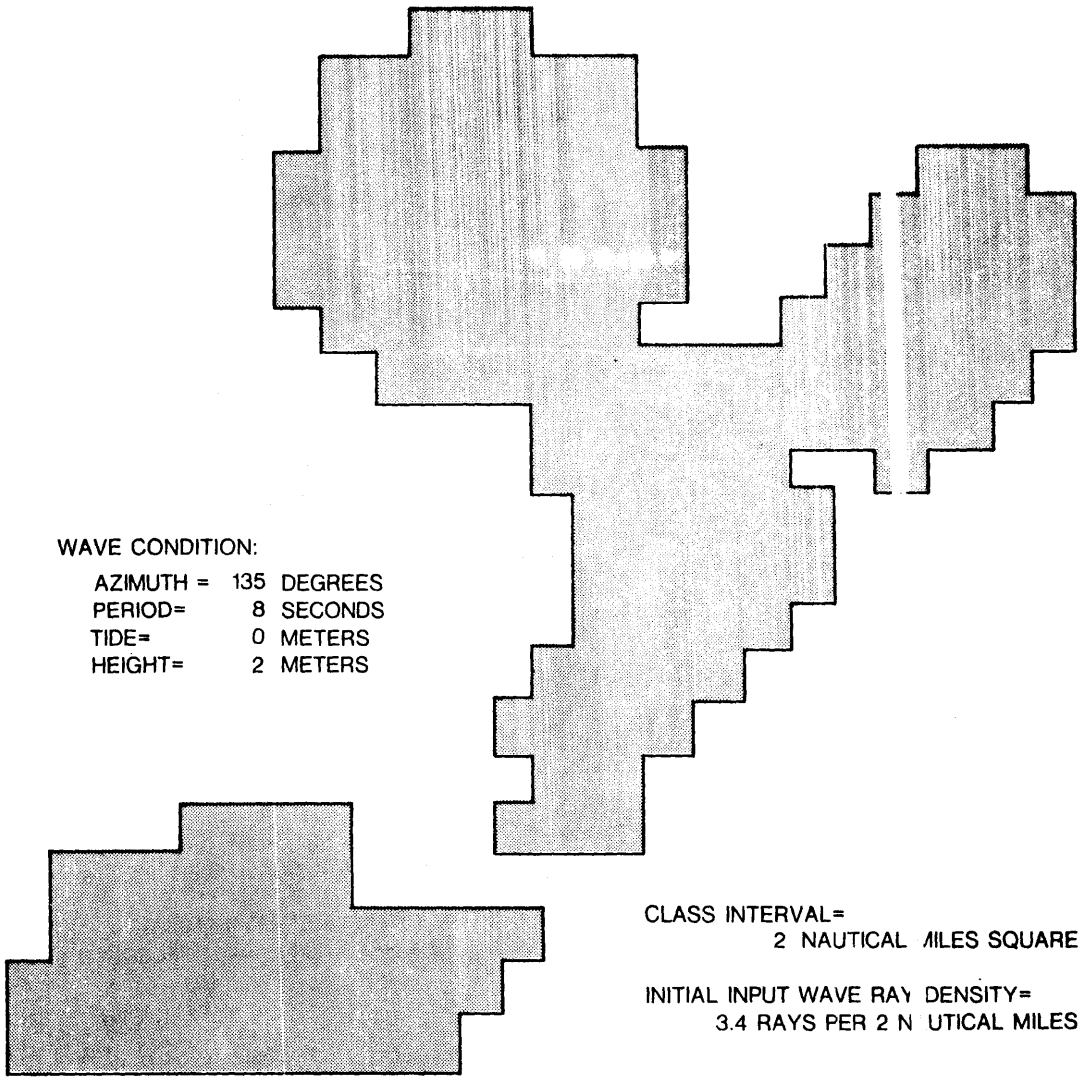

WAVE CONDITION:

AZIMUTH =	135	DEGREES
PERIOD=	8	SECONDS
TIDE=	0	METERS
HEIGHT=	2	METERS

CLASS INTERVAL=
2 NAUTICAL MILES SQUARE

INITIAL INPUT WAVE RAY DENSITY=
3.4 RAYS PER 2 NAUTICAL MILES

LEGEND

	RAY DENSITY (rays per 2 n.m. square)	$(Kr=(\frac{bo}{b})^{1/2})$
HIGH DIVERGENCE	< 1	< .559
DIVERGENCE	1-2	.559-.791
NO CHANGE	3-4	.968-1.118
CONVERGENCE	5-6	1.249-1.370
HIGH CONVERGENCE	7-8	1.478-1.581

VIMS-BLM BALTIMORE CANYON TROUGH
LEASE BLOCK AREA ORTHOGONAL DENSITY

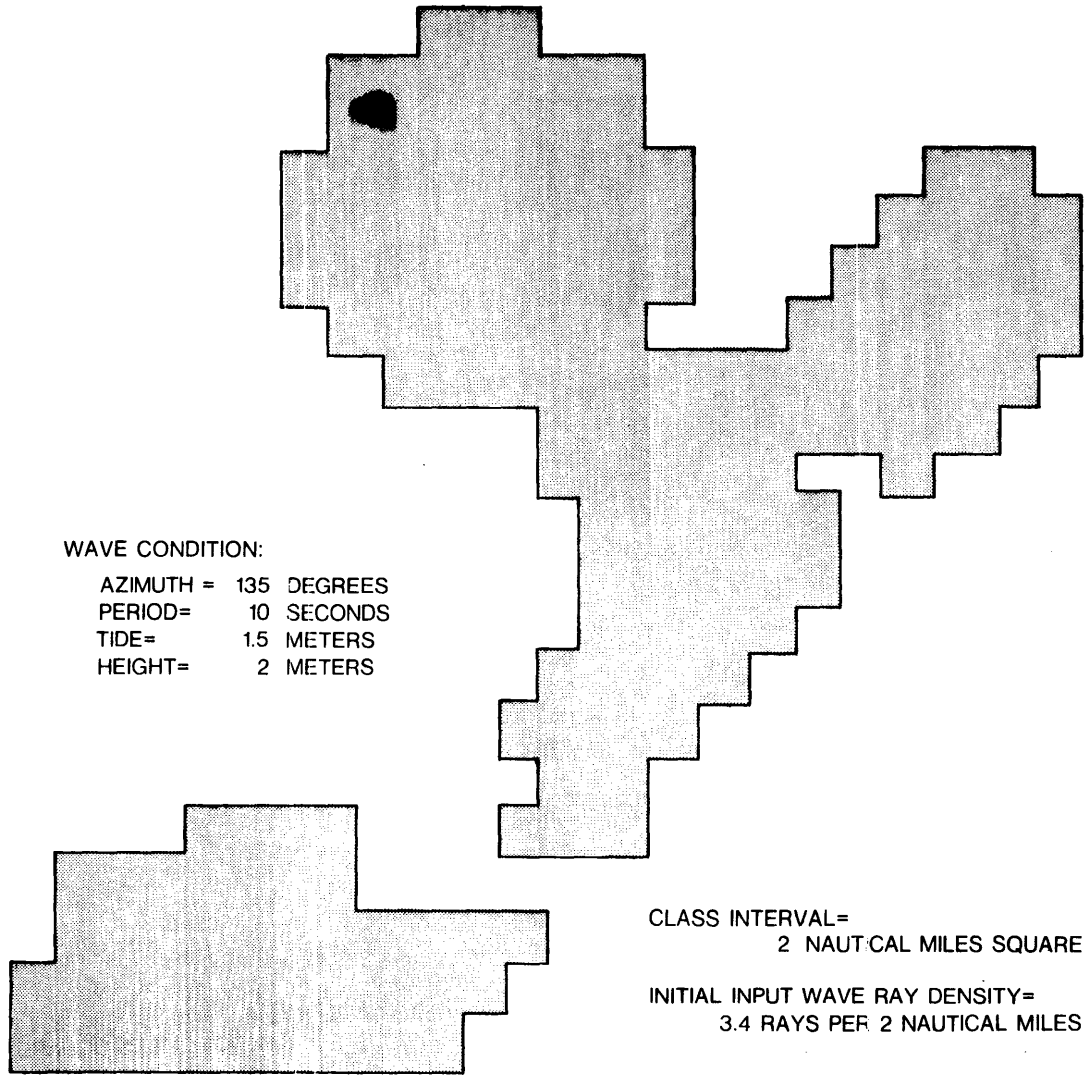

WAVE CONDITION:

AZIMUTH =	135	DEGREES
PERIOD=	10	SECONDS
TIDE=	1.5	METERS
HEIGHT=	2	METERS

CLASS INTERVAL=
2 NAUTICAL MILES SQUARE

INITIAL INPUT WAVE RAY DENSITY=
3.4 RAYS PER 2 NAUTICAL MILES

LEGEND

	RAY DENSITY (rays per 2 n.m. square)	($Kr=(\frac{bo}{b})^{1/2}$)
HIGH DIVERGENCE	< 1	< .559
DIVERGENCE	1-2	.559-.791
NO CHANGE	3-4	.968-1.118
CONVERGENCE	5-6	1.249-1.370
HIGH CONVERGENCE	7-8	1.478-1.581

VIMS-BLM BALTIMORE CANYON TROUGH
LEASE BLOCK AREA ORTHOGONAL DENSITY

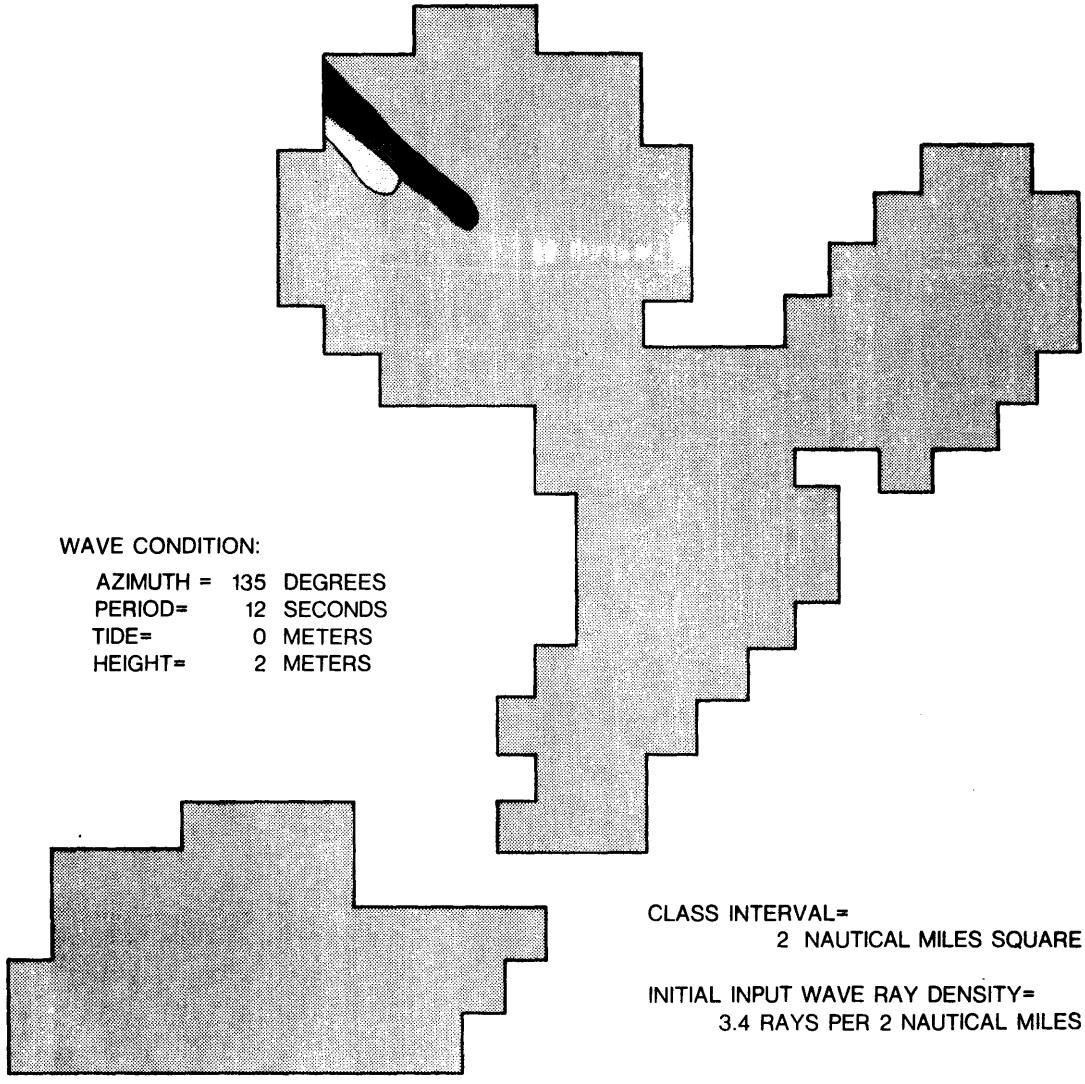

WAVE CONDITION:

AZIMUTH =	135	DEGREES
PERIOD=	12	SECONDS
TIDE=	0	METERS
HEIGHT=	2	METERS

CLASS INTERVAL=
2 NAUTICAL MILES SQUARE

INITIAL INPUT WAVE RAY DENSITY=
3.4 RAYS PER 2 NAUTICAL MILES

LEGEND

	RAY DENSITY (rays per 2 n.m. square)	($Kr=(\frac{bo}{b})^{1/2}$)
HIGH DIVERGENCE	< 1	< .559
DIVERGENCE	1-2	.559-.791
NO CHANGE	3-4	.968-1.118
CONVERGENCE	5-6	1.249-1.370
HIGH CONVERGENCE	7-8	1.478-1.581

VIMS-BLM BALTIMORE CANYON TROUGH
LEASE BLOCK AREA ORTHOGONAL DENSITY

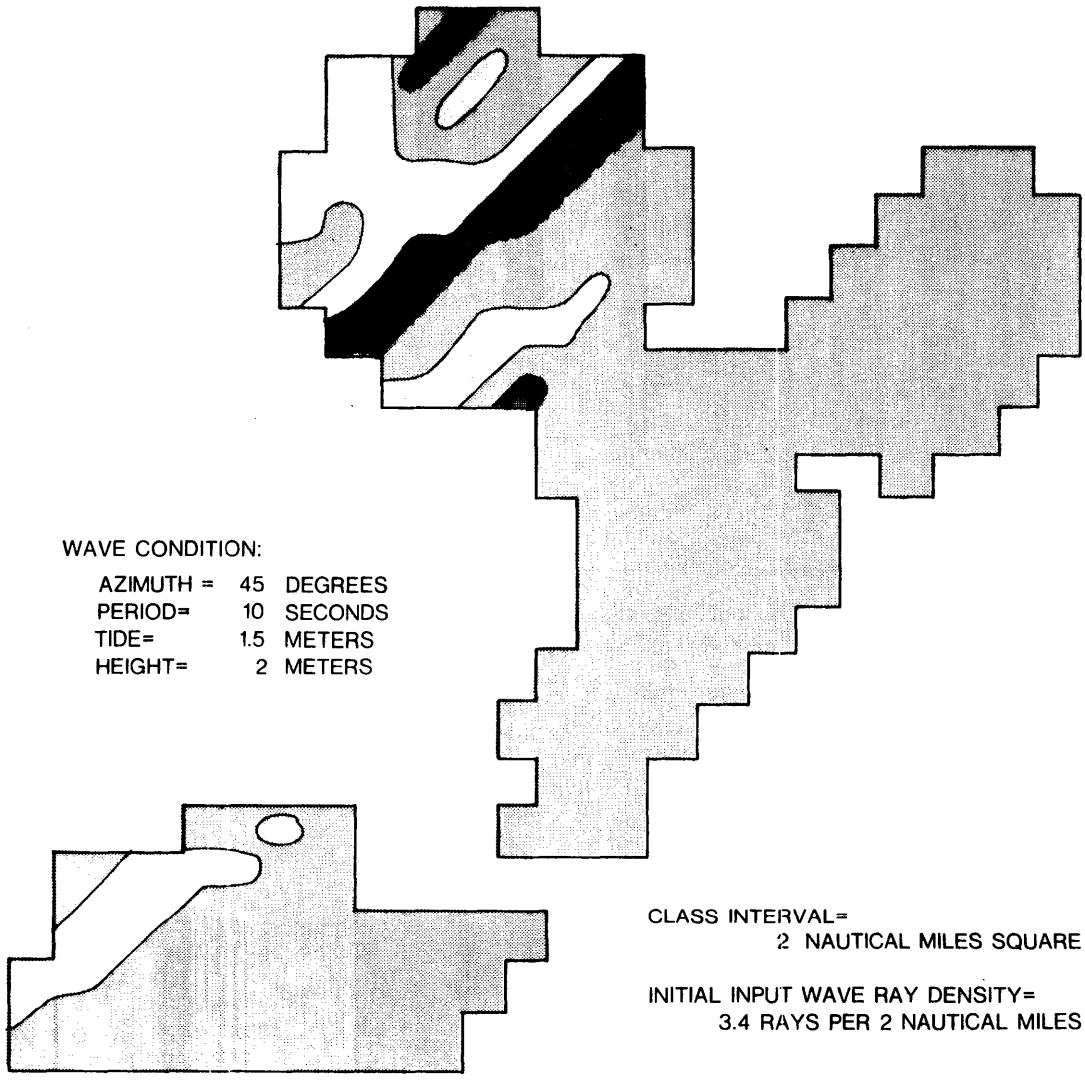

WAVE CONDITION:

AZIMUTH =	45	DEGREES
PERIOD=	10	SECONDS
TIDE=	1.5	METERS
HEIGHT=	2	METERS

CLASS INTERVAL=
2 NAUTICAL MILES SQUARE

INITIAL INPUT WAVE RAY DENSITY=
3.4 RAYS PER 2 NAUTICAL MILES

LEGEND

	RAY DENSITY (rays per 2 n.m. square)	($Kr=(\frac{bo}{b})^{1/2}$)
HIGH DIVERGENCE	< 1	< .559
DIVERGENCE	1-2	.559-.791
NO CHANGE	3-4	.968-1.118
CONVERGENCE	5-6	1.249-1.370
HIGH CONVERGENCE	7-8	1.478-1.581

VIMS-BLM BALTIMORE CANYON TROUGH
LEASE BLOCK AREA ORTHOGONAL DENSITY

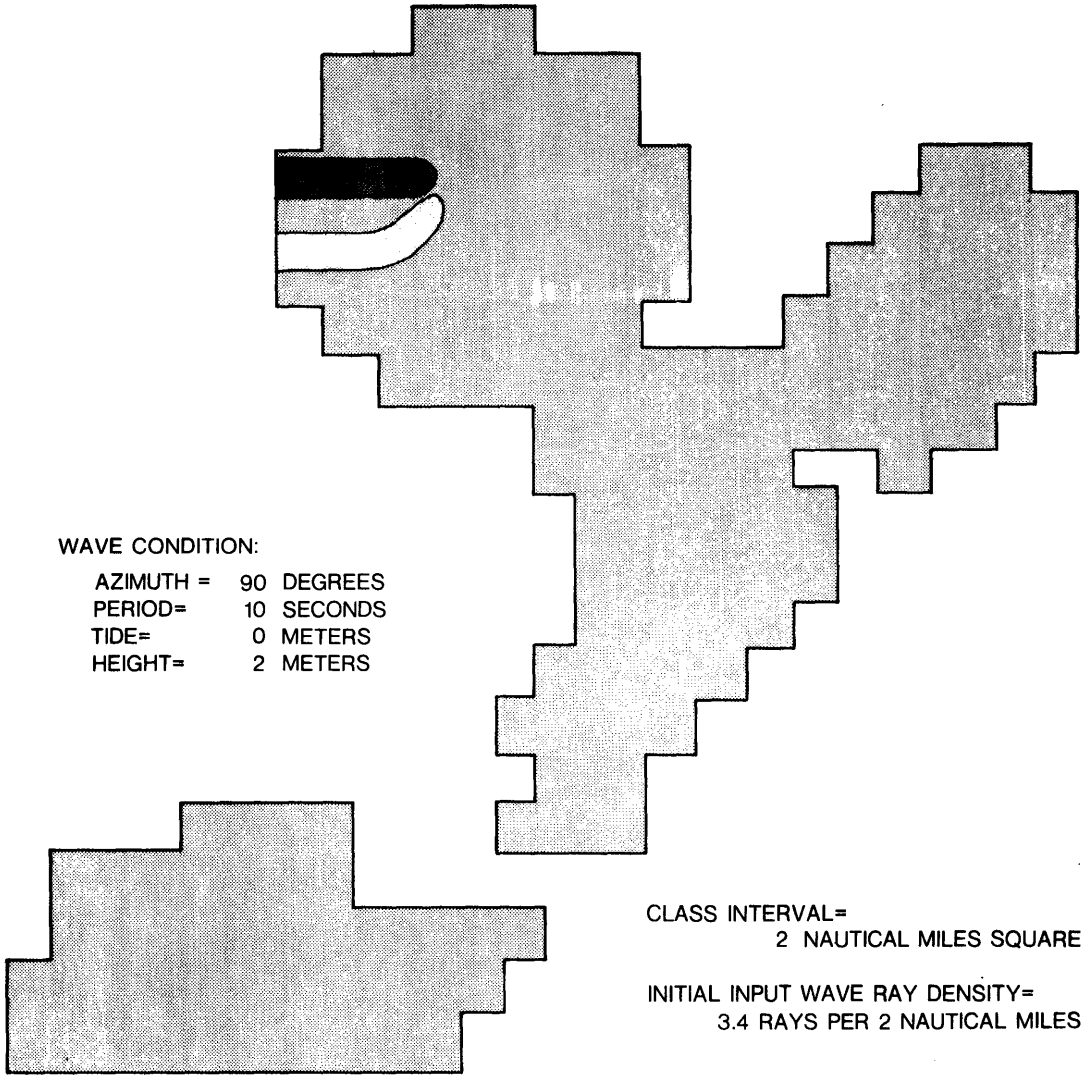

WAVE CONDITION:

AZIMUTH =	90	DEGREES
PERIOD=	10	SECONDS
TIDE=	0	METERS
HEIGHT=	2	METERS

CLASS INTERVAL=
2 NAUTICAL MILES SQUARE

INITIAL INPUT WAVE RAY DENSITY=
3.4 RAYS PER 2 NAUTICAL MILES

LEGEND

	RAY DENSITY (rays per 2 n.m. square)	($Kr=(\frac{bo}{b})^{1/2}$)
HIGH DIVERGENCE	< 1	< .559
DIVERGENCE	1-2	.559-.791
NO CHANGE	3-4	.968-1.118
CONVERGENCE	5-6	1.249-1.370
HIGH CONVERGENCE	7-8	1.478-1.581

VIMS-BLM BALTIMORE CANYON TROUGH
LEASE BLOCK AREA ORTHOGONAL DENSITY

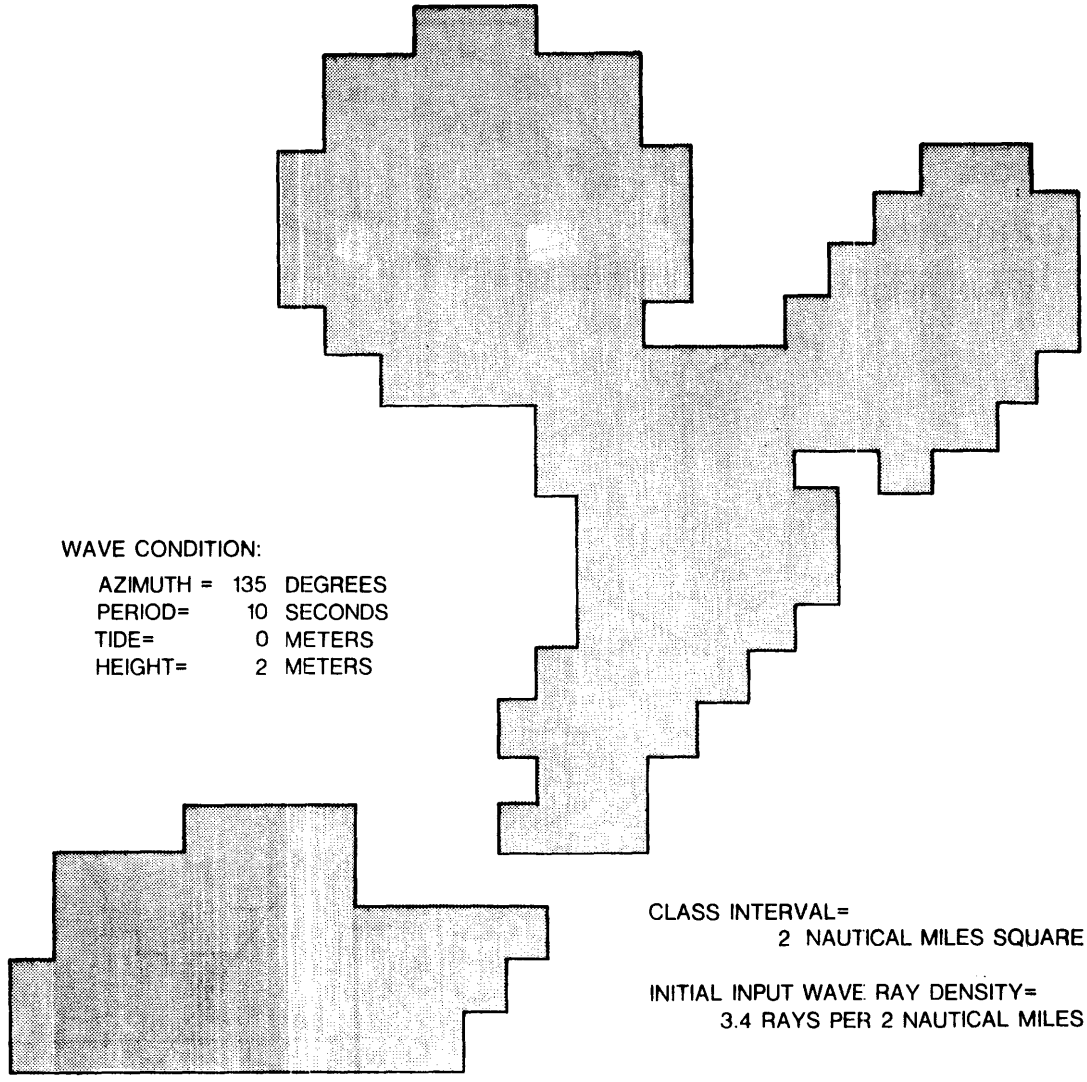

WAVE CONDITION:

AZIMUTH =	135	DEGREES
PERIOD=	10	SECONDS
TIDE=	0	METERS
HEIGHT=	2	METERS

CLASS INTERVAL=
2 NAUTICAL MILES SQUARE

INITIAL INPUT WAVE RAY DENSITY=
3.4 RAYS PER 2 NAUTICAL MILES

LEGEND

	RAY DENSITY (rays per 2 n.m. square)	$(Kr=(\frac{bo}{b})^{1/2})$
HIGH DIVERGENCE	< 1	< .559
DIVERGENCE	1-2	.559-.791
NO CHANGE	3-4	.968-1.118
CONVERGENCE	5-6	1.249-1.370
HIGH CONVERGENCE	7-8	1.478-1.581

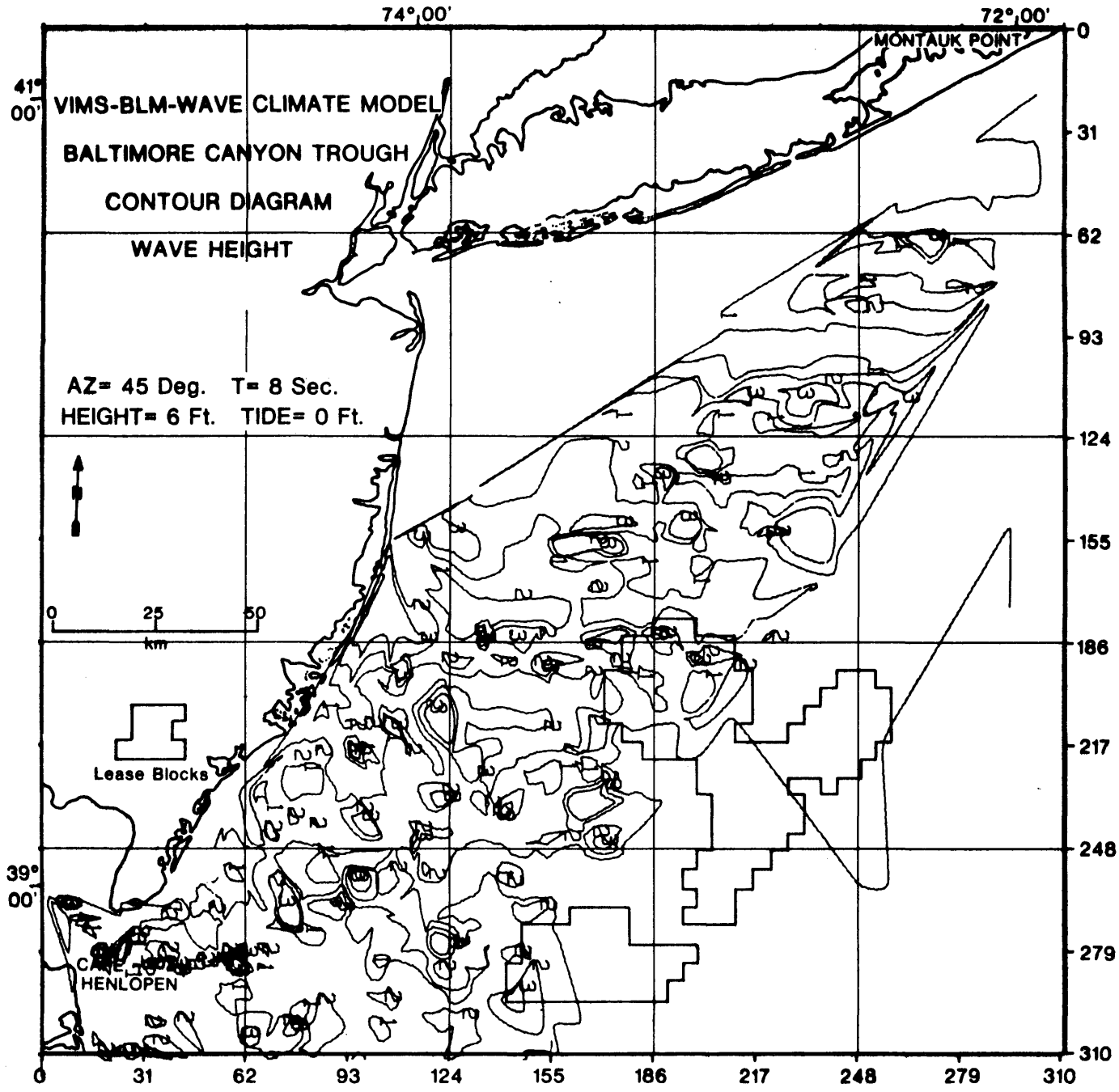
74°00'
72°00'
MONTAUK POINT
41° 00'
VIMS-BLM-WAVE CLIMATE MODEL
BALTIMORE CANYON TROUGH
CONTOUR DIAGRAM
WAVE HEIGHT
AZ= 45 Deg. T= 8 Sec.
HEIGHT= 6 Ft. TIDE= 0 Ft.
0 25 50
km
Lease Blocks
39° 00'
HENLOPEN
0 31 62 93 124 155 186 217 248 279 310
GRID UNITS (1=0.5 NM)

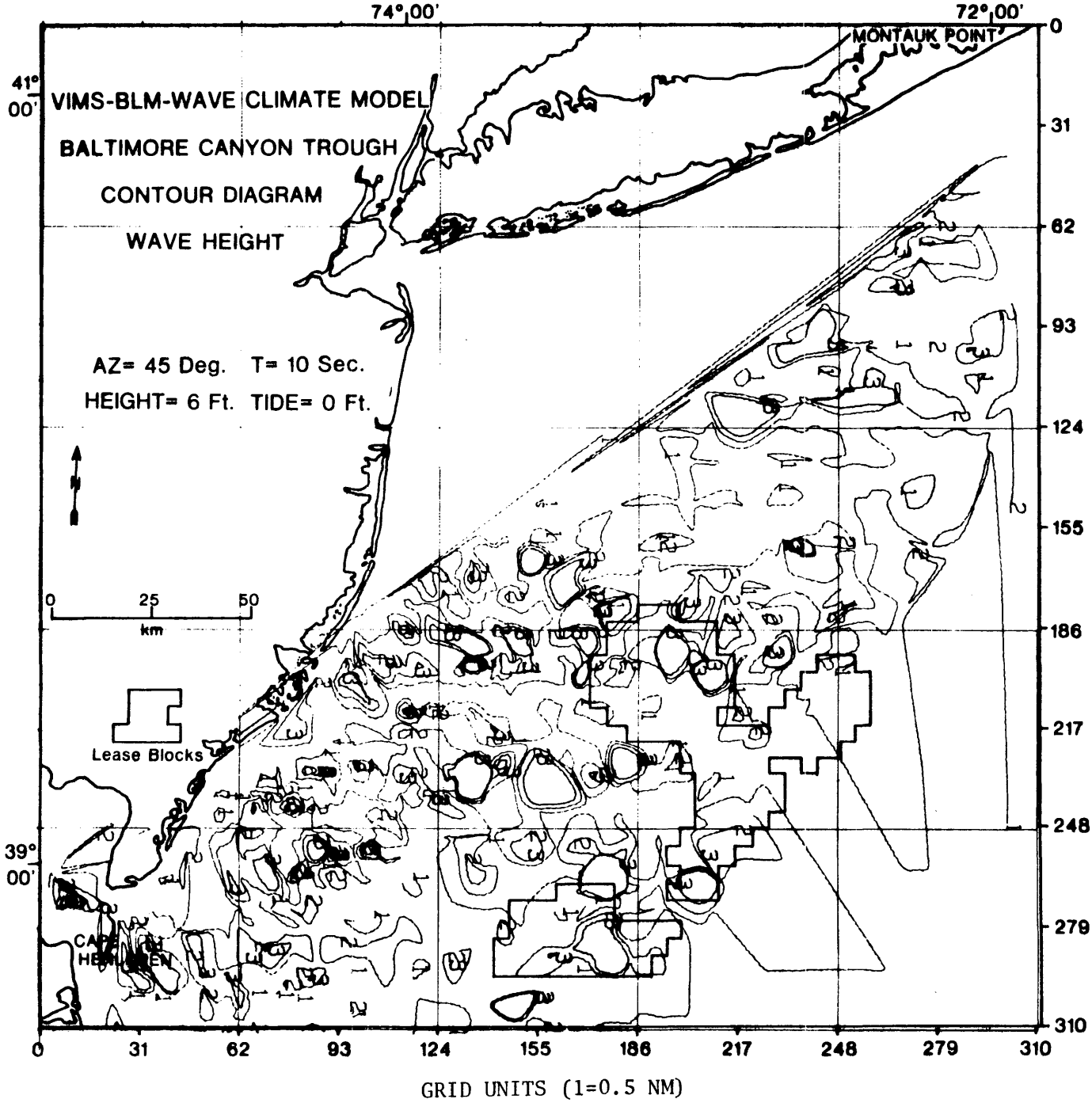
74°00'
72°00'
MONTAUK POINT
41° 00'
VIMS-BLM-WAVE CLIMATE MODEL
BALTIMORE CANYON TROUGH
CONTOUR DIAGRAM
WAVE HEIGHT
AZ= 45 Deg. T= 10 Sec.
HEIGHT= 6 Ft. TIDE= 0 Ft.
N
0 25 50
km
Lease Blocks
39° 00'
0 31 62 93 124 155 186 217 248 279 310
GRID UNITS (1=0.5 NM)

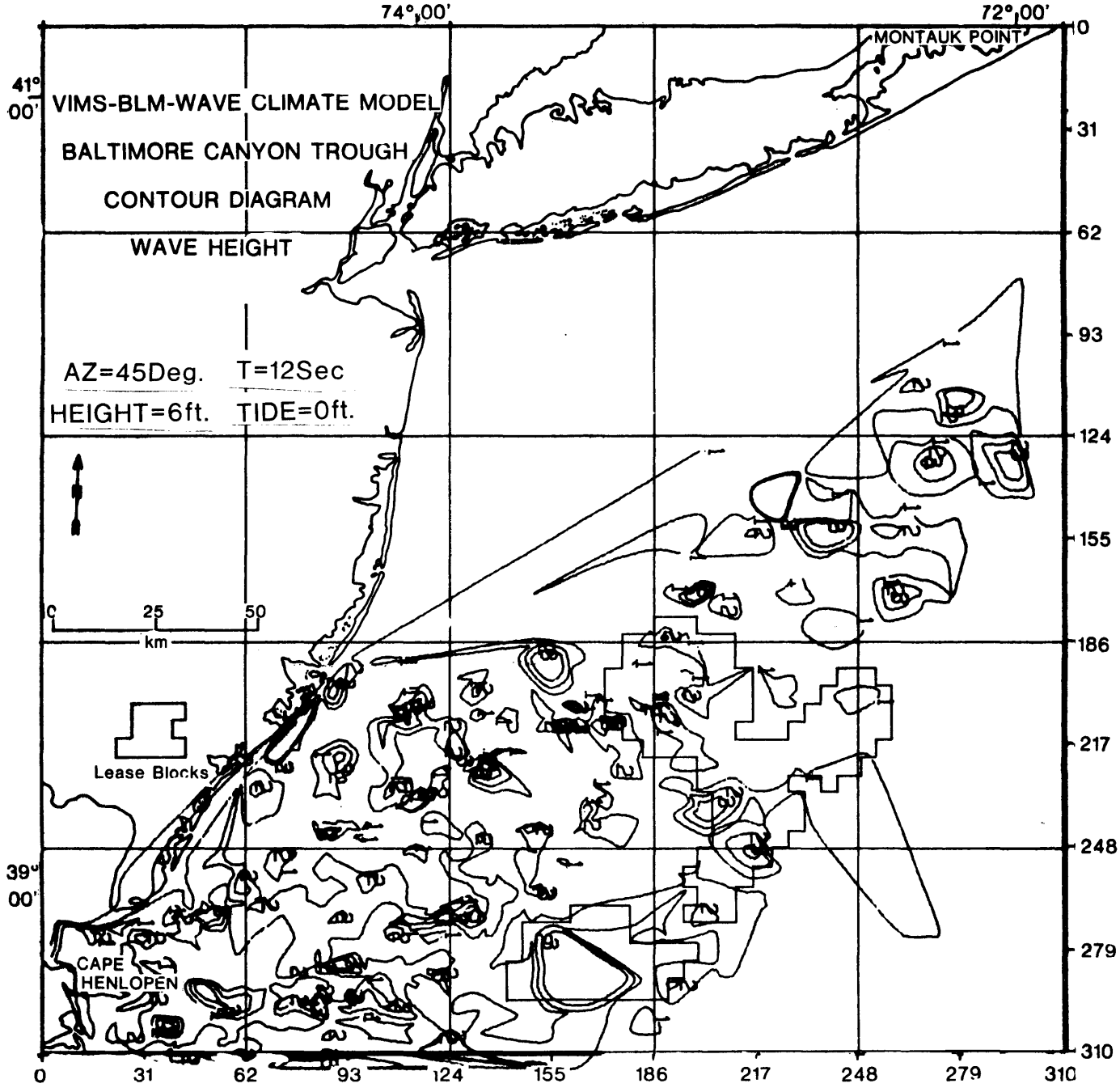
74°,00'
72°,00'
MONTAUK POINT
41° 00'
VIMS-BLM-WAVE CLIMATE MODEL
BALTIMORE CANYON TROUGH
CONTOUR DIAGRAM
WAVE HEIGHT
AZ=45Deg. T=12Sec
HEIGHT=6ft. TIDE=0ft.
0 25 50
km
Lease Blocks
39° 00'
CAPE HENLOPEN
0 31 62 93 124 155 186 217 248 279 310
GRID UNITS (1=0.5 NM)

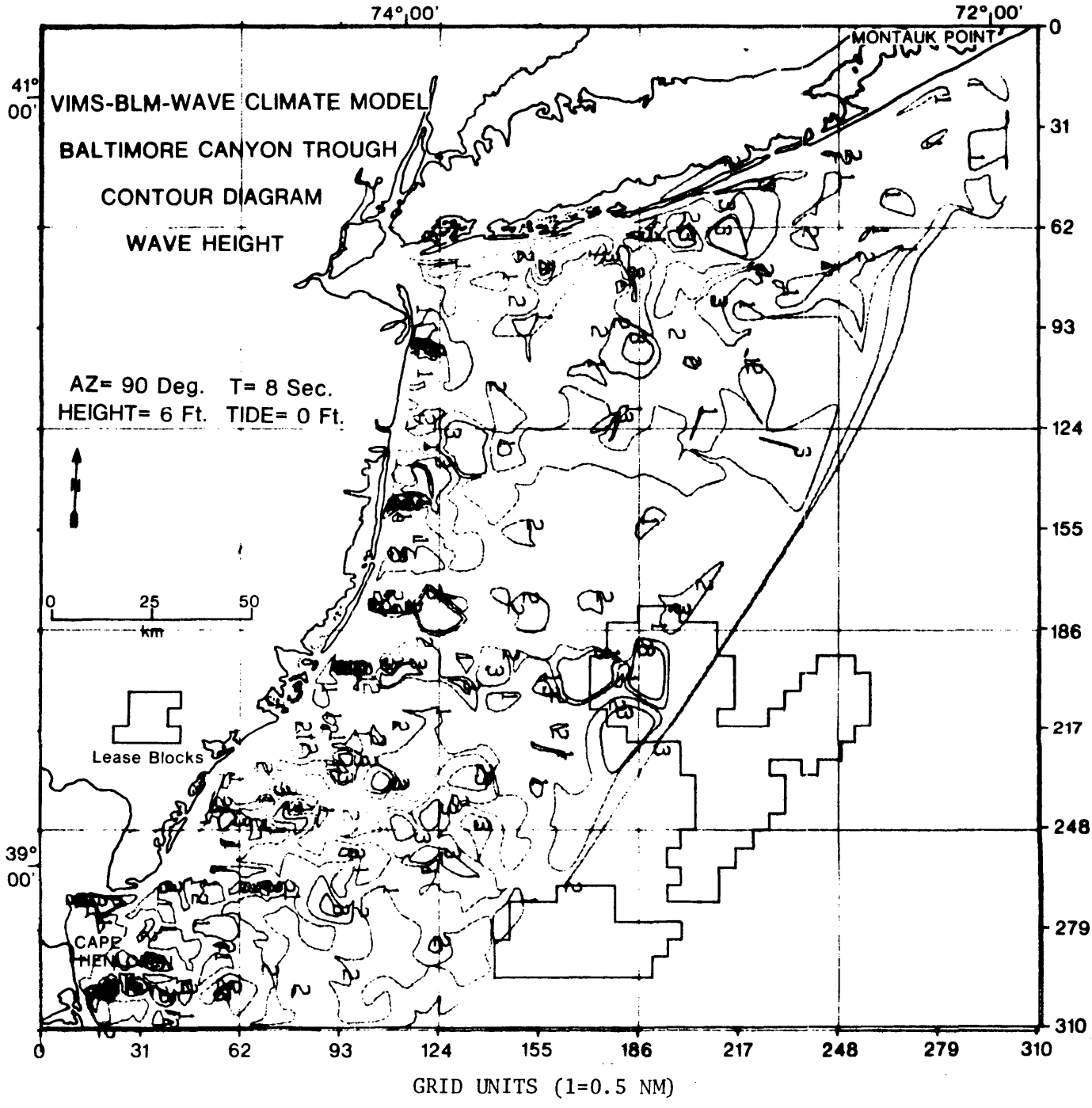
74°00'
72°00'
MONTAUK POINT
41° 00'
VIMS-BLM-WAVE CLIMATE MODEL
BALTIMORE CANYON TROUGH
CONTOUR DIAGRAM
WAVE HEIGHT
AZ= 90 Deg. T= 8 Sec.
HEIGHT= 6 Ft. TIDE= 0 Ft.
N
0 25 50
km
Lease Blocks
39° 00'
CAPE HENLOPEN
0 31 62 93 124 155 186 217 248 279 310
GRID UNITS (1=0.5 NM)

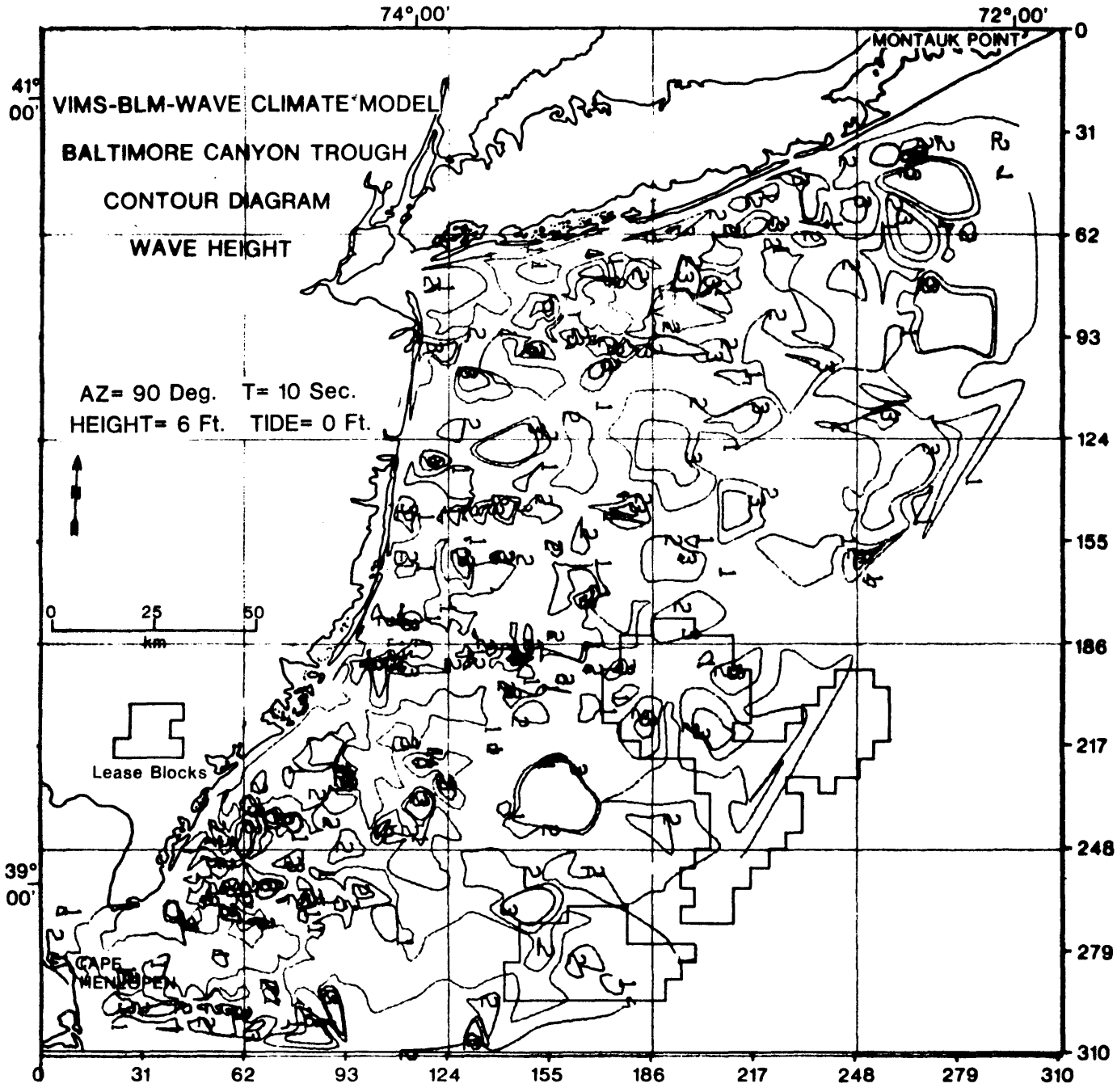
74°00'
72°00'
MONTAUK POINT
41° 00'
VIMS-BLM-WAVE CLIMATE MODEL
BALTIMORE CANYON TROUGH
CONTOUR DIAGRAM
WAVE HEIGHT
AZ= 90 Deg. T= 10 Sec.
HEIGHT= 6 Ft. TIDE= 0 Ft.
0 25 50
km
Lease Blocks
39° 00'
CAPE HENLOPEN
0 31 62 93 124 155 186 217 248 279 310
GRID UNITS (1=0.5 NM)

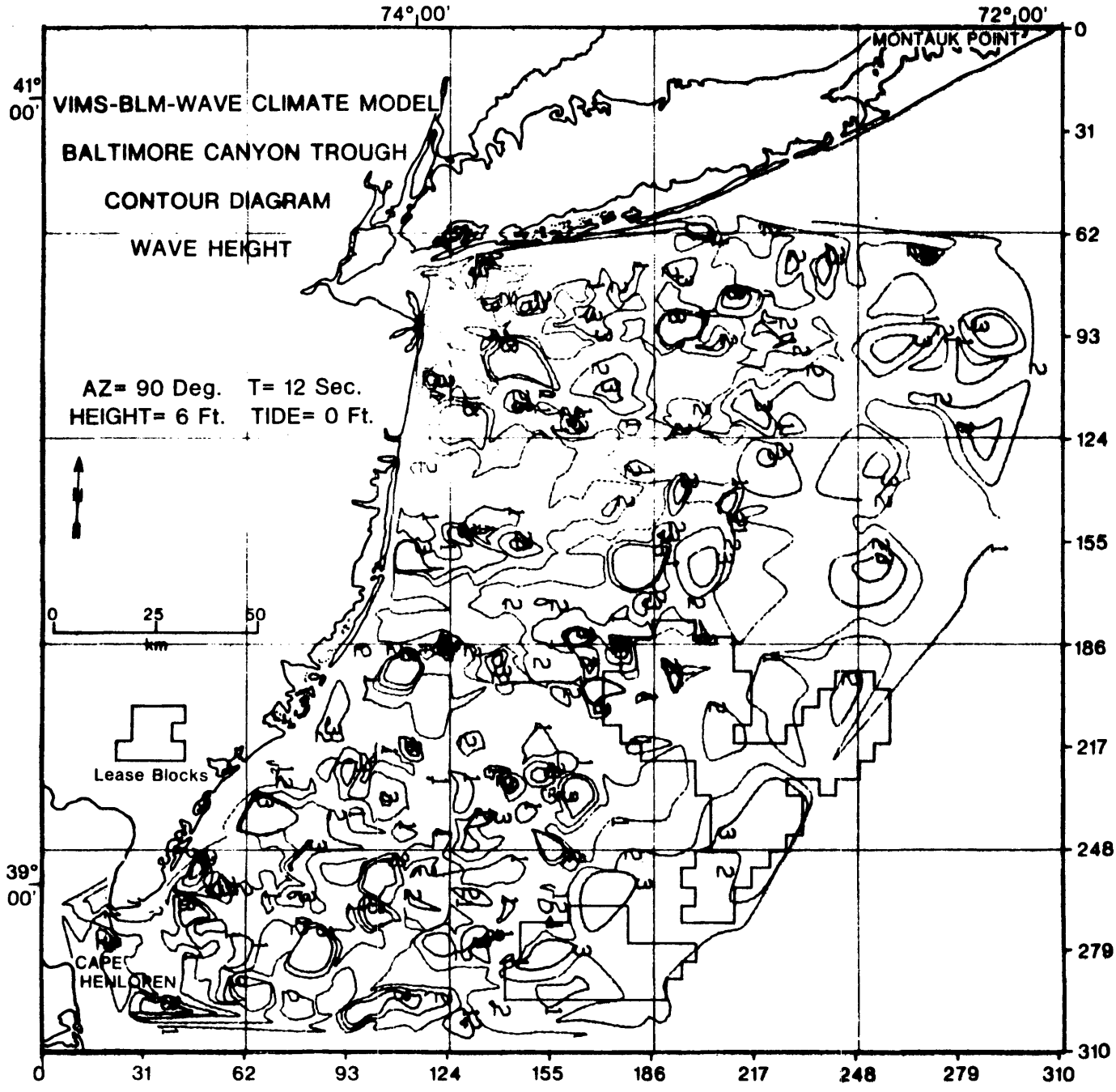
74°00'
72°00'
MONTAUK POINT
41° 00'
VIMS-BLM-WAVE CLIMATE MODEL
BALTIMORE CANYON TROUGH
CONTOUR DIAGRAM
WAVE HEIGHT
AZ= 90 Deg. T= 12 Sec.
HEIGHT= 6 Ft. TIDE= 0 Ft.
0 25 50
km
Lease Blocks
39° 00'
CAPE HENLOPEN
0 31 62 93 124 155 186 217 248 279 310
GRID UNITS (1=0.5 NM)

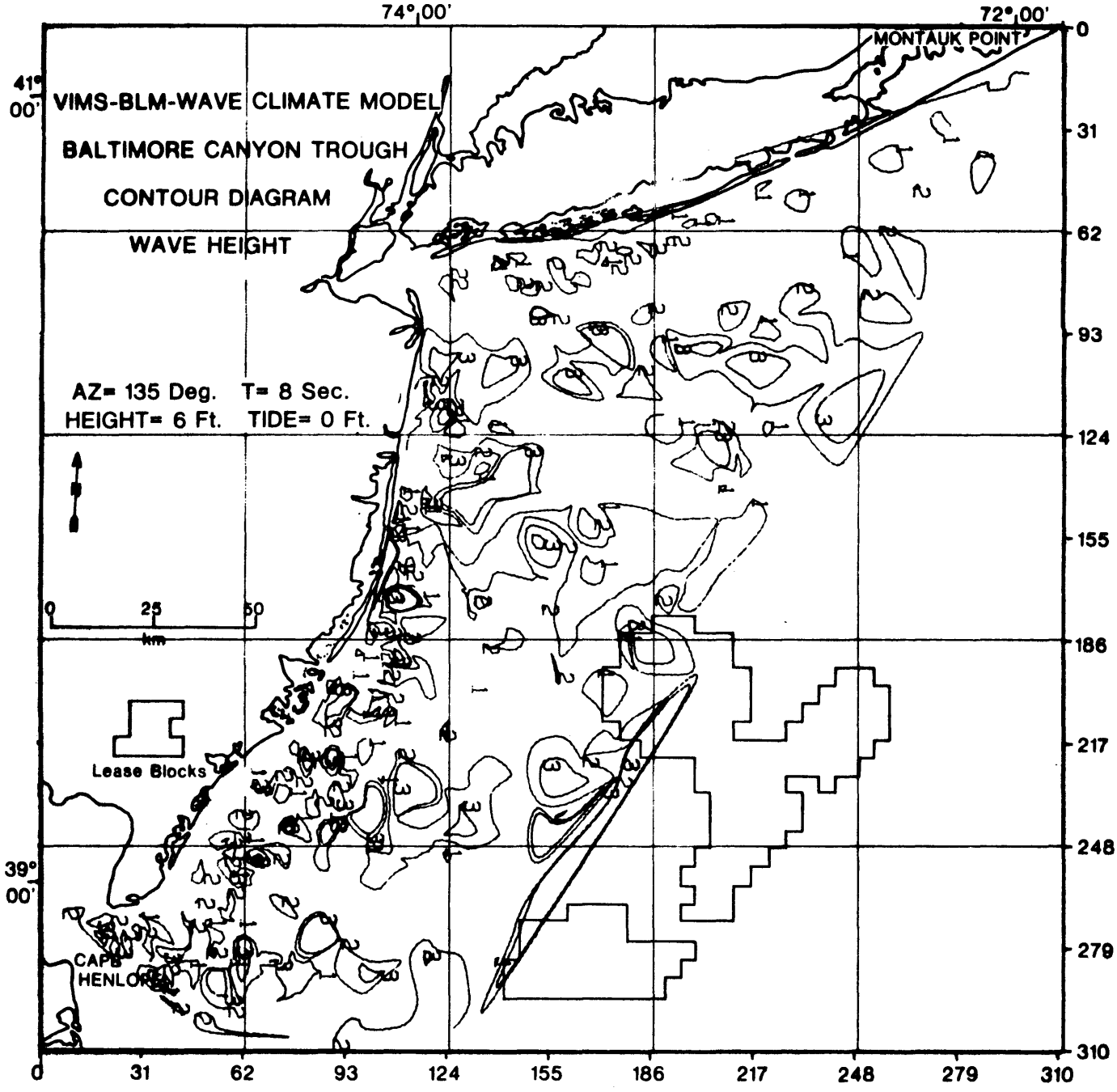

GRID UNITS (1=0.5 NM)

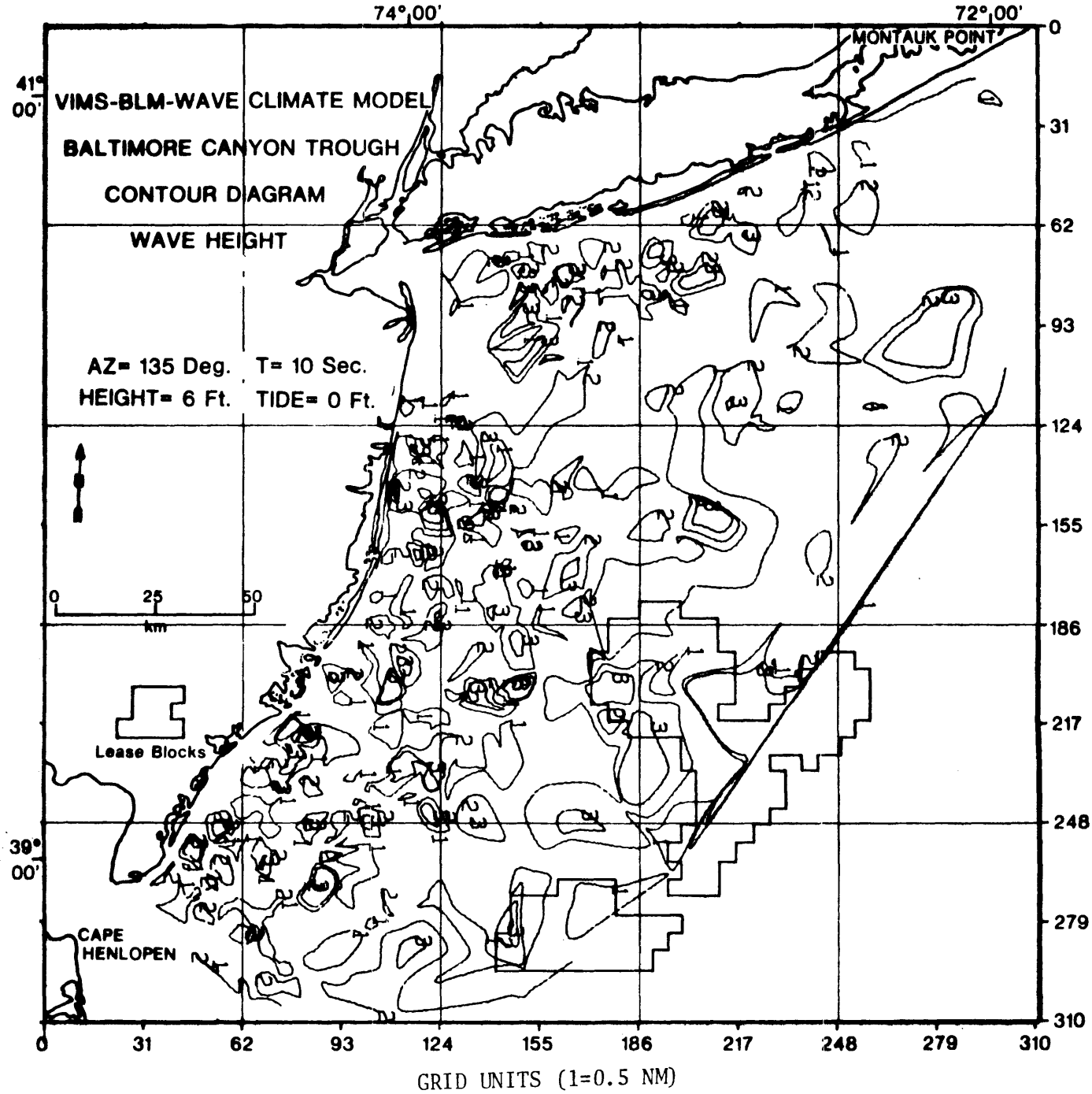
74°00'
72°00'
MONTAUK POINT
41° 00'
VIMS-BLM-WAVE CLIMATE MODEL
BALTIMORE CANYON TROUGH
CONTOUR DIAGRAM
WAVE HEIGHT
AZ= 135 Deg. T= 10 Sec.
HEIGHT= 6 Ft. TIDE= 0 Ft.
0 25 50
km
Lease Blocks
39° 00'
CAPE HENLOPEN
0 31 62 93 124 155 186 217 248 279 310
GRID UNITS (1=0.5 NM)

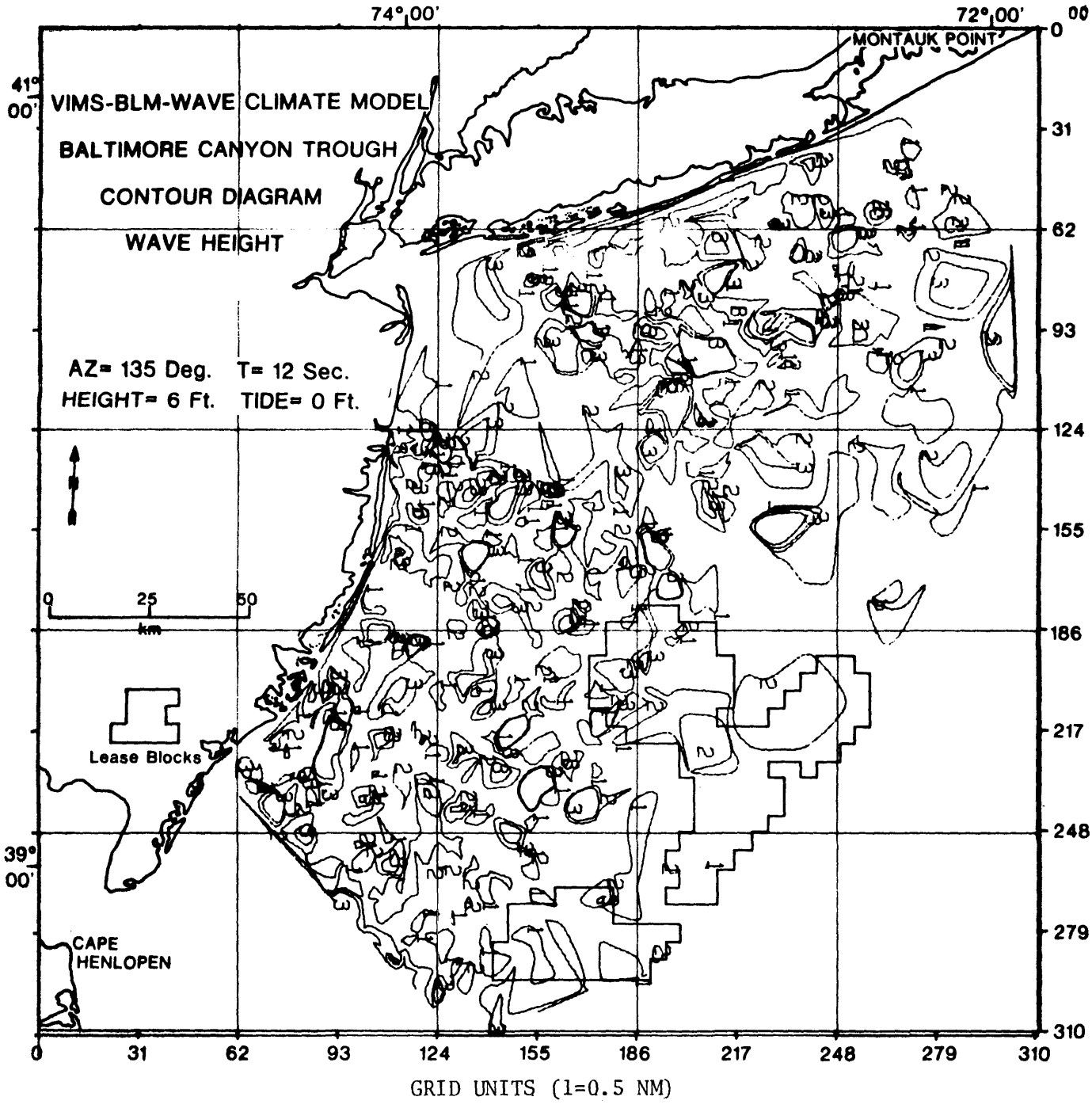
74°00'
72°00'
MONTAUK POINT
41° 00'
VIMS-BLM-WAVE CLIMATE MODEL
BALTIMORE CANYON TROUGH
CONTOUR DIAGRAM
WAVE HEIGHT
AZ= 135 Deg. T= 12 Sec.
HEIGHT= 6 Ft. TIDE= 0 Ft.
N
0 25 50
km
Lease Blocks
39° 00'
CAPE HENLOPEN
0 31 62 93 124 155 186 217 248 279 310
GRID UNITS (1=0.5 NM)

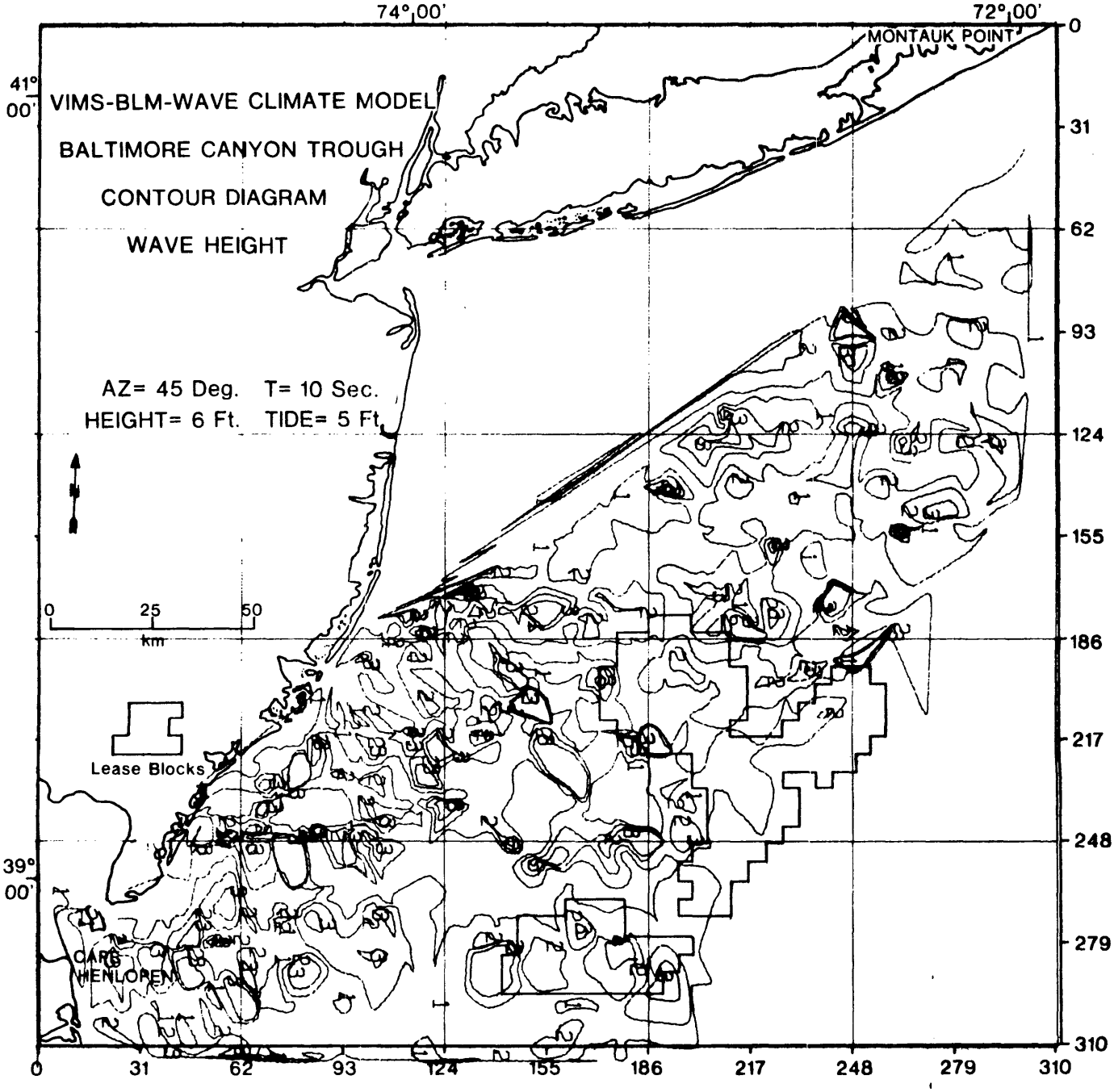

GRID UNITS (1=0.5 NM)

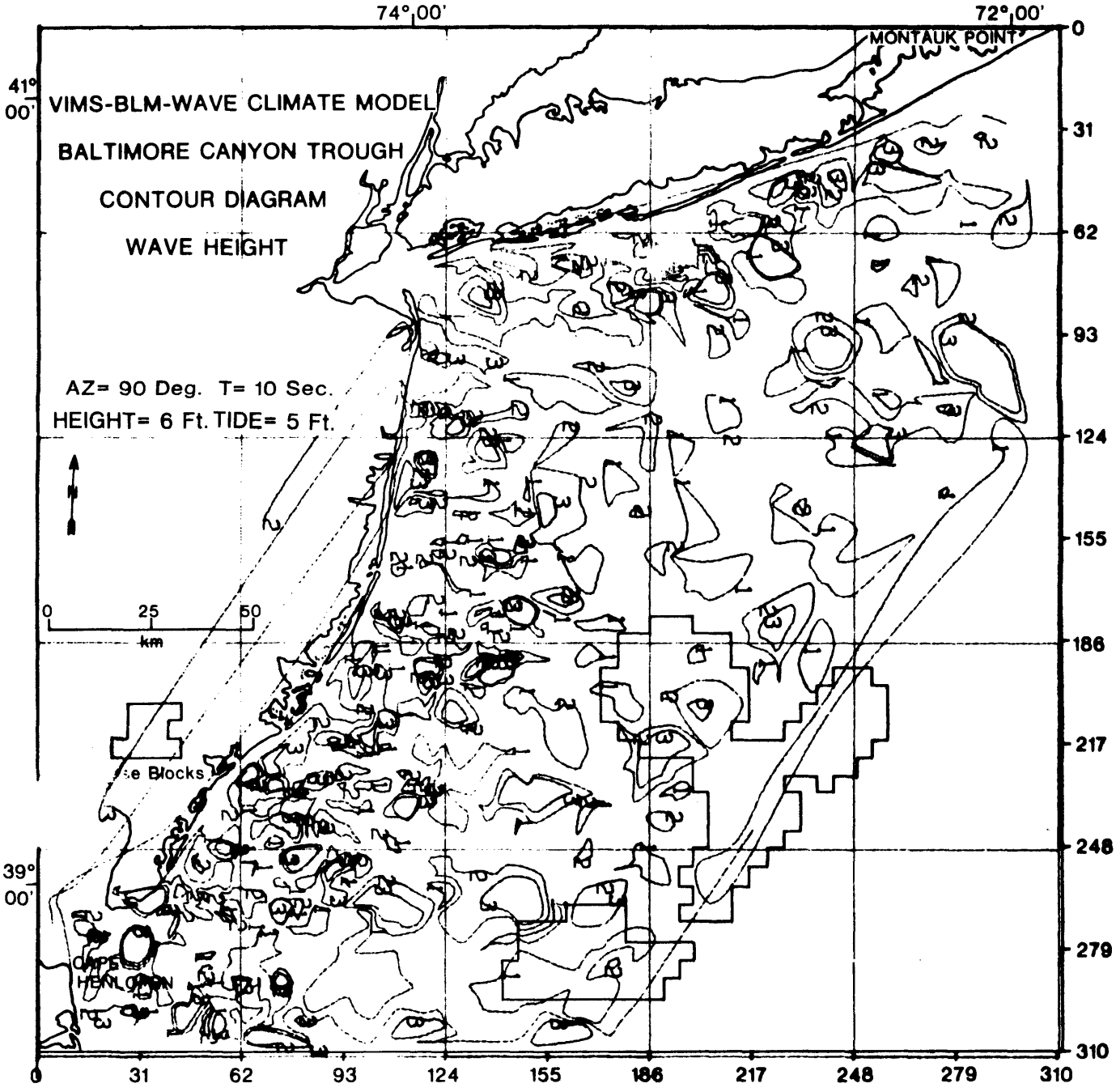

GRID UNITS (1=0.5 NM)

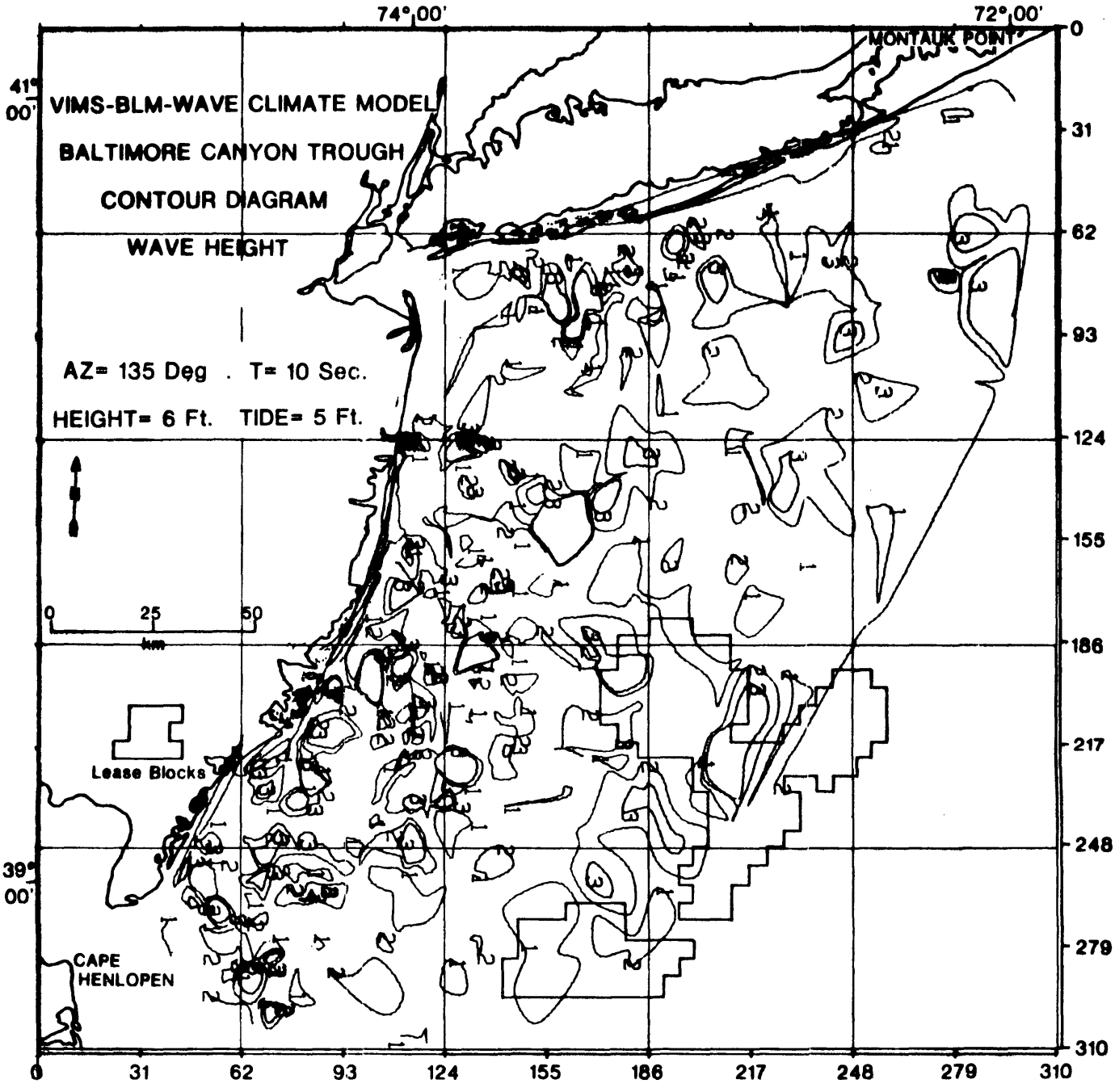
74°00'
72°00'
MONTAUK POINT
41° 00'
VIMS-BLM-WAVE CLIMATE MODEL
BALTIMORE CANYON TROUGH
CONTOUR DIAGRAM
WAVE HEIGHT
AZ= 135 Deg . T= 10 Sec.
HEIGHT= 6 Ft. TIDE= 5 Ft.
0 25 50
km
Lease Blocks
39° 00'
CAPE HENLOPEN
0 31 62 93 124 155 186 217 248 279 310
GRID UNITS (1=0.5 NM)

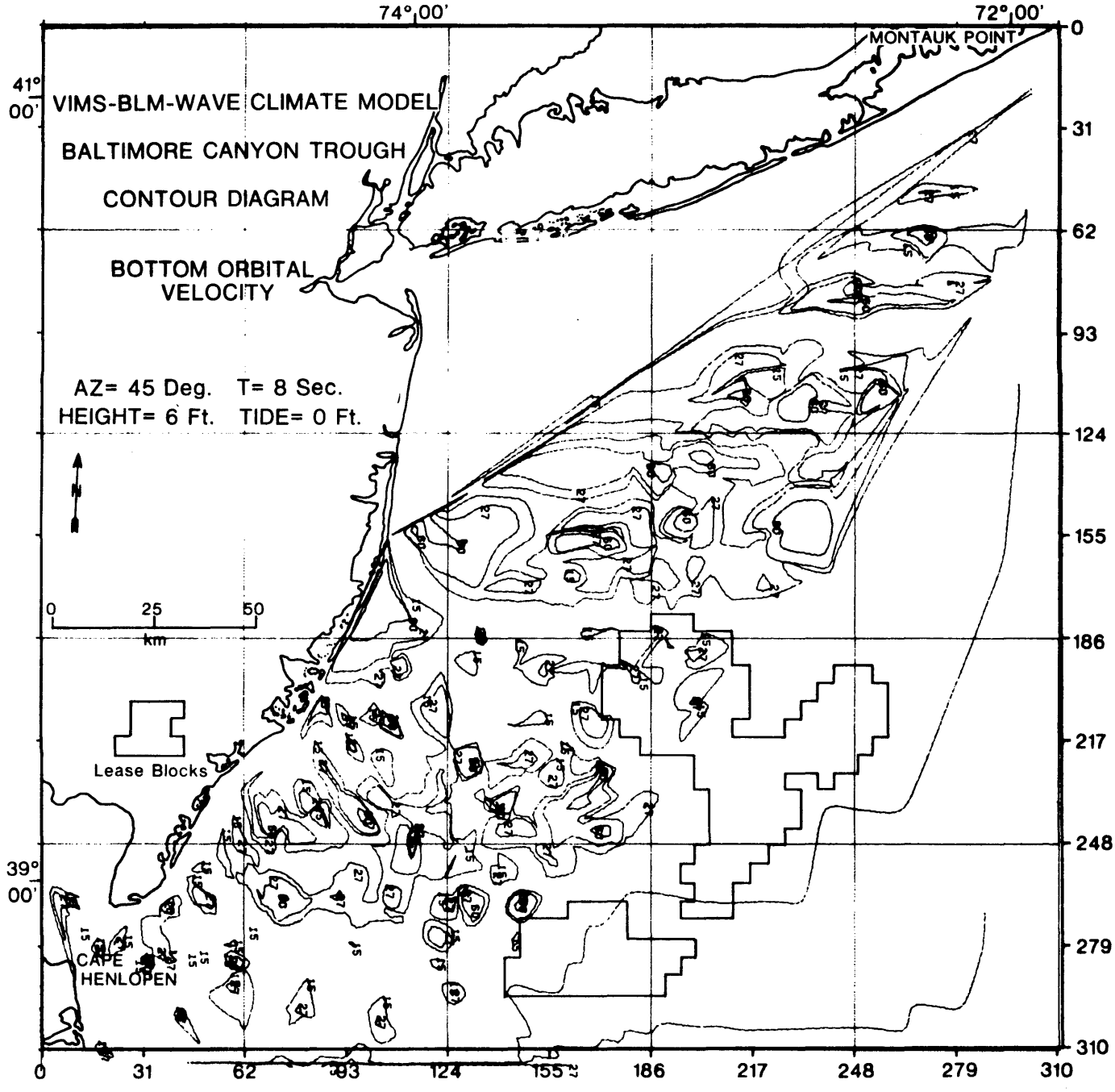
74°00'
72°00'
MONTAUK POINT
41° 00'
VIMS-BLM-WAVE CLIMATE MODEL
BALTIMORE CANYON TROUGH
CONTOUR DIAGRAM
BOTTOM ORBITAL VELOCITY
AZ= 45 Deg. T= 8 Sec.
HEIGHT= 6 Ft. TIDE= 0 Ft.
N
0 25 50
km
Lease Blocks
39° 00'
CAPE HENLOPEN
0 31 62 93 124 155 186 217 248 279 310
GRID UNITS (1=0.5 NM)

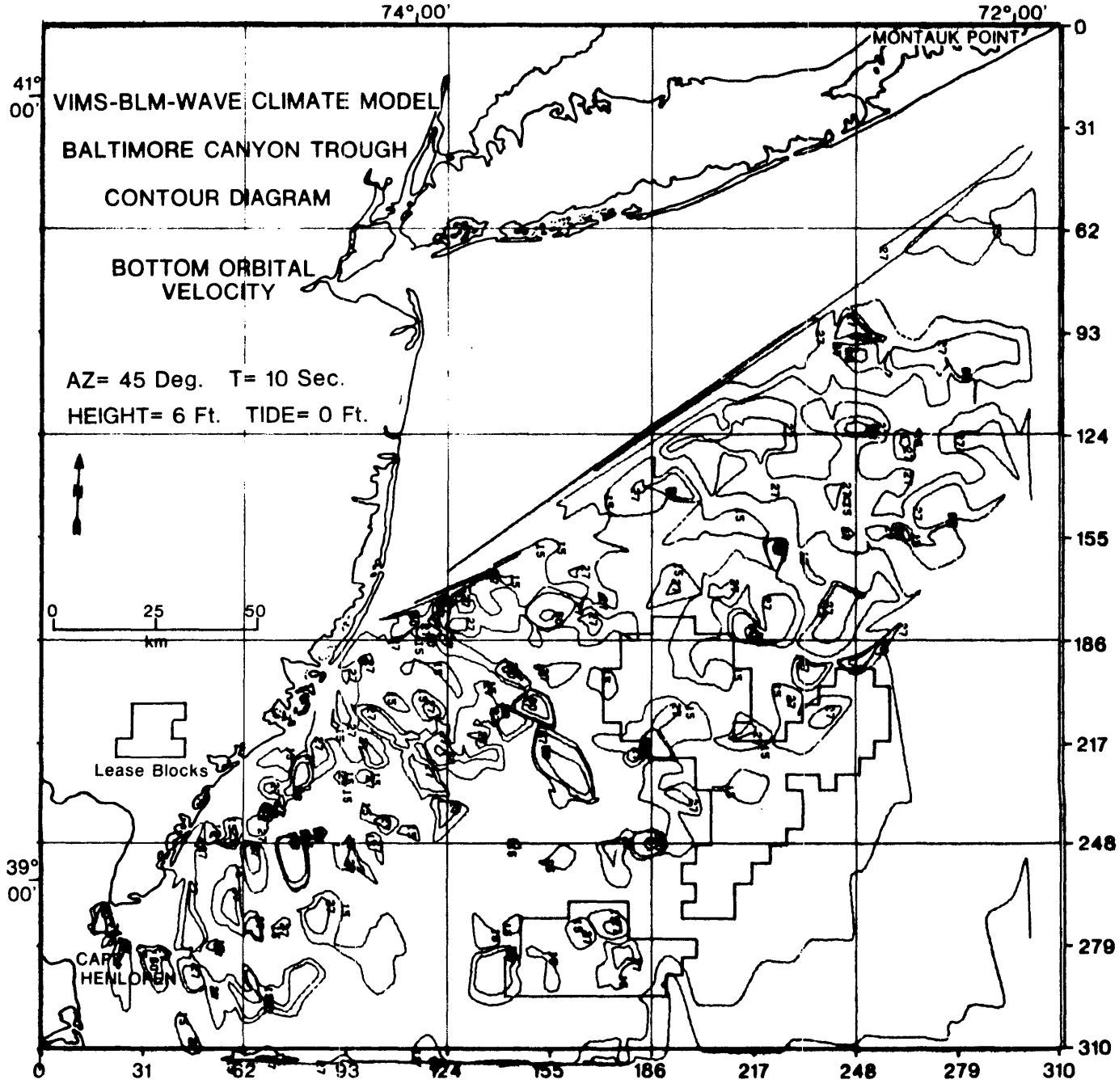
74°,00'
72°,00'
MONTAUK POINT
41° 00'
VIMS-BLM-WAVE CLIMATE MODEL
BALTIMORE CANYON TROUGH
CONTOUR DIAGRAM
BOTTOM ORBITAL VELOCITY
AZ= 45 Deg. T= 10 Sec.
HEIGHT= 6 Ft. TIDE= 0 Ft.
0 25 50
km
Lease Blocks
39° 00'
CAPE HENLOPEN
0 31 62 93 124 155 186 217 248 279 310
GRID UNITS (1=0.5 NM)

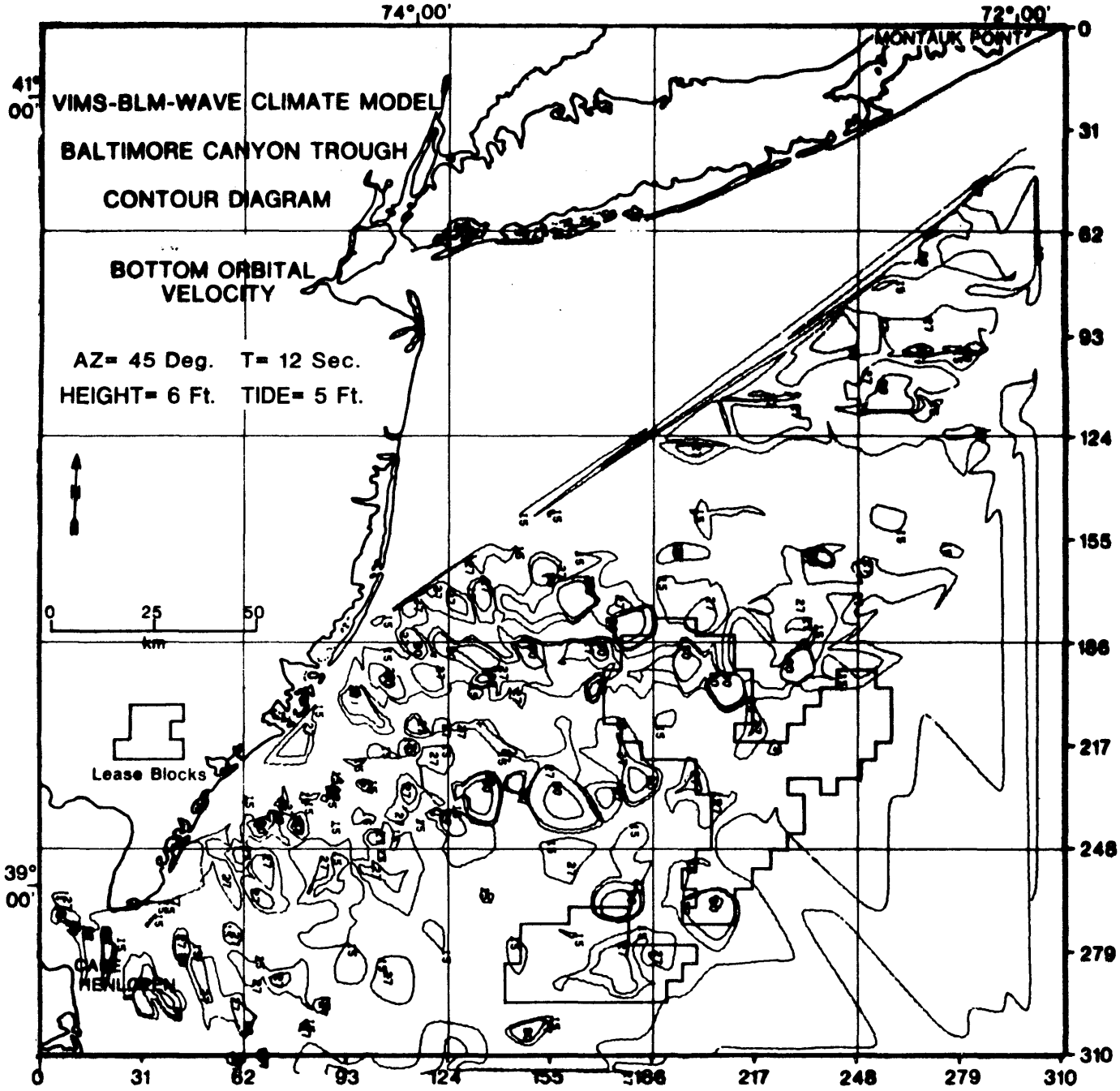

GRID UNITS (1=0.5 NM)

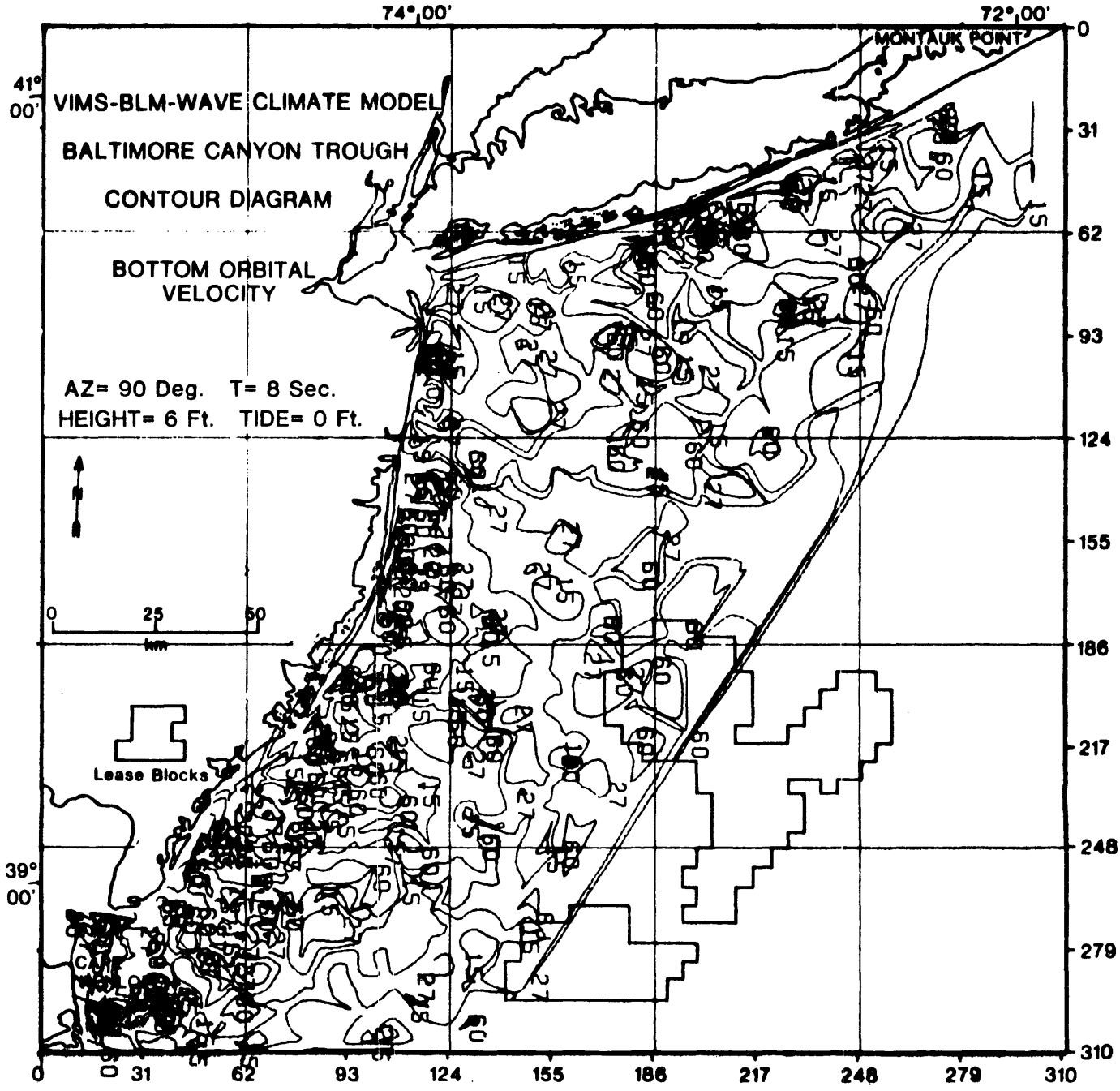

GRID UNITS (1=0.5 NM)

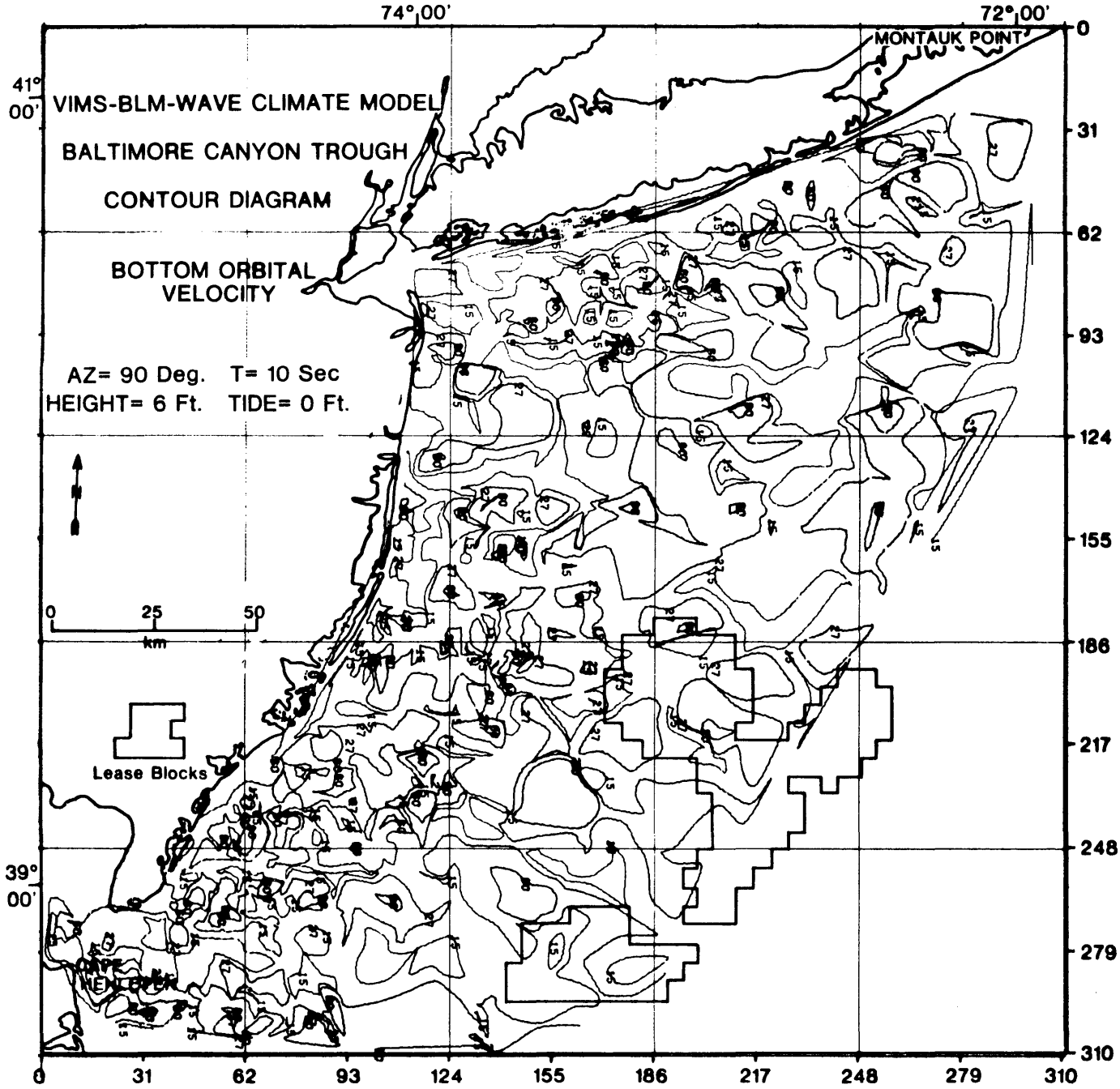
74°00'
72°00'
MONTAUK POINT
41° 00'
VIMS-BLM-WAVE CLIMATE MODEL
BALTIMORE CANYON TROUGH
CONTOUR DIAGRAM
BOTTOM ORBITAL VELOCITY
AZ= 90 Deg. T= 10 Sec
HEIGHT= 6 Ft. TIDE= 0 Ft.
N
0 25 50
km
Lease Blocks
39° 00'
0 31 62 93 124 155 186 217 248 279 310
GRID UNITS (1=0.5 NM)

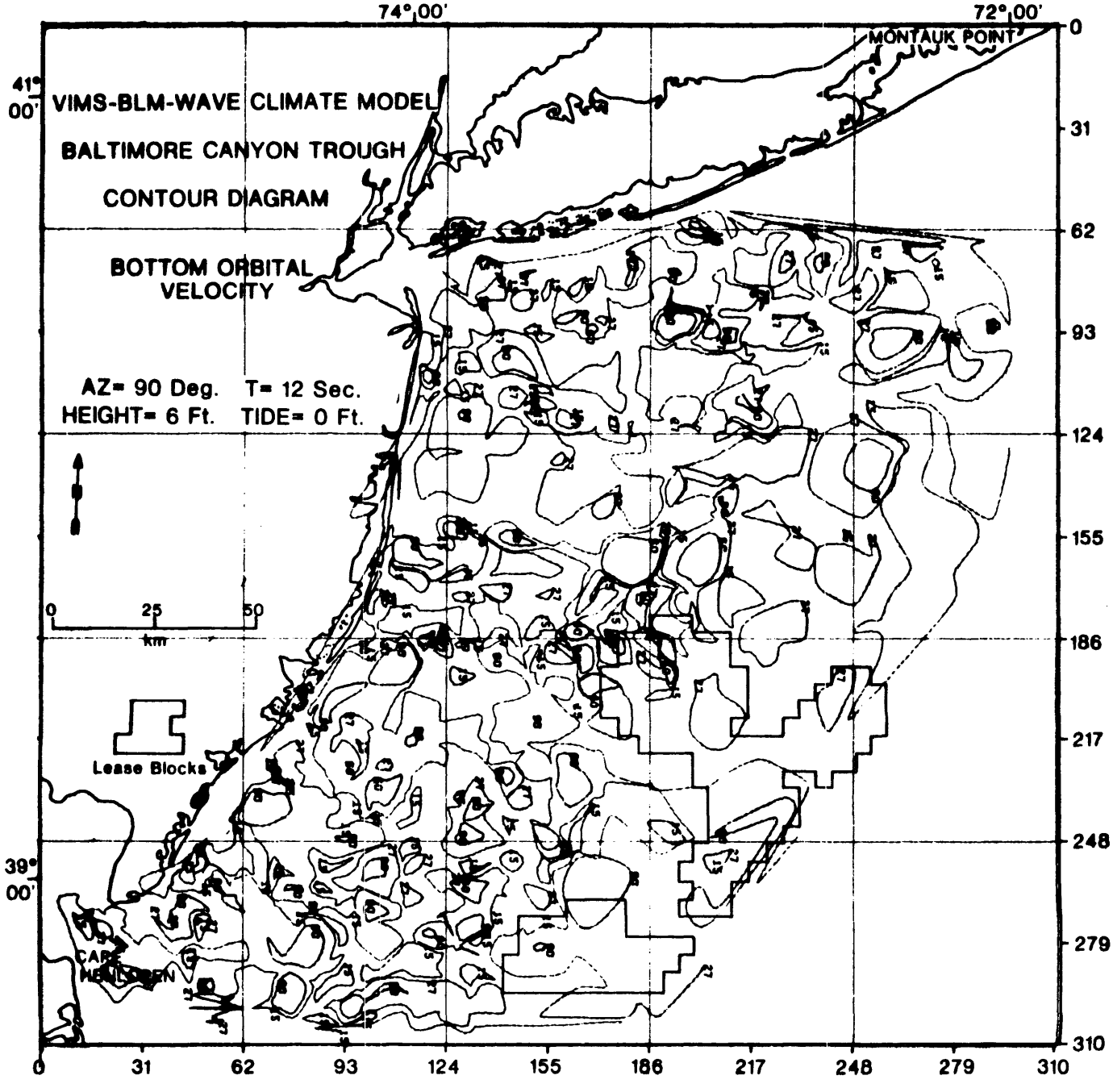
74°00'
72°00'
MONTAUK POINT
41° 00'
VIMS-BLM-WAVE CLIMATE MODEL
BALTIMORE CANYON TROUGH
CONTOUR DIAGRAM
BOTTOM ORBITAL VELOCITY
AZ= 90 Deg. T= 12 Sec.
HEIGHT= 6 Ft. TIDE= 0 Ft.
0 25 50
km
Lease Blocks
39° 00'
CAPE HENLOPEN
0 31 62 93 124 155 186 217 248 279 310
GRID UNITS (1=0.5 NM)

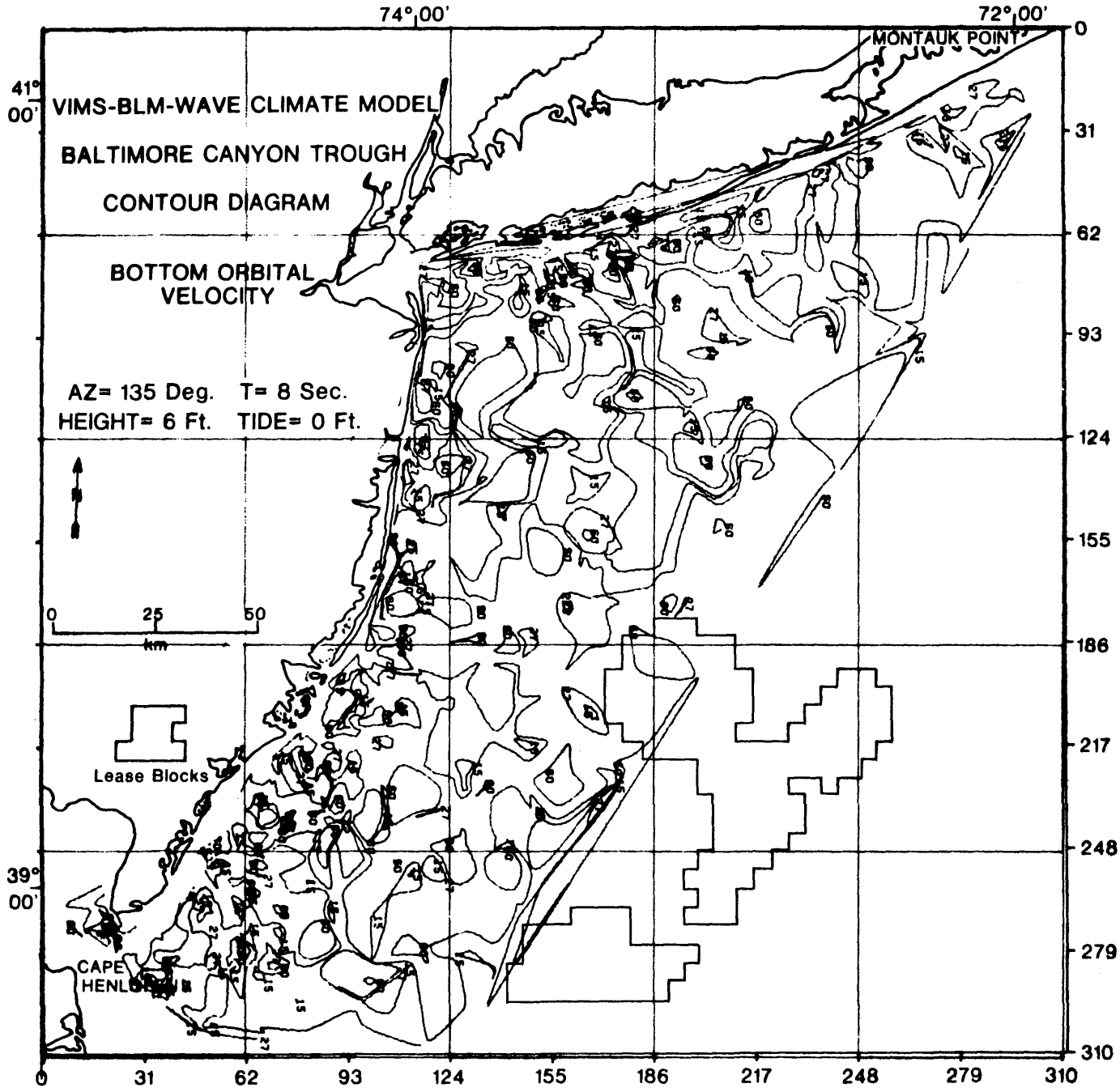

GRID UNITS (1-0.5 NM)

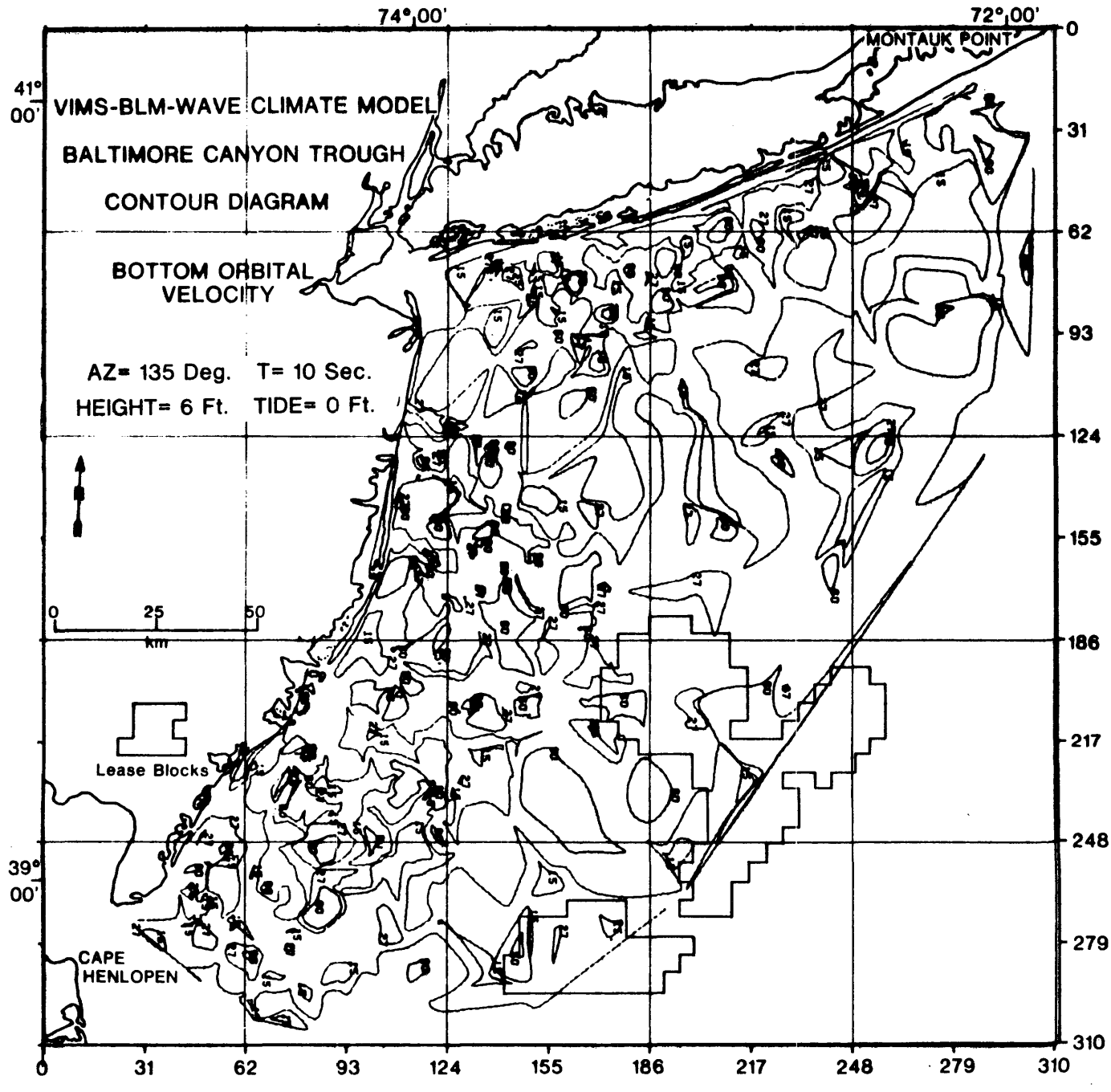

GRID UNITS (1=0.5 NM)

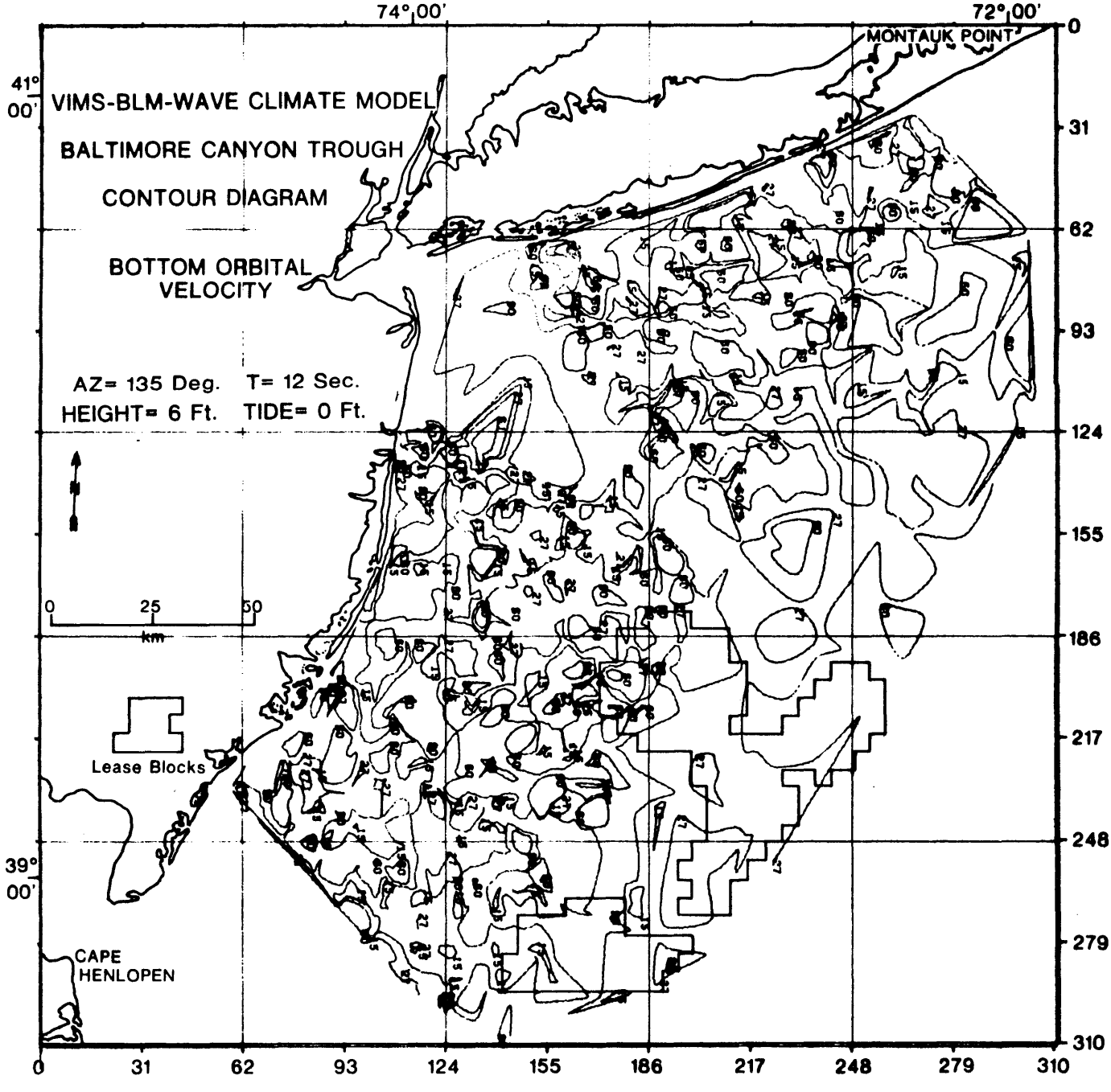

GRID UNITS (1=0.5 NM)

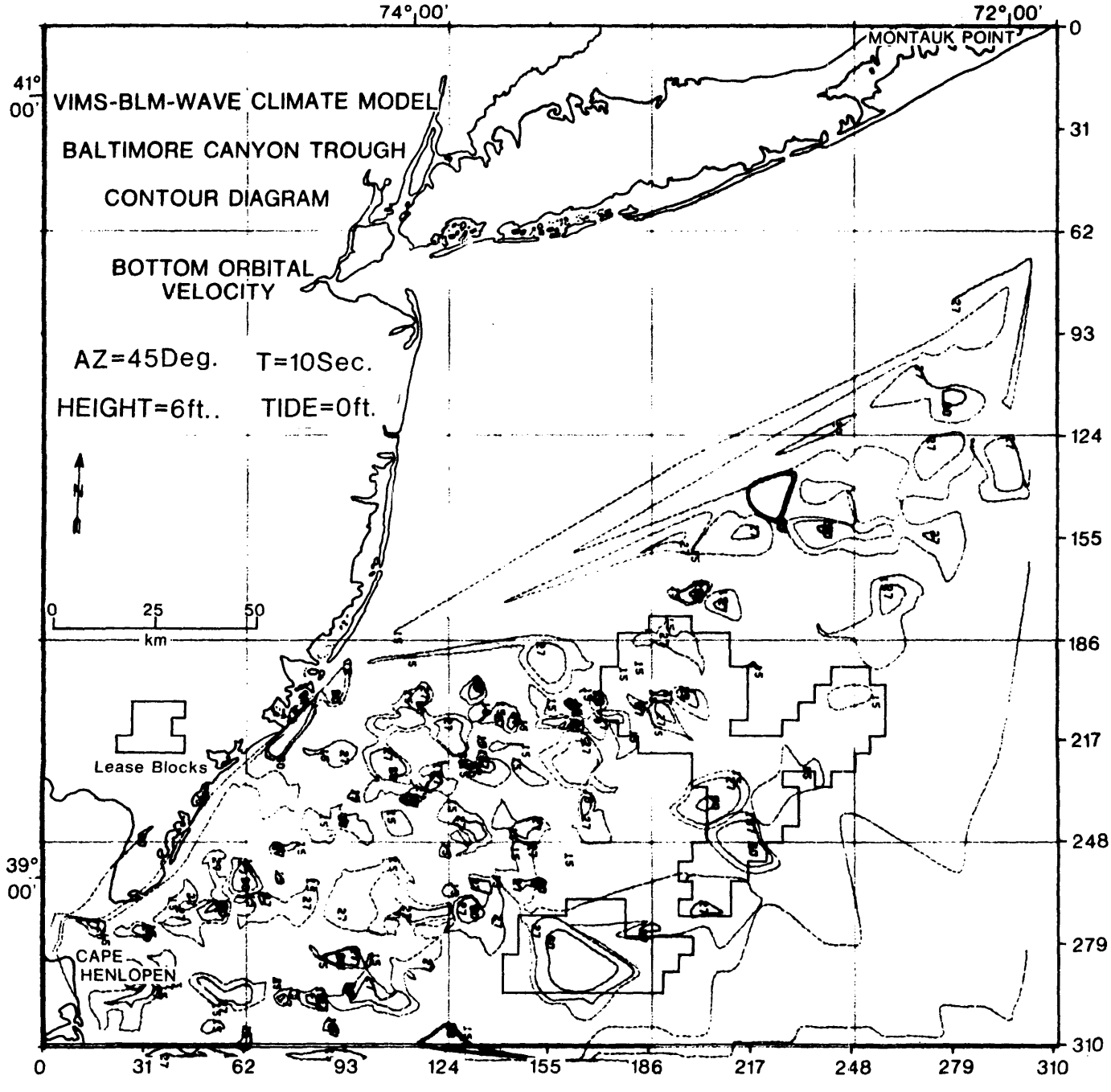
74°00'
72°00'
MONTAUK POINT
41°
00'
VIMS-BLM-WAVE CLIMATE MODEL
BALTIMORE CANYON TROUGH
CONTOUR DIAGRAM
BOTTOM ORBITAL
VELOCITY
AZ=45Deg.
T=10Sec.
HEIGHT=6ft..
TIDE=0ft.
N
0
25
50
km
Lease Blocks
39°
00'
CAPE
HENLOPEN
0
31
62
93
124
155
186
217
248
279
310
GRID UNITS (1=0.5 NM)

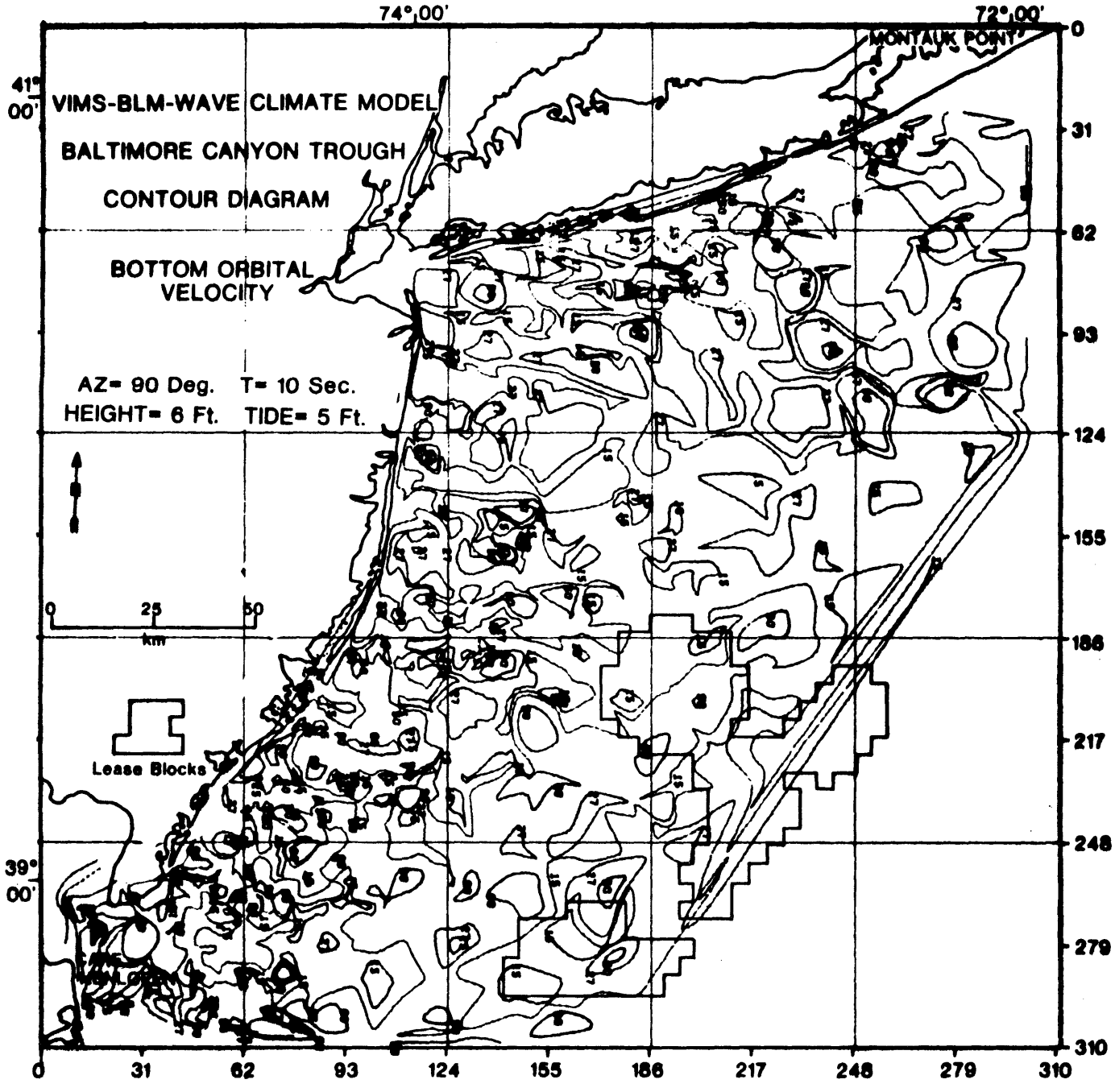
74°00'
72°00'
MONTAUK POINT
41° 00'
VIMS-BLM-WAVE CLIMATE MODEL
BALTIMORE CANYON TROUGH
CONTOUR DIAGRAM
BOTTOM ORBITAL VELOCITY
AZ= 90 Deg. T= 10 Sec.
HEIGHT= 6 Ft. TIDE= 5 Ft.
0 25 50
km
Lease Blocks
39° 00'
0 31 62 93 124 155 186 217 248 279 310
GRID UNITS (1=0.5 NM)

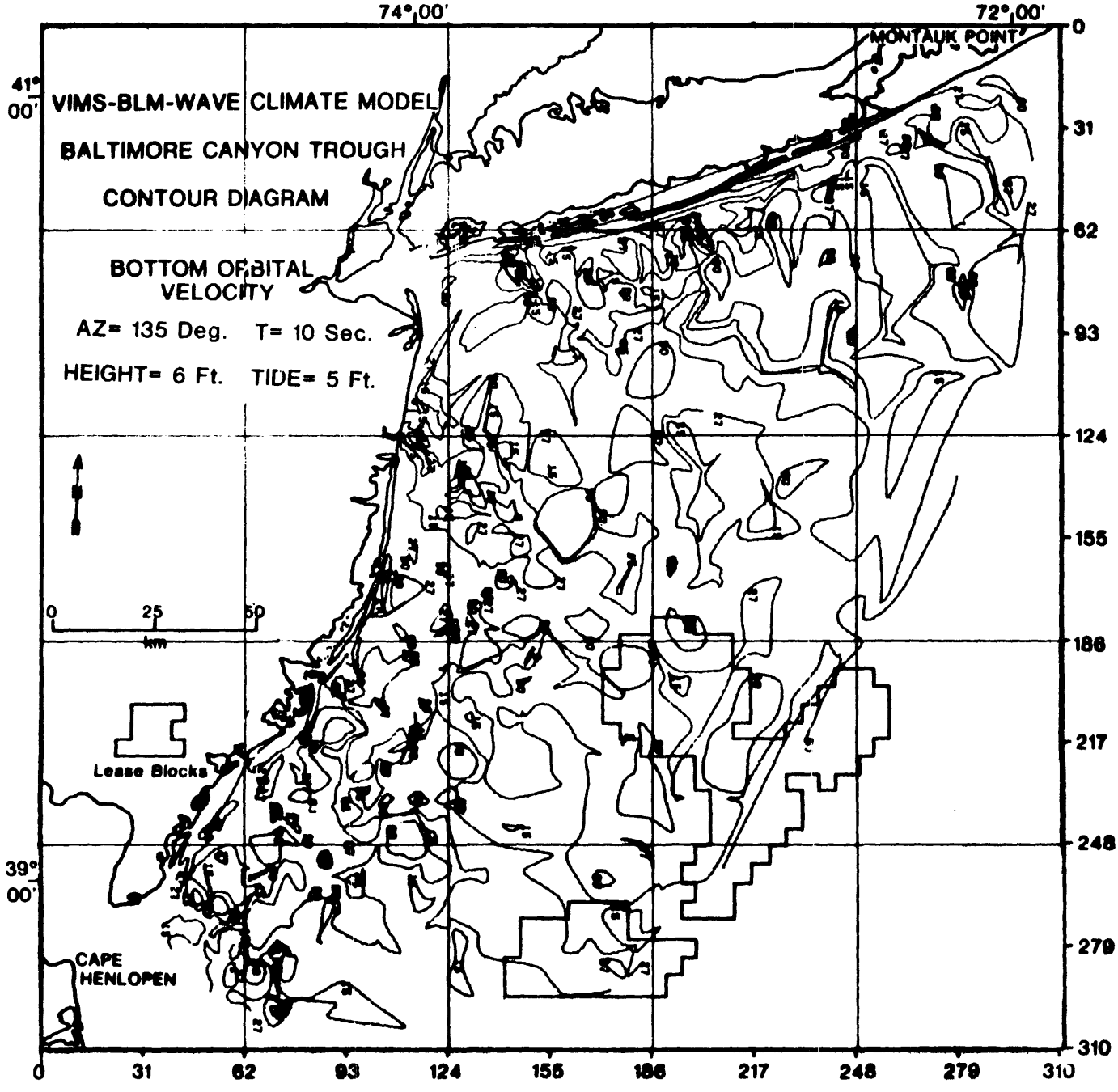
74°00'
72°00'
MONTAUK POINT
41° 00'
VIMS-BLM-WAVE CLIMATE MODEL
BALTIMORE CANYON TROUGH
CONTOUR DIAGRAM
BOTTOM ORBITAL VELOCITY
AZ= 135 Deg. T= 10 Sec.
HEIGHT= 6 Ft. TIDE= 5 Ft.
0 25 50
km
Lease Blocks
39° 00'
CAPE HENLOPEN
0 31 62 93 124 155 186 217 248 279 310
GRID UNITS (1=0.5 NM)

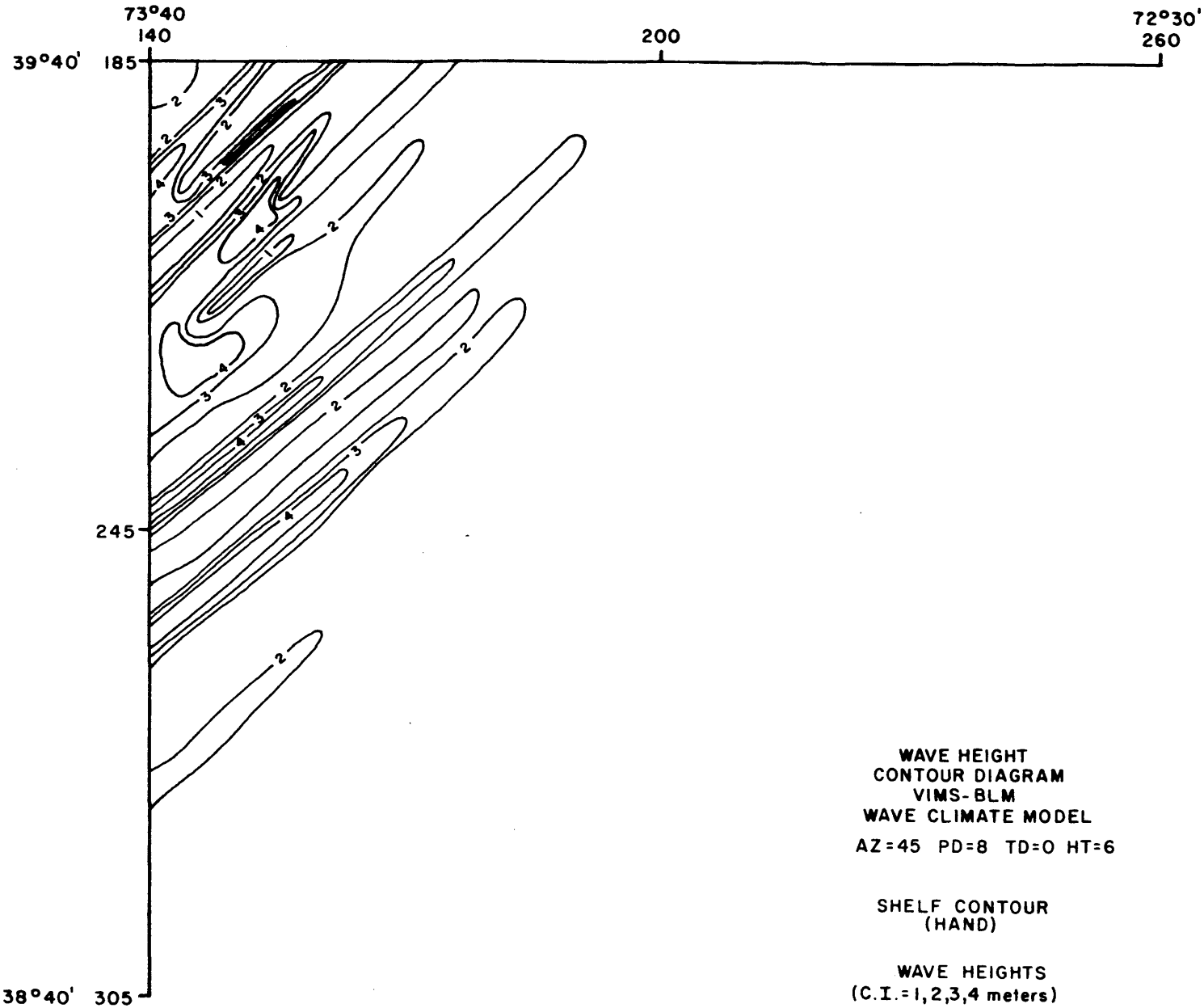
73°40
140
200
72°30'
260
39°40'
185
245
38°40'
305
WAVE HEIGHT
CONTOUR DIAGRAM
VIMS-BLM
WAVE CLIMATE MODEL
AZ=45 PD=8 TD=0 HT=6
SHELF CONTOUR
(HAND)
WAVE HEIGHTS
(C.I.=1,2,3,4 meters)

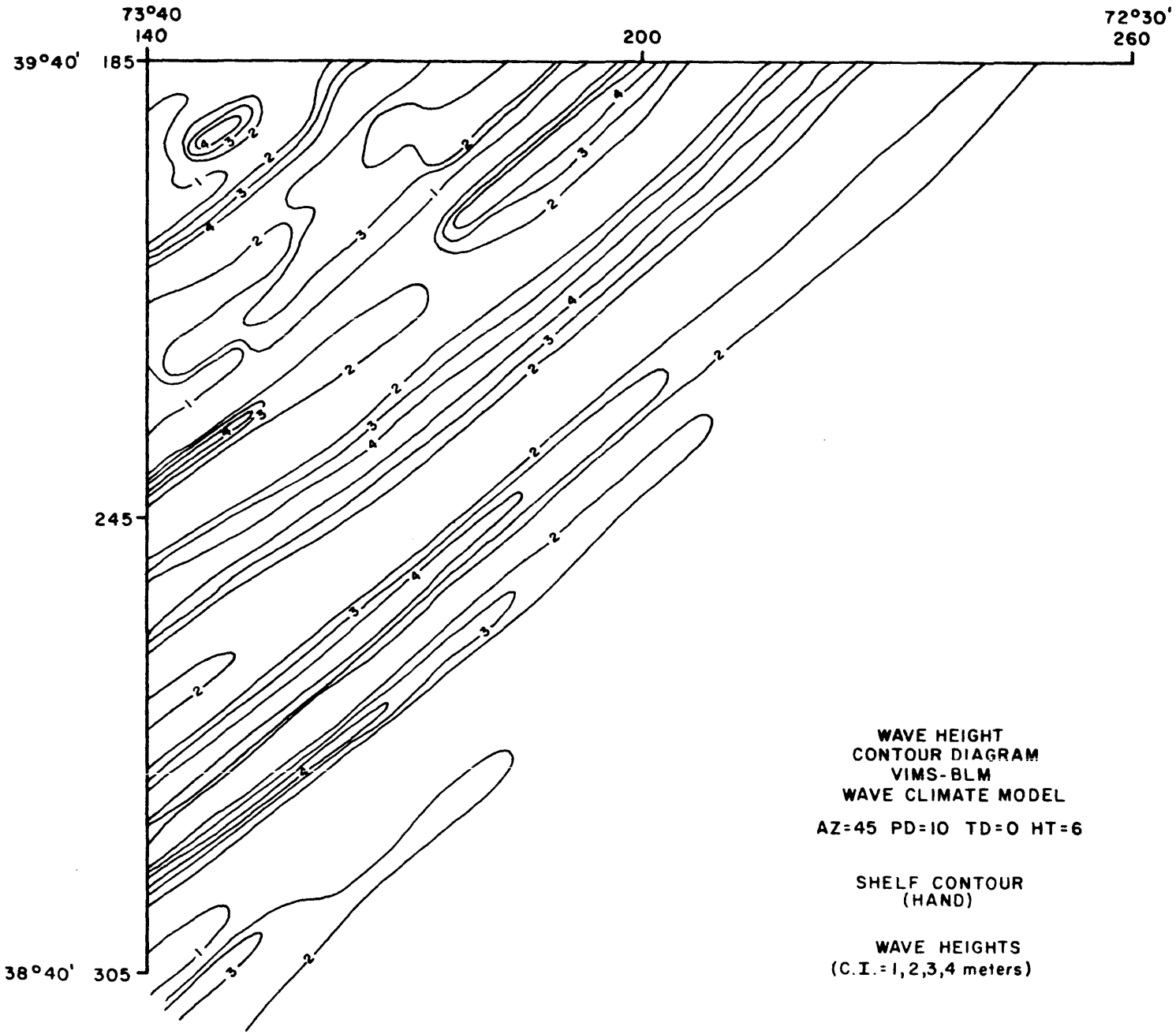
73°40
140
200
72°30'
260
39°40'
185
245
38°40'
305
WAVE HEIGHT
CONTOUR DIAGRAM
VIMS-BLM
WAVE CLIMATE MODEL
AZ=45 PD=10 TD=0 HT=6
SHELF CONTOUR
(HAND)
WAVE HEIGHTS
(C.I.=1,2,3,4 meters)

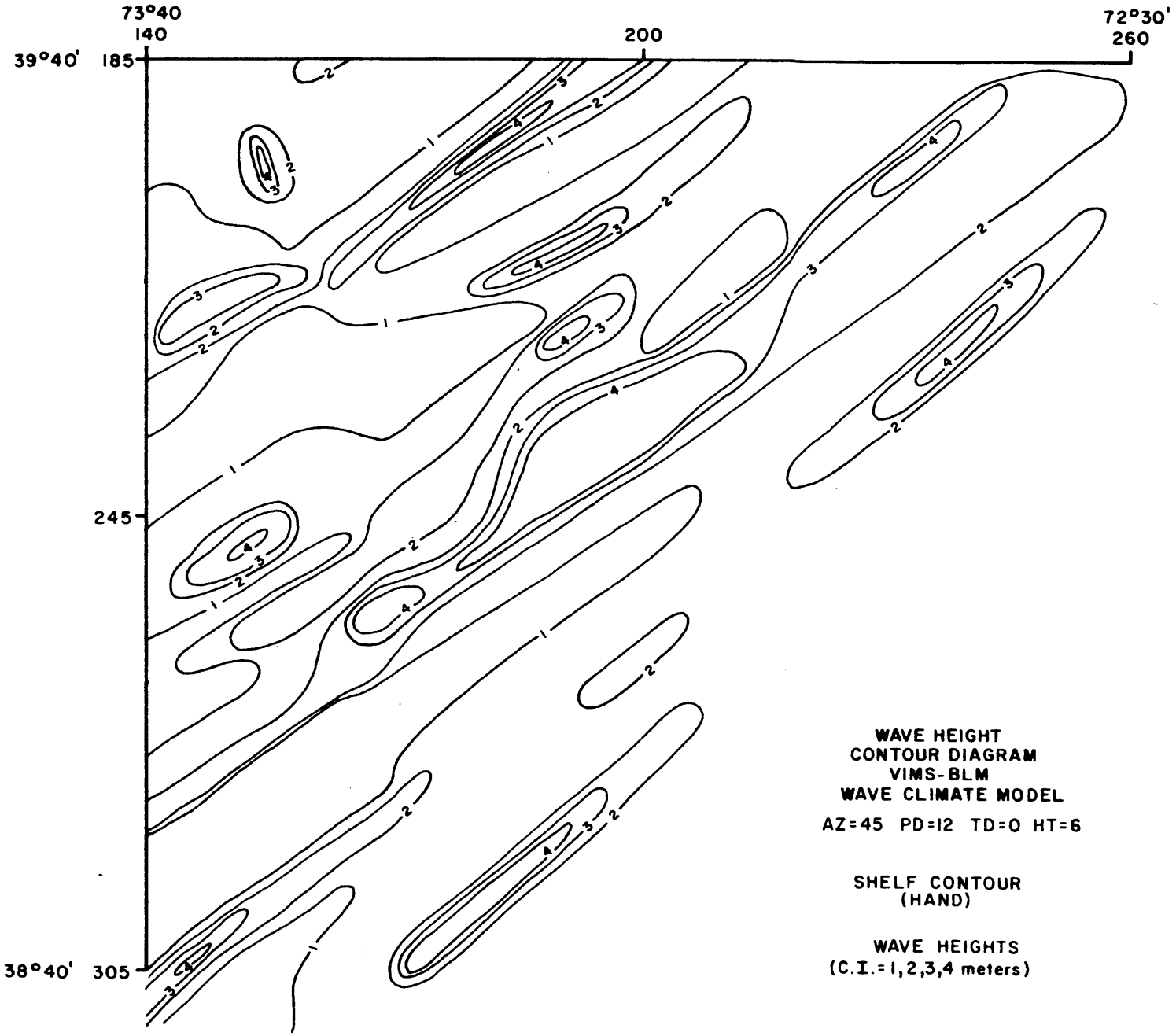
73°40
140
200
72°30'
260
39°40'
185
245
38°40'
305
WAVE HEIGHT
CONTOUR DIAGRAM
VIMS-BLM
WAVE CLIMATE MODEL
AZ=45 PD=12 TD=0 HT=6
SHELF CONTOUR
(HAND)
WAVE HEIGHTS
(C.I.=1,2,3,4 meters)

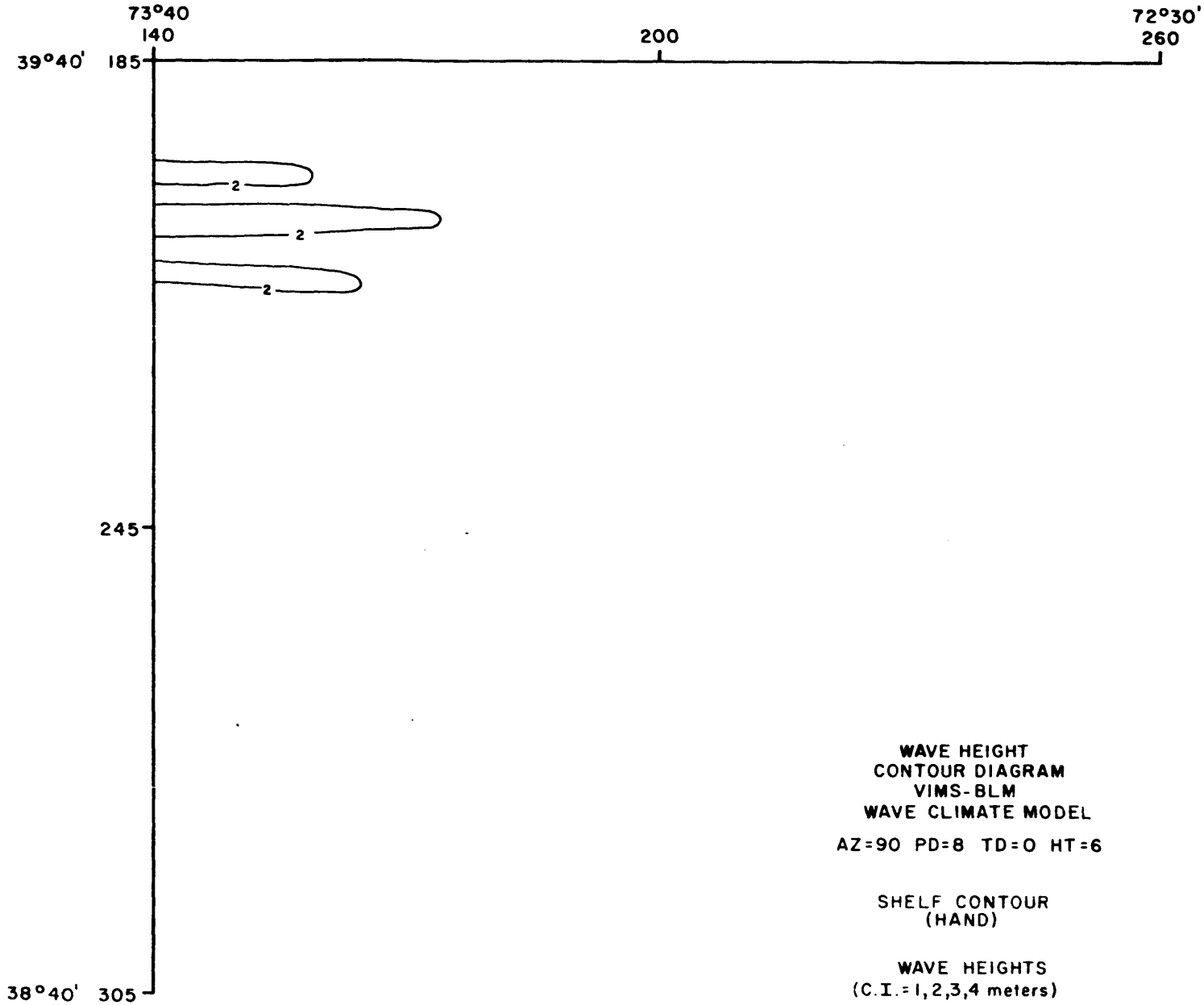

WAVE HEIGHT
CONTOUR DIAGRAM
VIMS-BLM
WAVE CLIMATE MODEL

AZ=90 PD=8 TD=0 HT=6

SHELF CONTOUR
(HAND)

WAVE HEIGHTS
(C.I.=1,2,3,4 meters)

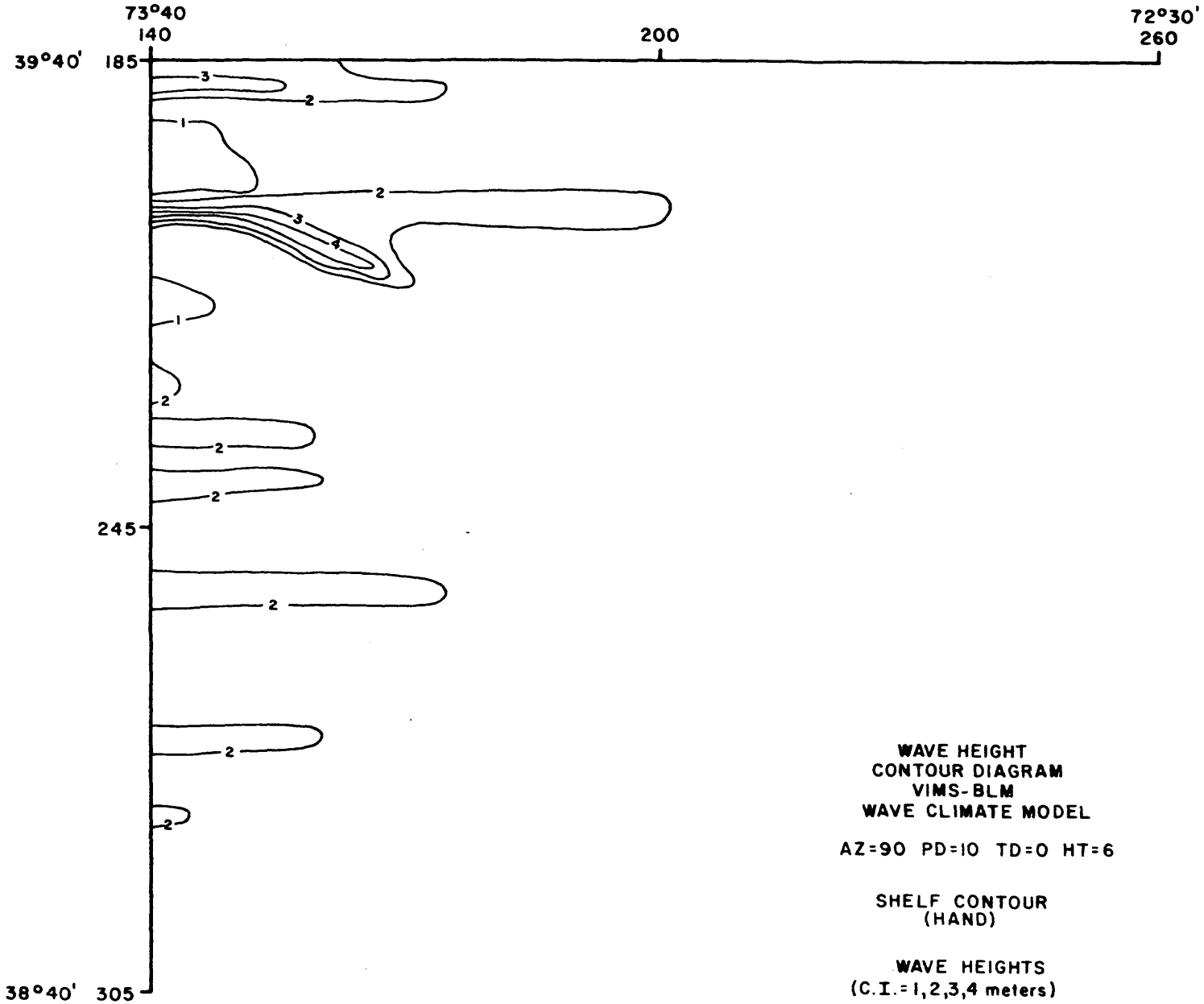
73°40
140
200
72°30'
260
39°40'
185
245
38°40'
305
3
2
1
2
3
4
1
2
2
2
2
2
2
2
WAVE HEIGHT
CONTOUR DIAGRAM
VIMS-BLM
WAVE CLIMATE MODEL
AZ=90 PD=10 TD=0 HT=6
SHELF CONTOUR
(HAND)
WAVE HEIGHTS
(C.I.=1,2,3,4 meters)

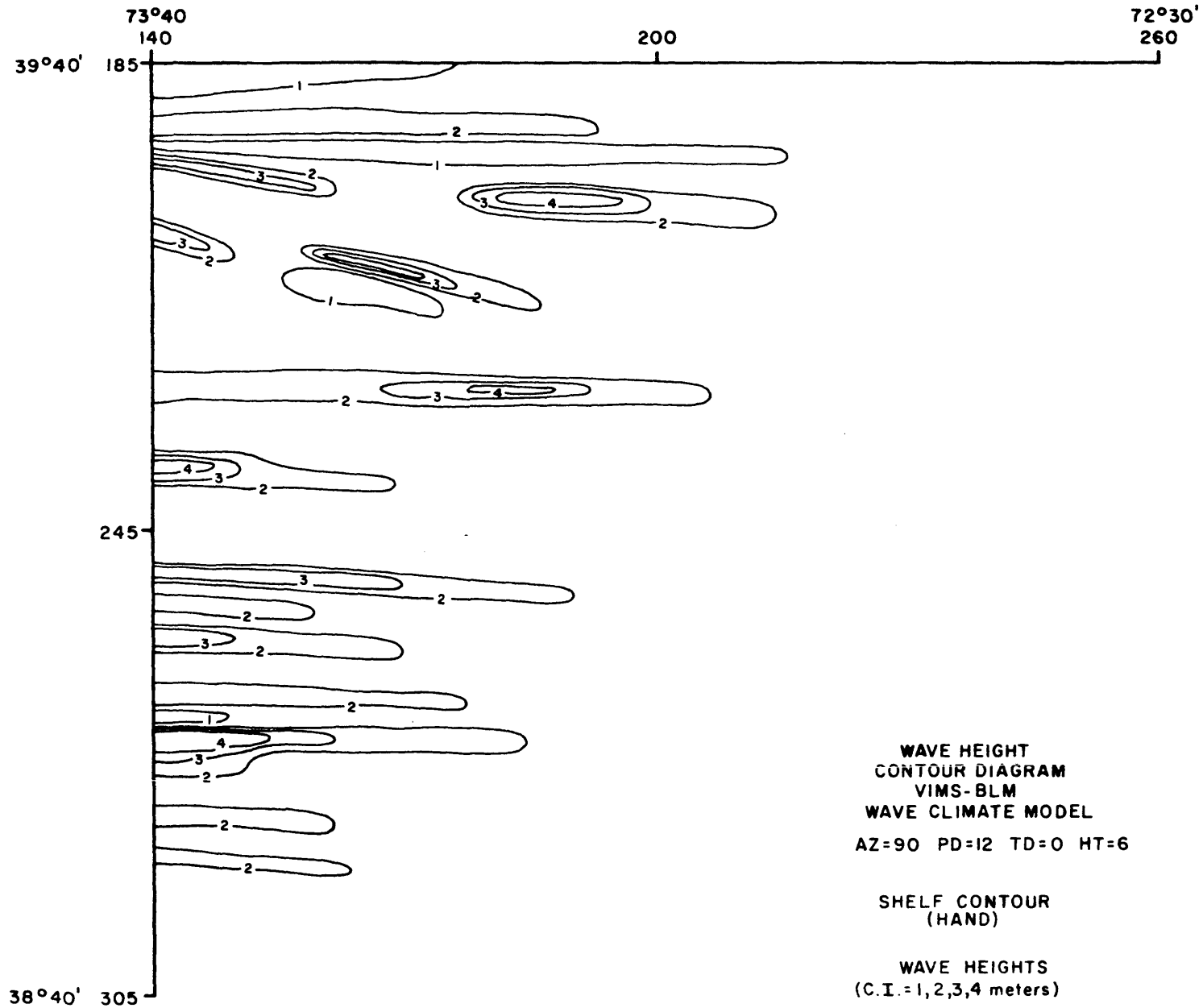
73°40
140
200
72°30'
260
39°40'
185
245
38°40'
305
WAVE HEIGHT
CONTOUR DIAGRAM
VIMS-BLM
WAVE CLIMATE MODEL
AZ=90 PD=12 TD=0 HT=6
SHELF CONTOUR
(HAND)
WAVE HEIGHTS
(C.I.=1,2,3,4 meters)

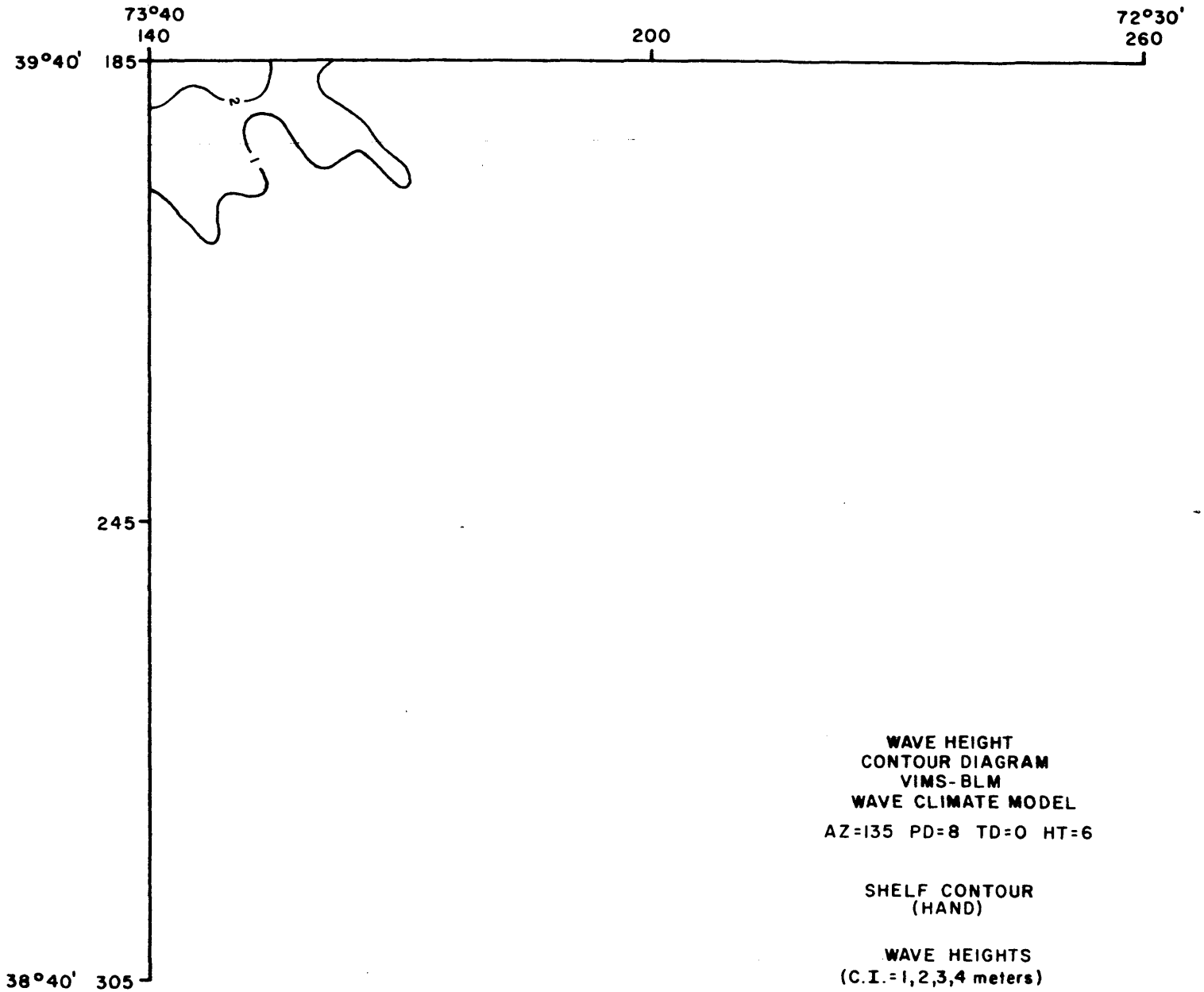

WAVE HEIGHT
CONTOUR DIAGRAM
VIMS-BLM
WAVE CLIMATE MODEL

AZ=135 PD=8 TD=0 HT=6

SHELF CONTOUR
(HAND)

WAVE HEIGHTS
(C.I.=1,2,3,4 meters)

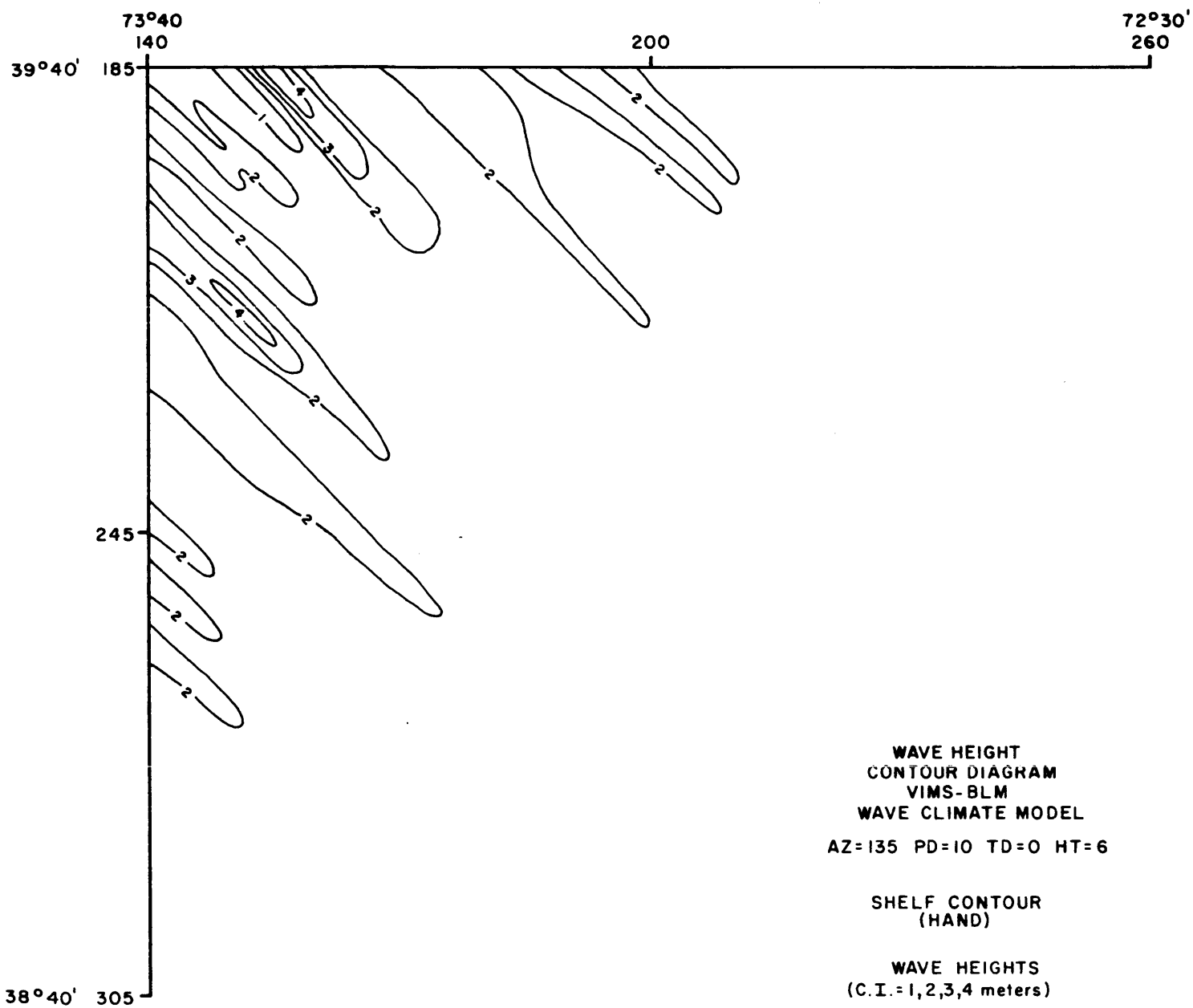

WAVE HEIGHT
CONTOUR DIAGRAM
VIMS-BLM
WAVE CLIMATE MODEL

AZ=135 PD=10 TD=0 HT=6

SHELF CONTOUR
(HAND)

WAVE HEIGHTS
(C.I.=1,2,3,4 meters)

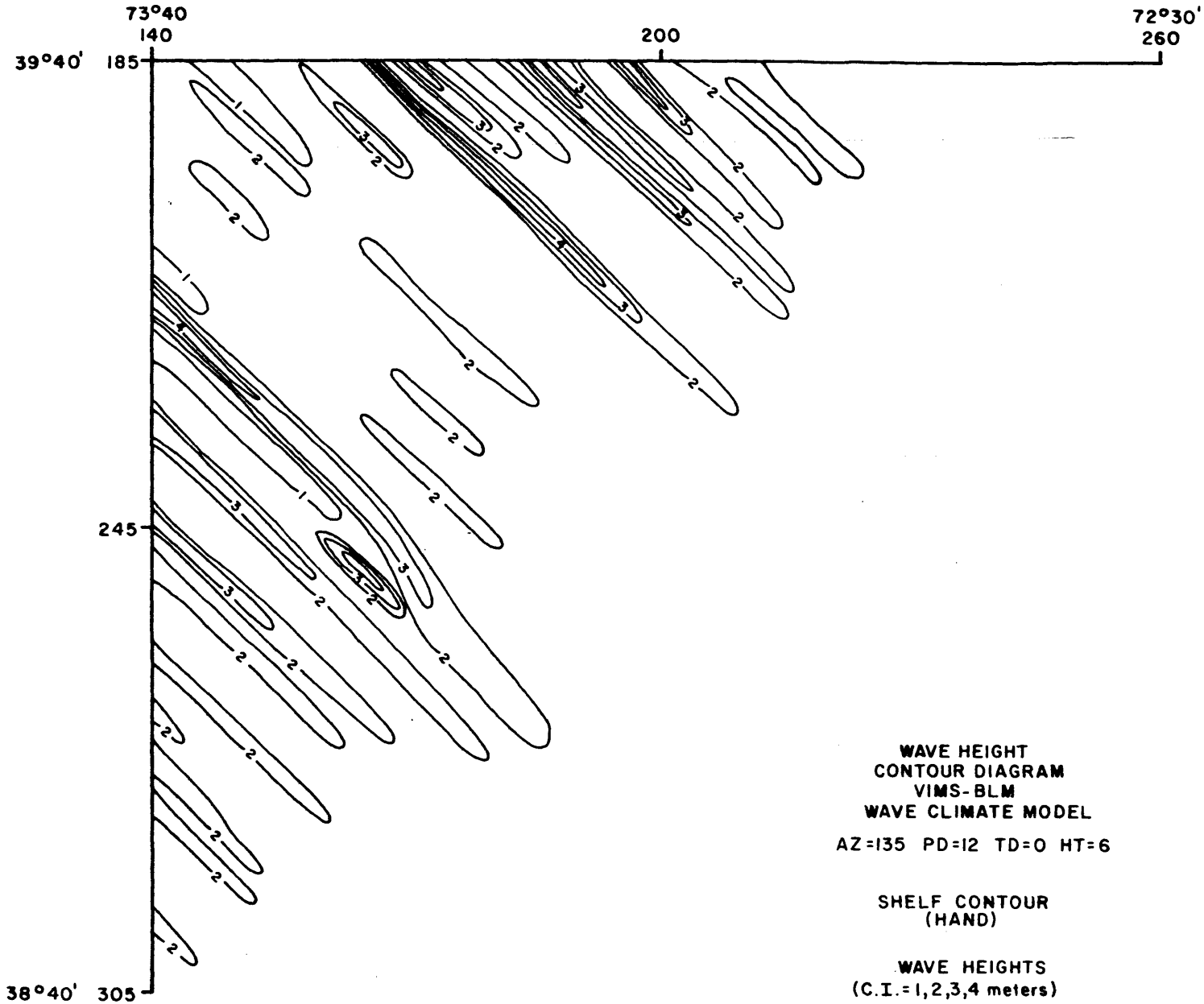
73°40
140
200
72°30'
260
39°40'
185
245
38°40'
305
WAVE HEIGHT
CONTOUR DIAGRAM
VIMS-BLM
WAVE CLIMATE MODEL
AZ=135 PD=12 TD=0 HT=6
SHELF CONTOUR
(HAND)
WAVE HEIGHTS
(C.I.=1,2,3,4 meters)

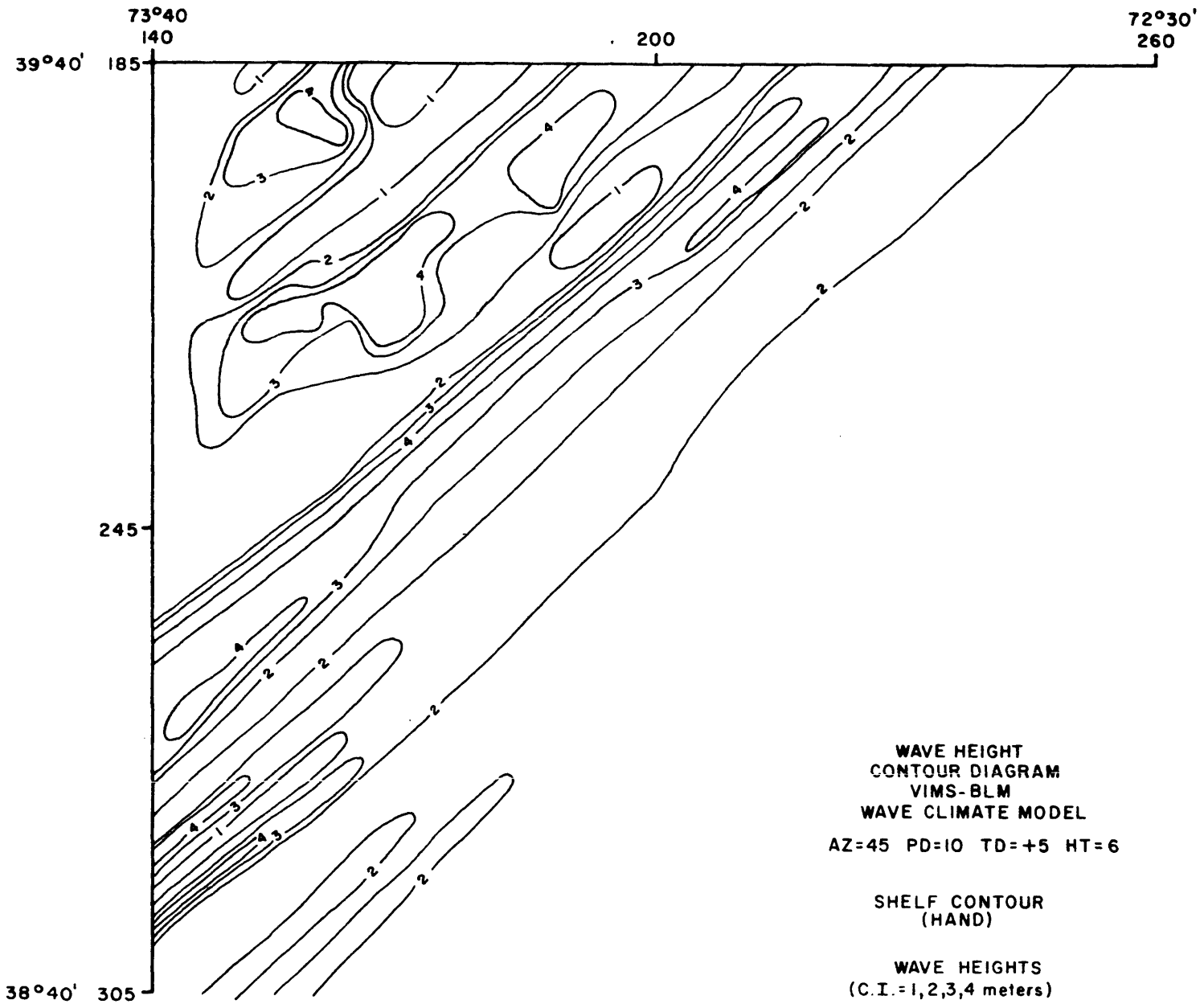
73°40
140
200
72°30'
260
39°40'
185
245
38°40'
305
WAVE HEIGHT
CONTOUR DIAGRAM
VIMS-BLM
WAVE CLIMATE MODEL
AZ=45 PD=10 TD=+5 HT=6
SHELF CONTOUR
(HAND)
WAVE HEIGHTS
(C.I.=1,2,3,4 meters)

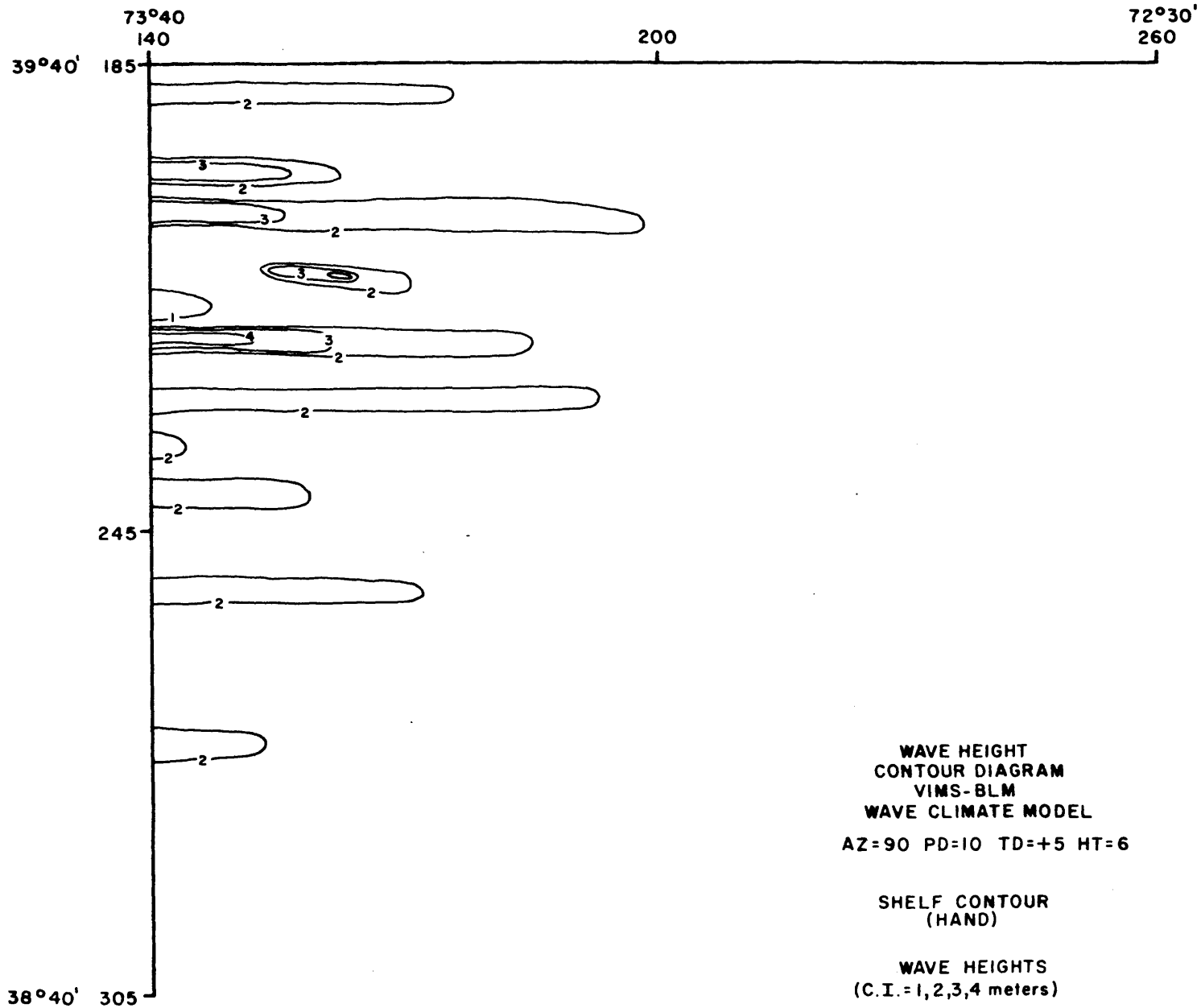

WAVE HEIGHT
CONTOUR DIAGRAM
VIMS-BLM
WAVE CLIMATE MODEL

AZ=90 PD=10 TD=+5 HT=6

SHELF CONTOUR
(HAND)

WAVE HEIGHTS
(C.I.=1,2,3,4 meters)

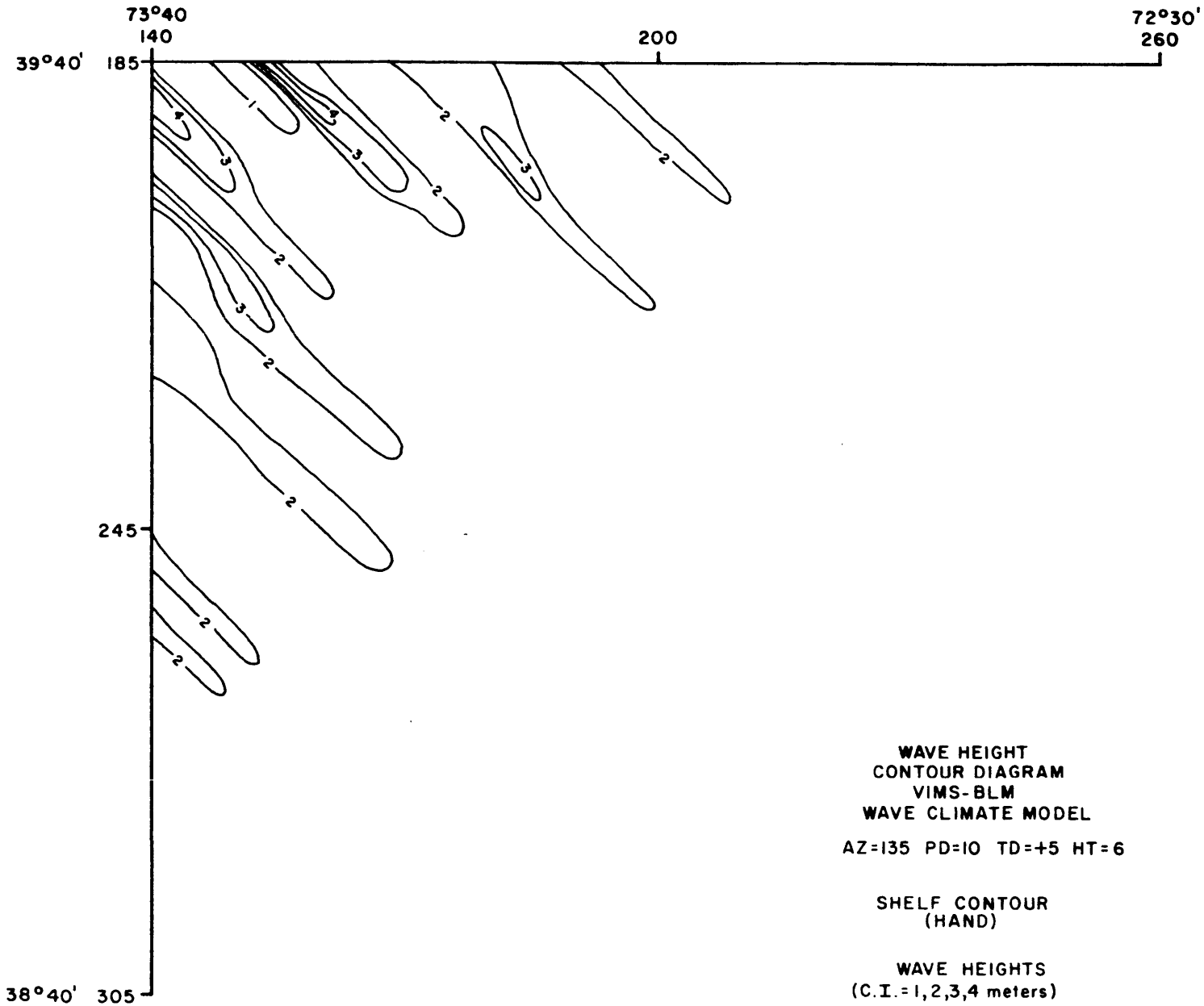
73°40
140
200
72°30'
260
39°40'
185
245
38°40'
305
WAVE HEIGHT
CONTOUR DIAGRAM
VIMS-BLM
WAVE CLIMATE MODEL
AZ=135 PD=10 TD=+5 HT=6
SHELF CONTOUR
(HAND)
WAVE HEIGHTS
(C.I.=1,2,3,4 meters)

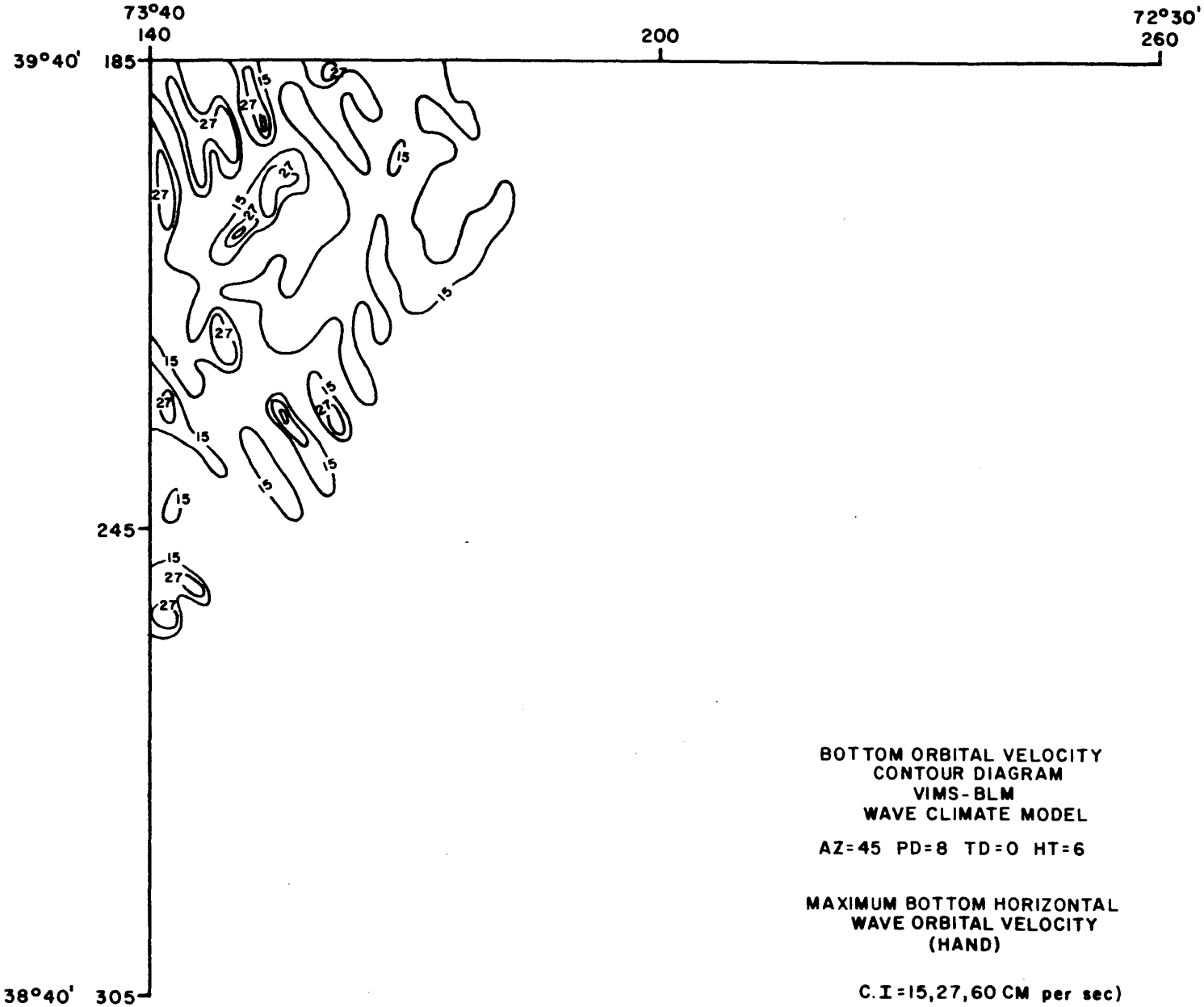

BOTTOM ORBITAL VELOCITY
CONTOUR DIAGRAM
VIMS-BLM
WAVE CLIMATE MODEL

AZ=45 PD=8 TD=0 HT=6

MAXIMUM BOTTOM HORIZONTAL
WAVE ORBITAL VELOCITY
(HAND)

C.I=15,27,60 CM per sec)

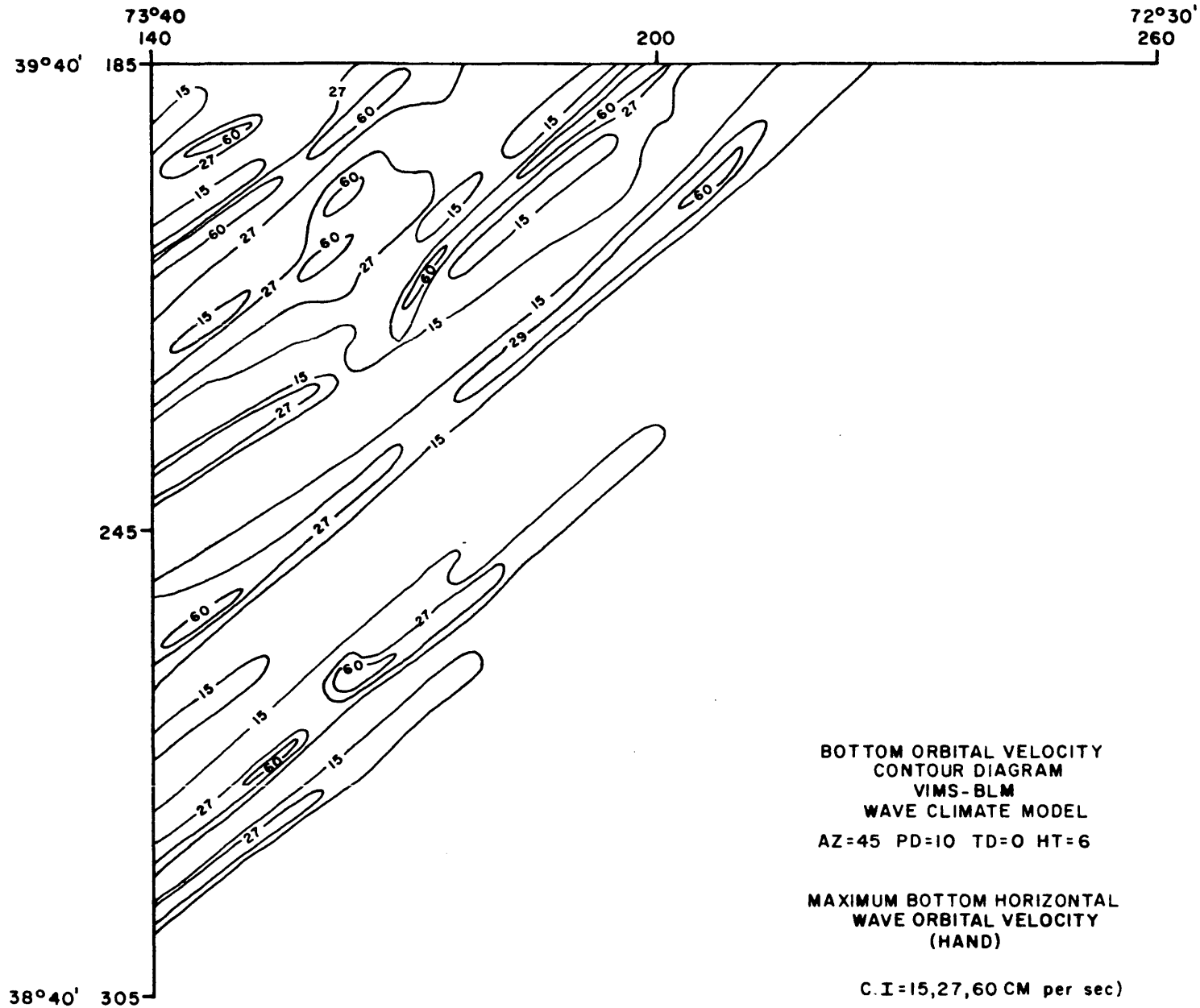

BOTTOM ORBITAL VELOCITY
CONTOUR DIAGRAM
VIMS-BLM
WAVE CLIMATE MODEL

AZ=45 PD=10 TD=0 HT=6

MAXIMUM BOTTOM HORIZONTAL
WAVE ORBITAL VELOCITY
(HAND)

C.I=15,27,60 CM per sec)

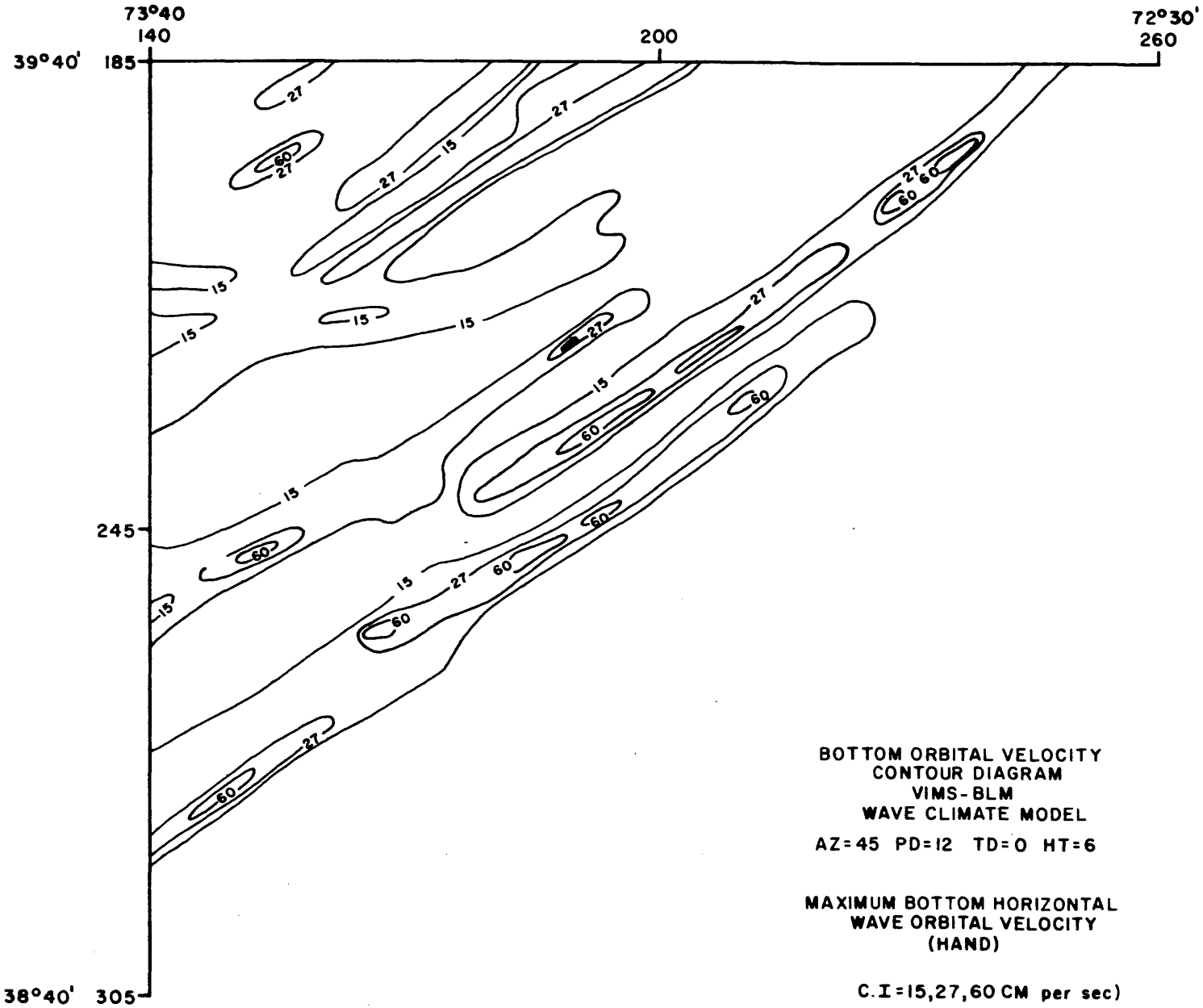

BOTTOM ORBITAL VELOCITY
CONTOUR DIAGRAM
VIMS-BLM
WAVE CLIMATE MODEL

AZ=45 PD=12 TD=0 HT=6

MAXIMUM BOTTOM HORIZONTAL
WAVE ORBITAL VELOCITY
(HAND)

C.I=15,27,60 CM per sec)

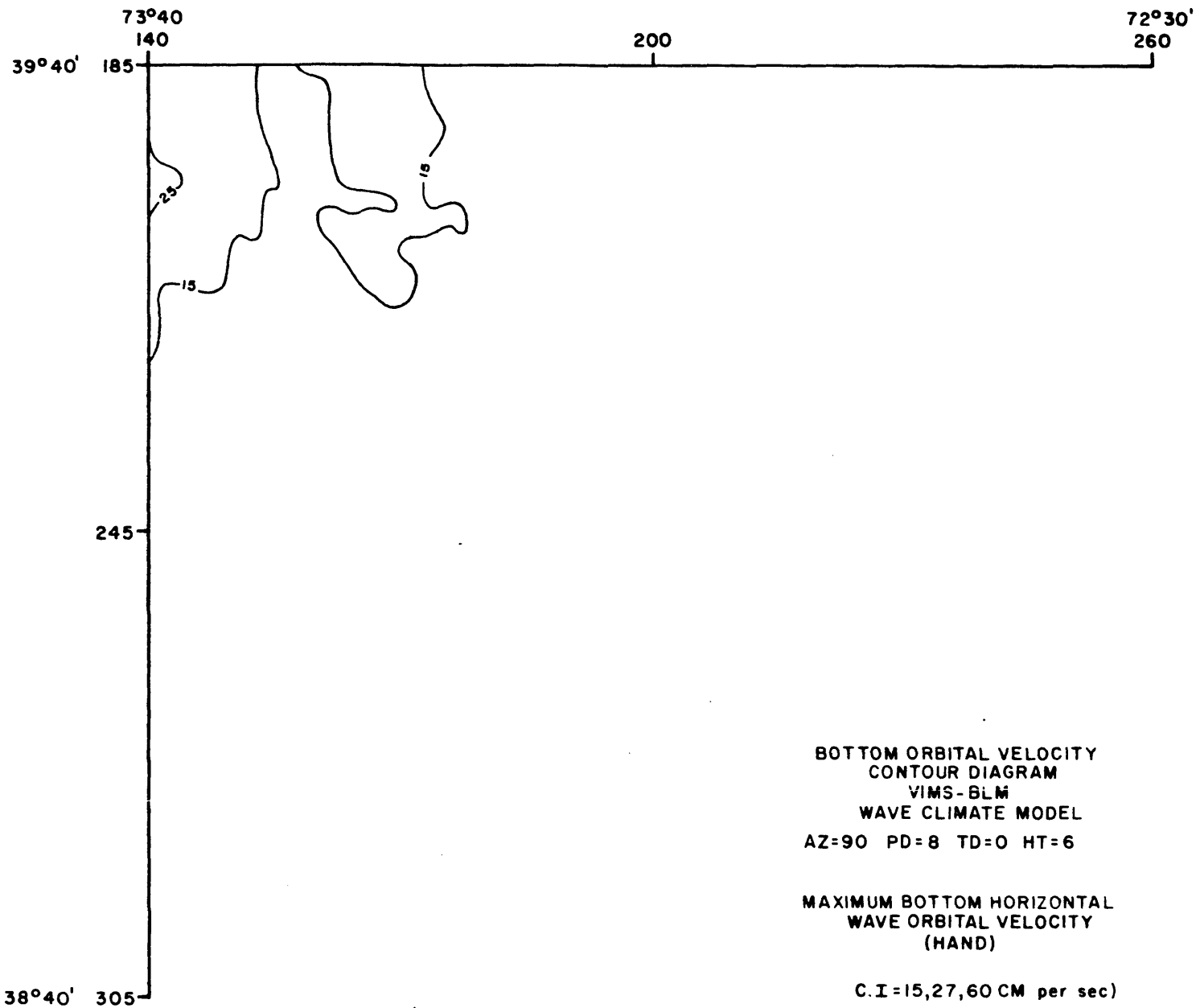

BOTTOM ORBITAL VELOCITY
CONTOUR DIAGRAM
VIMS-BLM
WAVE CLIMATE MODEL
AZ=90 PD=8 TD=0 HT=6

MAXIMUM BOTTOM HORIZONTAL
WAVE ORBITAL VELOCITY
(HAND)

C.I=15,27,60 CM per sec)

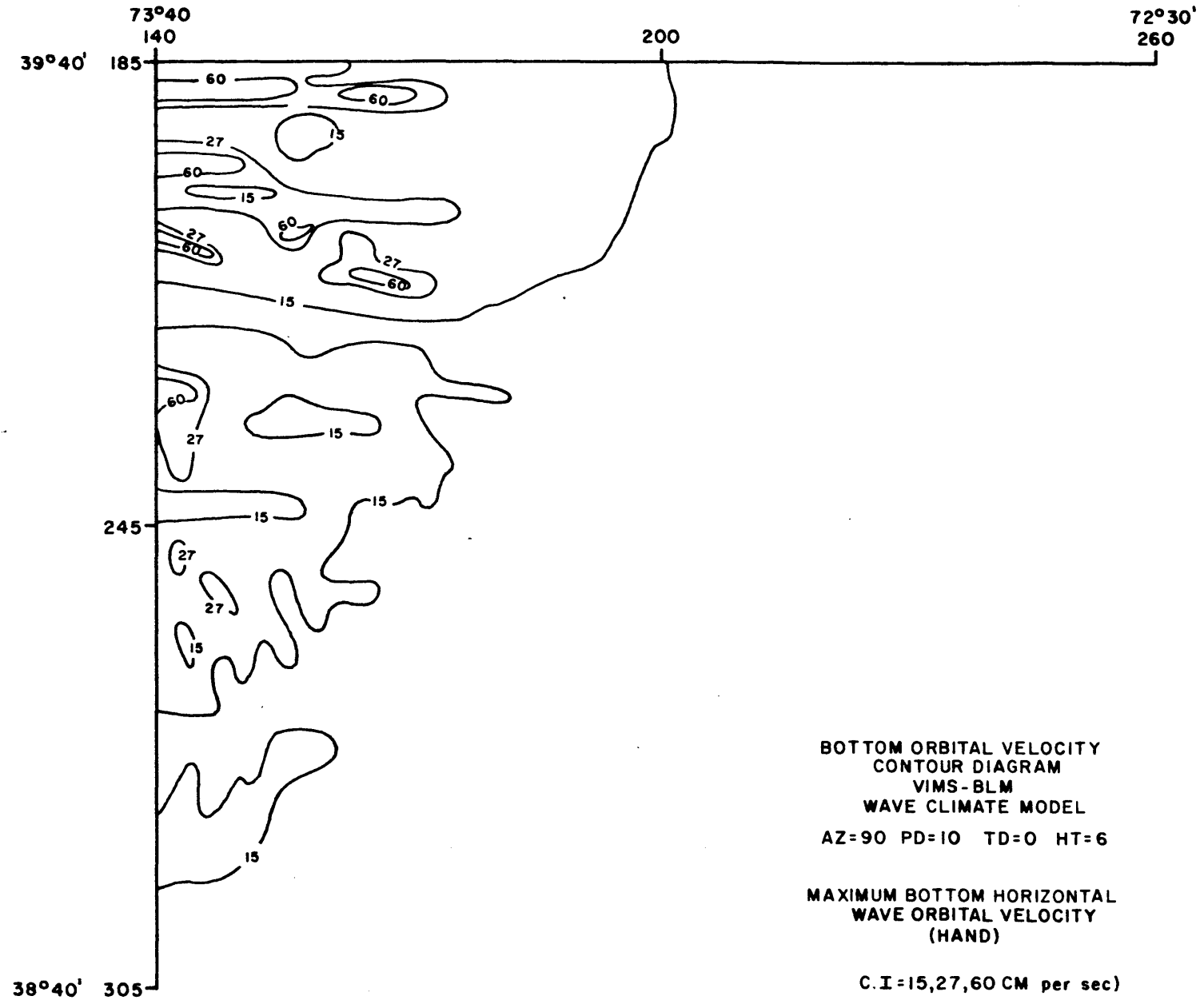

BOTTOM ORBITAL VELOCITY
CONTOUR DIAGRAM
VIMS-BLM
WAVE CLIMATE MODEL

AZ=90 PD=10 TD=0 HT=6

MAXIMUM BOTTOM HORIZONTAL
WAVE ORBITAL VELOCITY
(HAND)

C.I=15,27,60 CM per sec)

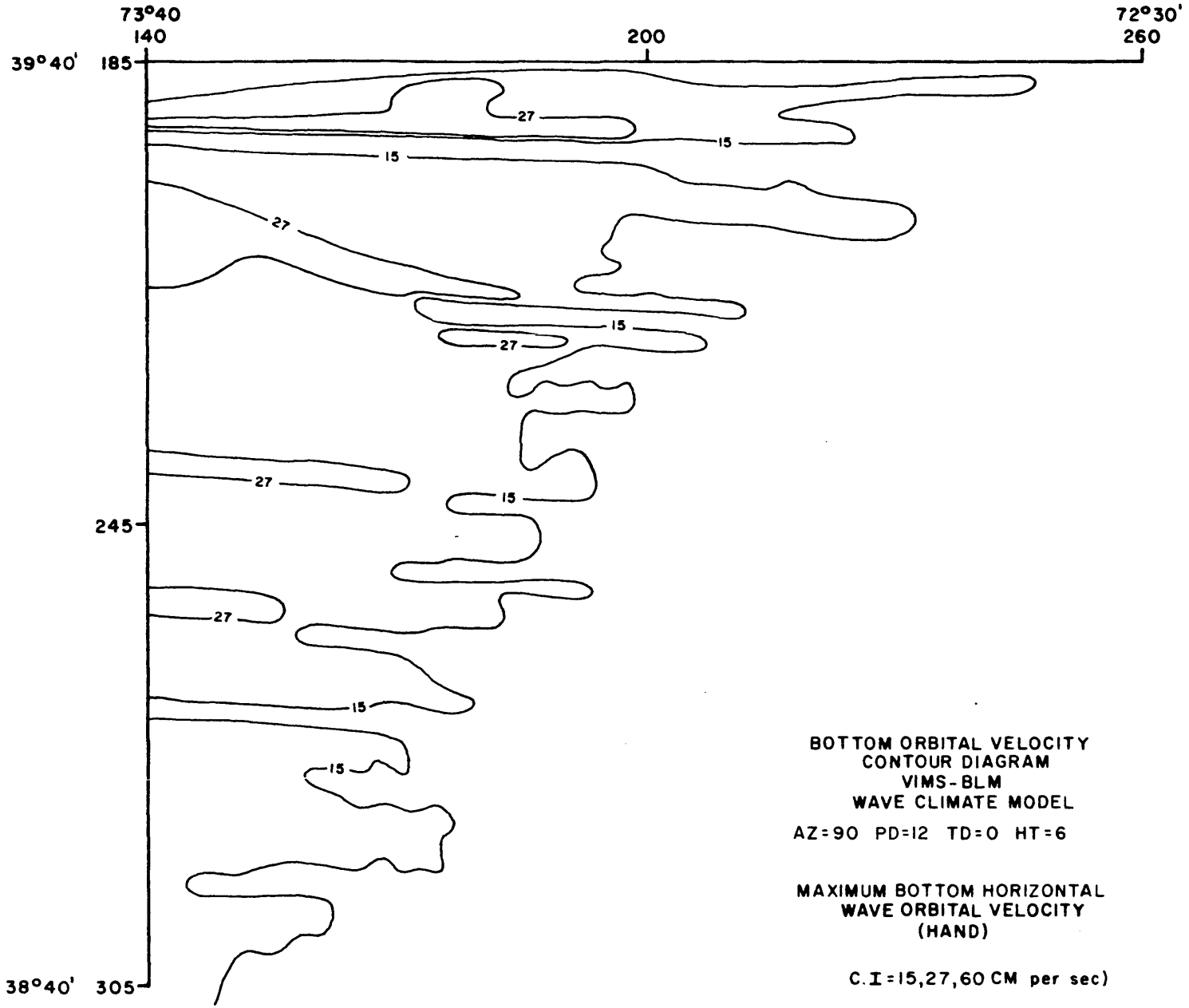
73°40
140
200
72°30'
260
39°40'
185
245
38°40'
305
27
15
BOTTOM ORBITAL VELOCITY
CONTOUR DIAGRAM
VIMS-BLM
WAVE CLIMATE MODEL
AZ=90 PD=12 TD=0 HT=6
MAXIMUM BOTTOM HORIZONTAL
WAVE ORBITAL VELOCITY
(HAND)
C.I=15,27,60 CM per sec)

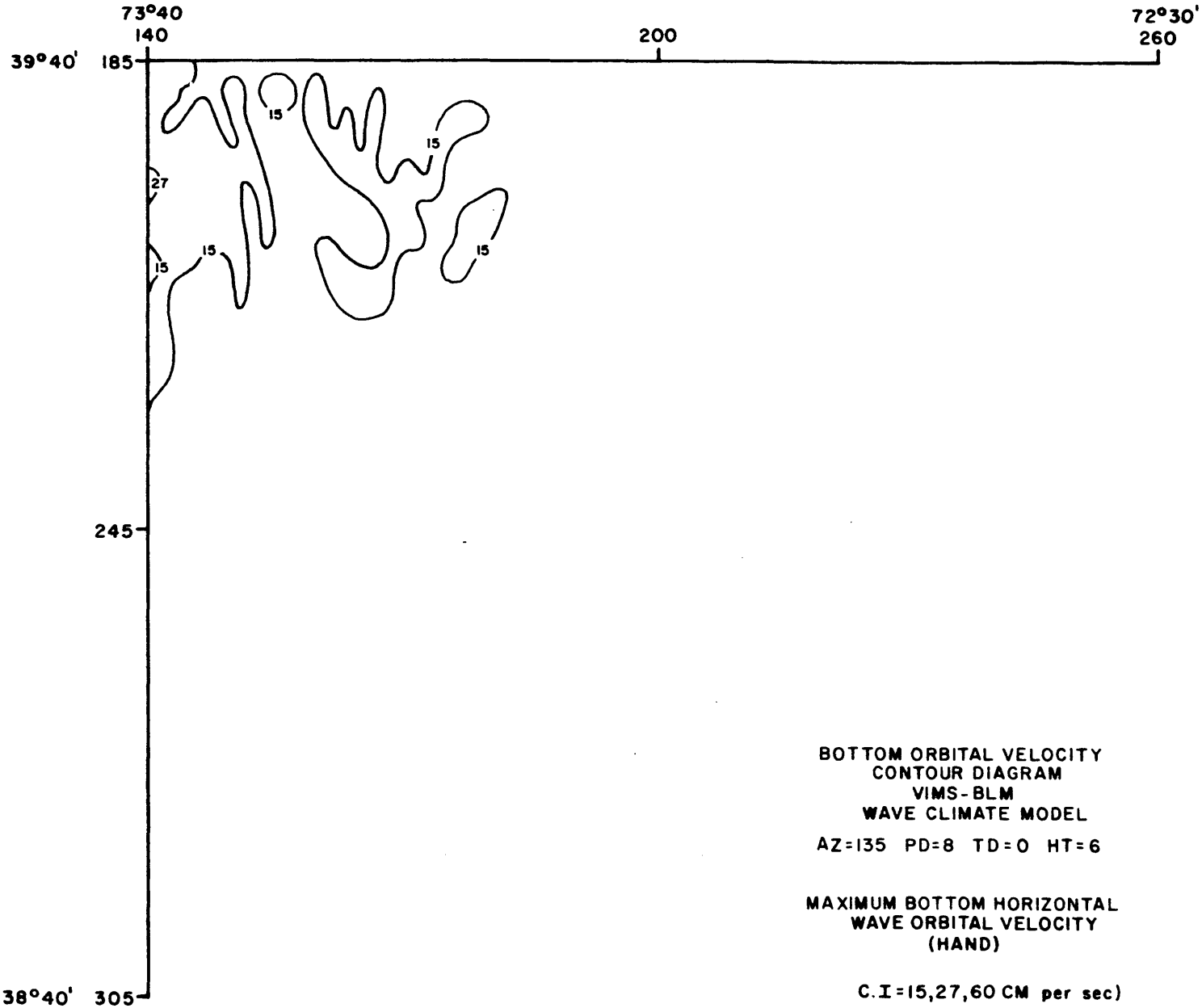

BOTTOM ORBITAL VELOCITY
CONTOUR DIAGRAM
VIMS-BLM
WAVE CLIMATE MODEL

AZ=135 PD=8 TD=0 HT=6

MAXIMUM BOTTOM HORIZONTAL
WAVE ORBITAL VELOCITY
(HAND)

C.I=15,27,60 CM per sec)

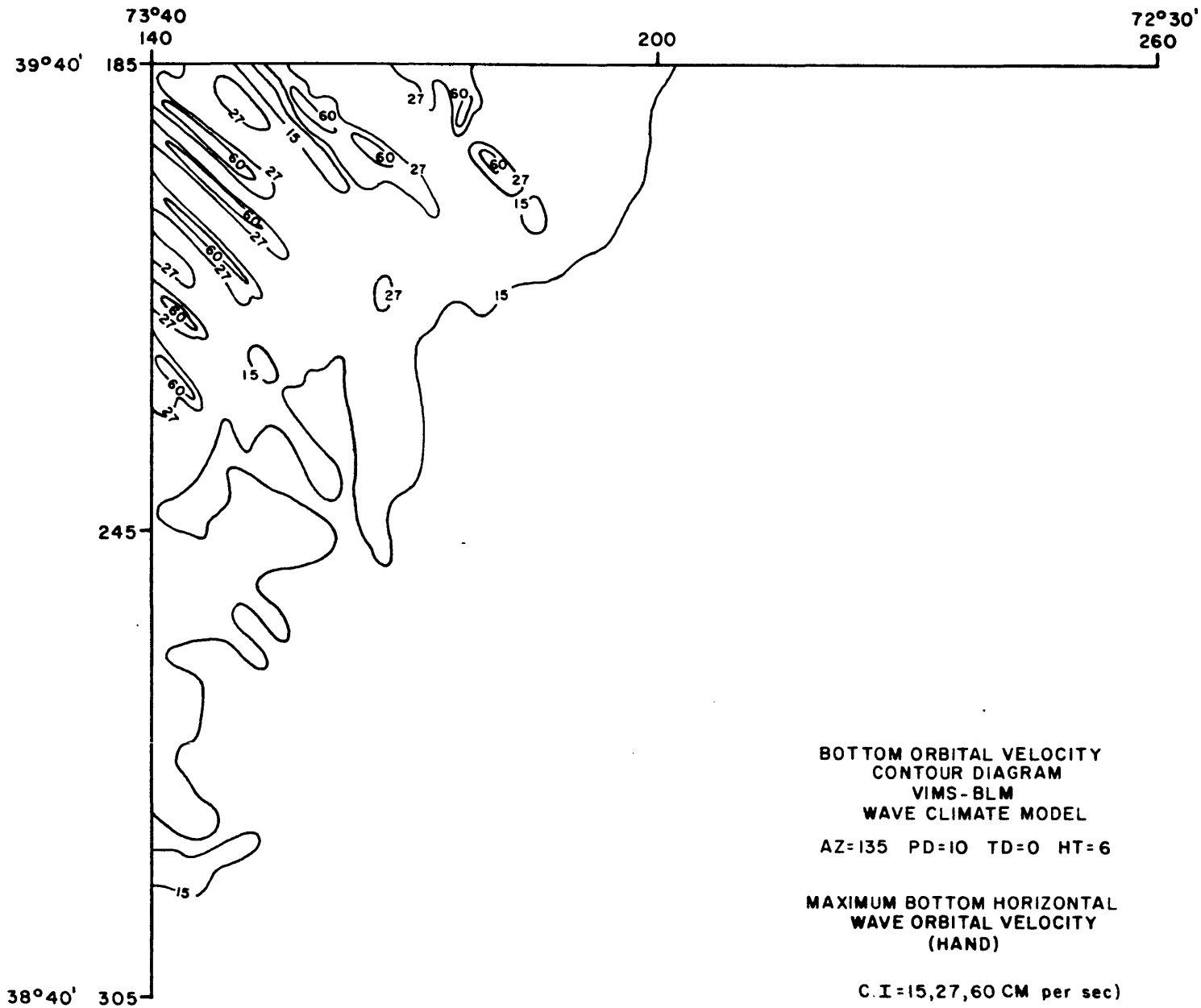

BOTTOM ORBITAL VELOCITY
CONTOUR DIAGRAM
VIMS-BLM
WAVE CLIMATE MODEL

AZ=135 PD=10 TD=0 HT=6

MAXIMUM BOTTOM HORIZONTAL
WAVE ORBITAL VELOCITY
(HAND)

C.I=15,27,60 CM per sec)

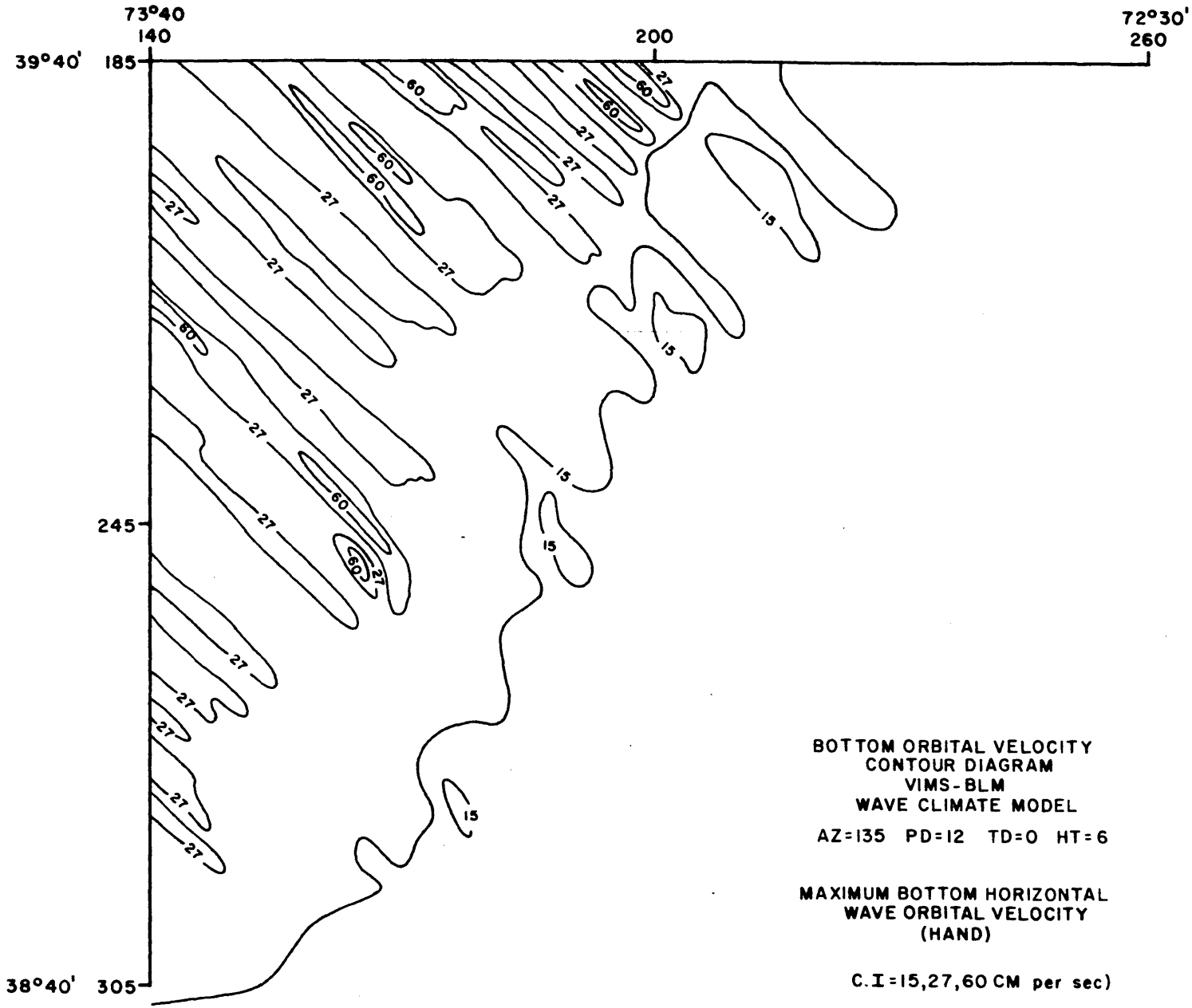
73°40
140
200
72°30'
260
39°40'
185
245
38°40'
305
60
27
15
BOTTOM ORBITAL VELOCITY
CONTOUR DIAGRAM
VIMS-BLM
WAVE CLIMATE MODEL
AZ=135 PD=12 TD=0 HT=6
MAXIMUM BOTTOM HORIZONTAL
WAVE ORBITAL VELOCITY
(HAND)
C.I=15,27,60 CM per sec)

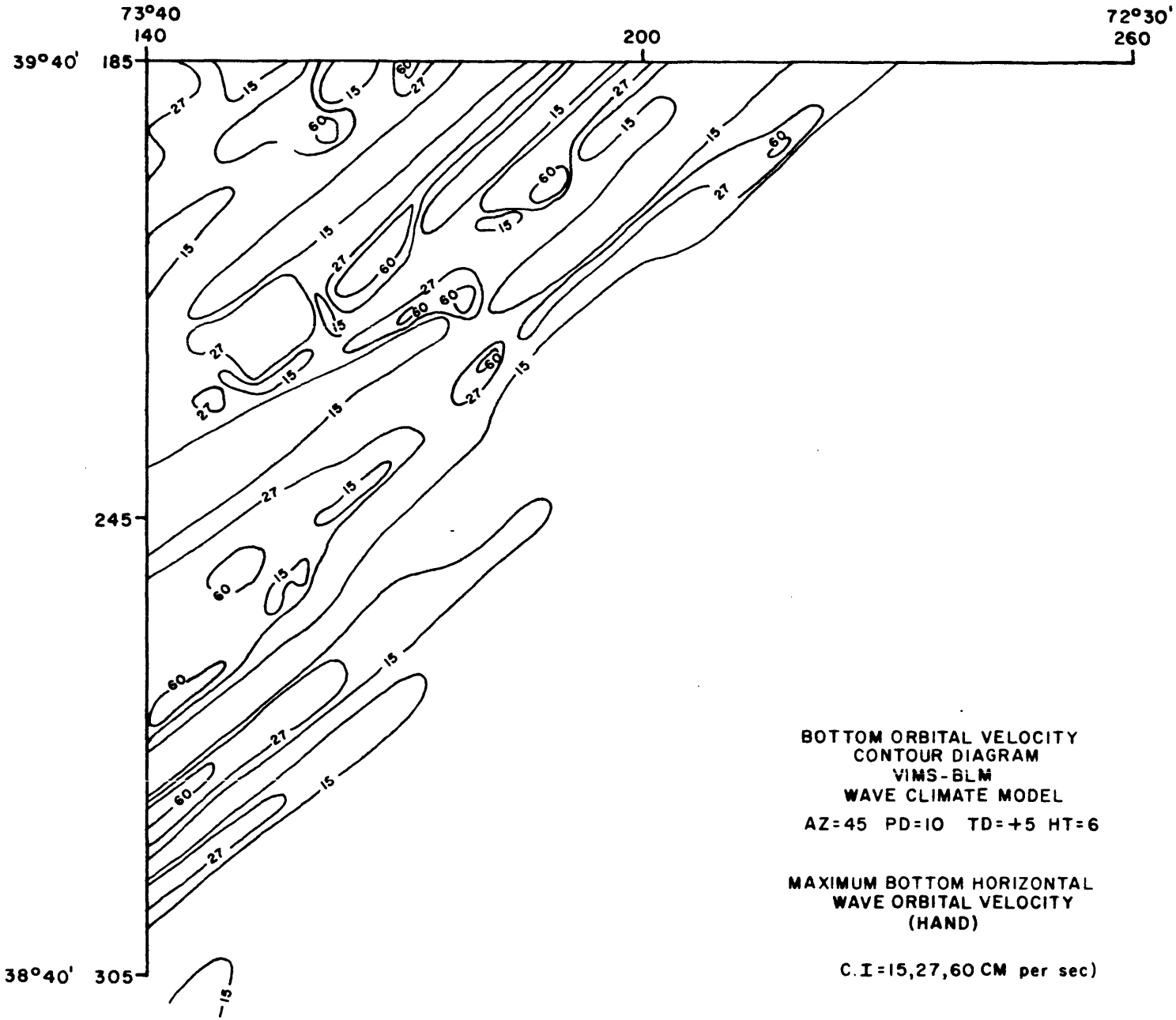

BOTTOM ORBITAL VELOCITY
CONTOUR DIAGRAM
VIMS-BLM
WAVE CLIMATE MODEL

AZ=45 PD=10 TD=+5 HT=6

MAXIMUM BOTTOM HORIZONTAL
WAVE ORBITAL VELOCITY
(HAND)

C.I=15,27,60 CM per sec)

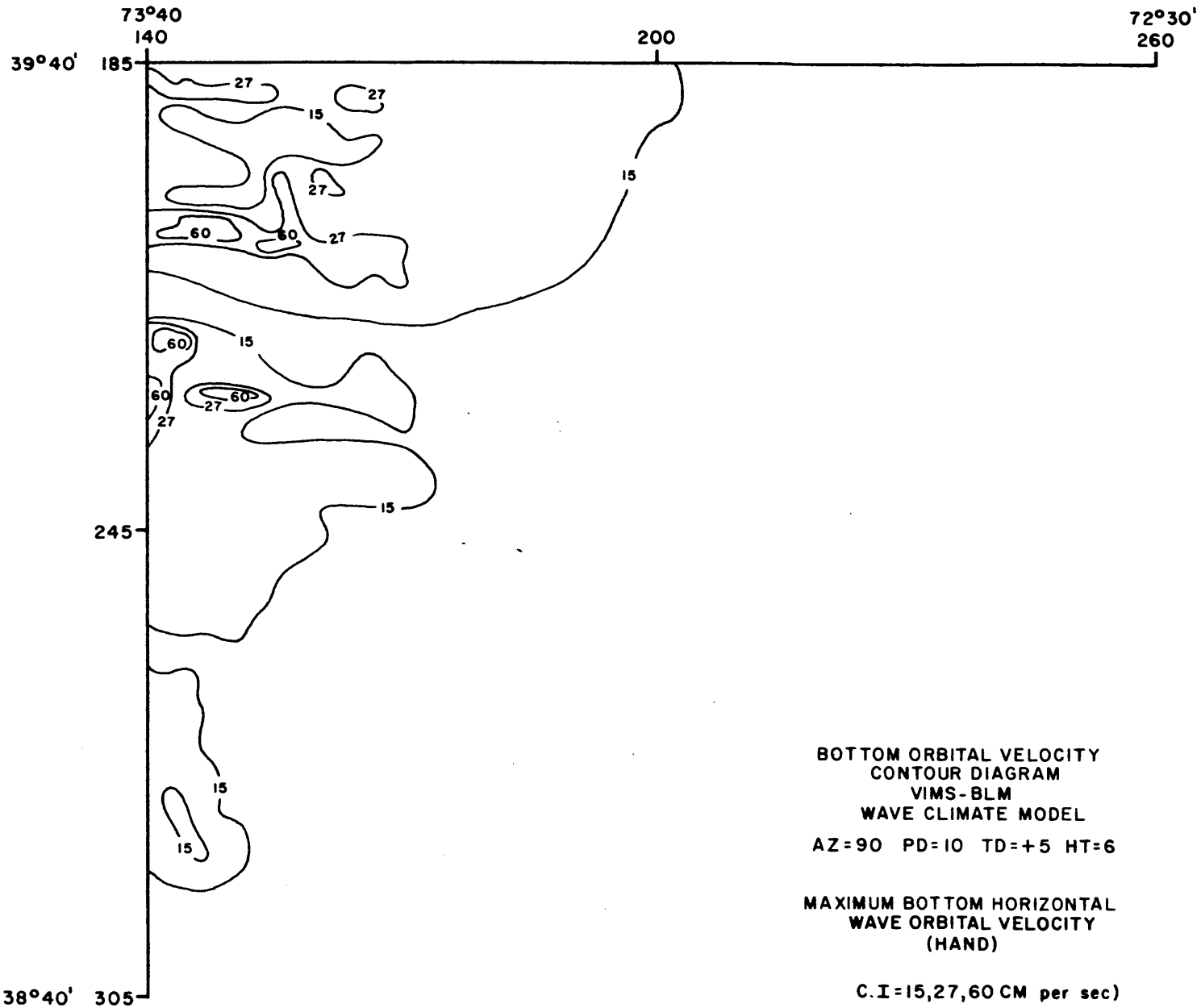

BOTTOM ORBITAL VELOCITY
CONTOUR DIAGRAM
VIMS-BLM
WAVE CLIMATE MODEL

AZ=90 PD=10 TD=+5 HT=6

MAXIMUM BOTTOM HORIZONTAL
WAVE ORBITAL VELOCITY
(HAND)

C.I=15,27,60 CM per sec)

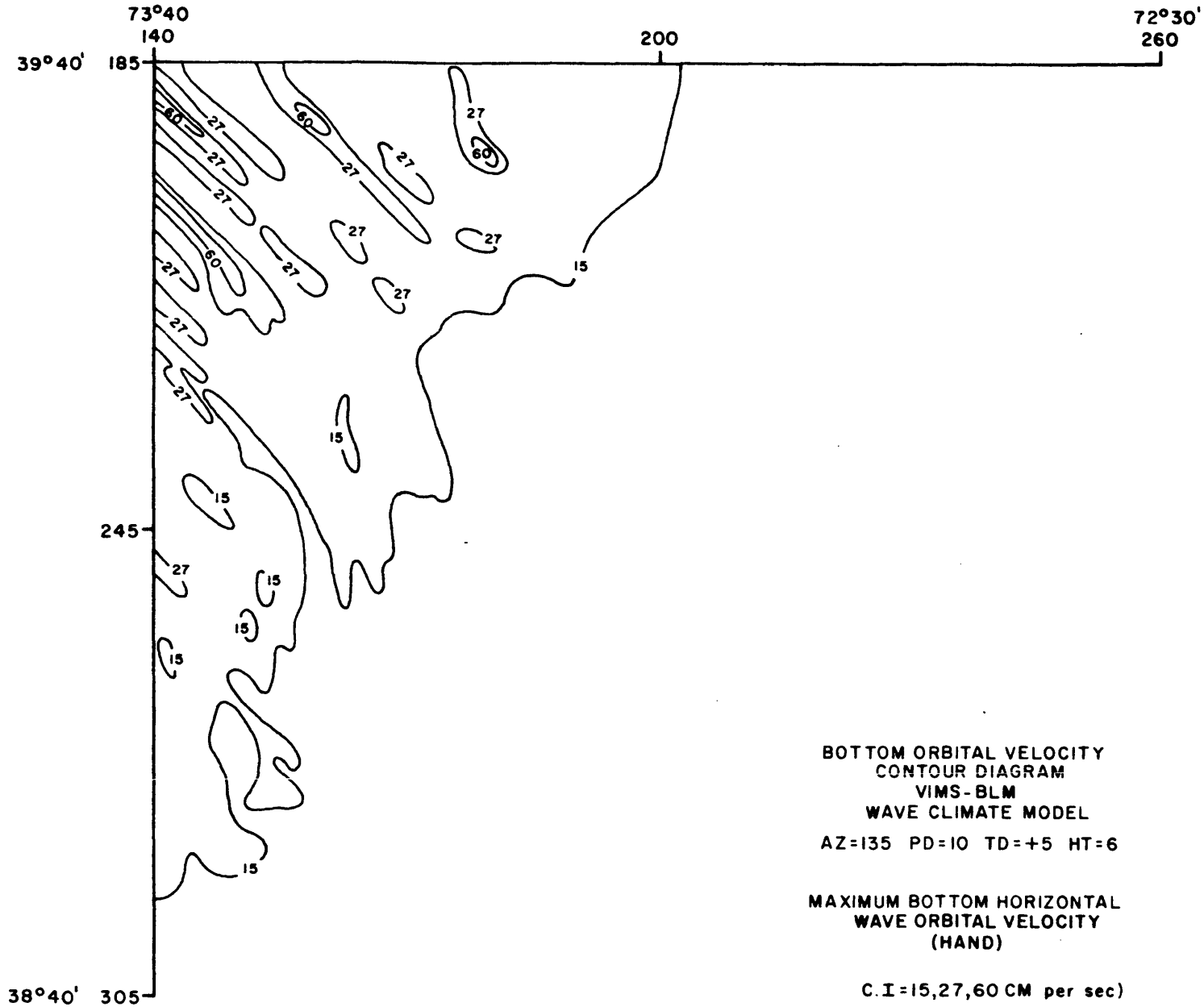

BOTTOM ORBITAL VELOCITY
CONTOUR DIAGRAM
VIMS-BLM
WAVE CLIMATE MODEL

AZ=135 PD=10 TD=+5 HT=6

MAXIMUM BOTTOM HORIZONTAL
WAVE ORBITAL VELOCITY
(HAND)

C.I=15,27,60 CM per sec)

NEW JERSEY - DELAWARE SHORELINE (N-S)

VIMS - BLM - BALTIMORE CANYON SHELF WAVES

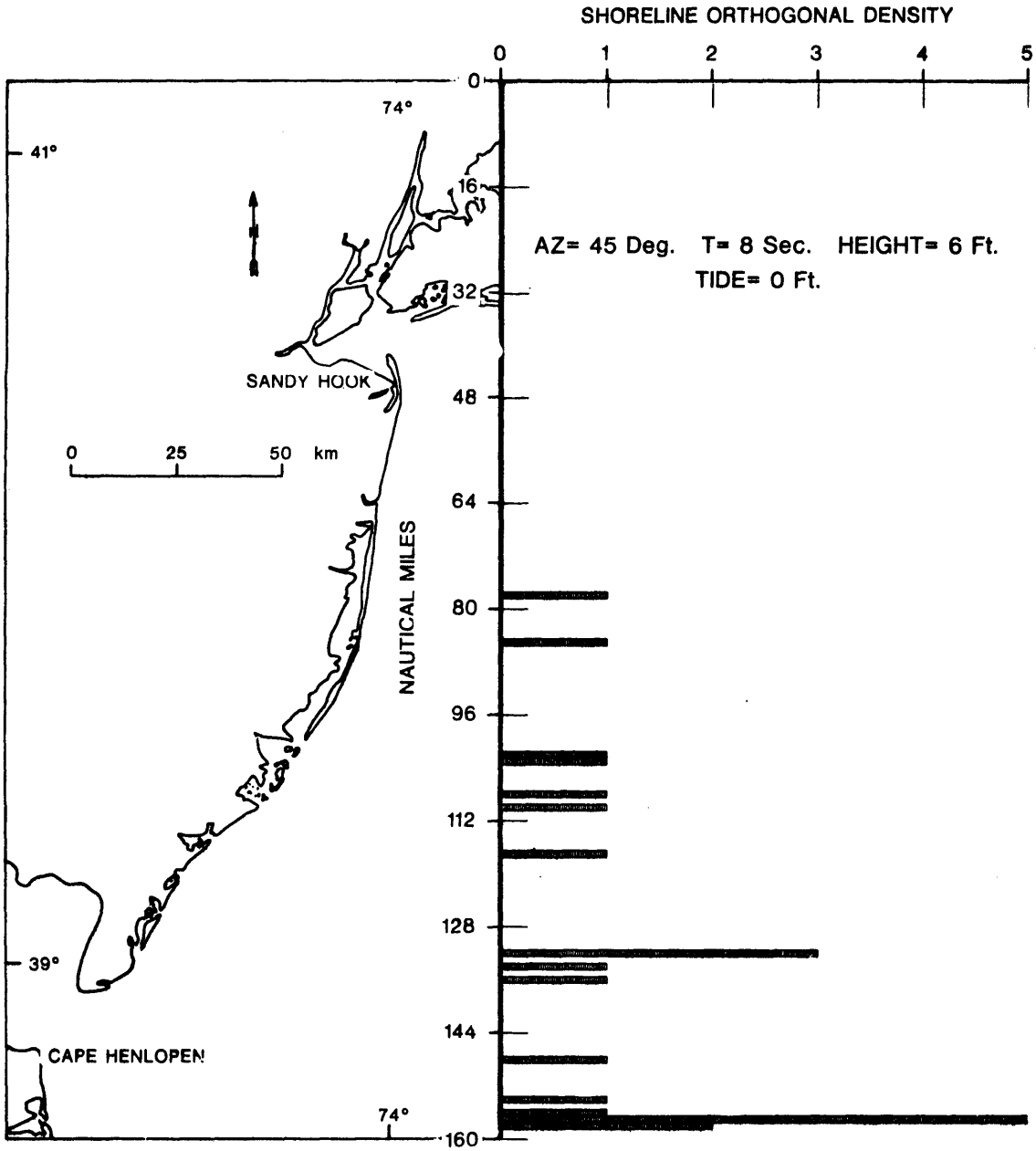

NEW JERSEY - DELAWARE SHORELINE (N-S)
VIMS - BLM - BALTIMORE CANYON SHELF WAVES

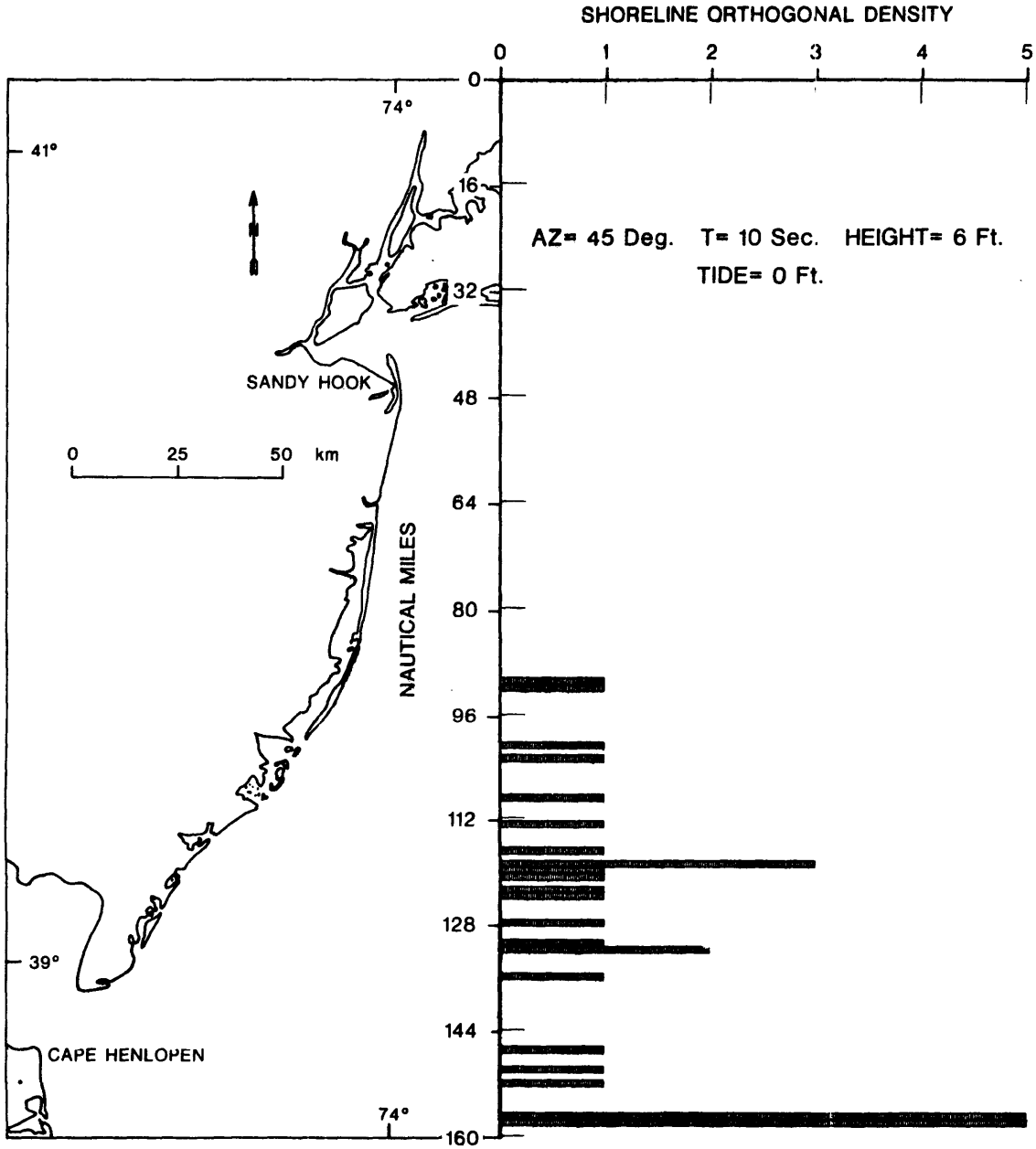

NEW JERSEY - DELAWARE SHORELINE (N-S)

VIMS - BLM - BALTIMORE CANYON SHELF WAVES

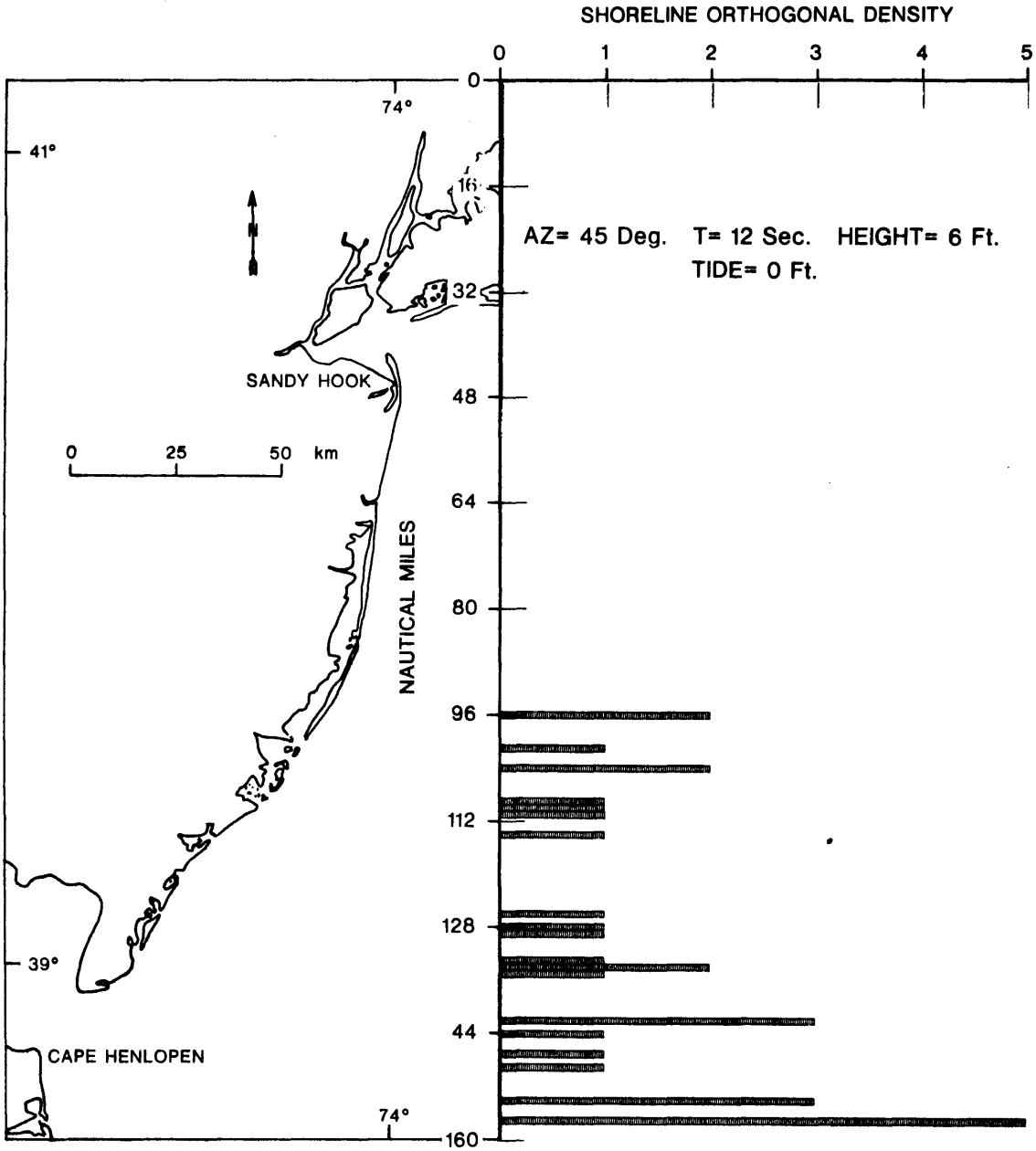

NEW JERSEY - DELAWARE SHORELINE (N-S)

VIMS - BLM - BALTIMORE CANYON SHELF WAVES

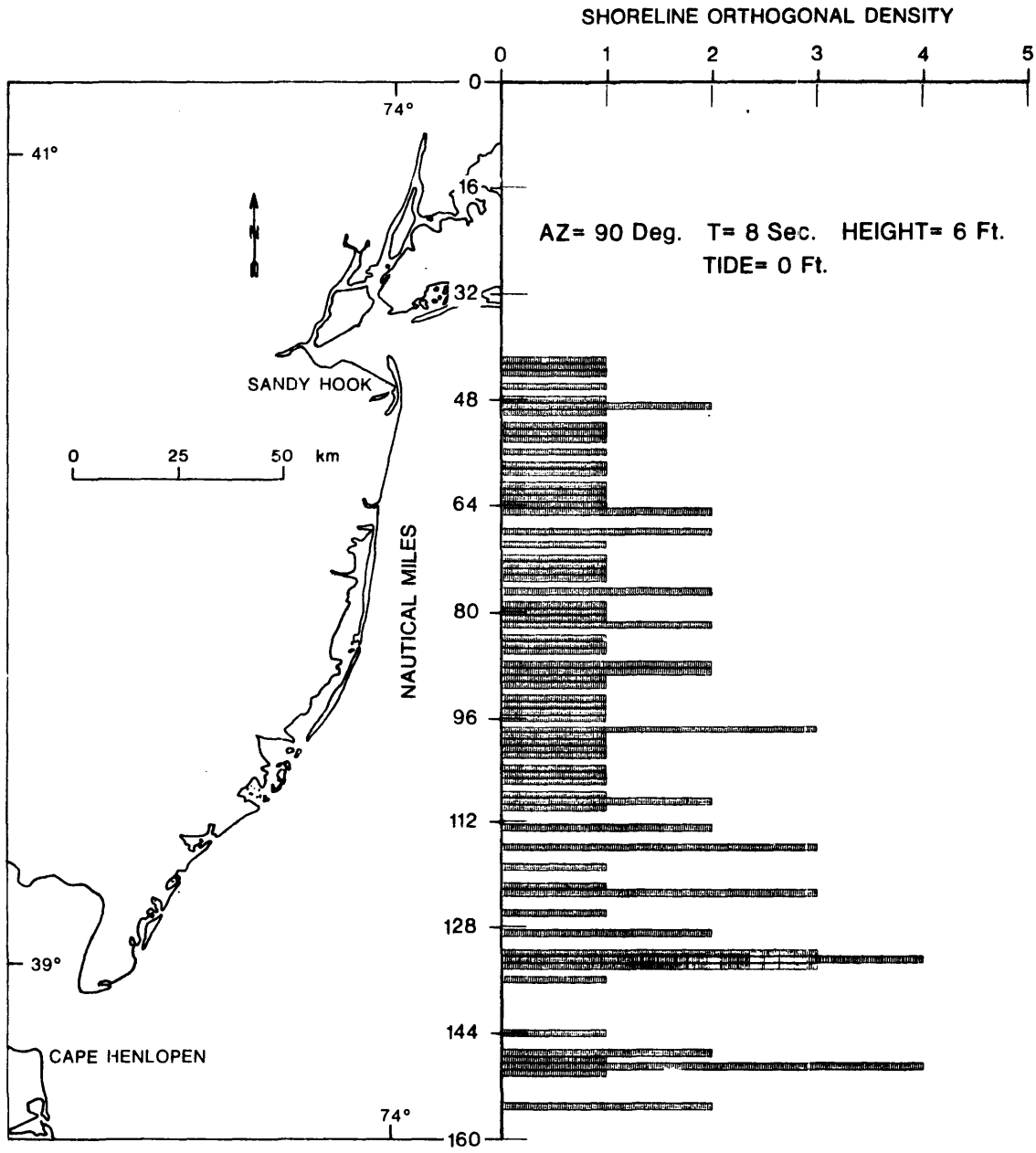

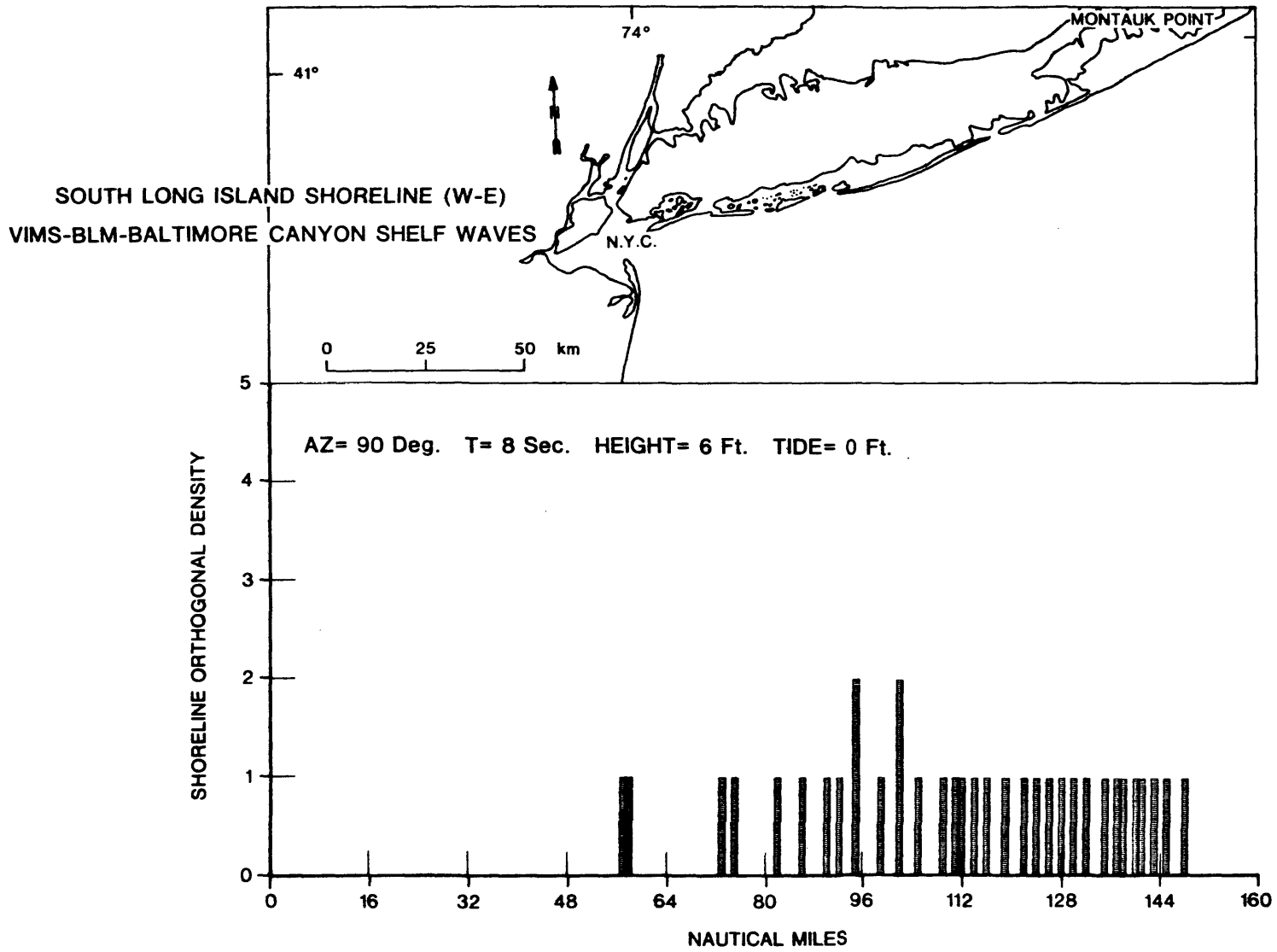
SOUTH LONG ISLAND SHORELINE (W-E)
VIMS-BLM-BALTIMORE CANYON SHELF WAVES
74°
41°
MONTAUK POINT
N.Y.C.
0 25 50 km
AZ= 90 Deg. T= 8 Sec. HEIGHT= 6 Ft. TIDE= 0 Ft.
SHORELINE ORTHOGONAL DENSITY
0
1
2
3
4
5
0 16 32 48 64 80 96 112 128 144 160
NAUTICAL MILES

G-4b

NEW JERSEY - DELAWARE SHORELINE (N-S)

VIMS - BLM - BALTIMORE CANYON SHELF WAVES

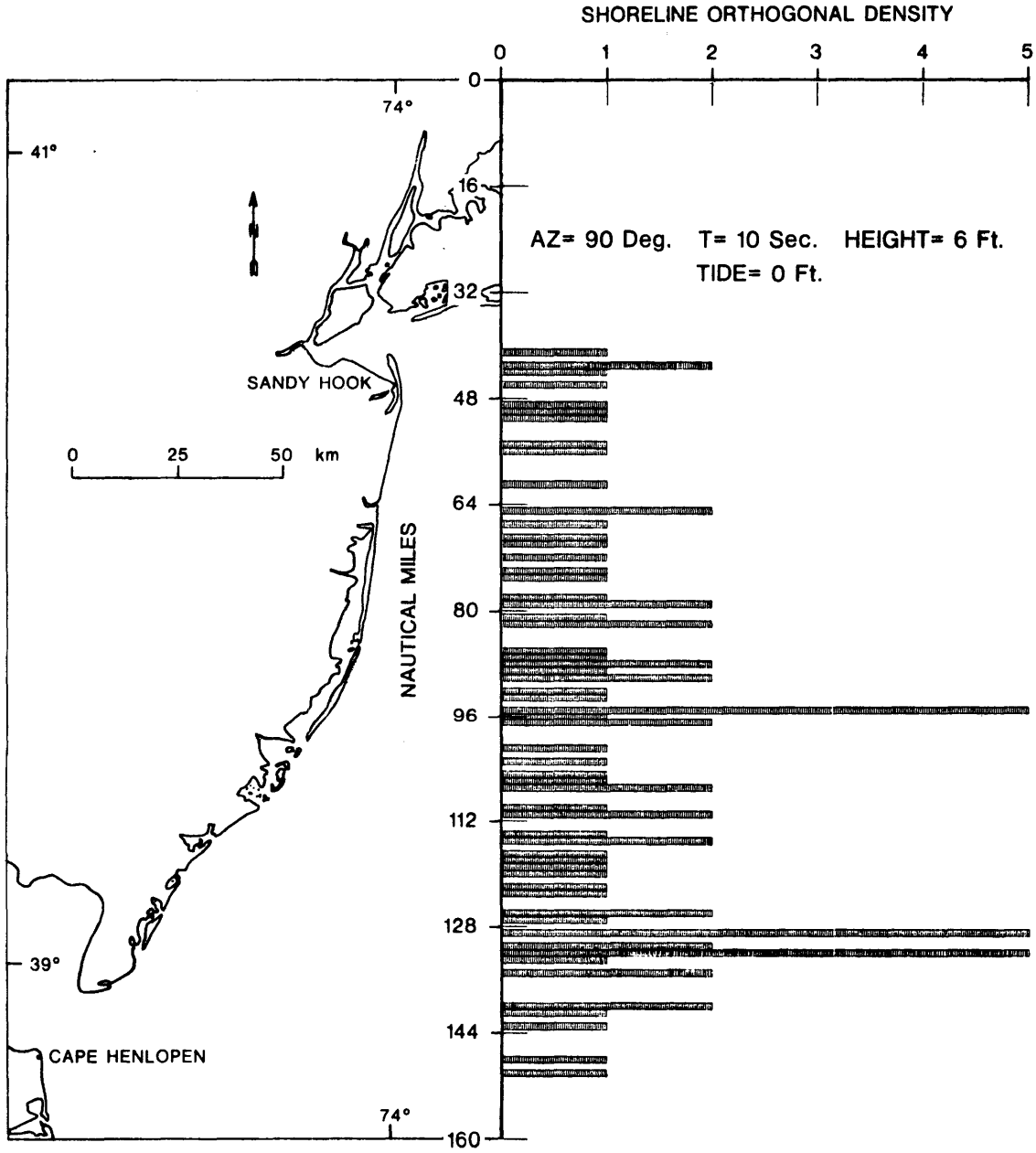

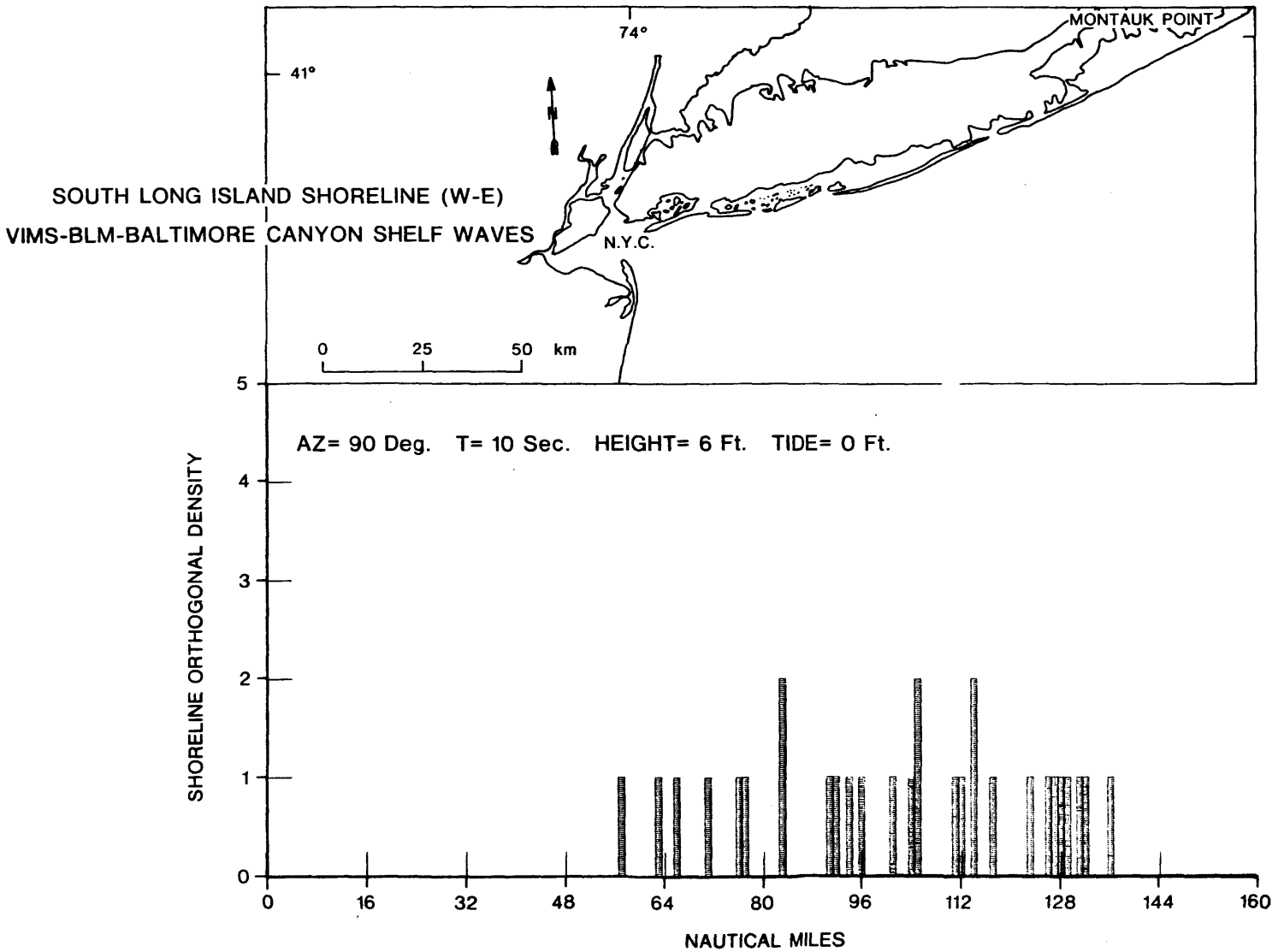
SOUTH LONG ISLAND SHORELINE (W-E)
VIMS-BLM-BALTIMORE CANYON SHELF WAVES
74°
41°
MONTAUK POINT
N.Y.C.
0 25 50 km
AZ= 90 Deg. T= 10 Sec. HEIGHT= 6 Ft. TIDE= 0 Ft.
SHORELINE ORTHOGONAL DENSITY
0
1
2
3
4
5
0 16 32 48 64 80 96 112 128 144 160
NAUTICAL MILES

G-5b

NEW JERSEY - DELAWARE SHORELINE (N-S)

VIMS - BLM - BALTIMORE CANYON SHELF WAVES

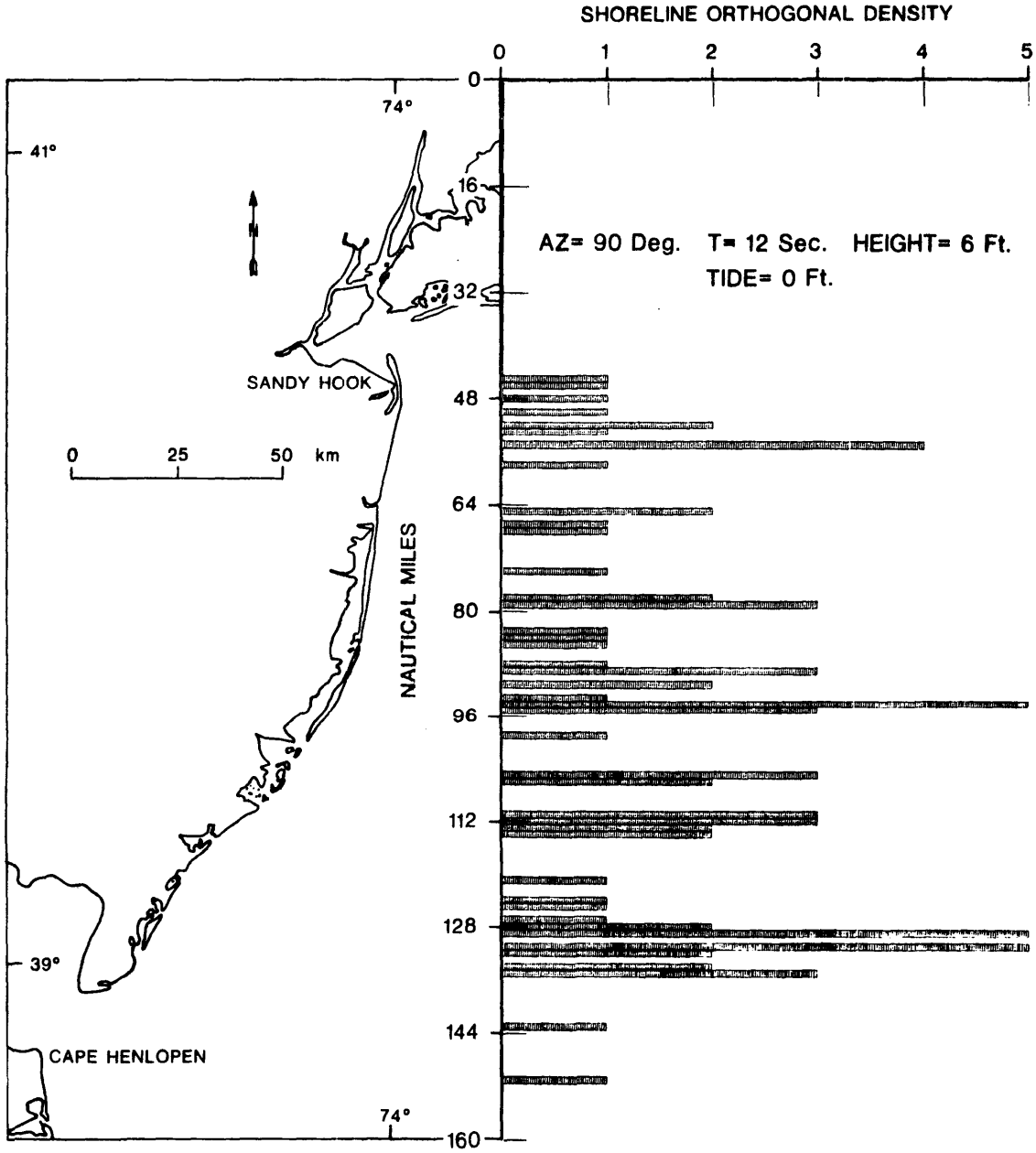

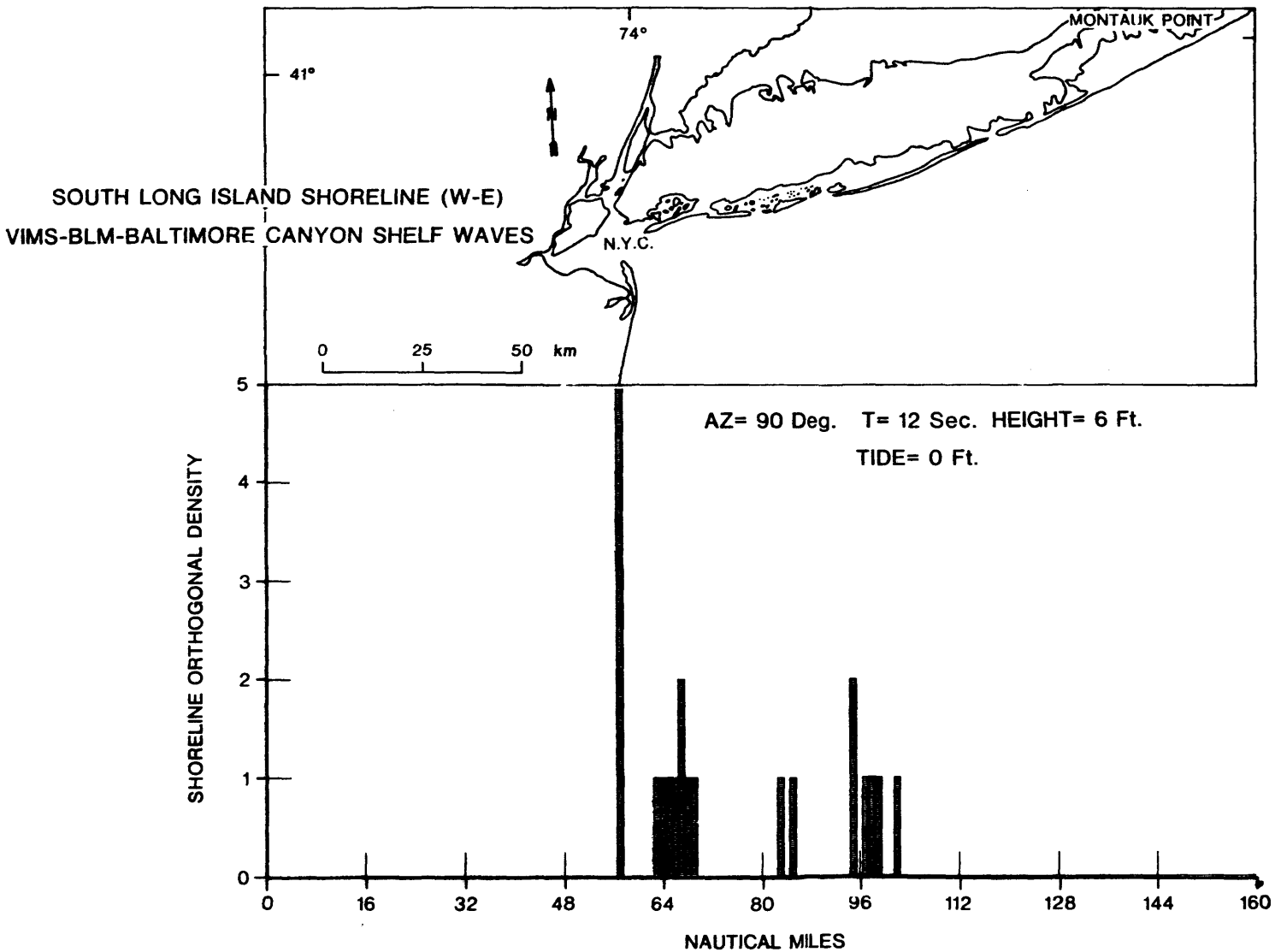
SOUTH LONG ISLAND SHORELINE (W-E)
VIMS-BLM-BALTIMORE CANYON SHELF WAVES
74°
41°
MONTAUK POINT
N.Y.C.
0 25 50 km
AZ= 90 Deg. T= 12 Sec. HEIGHT= 6 Ft.
TIDE= 0 Ft.
SHORELINE ORTHOGONAL DENSITY
0
1
2
3
4
5
0 16 32 48 64 80 96 112 128 144 160
NAUTICAL MILES

NEW JERSEY - DELAWARE SHORELINE (N-S)

VIMS - BLM - BALTIMORE CANYON SHELF WAVES

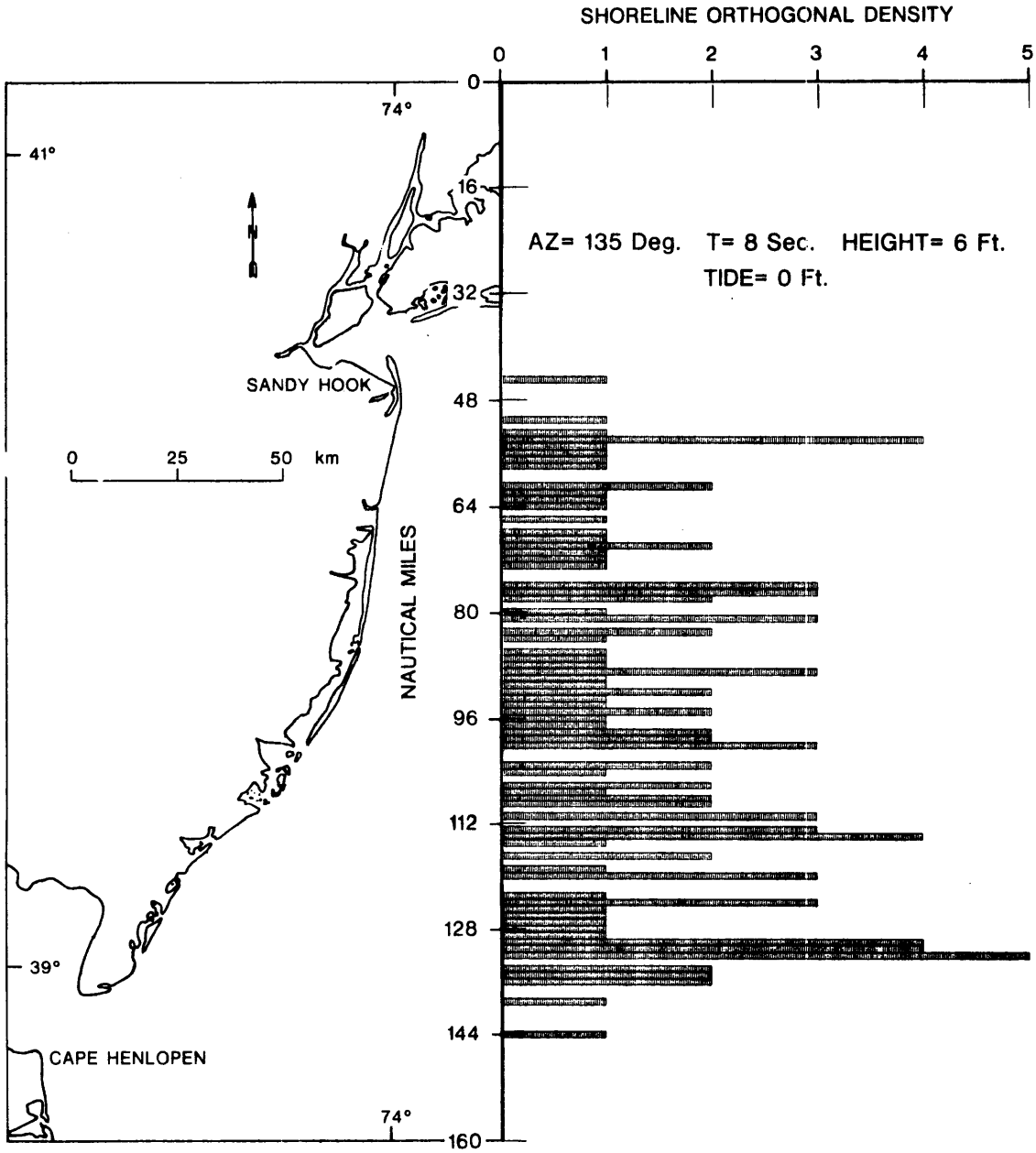

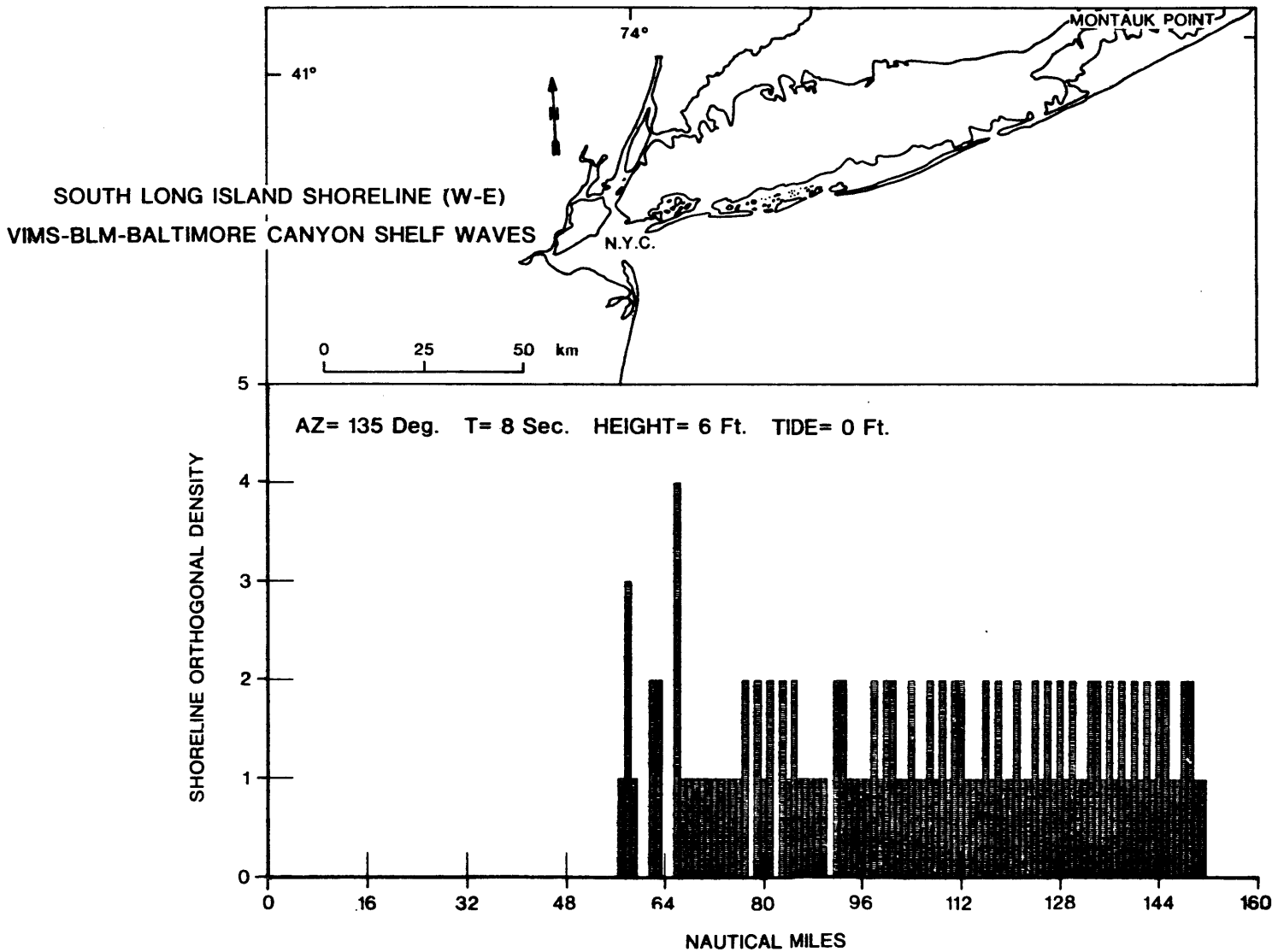
SOUTH LONG ISLAND SHORELINE (W-E)
VIMS-BLM-BALTIMORE CANYON SHELF WAVES
74°
41°
MONTAUK POINT
N.Y.C.
0 25 50 km
AZ= 135 Deg. T= 8 Sec. HEIGHT= 6 Ft. TIDE= 0 Ft.
SHORELINE ORTHOGONAL DENSITY
0
1
2
3
4
5
0 16 32 48 64 80 96 112 128 144 160
NAUTICAL MILES

NEW JERSEY - DELAWARE SHORELINE (N-S)
VIMS - BLM - BALTIMORE CANYON SHELF WAVES

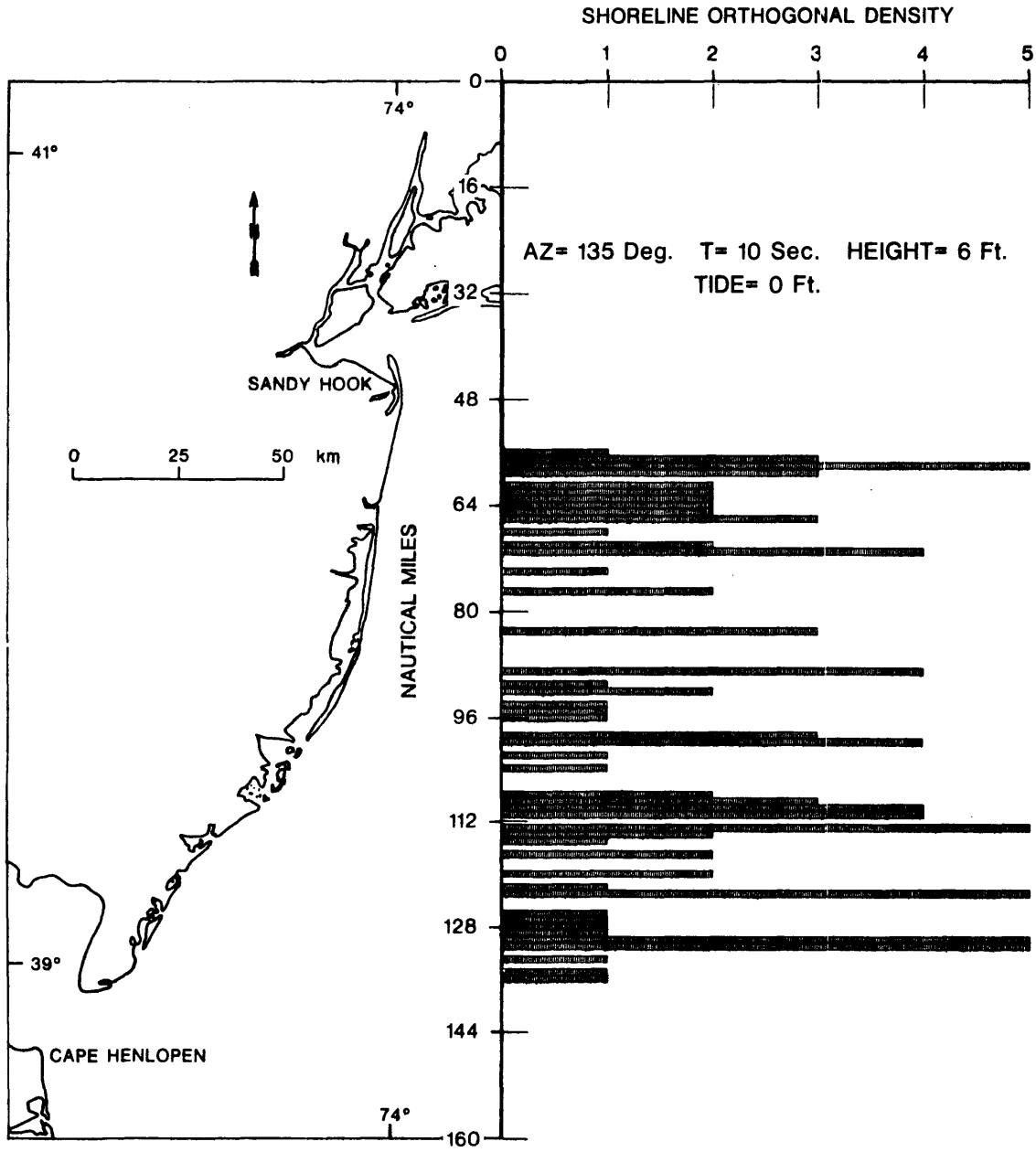

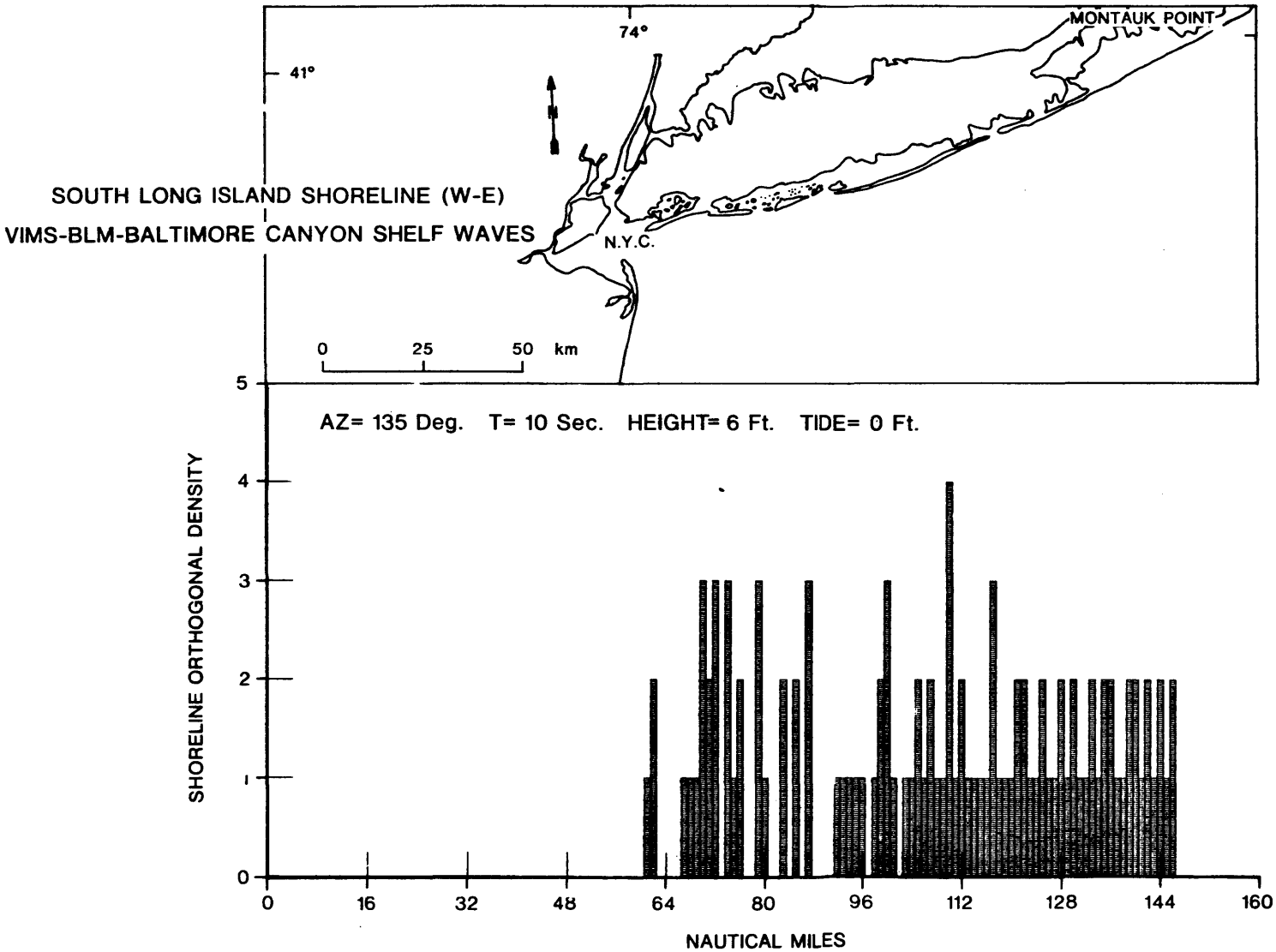
SOUTH LONG ISLAND SHORELINE (W-E)
VIMS-BLM-BALTIMORE CANYON SHELF WAVES
74°
41°
MONTAUK POINT
N.Y.C.
0 25 50 km
AZ= 135 Deg. T= 10 Sec. HEIGHT= 6 Ft. TIDE= 0 Ft.
SHORELINE ORTHOGONAL DENSITY
0
1
2
3
4
5
0 16 32 48 64 80 96 112 128 144 160
NAUTICAL MILES

NEW JERSEY - DELAWARE SHORELINE (N-S)

VIMS - BLM - BALTIMORE CANYON SHELF WAVES

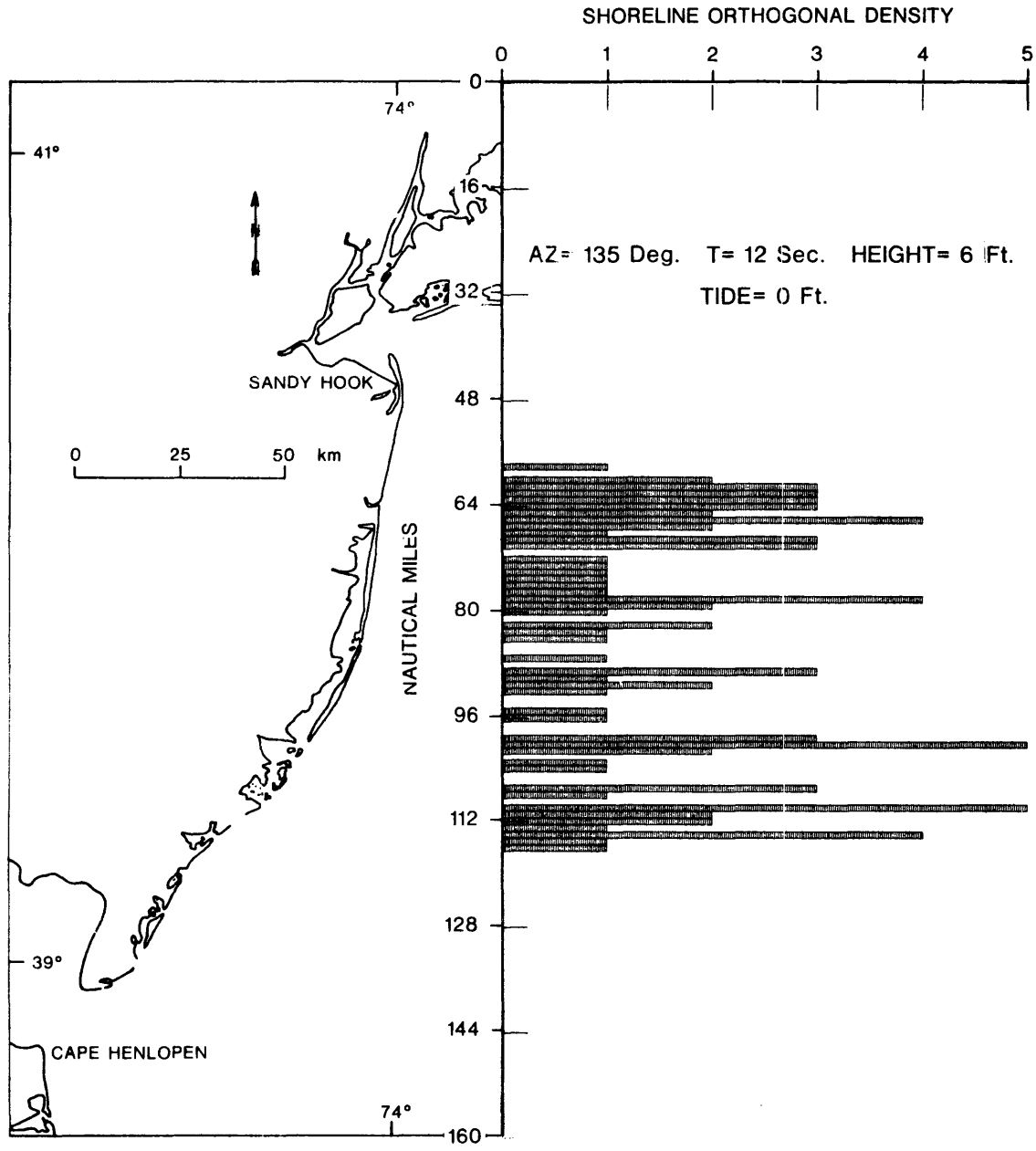

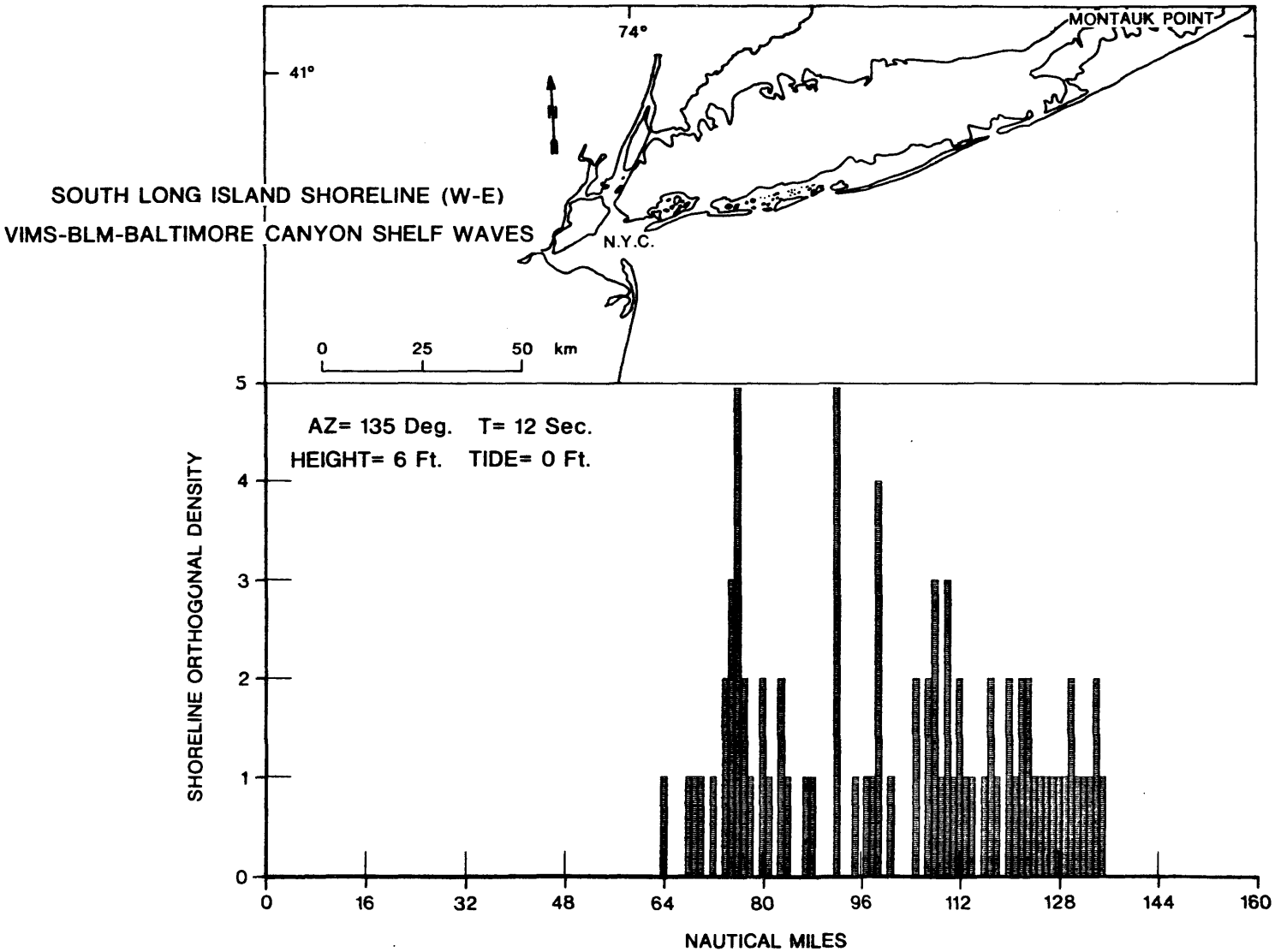
SOUTH LONG ISLAND SHORELINE (W-E)
VIMS-BLM-BALTIMORE CANYON SHELF WAVES
74°
41°
MONTAUK POINT
N.Y.C.
0 25 50 km
AZ= 135 Deg. T= 12 Sec.
HEIGHT= 6 Ft. TIDE= 0 Ft.
SHORELINE ORTHOGONAL DENSITY
0
1
2
3
4
5
0 16 32 48 64 80 96 112 128 144 160
NAUTICAL MILES

NEW JERSEY - DELAWARE SHORELINE (N-S)
VIMS - BLM - BALTIMORE CANYON SHELF WAVES

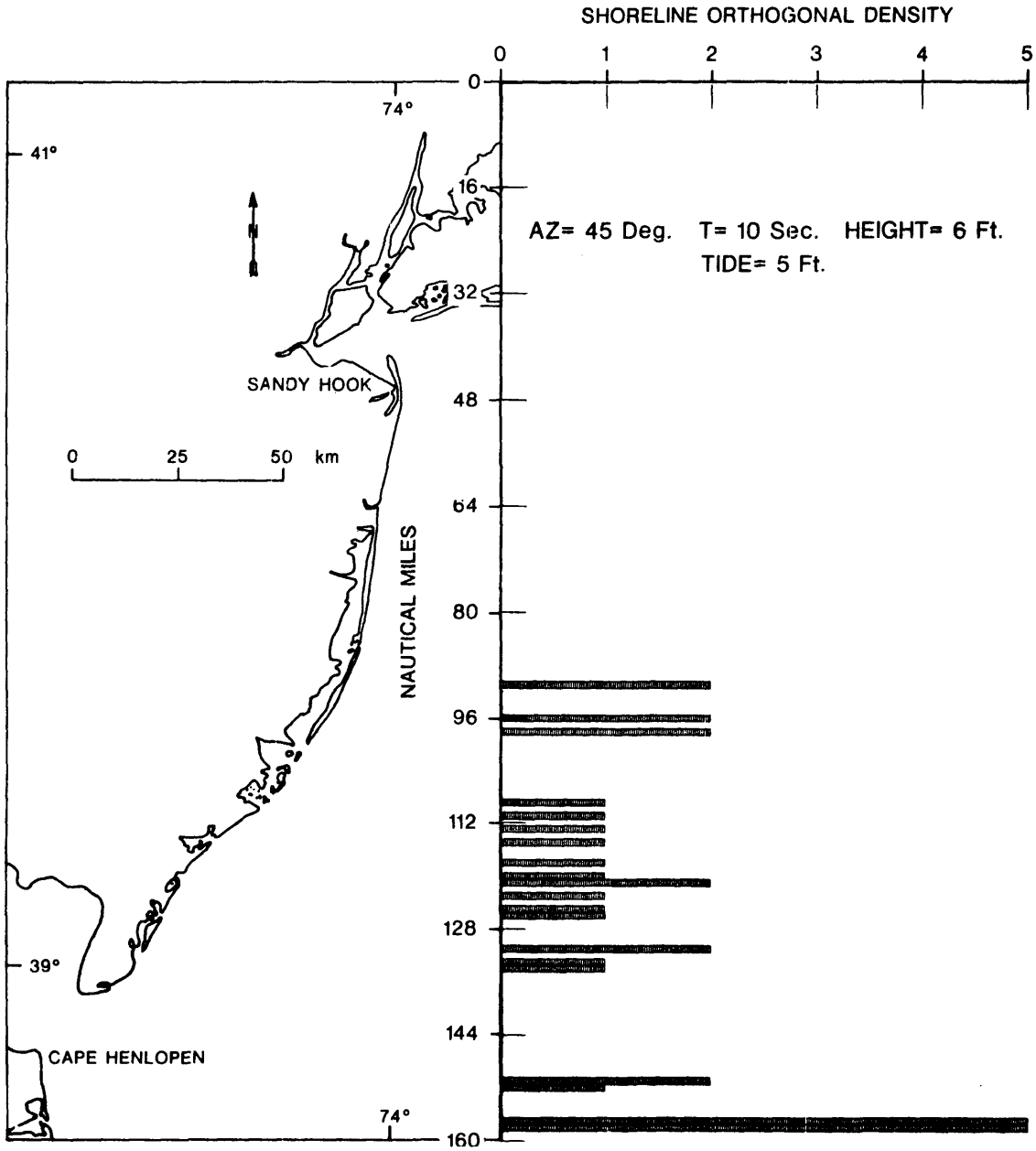

NEW JERSEY - DELAWARE SHORELINE (N-S)

VIMS - BLM - BALTIMORE CANYON SHELF WAVES

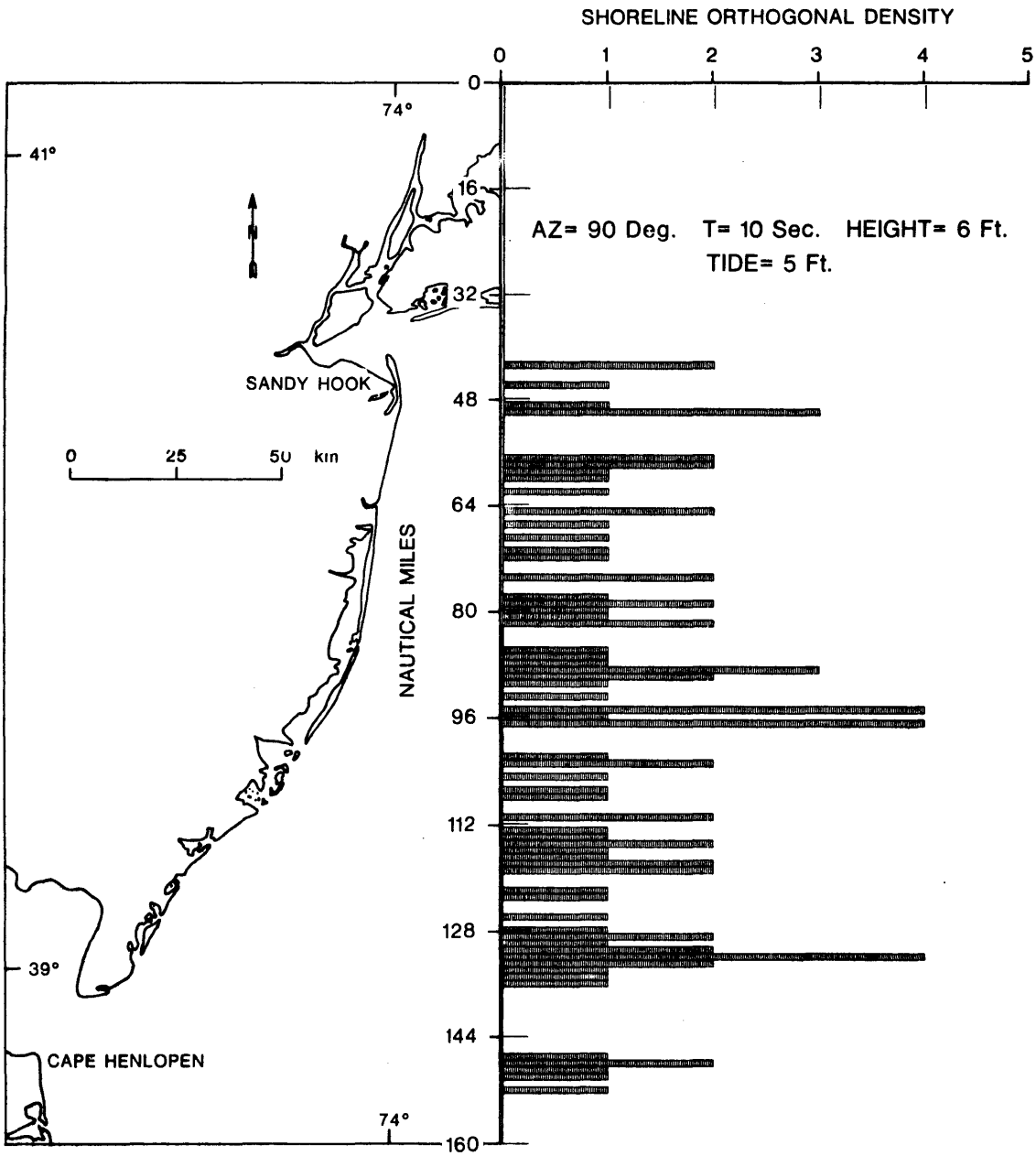

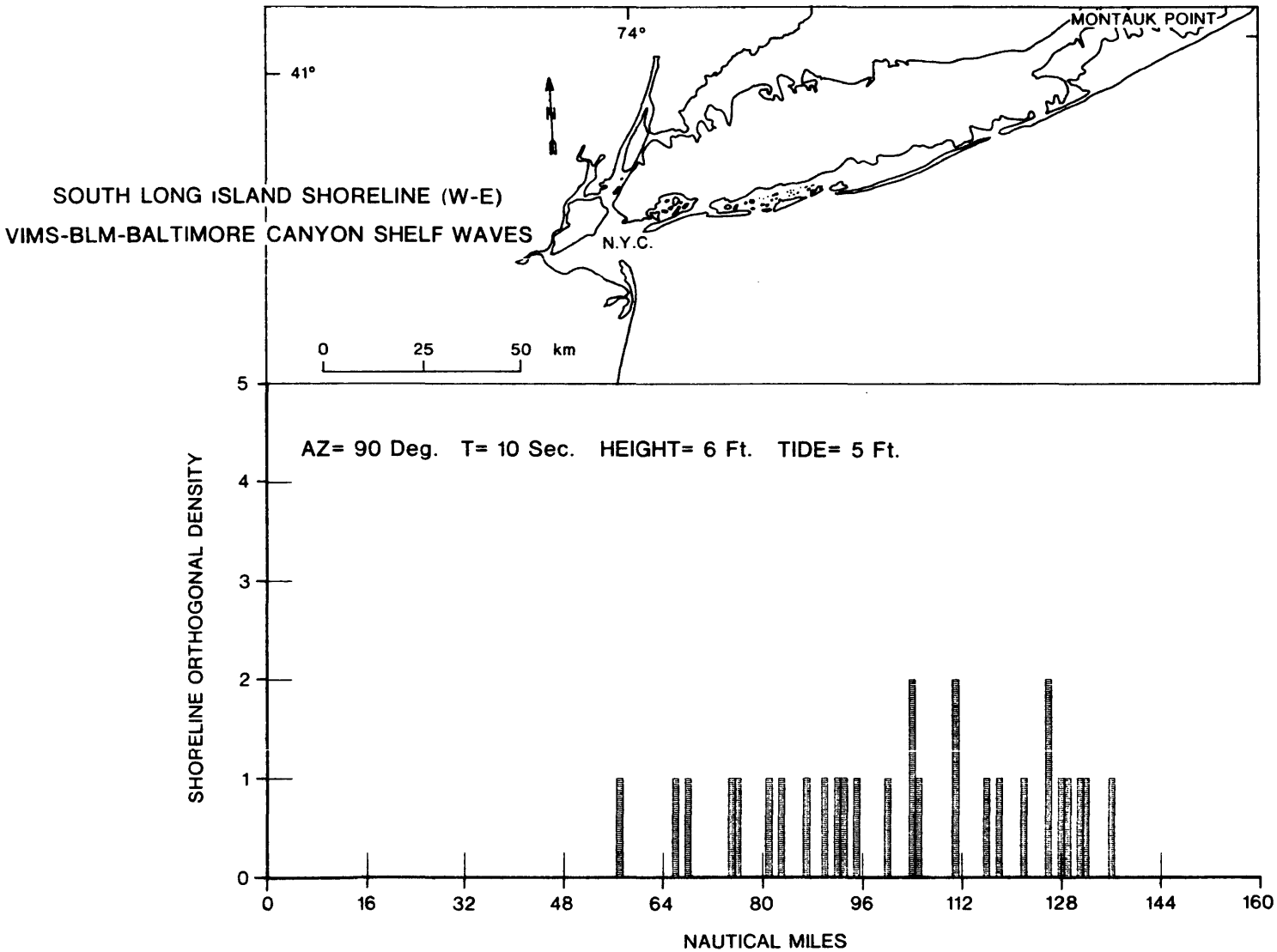
SOUTH LONG ISLAND SHORELINE (W-E)
VIMS-BLM-BALTIMORE CANYON SHELF WAVES
74°
41°
MONTAUK POINT
N.Y.C.
0 25 50 km
AZ= 90 Deg. T= 10 Sec. HEIGHT= 6 Ft. TIDE= 5 Ft.
SHORELINE ORTHOGONAL DENSITY
0
1
2
3
4
5
0 16 32 48 64 80 96 112 128 144 160
NAUTICAL MILES

NEW JERSEY - DELAWARE SHORELINE (N-S)
VIMS - BLM - BALTIMORE CANYON SHELF WAVES

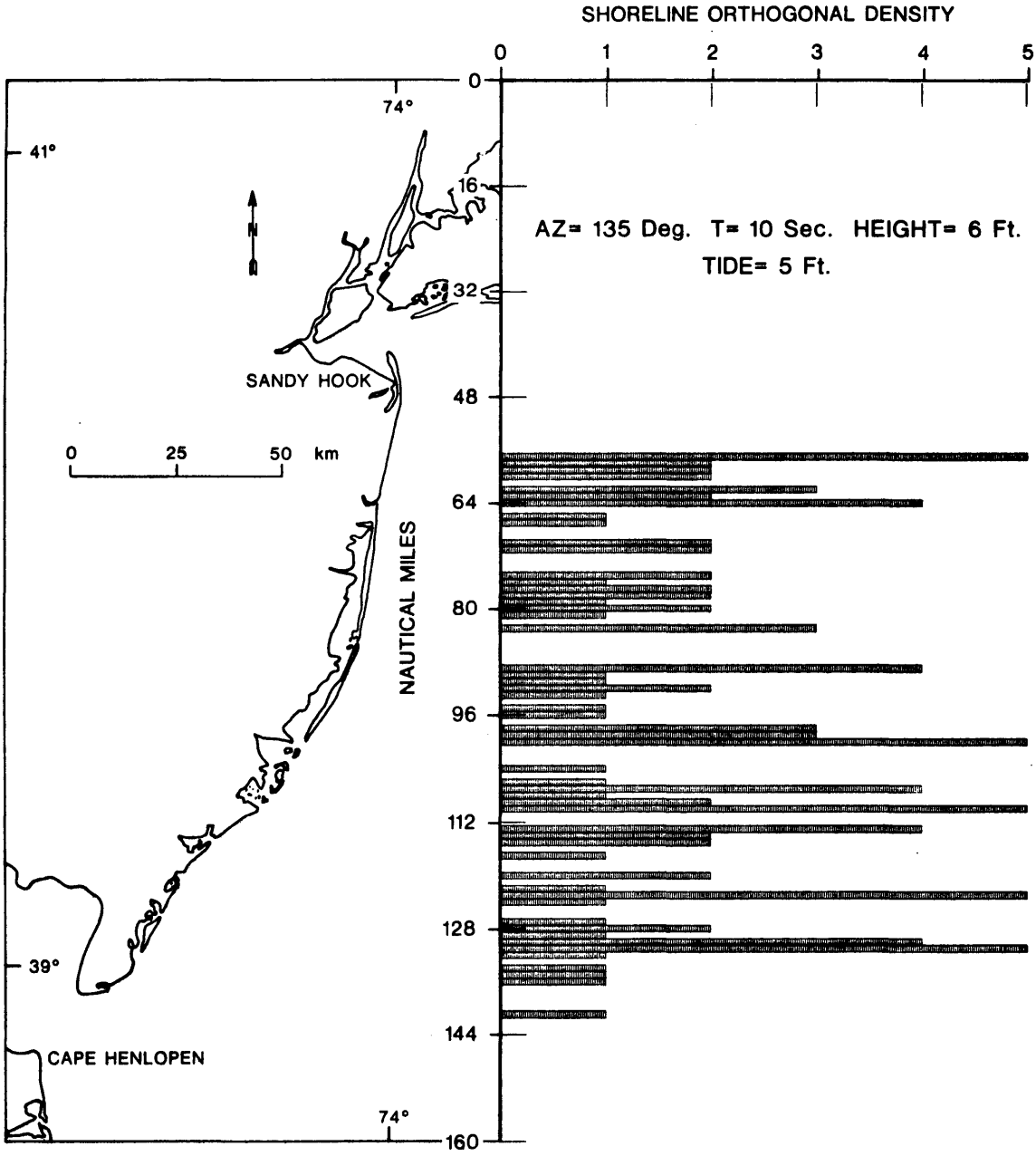

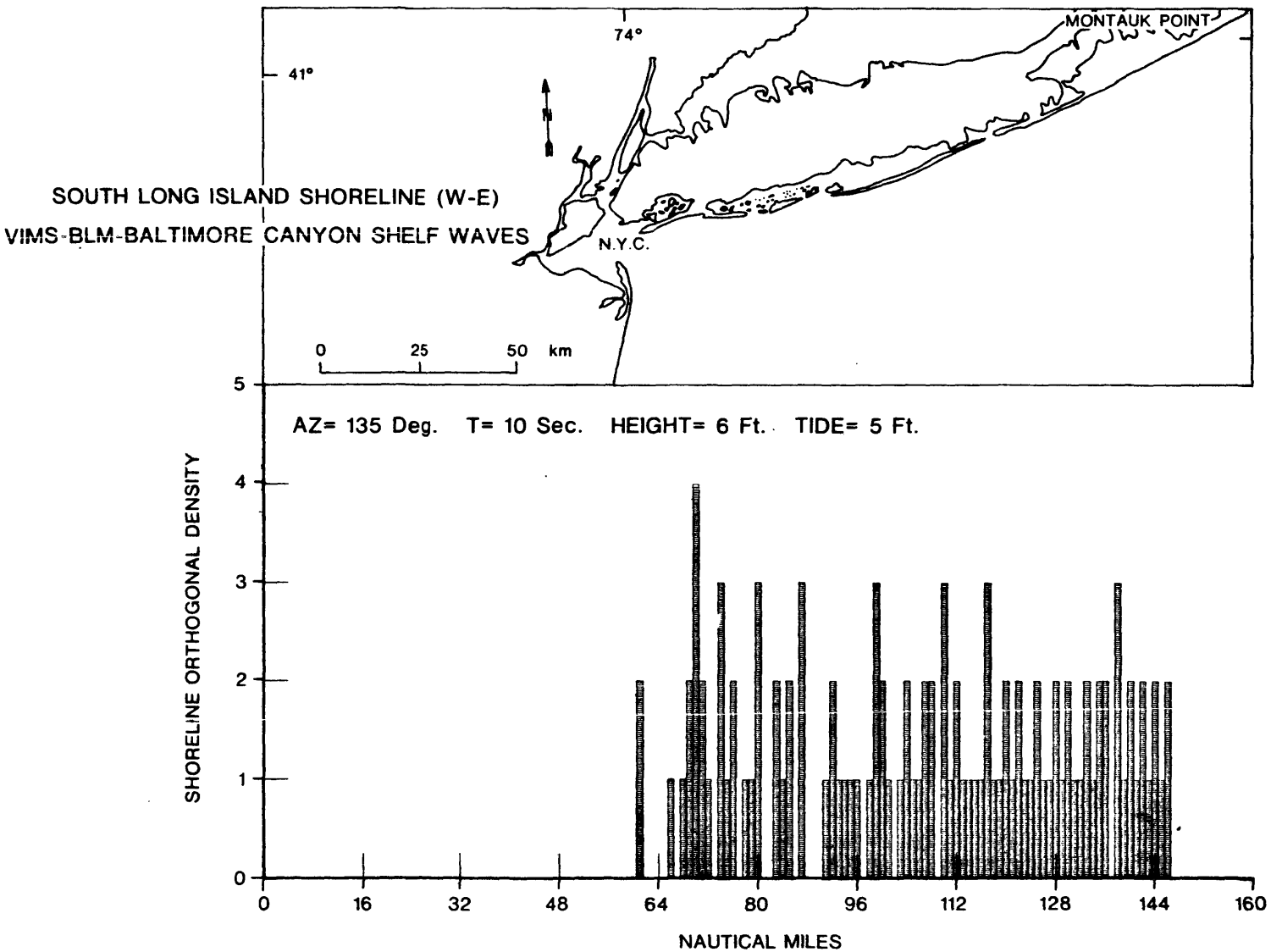
SOUTH LONG ISLAND SHORELINE (W-E)
VIMS-BLM-BALTIMORE CANYON SHELF WAVES
74°
41°
MONTAUK POINT
N.Y.C.
0 25 50 km
AZ= 135 Deg. T= 10 Sec. HEIGHT= 6 Ft. TIDE= 5 Ft.
SHORELINE ORTHOGONAL DENSITY
0 1 2 3 4 5
0 16 32 48 64 80 96 112 128 144 160
NAUTICAL MILES

G-12b

NEW JERSEY - DELAWARE SHORELINE (N-S)

VIMS - BLM - BALTIMORE CANYON SHELF WAVES

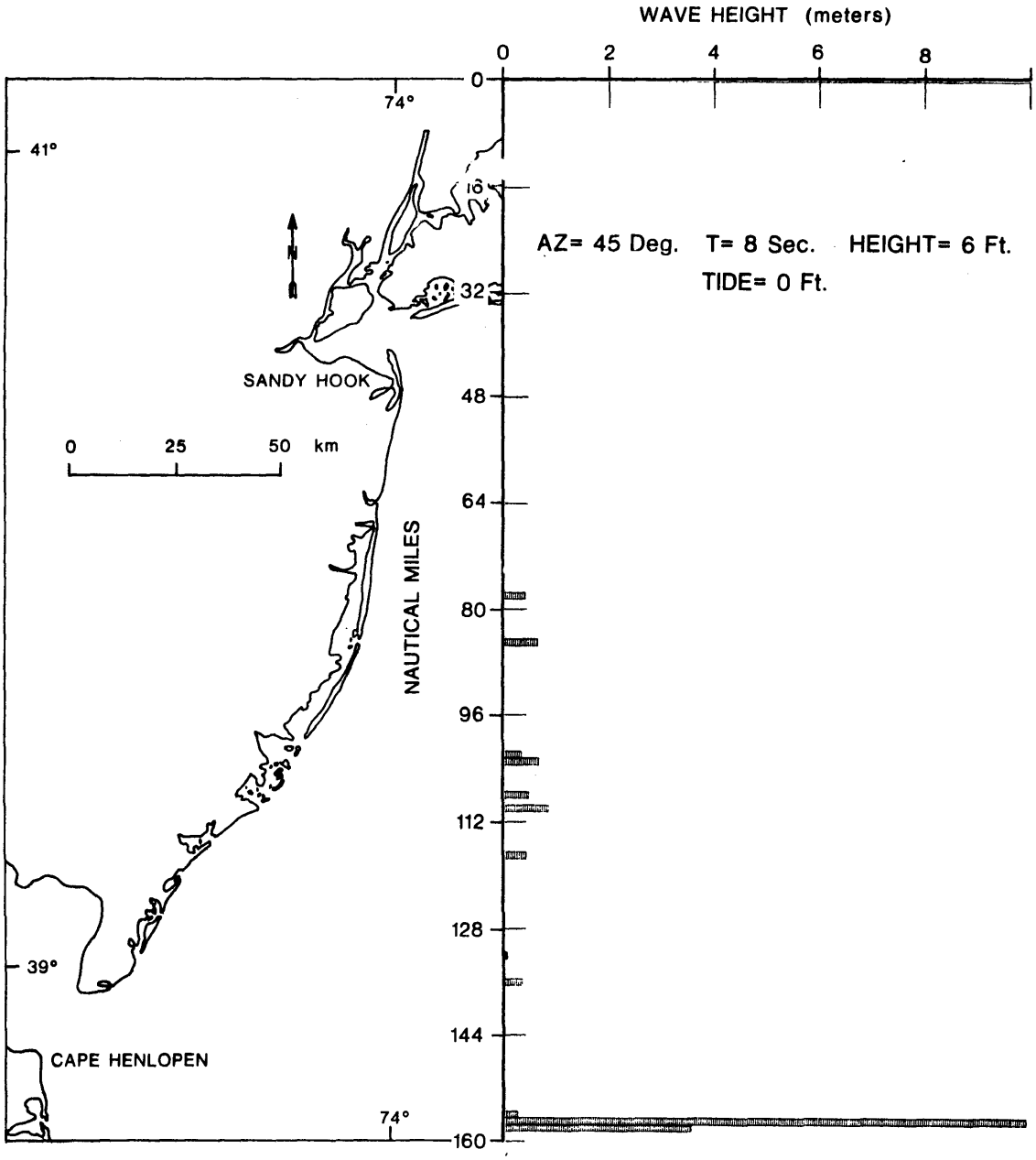

NEW JERSEY - DELAWARE SHORELINE (N-S)

VIMS - BLM - BALTIMORE CANYON SHELF WAVES

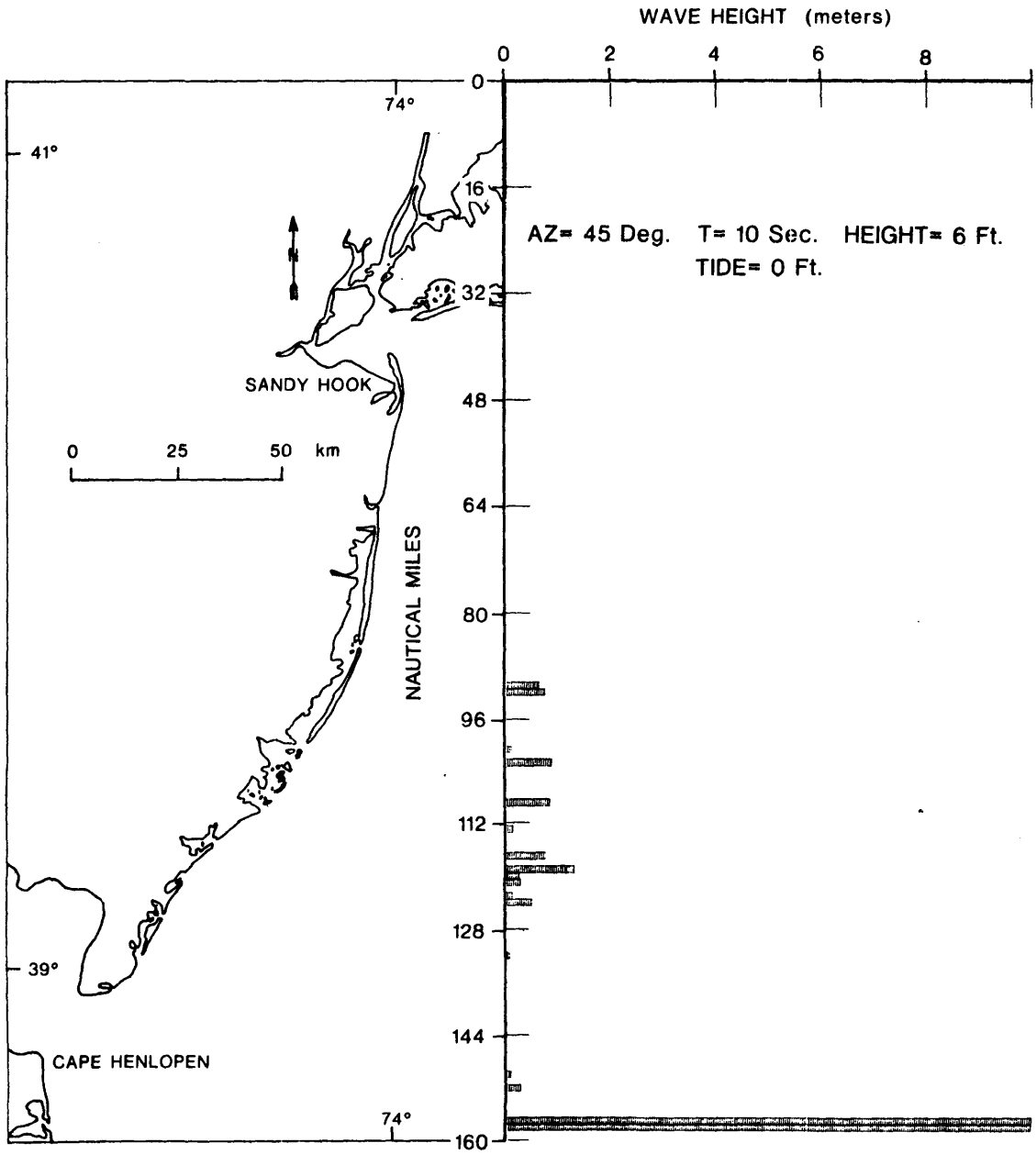

NEW JERSEY - DELAWARE SHORELINE (N-S)

VIMS - BLM - BALTIMORE CANYON SHELF WAVES

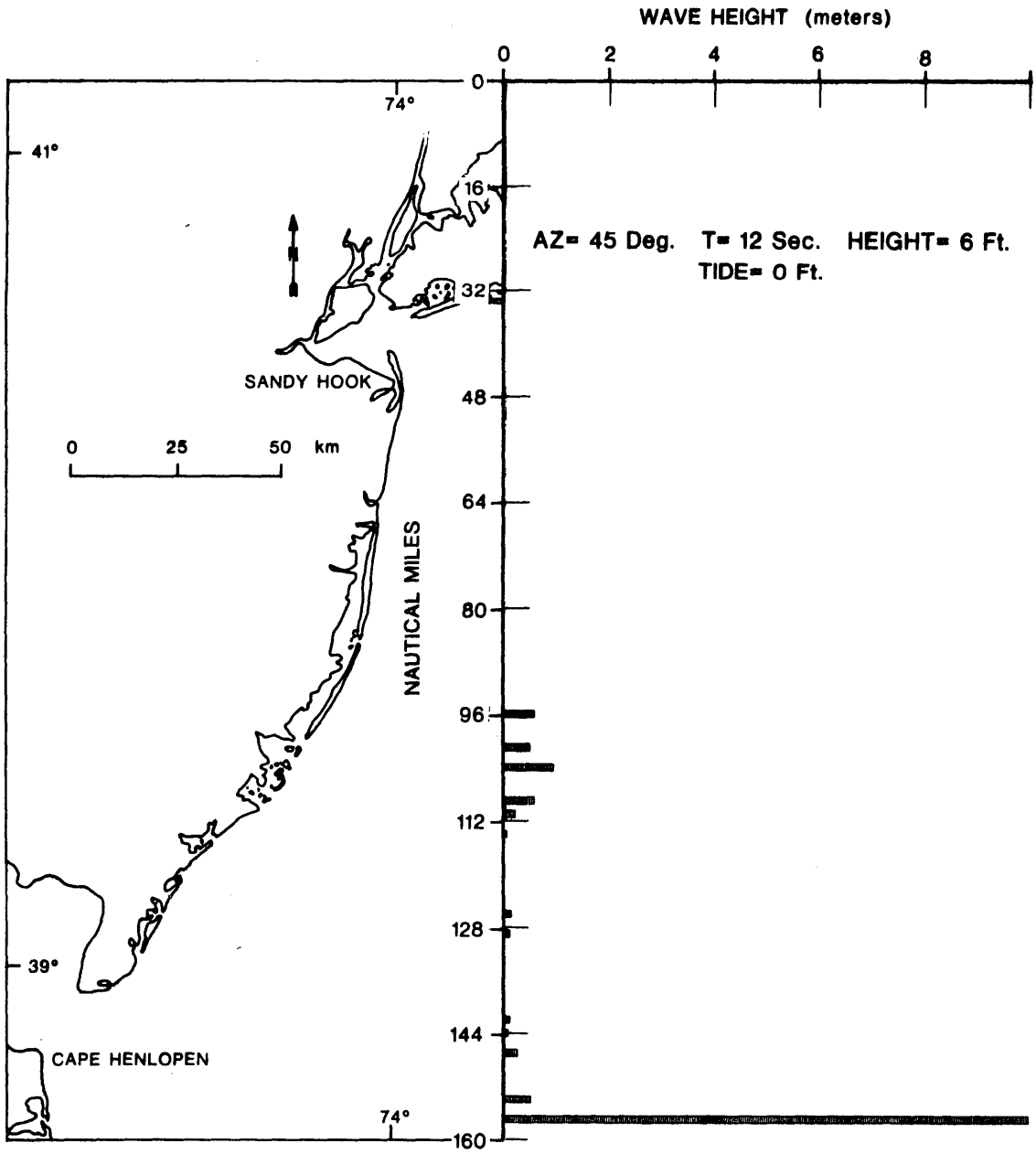

NEW JERSEY - DELAWARE SHORELINE (N-S)

VIMS - BLM - BALTIMORE CANYON SHELF WAVES

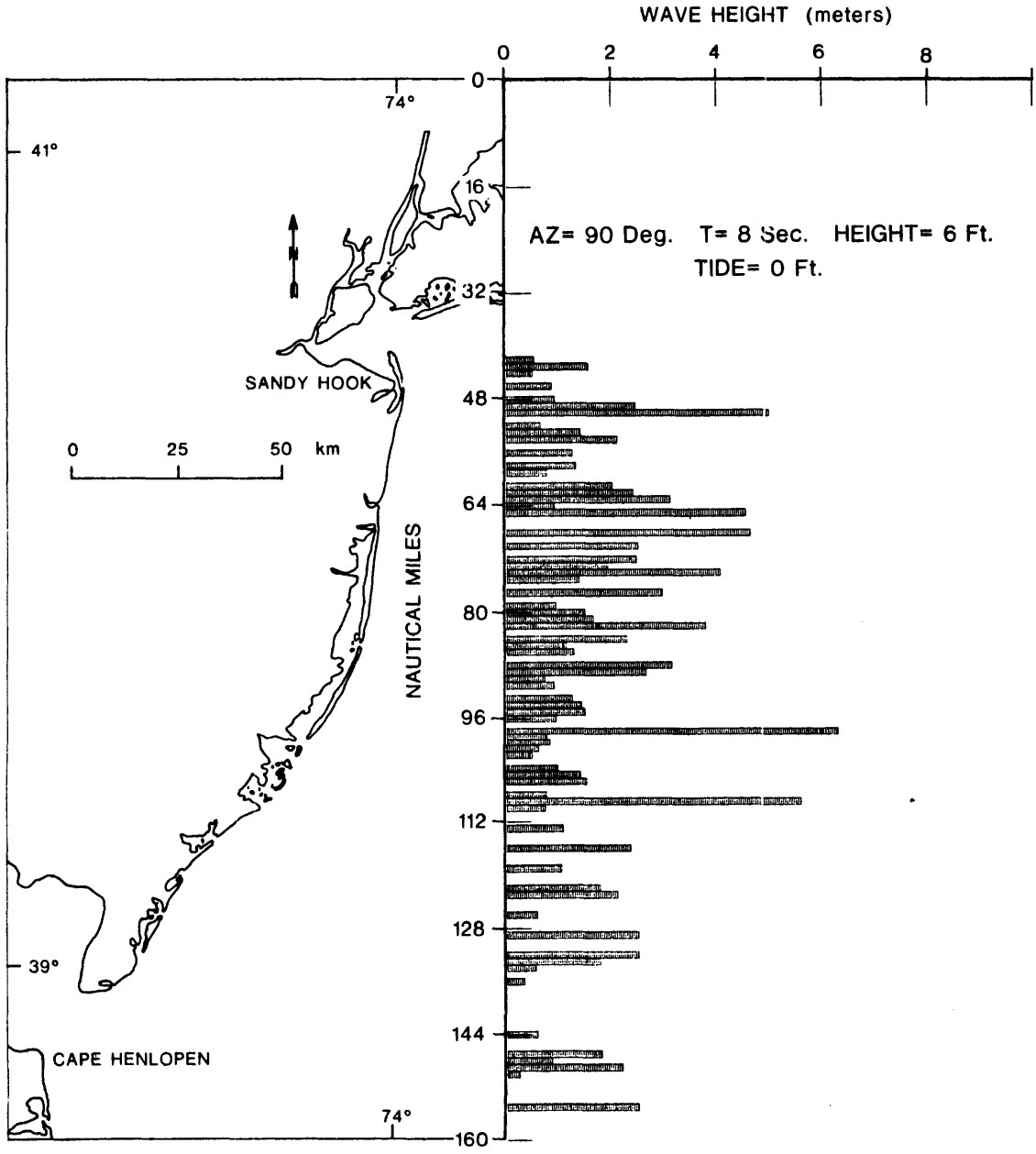

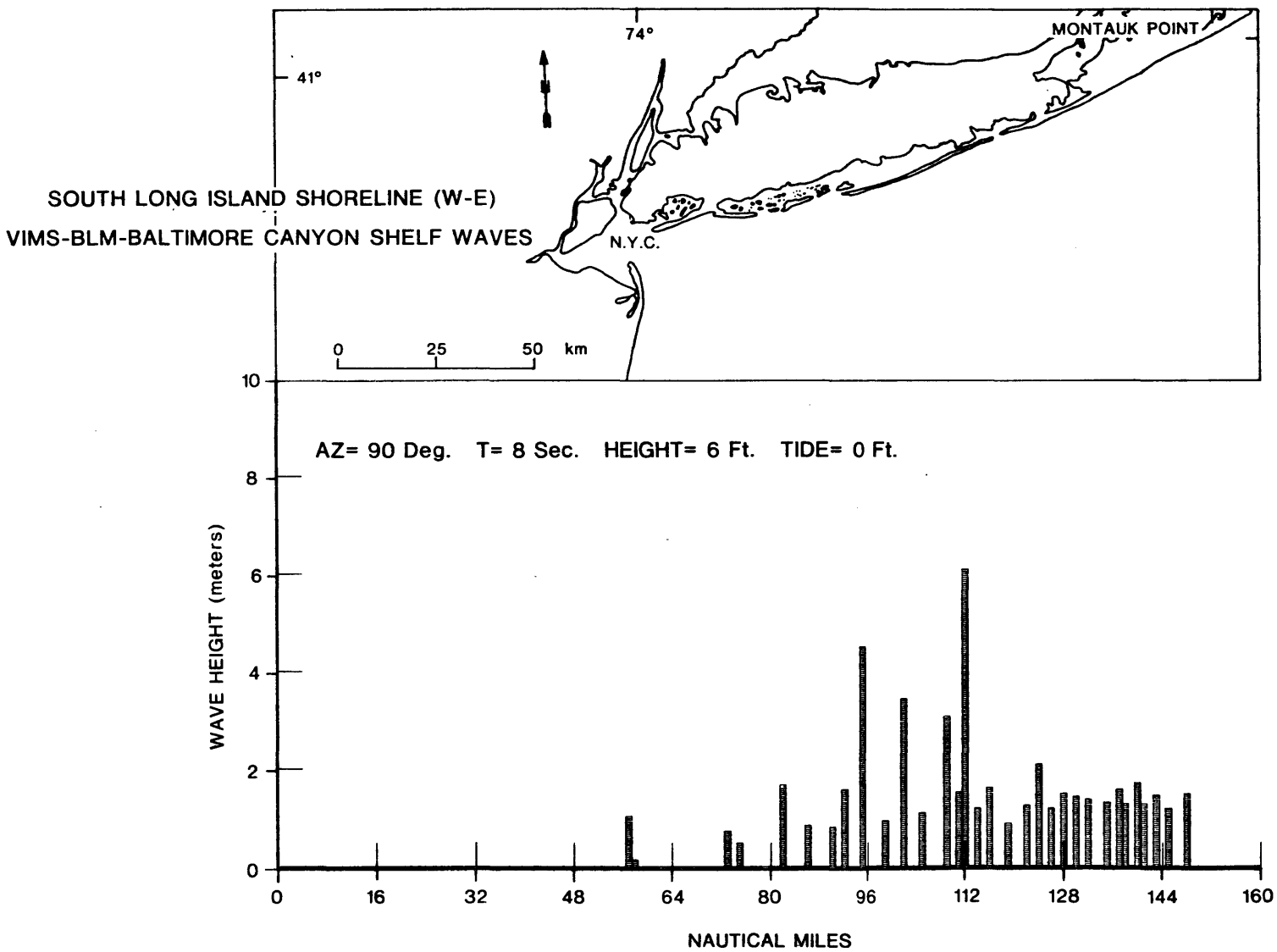
SOUTH LONG ISLAND SHORELINE (W-E)
VIMS-BLM-BALTIMORE CANYON SHELF WAVES
74°
41°
MONTAUK POINT
N.Y.C.
0 25 50 km
AZ= 90 Deg. T= 8 Sec. HEIGHT= 6 Ft. TIDE= 0 Ft.
WAVE HEIGHT (meters)
0 2 4 6 8 10
0 16 32 48 64 80 96 112 128 144 160
NAUTICAL MILES

H-4b

NEW JERSEY - DELAWARE SHORELINE (N-S)

VIMS - BLM - BALTIMORE CANYON SHELF WAVES

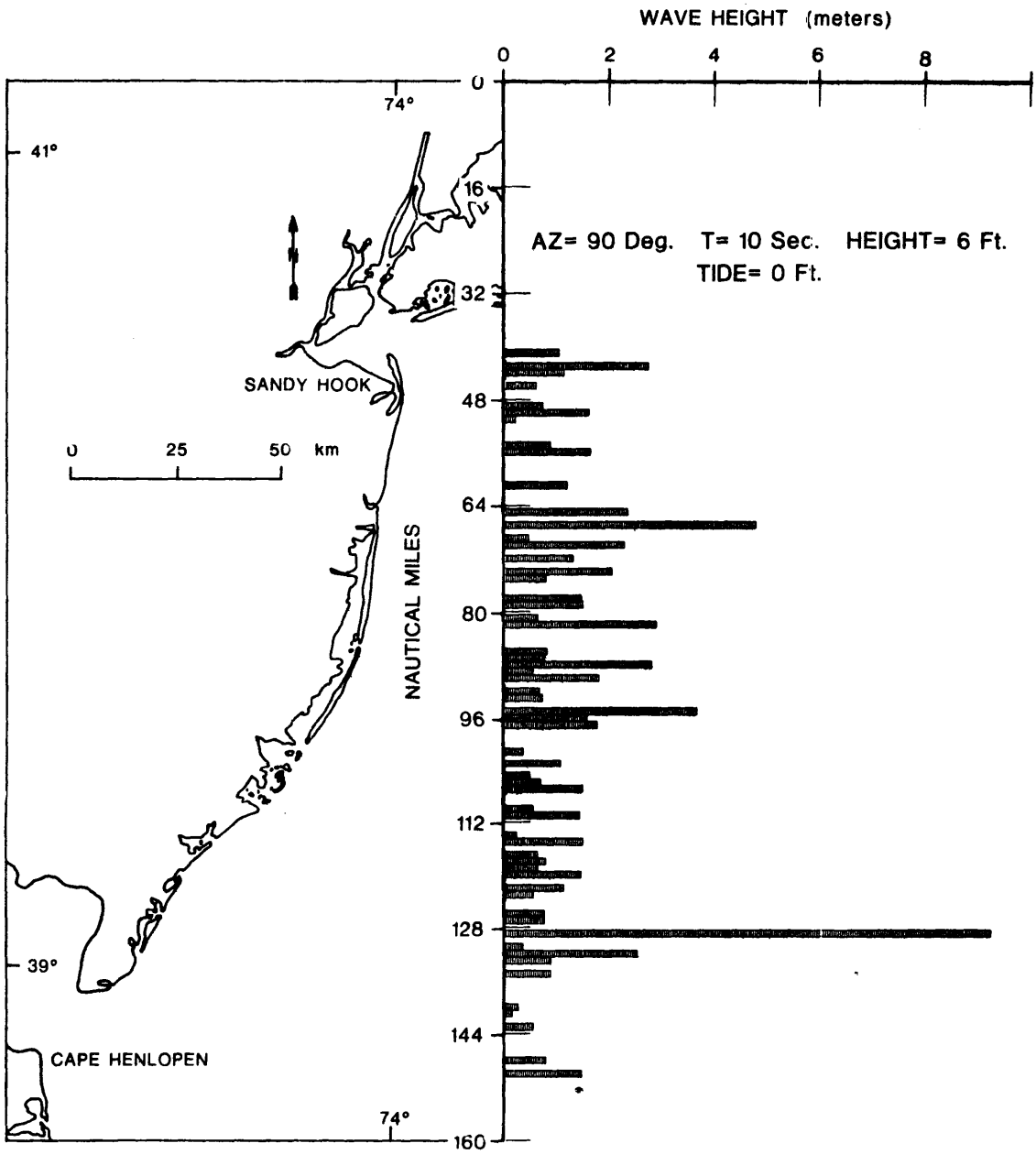

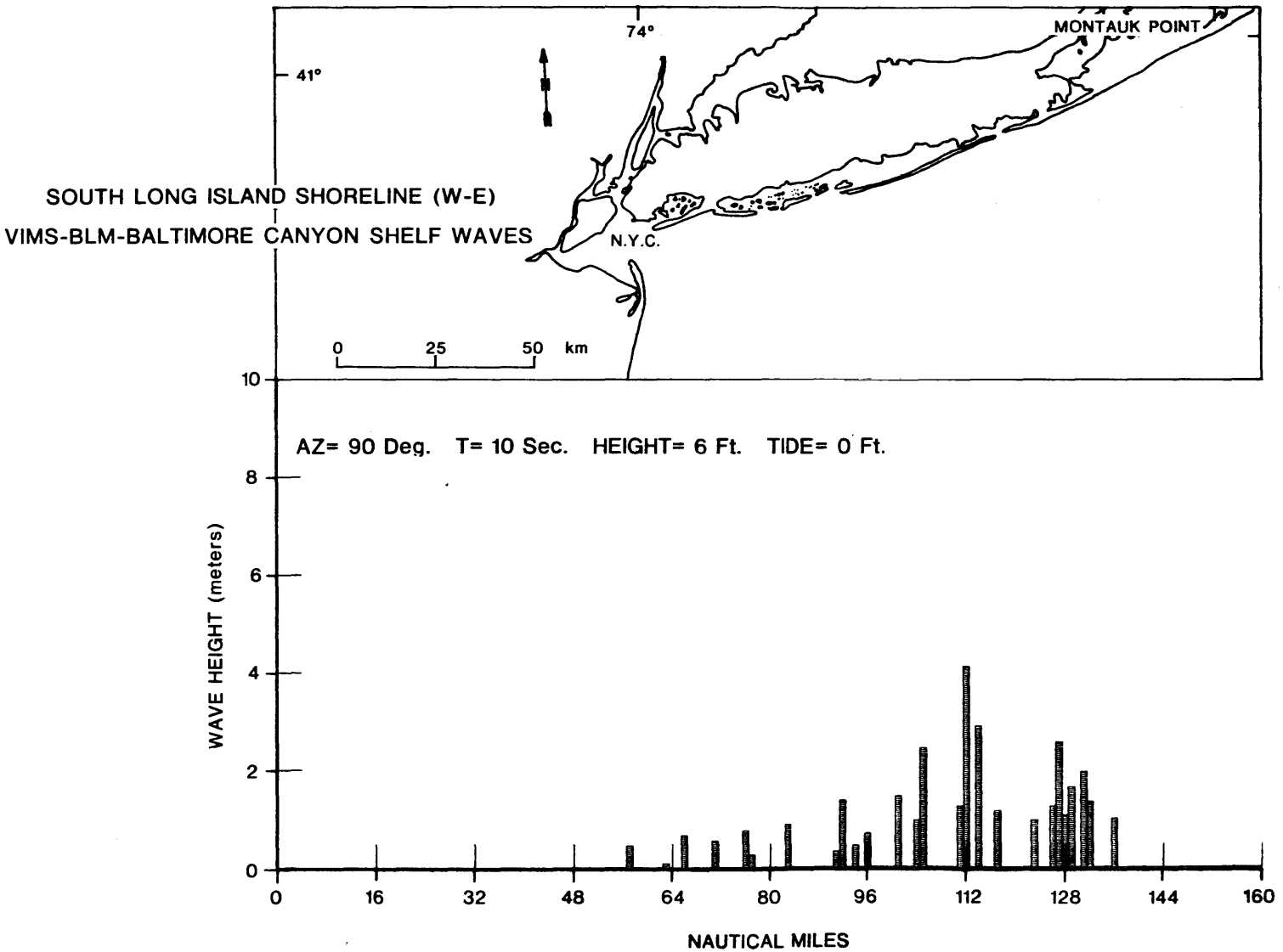
SOUTH LONG ISLAND SHORELINE (W-E)
VIMS-BLM-BALTIMORE CANYON SHELF WAVES
74°
41°
MONTAUK POINT
N.Y.C.
0 25 50 km
AZ= 90 Deg. T= 10 Sec. HEIGHT= 6 Ft. TIDE= 0 Ft.
WAVE HEIGHT (meters)
0
2
4
6
8
10
0 16 32 48 64 80 96 112 128 144 160
NAUTICAL MILES

NEW JERSEY - DELAWARE SHORELINE (N-S)

VIMS - BLM - BALTIMORE CANYON SHELF WAVES

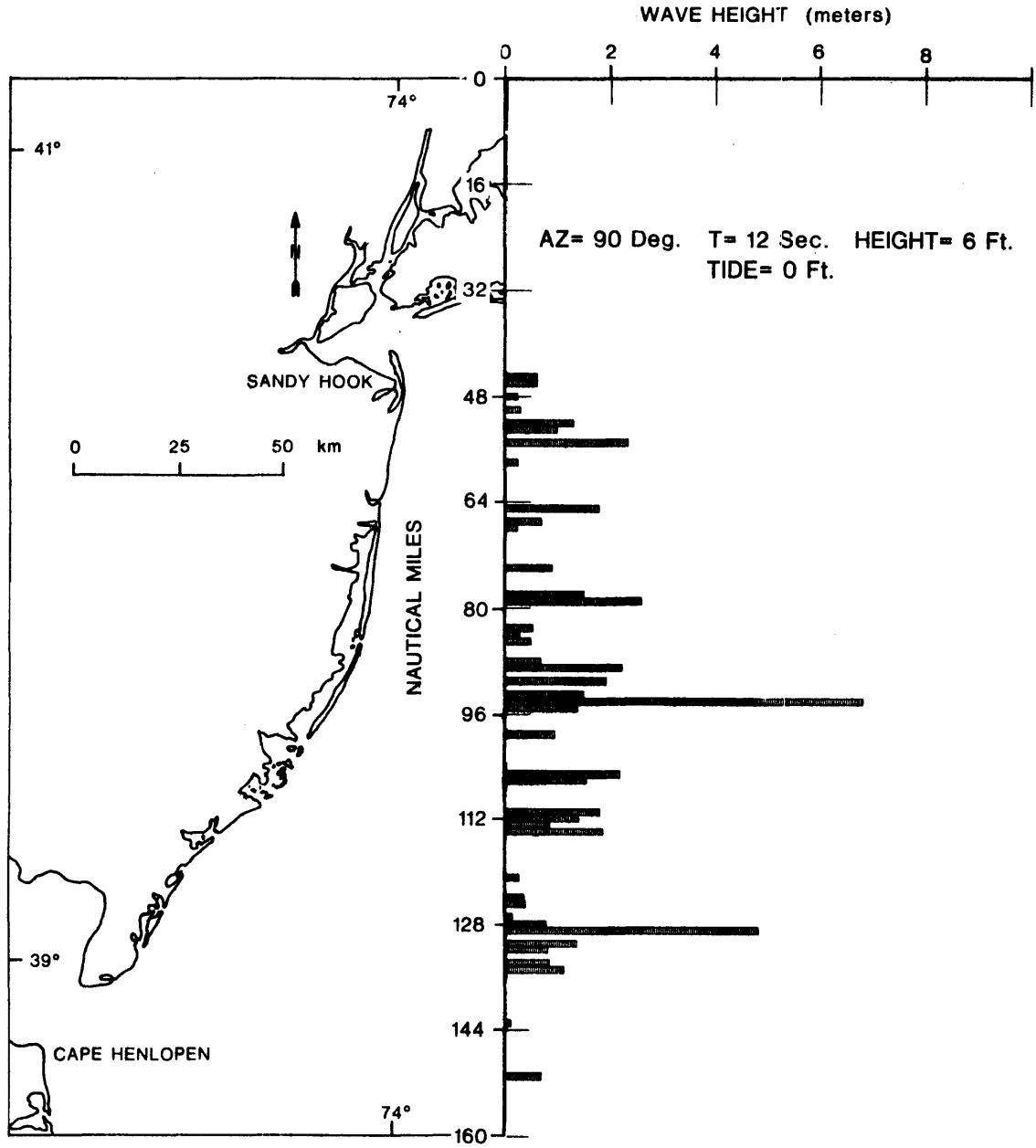

SOUTH LONG ISLAND SHORELINE (W-E)
VIMS-BLM-BALTIMORE CANYON SHELF WAVES

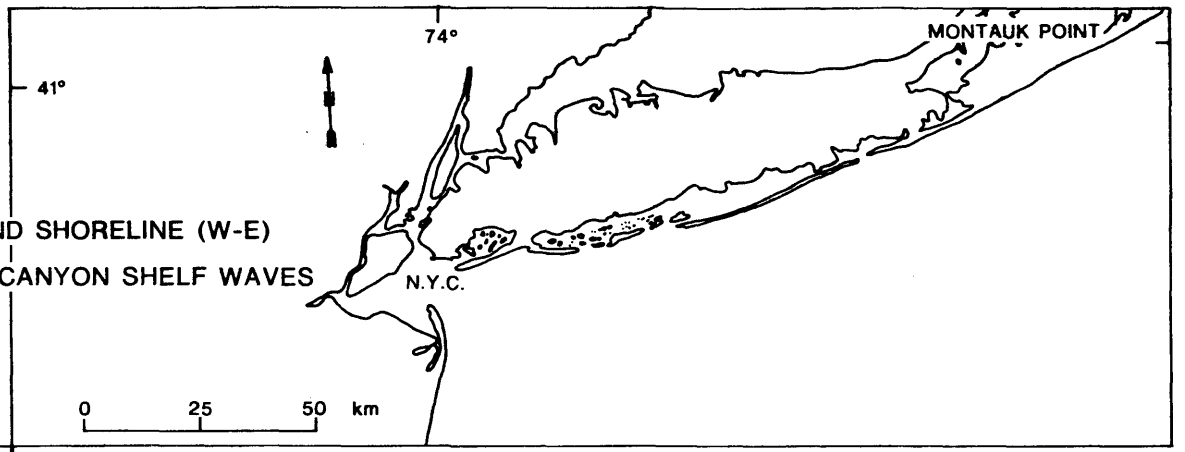

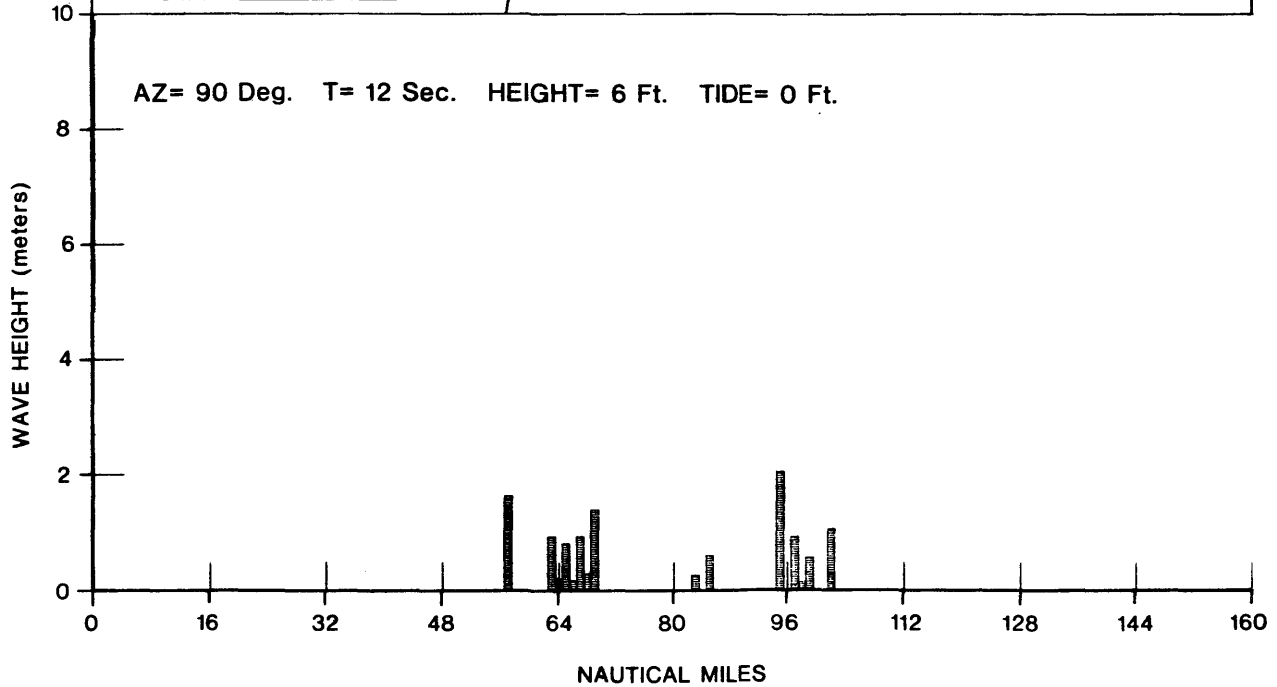

NEW JERSEY - DELAWARE SHORELINE (N-S)

VIMS - BLM - BALTIMORE CANYON SHELF WAVES

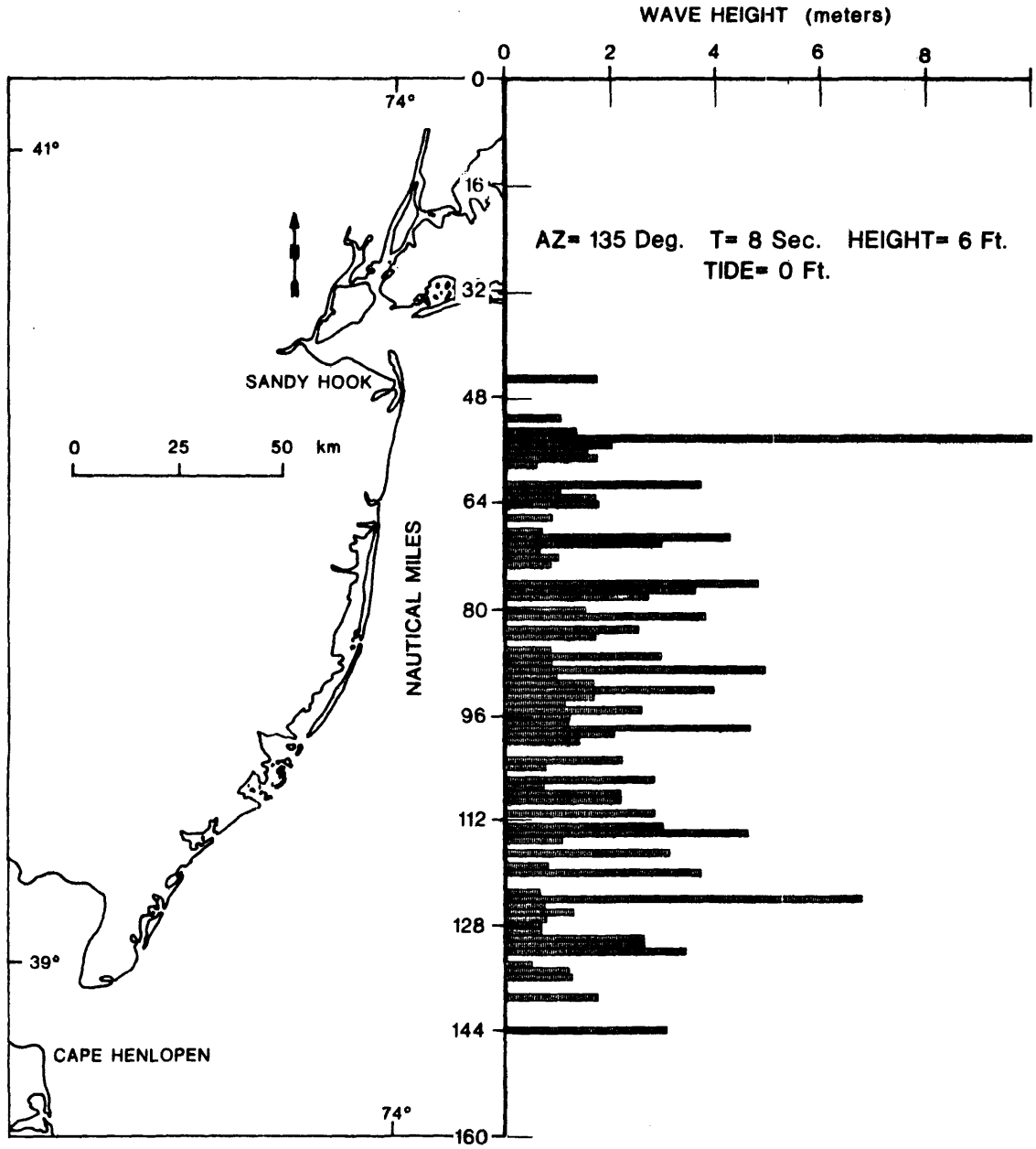

SOUTH LONG ISLAND SHORELINE (W-E)
VIMS-BLM-BALTIMORE CANYON SHELF WAVES

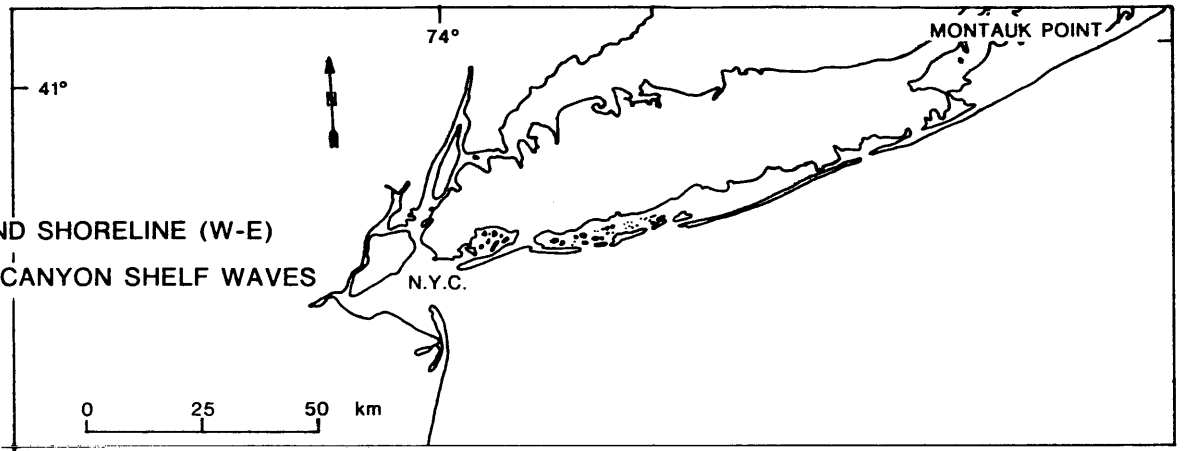

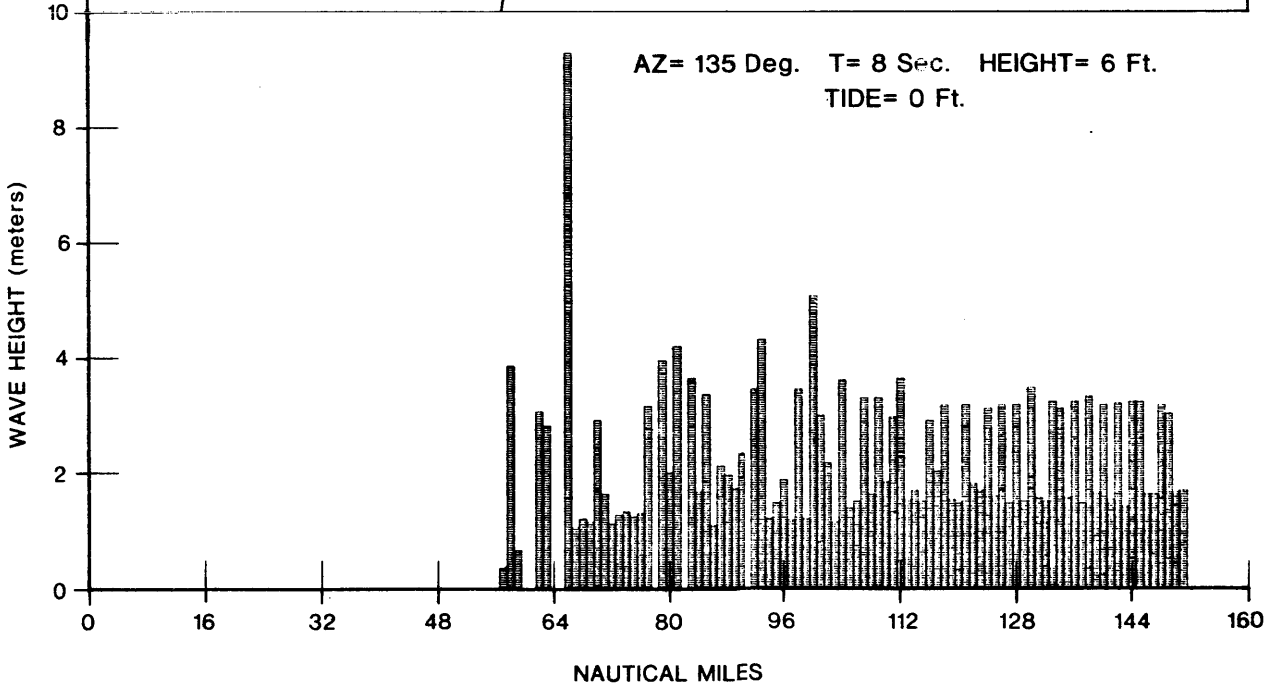

NEW JERSEY - DELAWARE SHORELINE (N-S)

VIMS - BLM - BALTIMORE CANYON SHELF WAVES

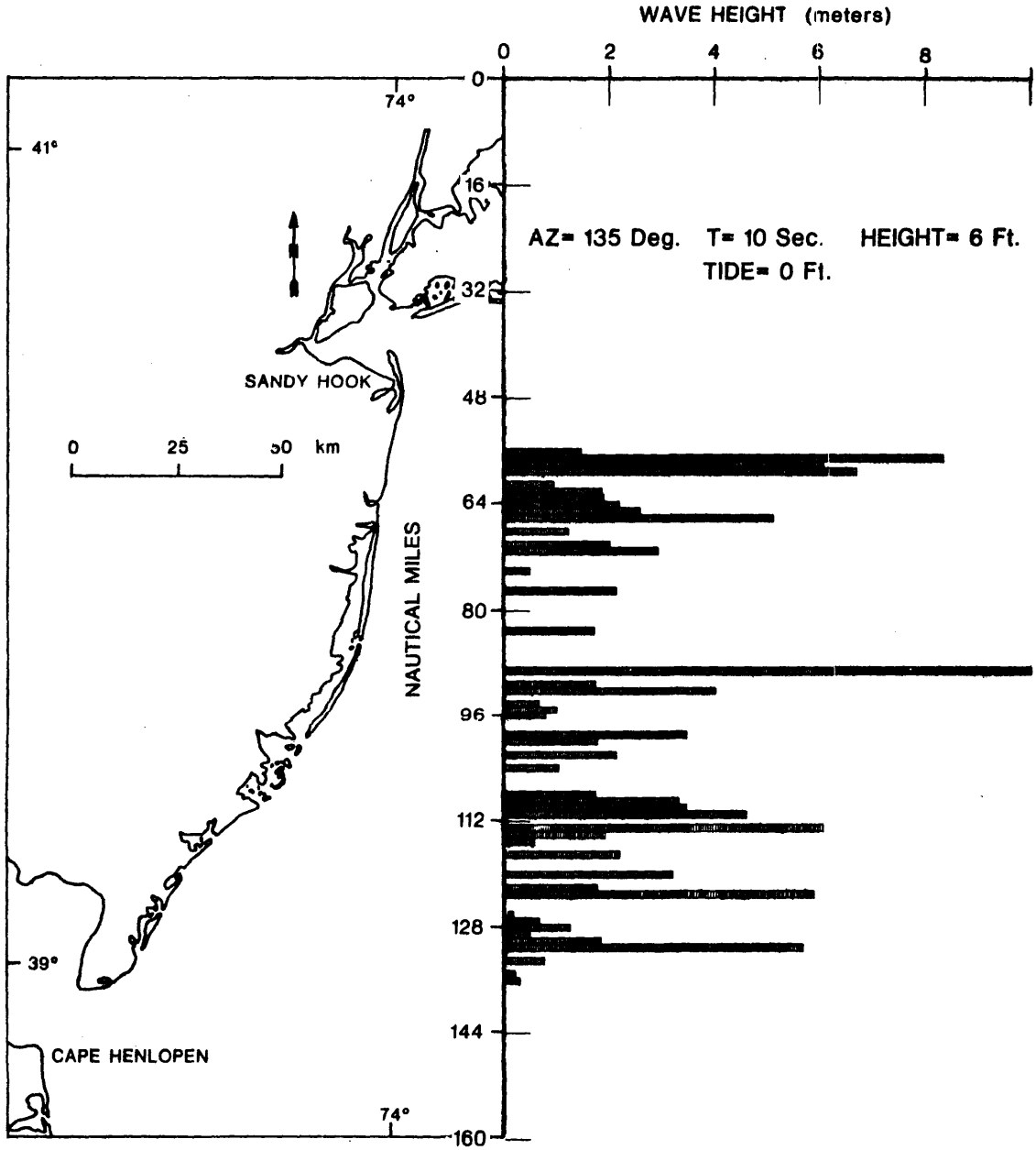

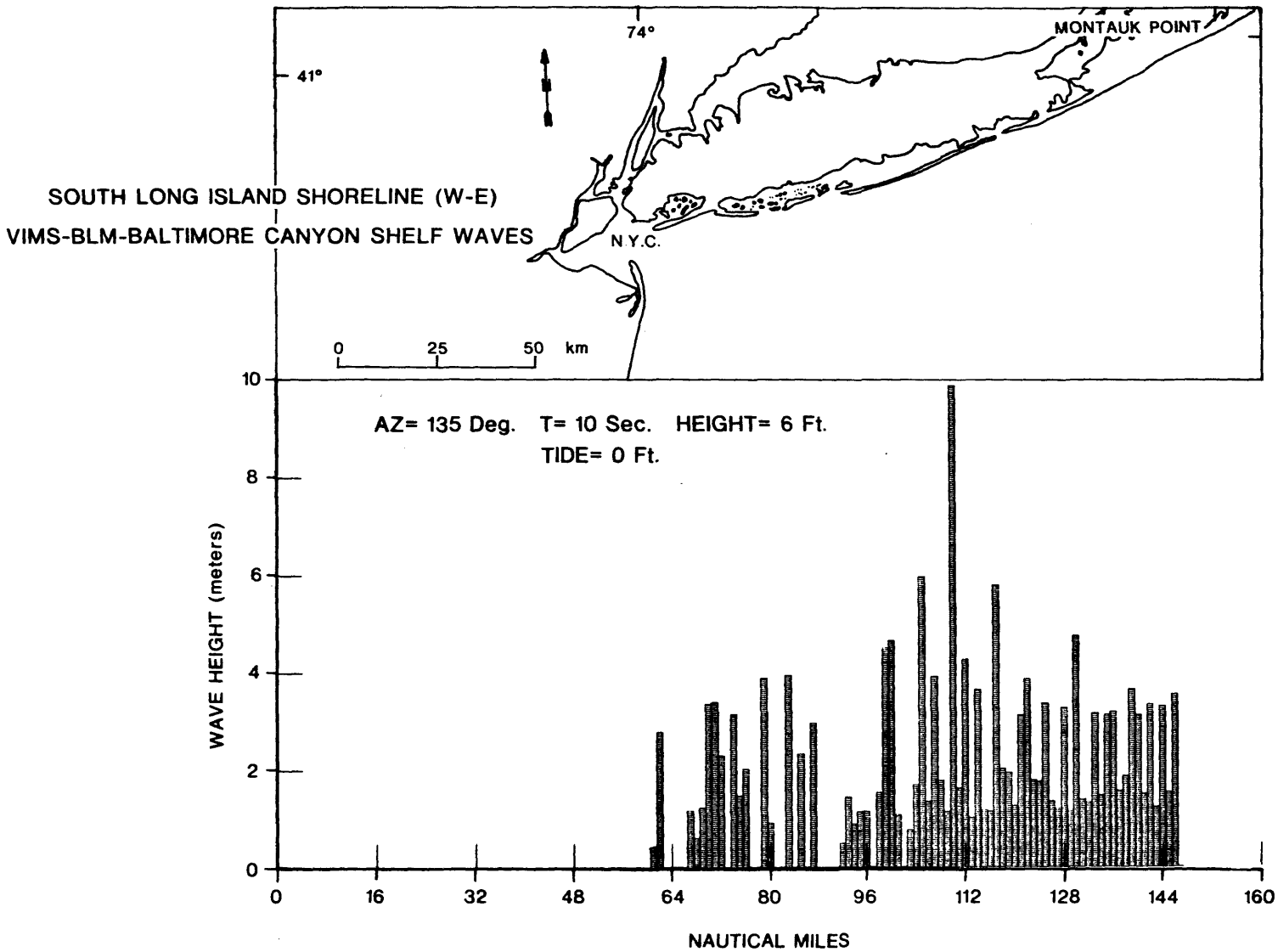
SOUTH LONG ISLAND SHORELINE (W-E)
VIMS-BLM-BALTIMORE CANYON SHELF WAVES
74°
41°
MONTAUK POINT
N.Y.C.
0 25 50 km
AZ= 135 Deg. T= 10 Sec. HEIGHT= 6 Ft.
TIDE= 0 Ft.
WAVE HEIGHT (meters)
0
2
4
6
8
10
0 16 32 48 64 80 96 112 128 144 160
NAUTICAL MILES

NEW JERSEY - DELAWARE SHORELINE (N-S)
VIMS - BLM - BALTIMORE CANYON SHELF WAVES

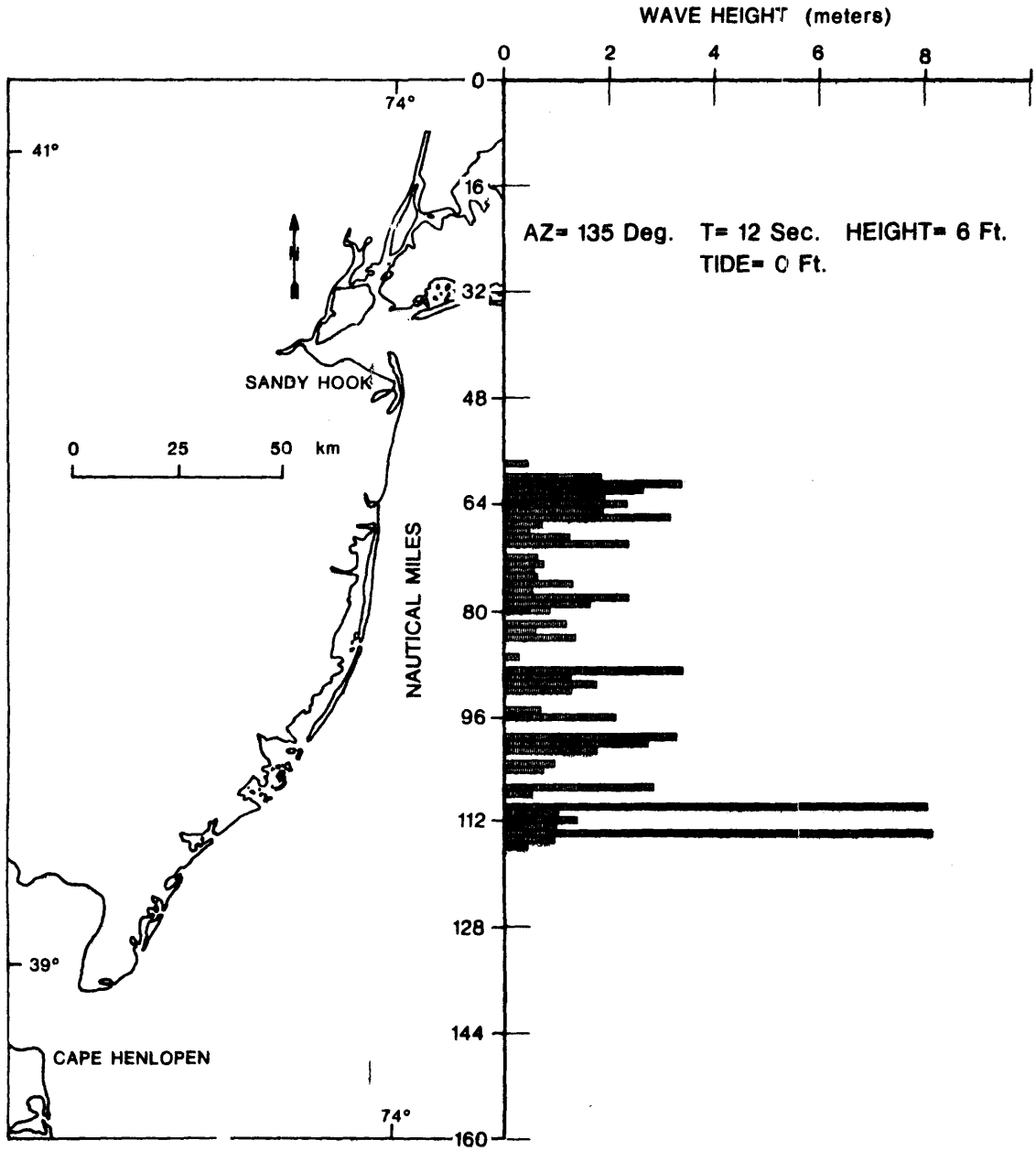

SOUTH LONG ISLAND SHORELINE (W-E)
VIMS-BLM-BALTIMORE CANYON SHELF WAVES

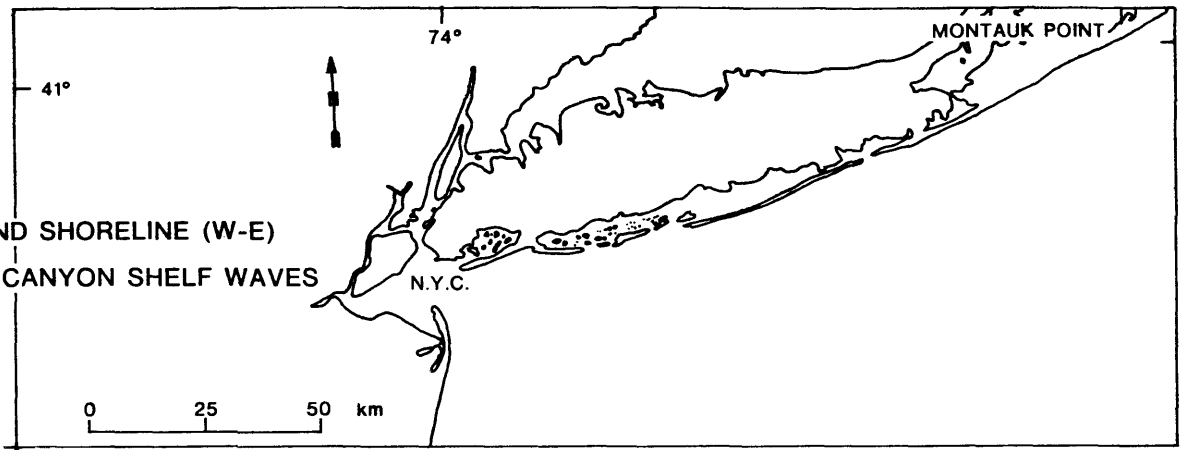

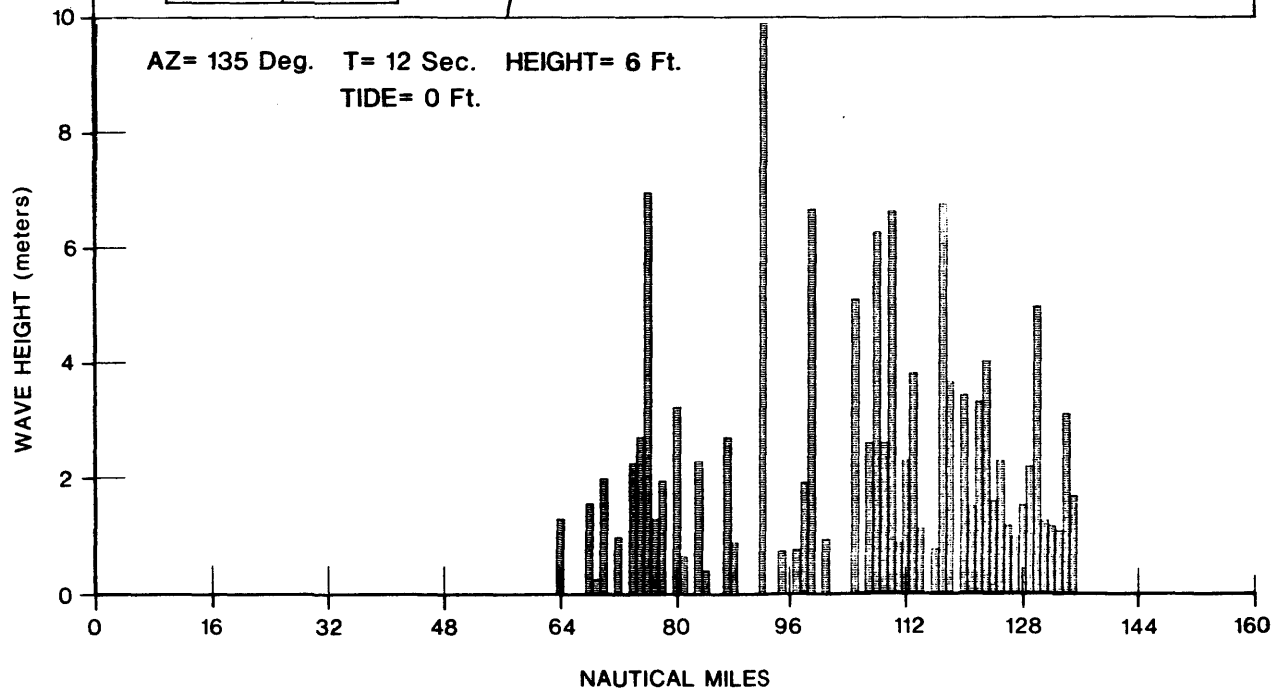

EW JERSEY - DELAWARE SHORELINE (N-S)

VIM ; - BLM - BALTIMORE CANYON SHELF WAVES

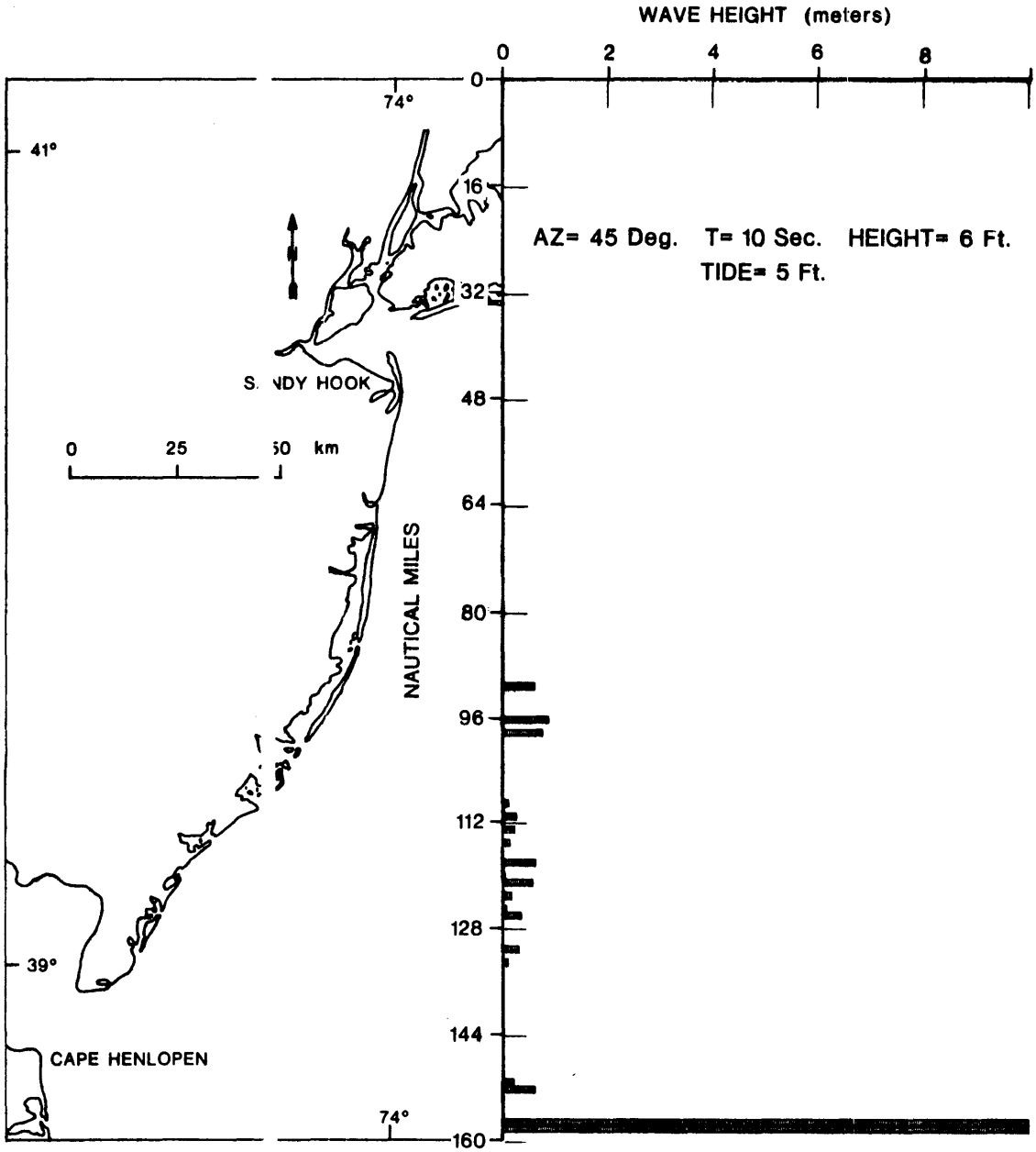

NEW JERSEY - DELAWARE SHORELINE (N-S)

VIMS - BLM - BALTIMORE CANYON SHELF WAVES

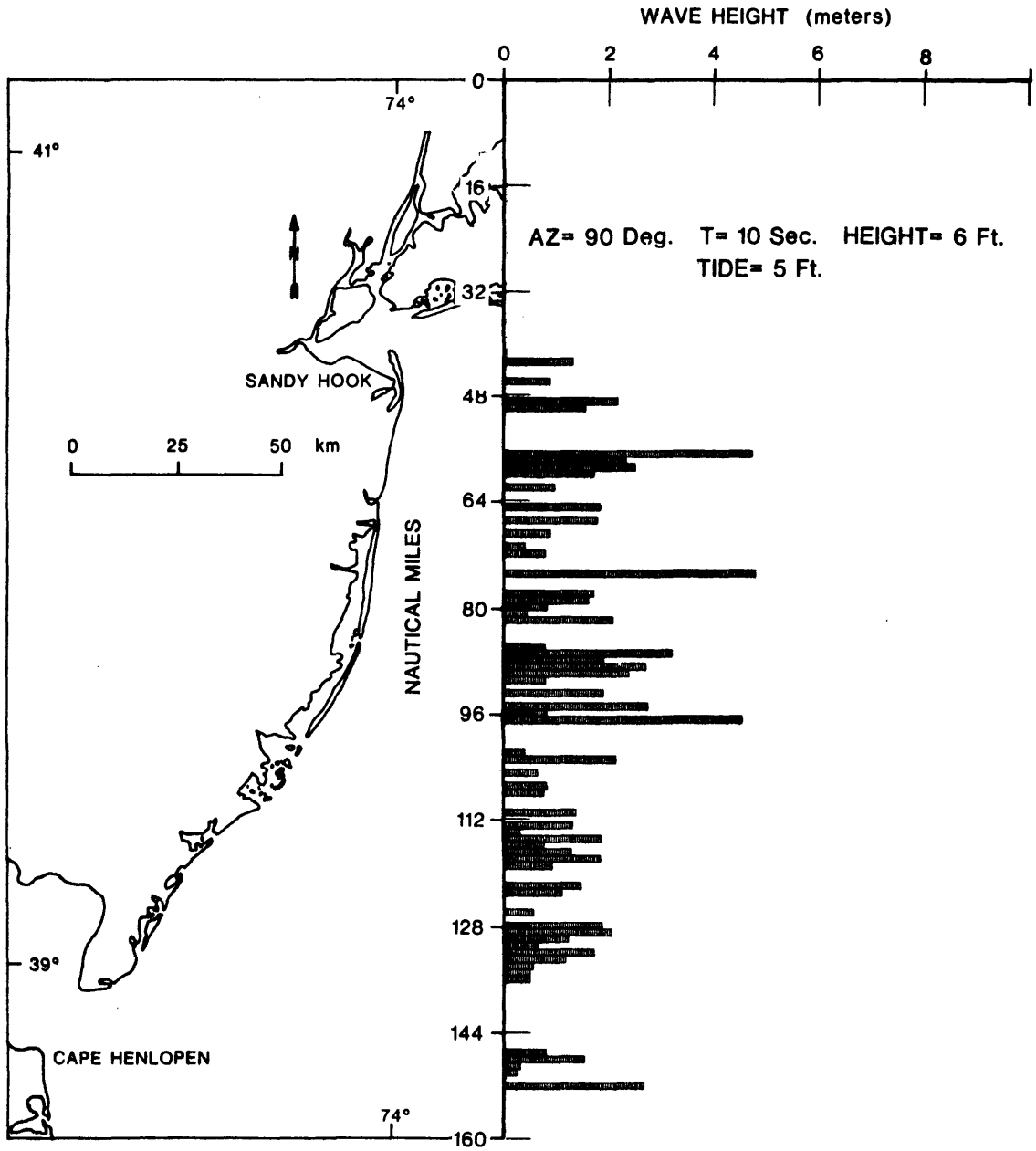

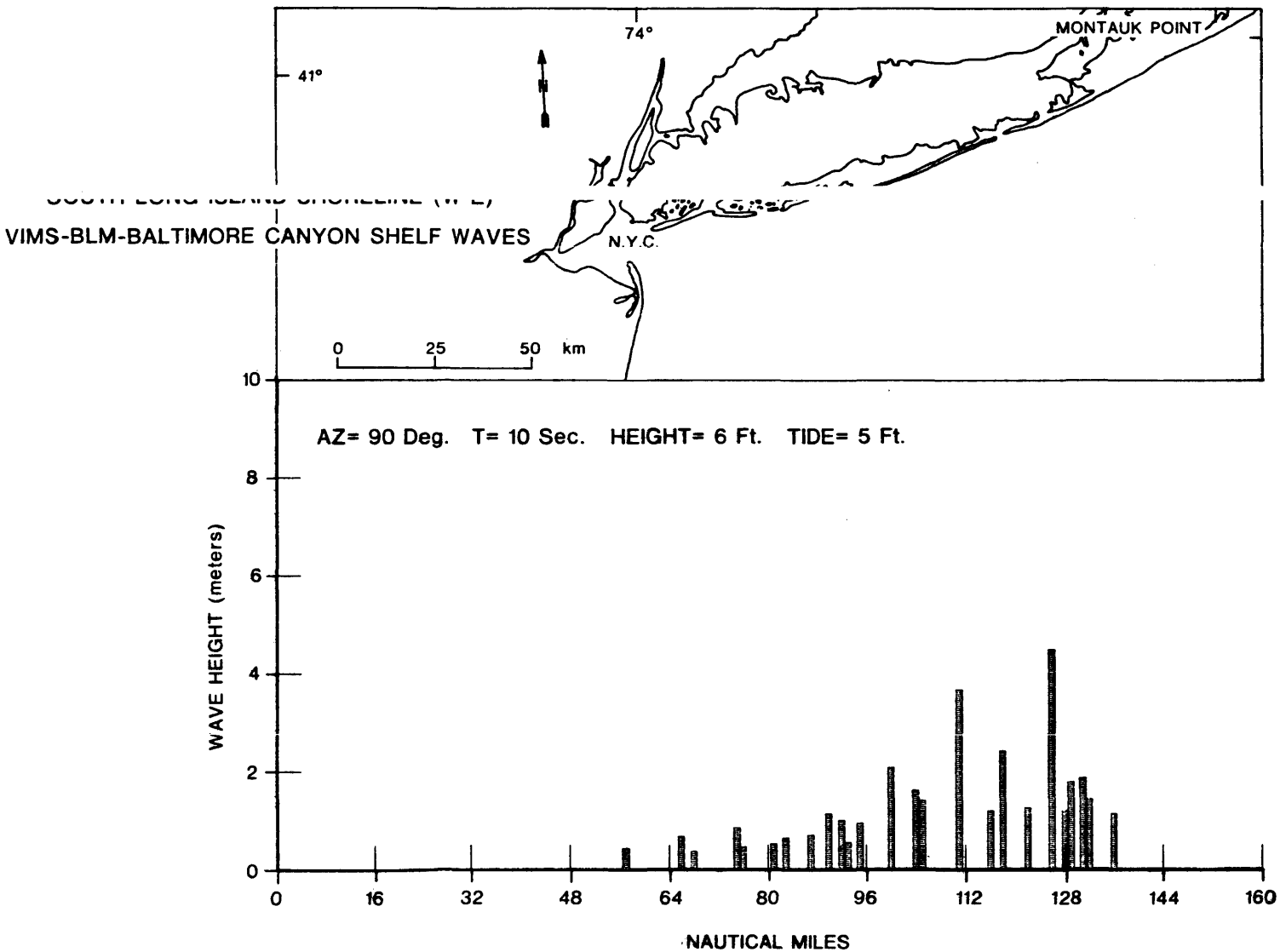
74°
41°
MONTAUK POINT
N.Y.C.
0 25 50 km
VIMS-BLM-BALTIMORE CANYON SHELF WAVES
AZ= 90 Deg. T= 10 Sec. HEIGHT= 6 Ft. TIDE= 5 Ft.
WAVE HEIGHT (meters)
0
2
4
6
8
10
0 16 32 48 64 80 96 112 128 144 160
NAUTICAL MILES

H-11b

NEW JERSEY - DELAWARE SHORELINE (N-S)

VIMS - BLM - BALTIMORE CANYON SHELF WAVES

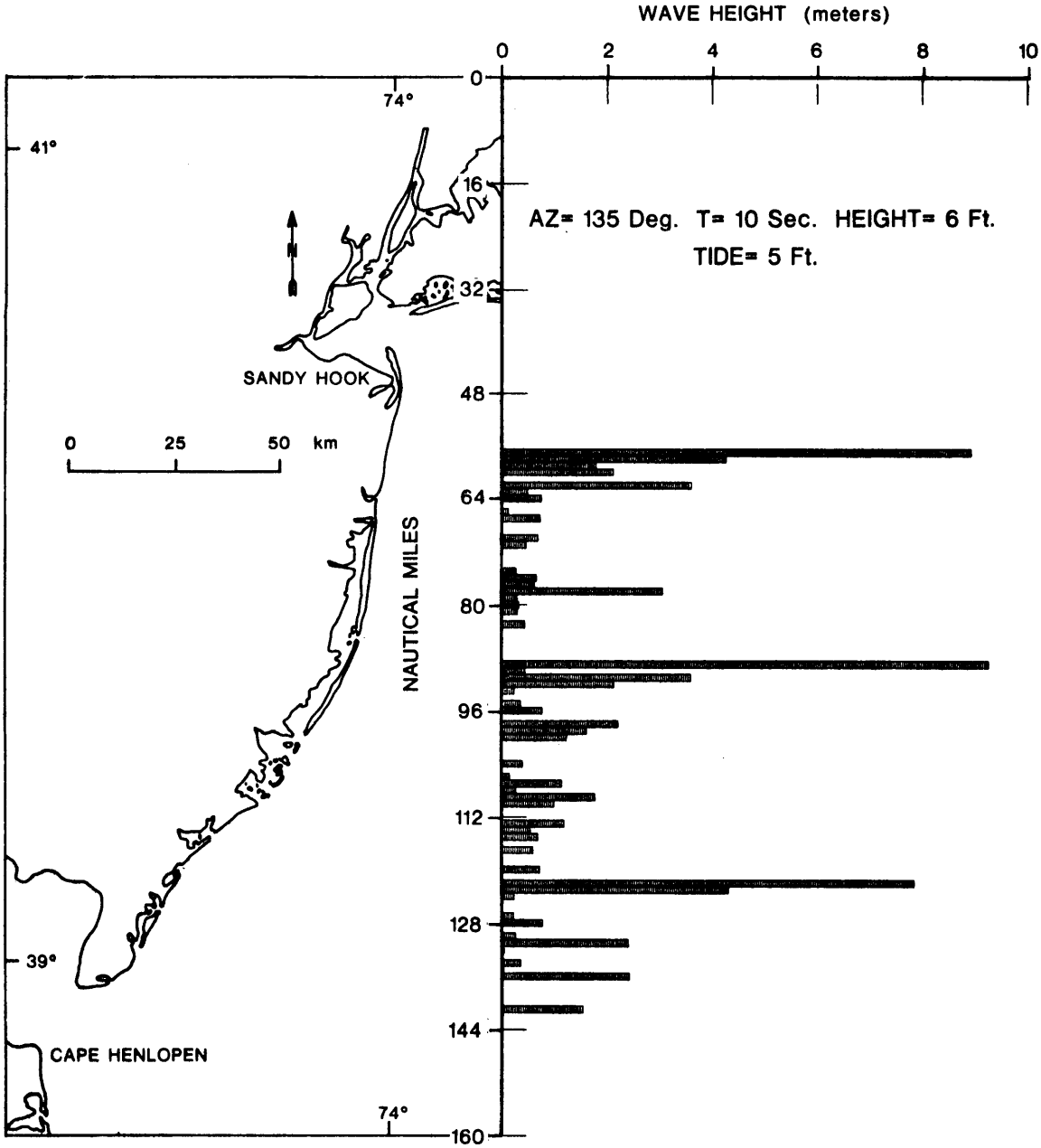

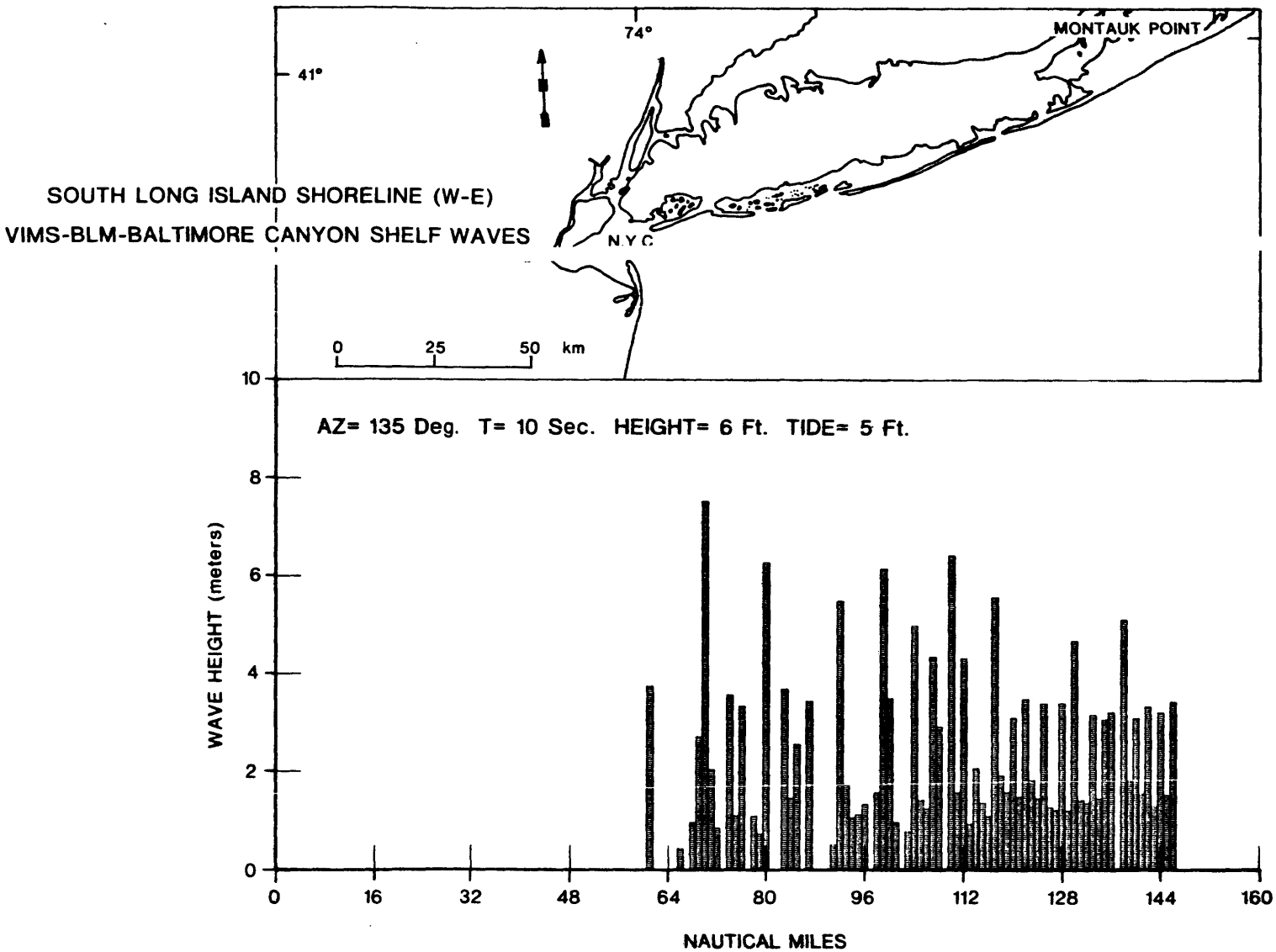
SOUTH LONG ISLAND SHORELINE (W-E)
VIMS-BLM-BALTIMORE CANYON SHELF WAVES
74°
41°
MONTAUK POINT
N.Y.C.
0 25 50 km
AZ= 135 Deg. T= 10 Sec. HEIGHT= 6 Ft. TIDE= 5 Ft.
WAVE HEIGHT (meters)
0
2
4
6
8
10
0 16 32 48 64 80 96 112 128 144 160
NAUTICAL MILES

NEW JERSEY - DELAWARE SHORELINE (N-S)
VIMS - BLM - BALTIMORE CANYON SHELF WAVES

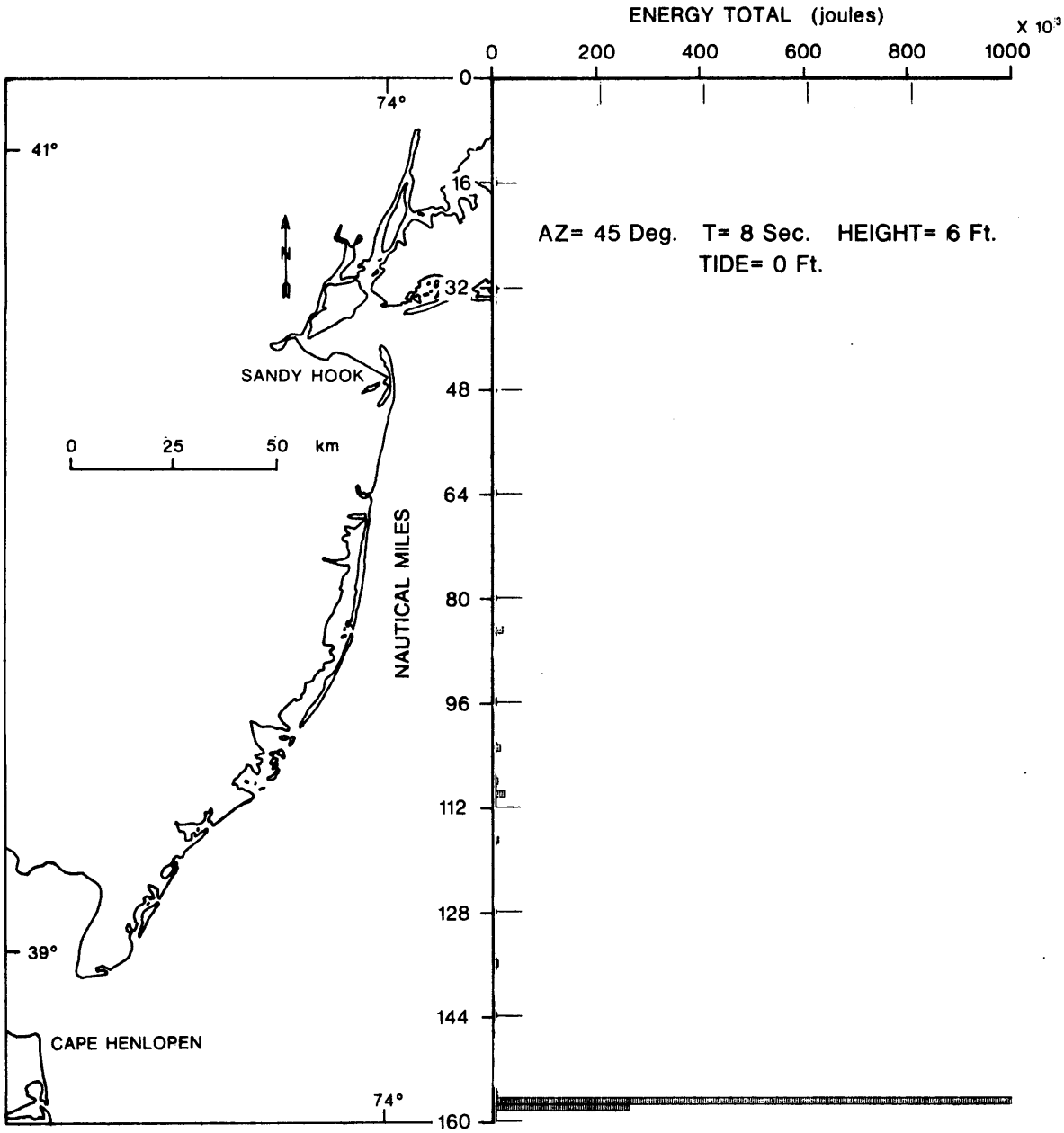

NEW JERSEY - DELAWARE SHORELINE (N-S)

/IMS - BLM - BALTIMORE CANYON SHELF WAVES

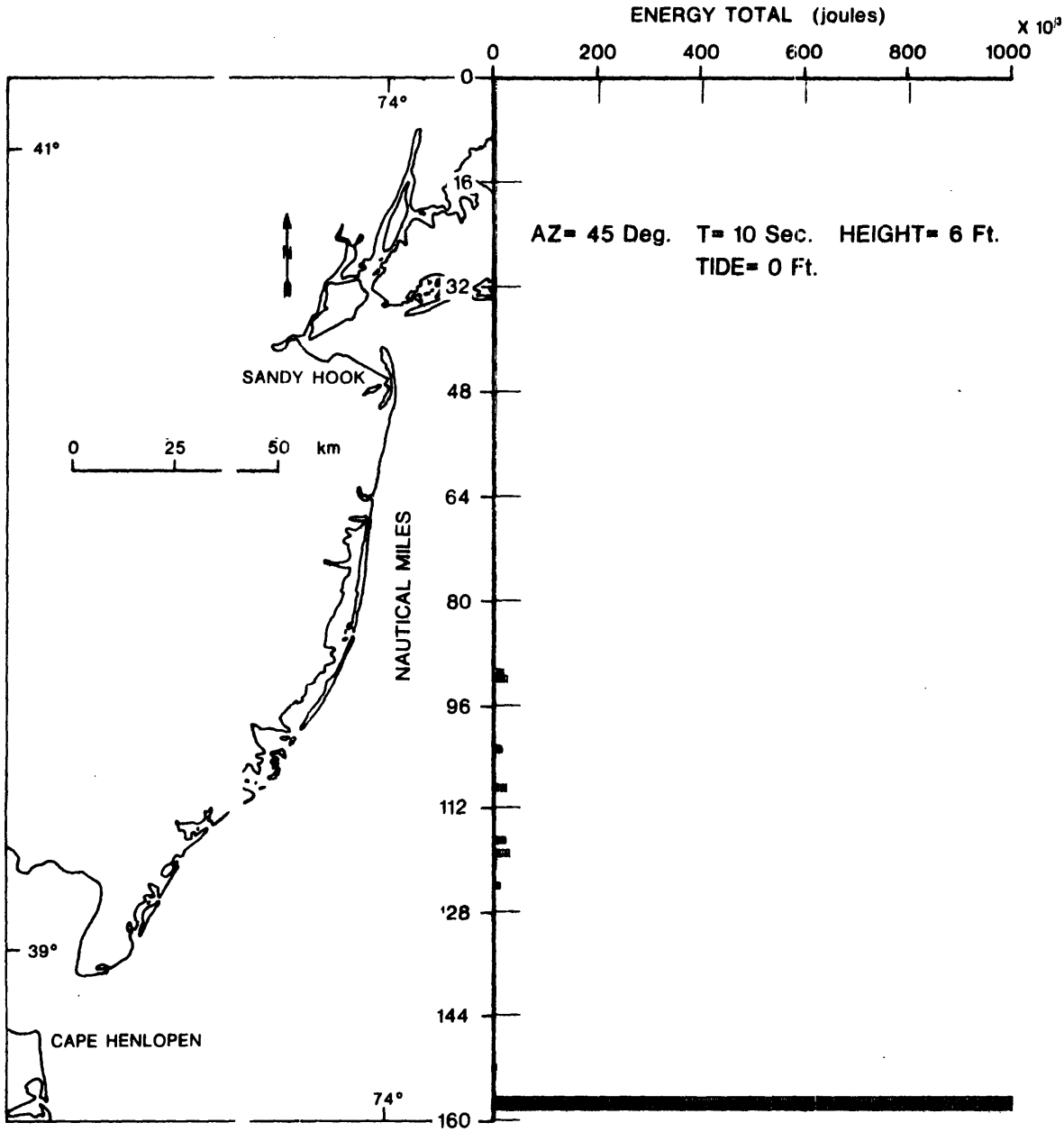

NEW JERSEY - DELAWARE SHORELINE (N-S)
VIMS - BLM - BALTIMORE CANYON SHELF WAVES

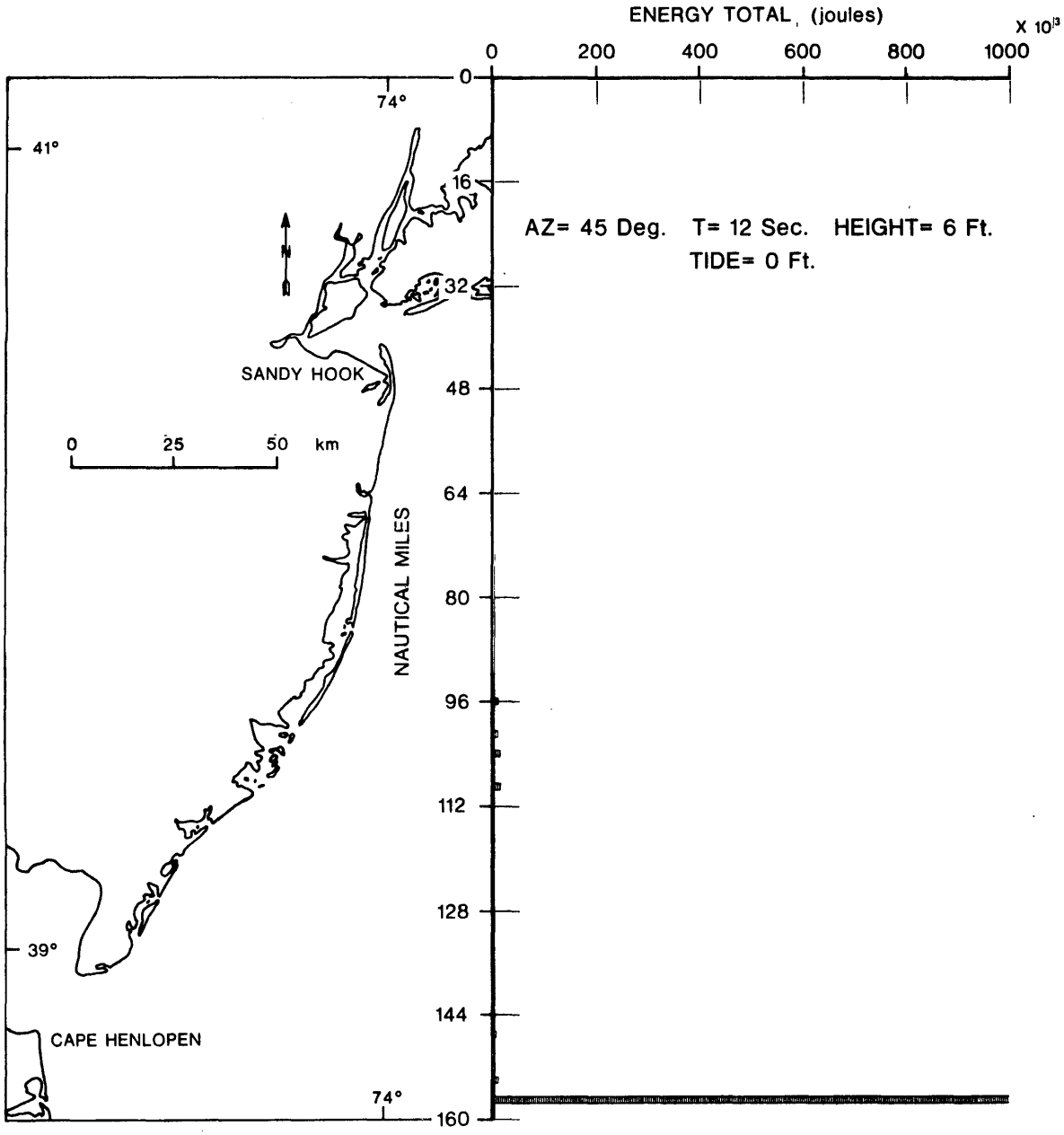

NEW JERSEY - DELAWARE SHORELINE (N-S)
VIMS - BLM - BALTIMORE CANYON SHELF WAVES

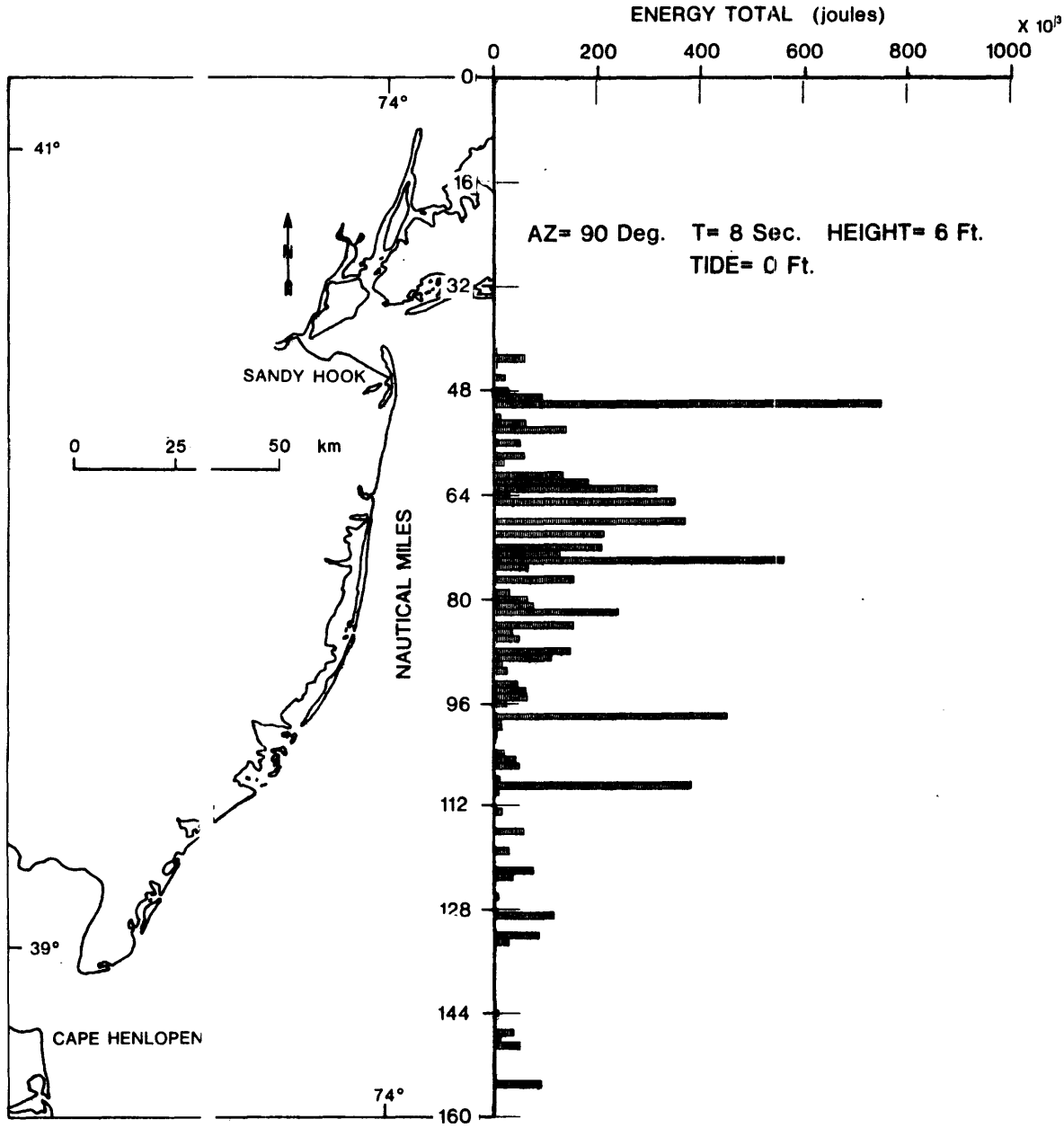

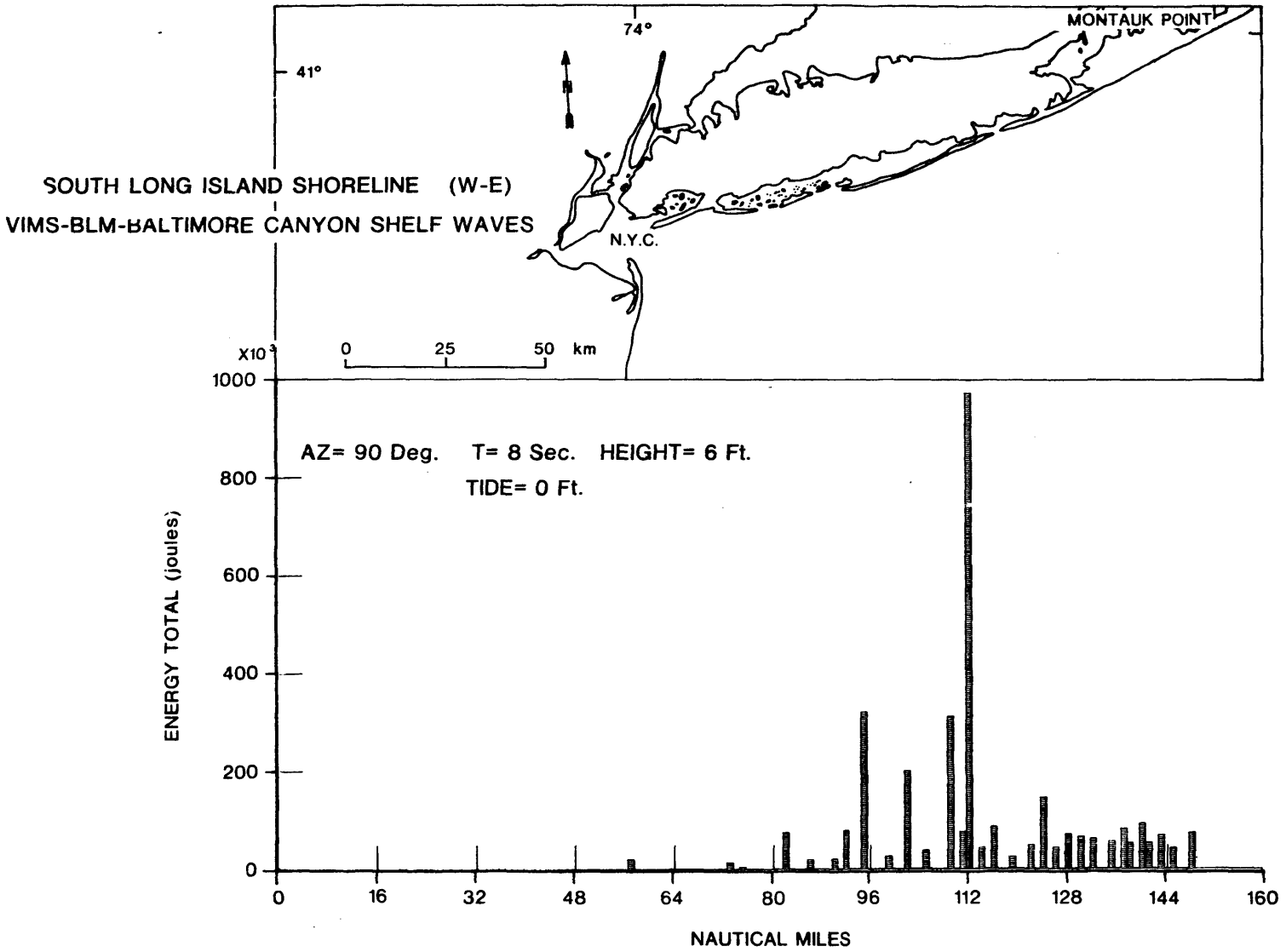
SOUTH LONG ISLAND SHORELINE (W-E)
VIMS-BLM-BALTIMORE CANYON SHELF WAVES
74°
41°
MONTAUK POINT
N.Y.C.
0 25 50 km
AZ= 90 Deg. T= 8 Sec. HEIGHT= 6 Ft.
TIDE= 0 Ft.
X10³
1000
800
600
400
200
0
ENERGY TOTAL (joules)
0 16 32 48 64 80 96 112 128 144 160
NAUTICAL MILES

NEW JERSEY - DELAWARE SHORELINE (N-S)
VIMS - BLM - BALTIMORE CANYON SHELF WAVES

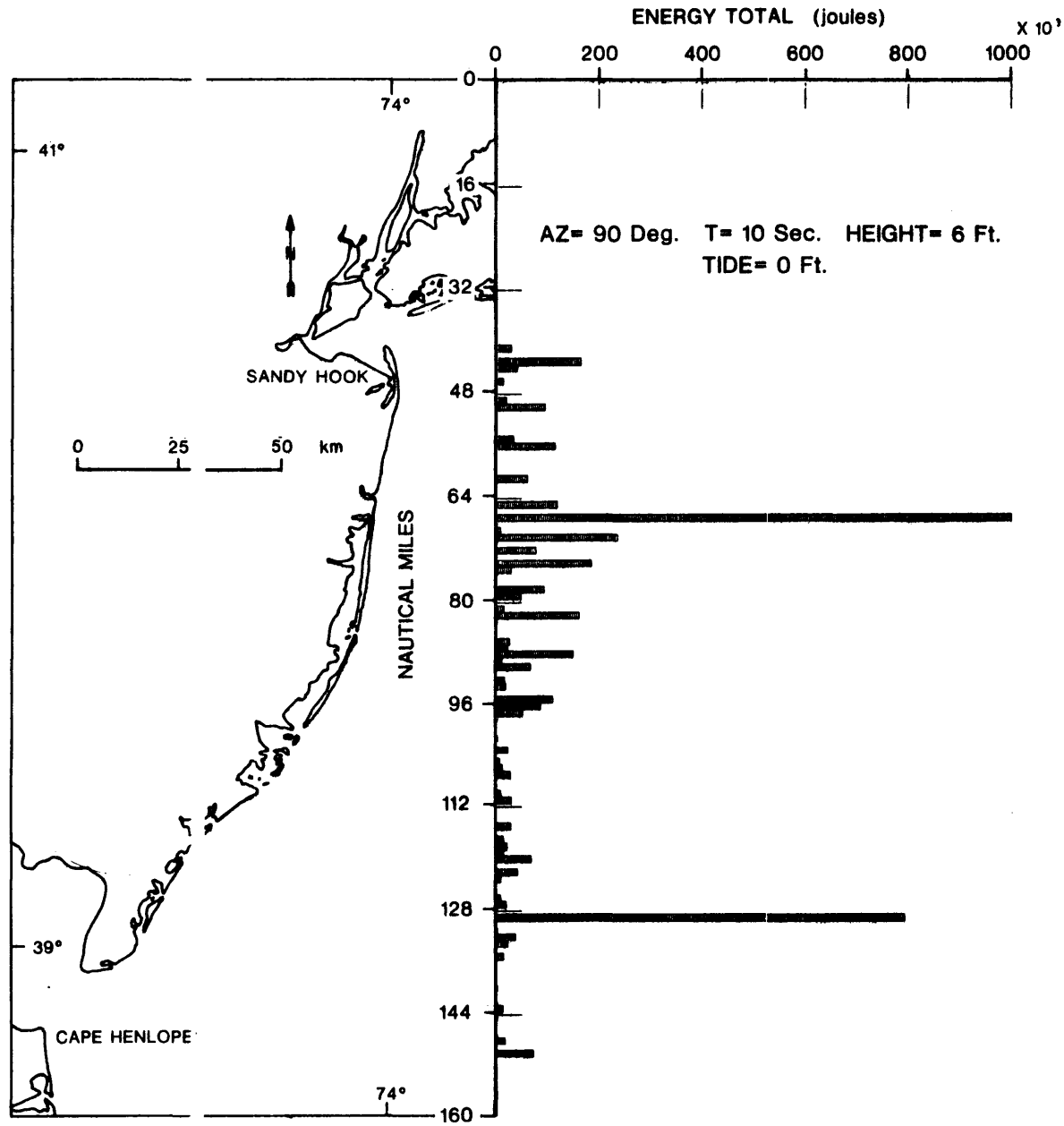

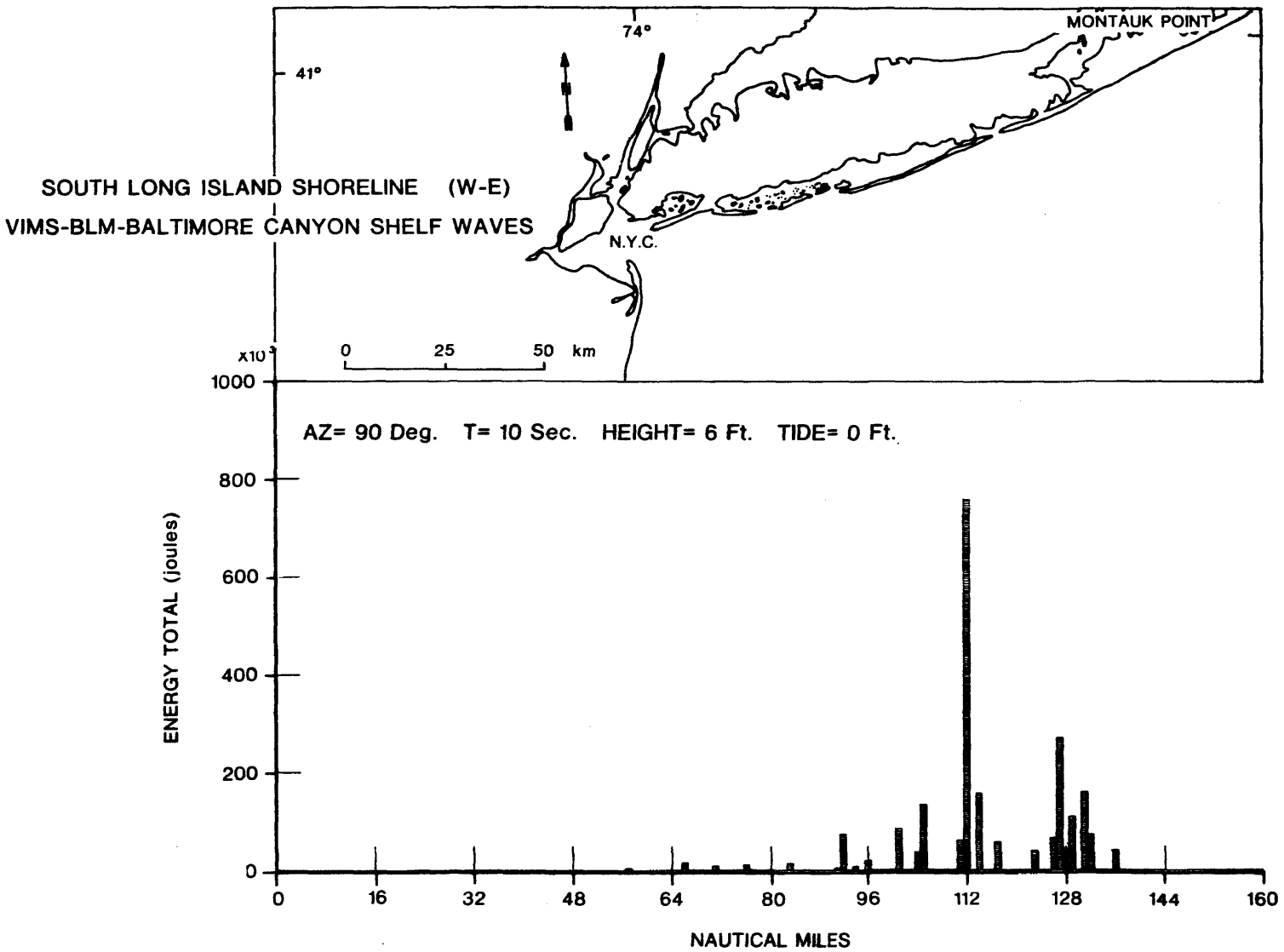
SOUTH LONG ISLAND SHORELINE (W-E)
VIMS-BLM-BALTIMORE CANYON SHELF WAVES
74°
41°
MONTAUK POINT
N.Y.C.
0 25 50 km
AZ= 90 Deg. T= 10 Sec. HEIGHT= 6 Ft. TIDE= 0 Ft.
ENERGY TOTAL (joules)
x10³
1000
800
600
400
200
0
0 16 32 48 64 80 96 112 128 144 160
NAUTICAL MILES

NEW JERSEY - DELAWARE SHORELINE (N-S)

' IMS - BLM - BALTIMORE CANYON SHELF WAVES

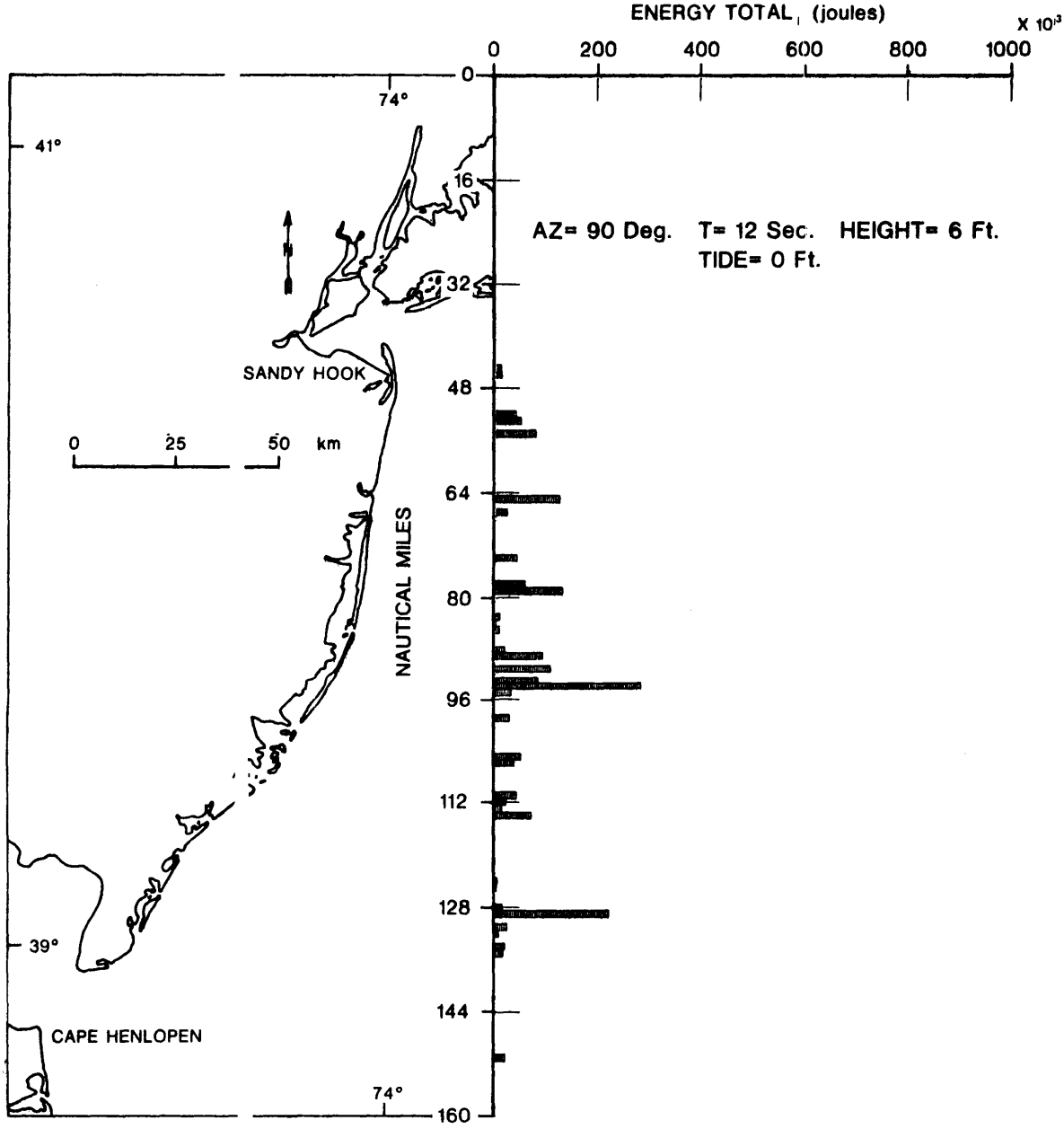

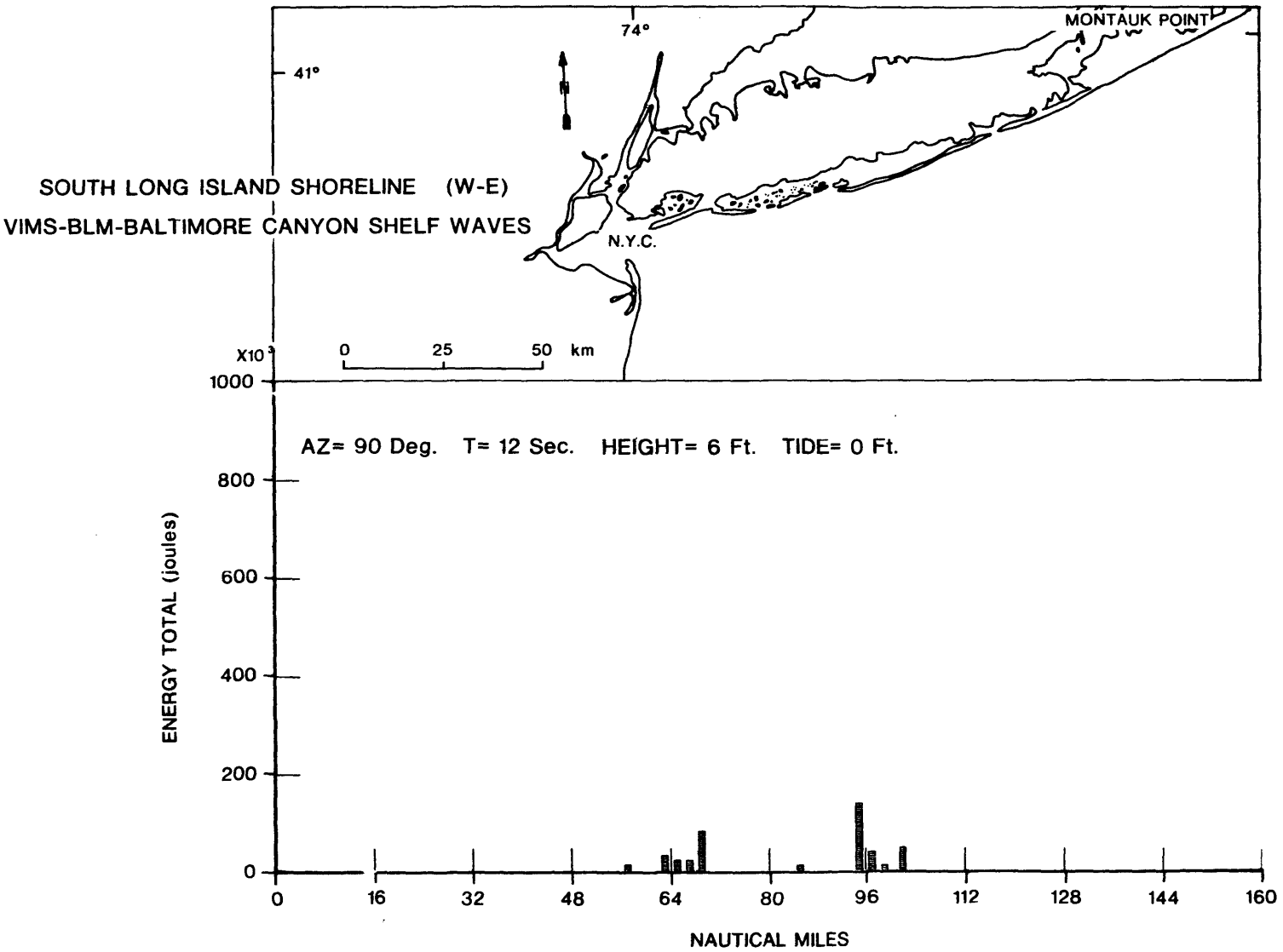
SOUTH LONG ISLAND SHORELINE (W-E)
VIMS-BLM-BALTIMORE CANYON SHELF WAVES
74°
41°
MONTAUK POINT
N.Y.C.
X10³
0 25 50 km
1000
AZ= 90 Deg. T= 12 Sec. HEIGHT= 6 Ft. TIDE= 0 Ft.
800
600
400
200
0
ENERGY TOTAL (joules)
0 16 32 48 64 80 96 112 128 144 160
NAUTICAL MILES

NEW JERSEY - DELAWARE SHORELINE (N-S)

MS - BLM - BALTIMORE CANYON SHELF WAVES

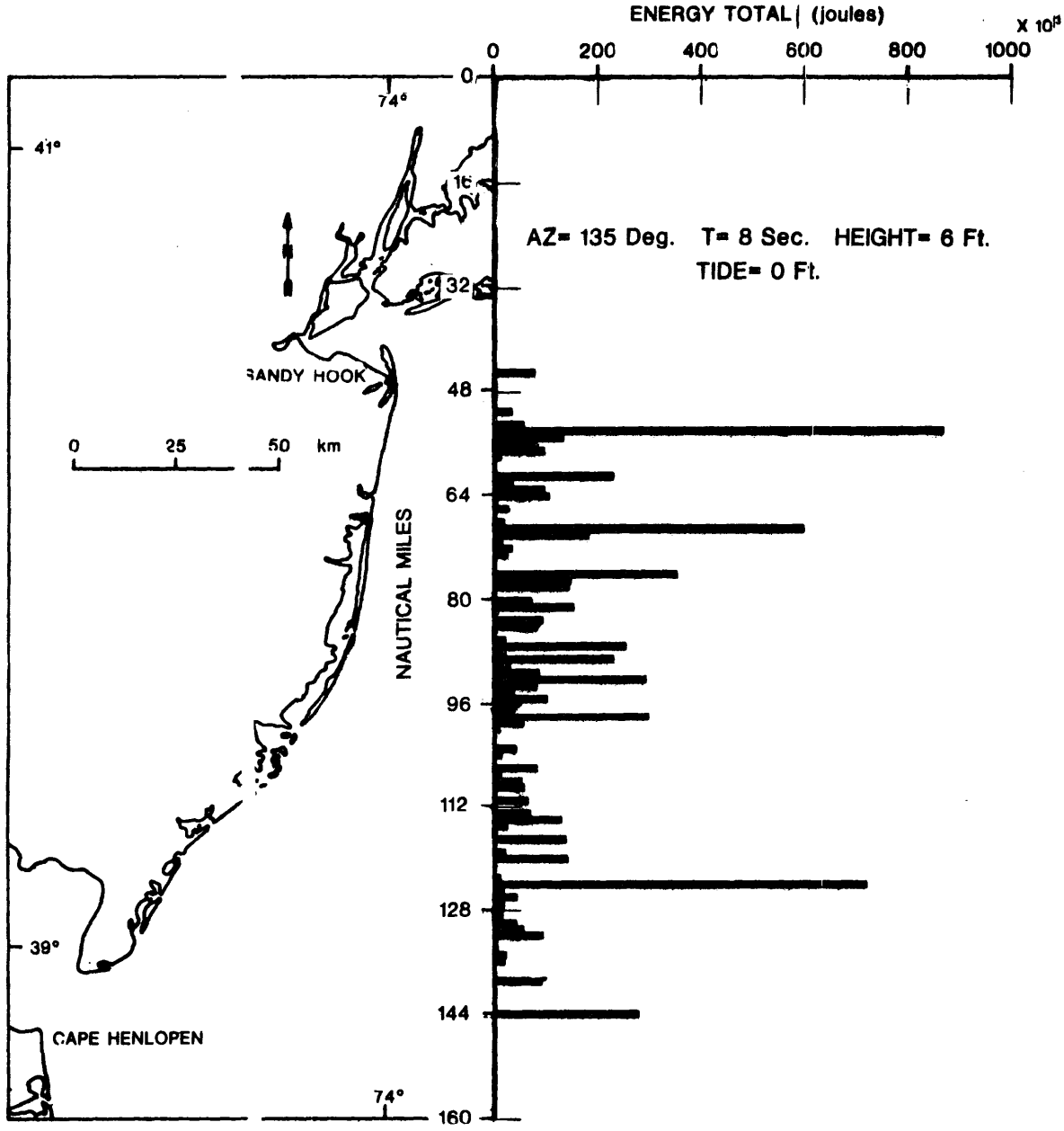

SOUTH LONG ISLAND SHORELINE (W-E)

VIMS-BLM-BALTIMORE CANYON SHELF WAVES

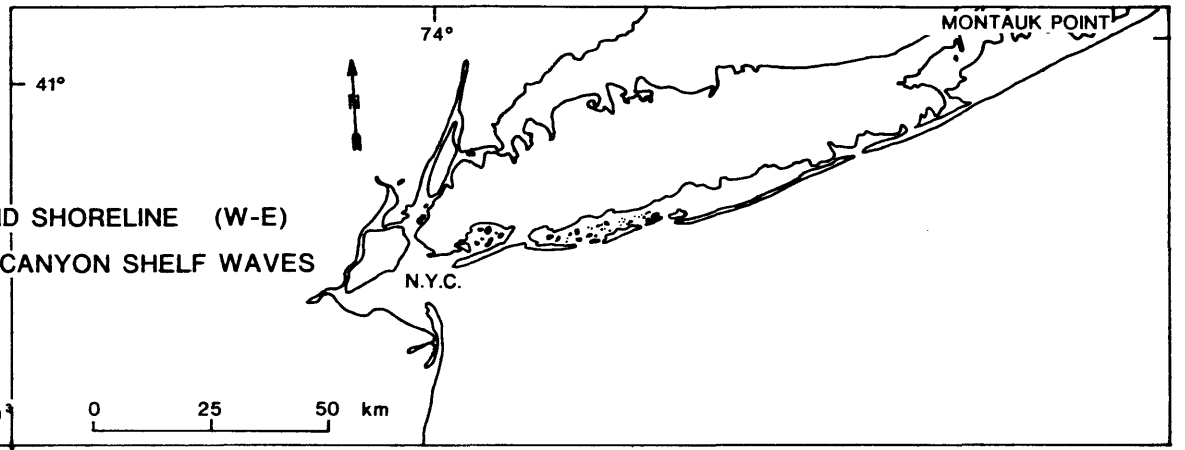

AZ= 135 Deg. T= 8 Sec. HEIGHT= 6 Ft. TIDE= 0 Ft.

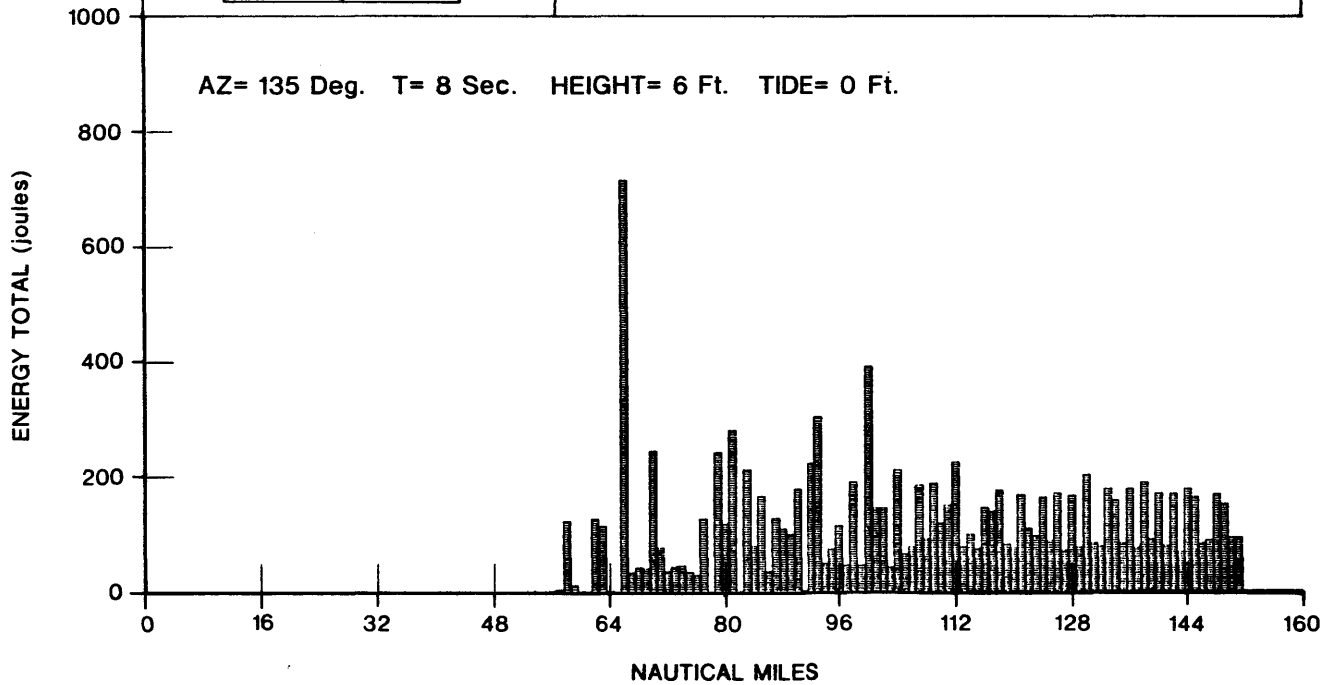

NEW JERSEY - DELAWARE SHORELINE (N-S)

VI IS - BLM - BALTIMORE CANYON SHELF WAVES

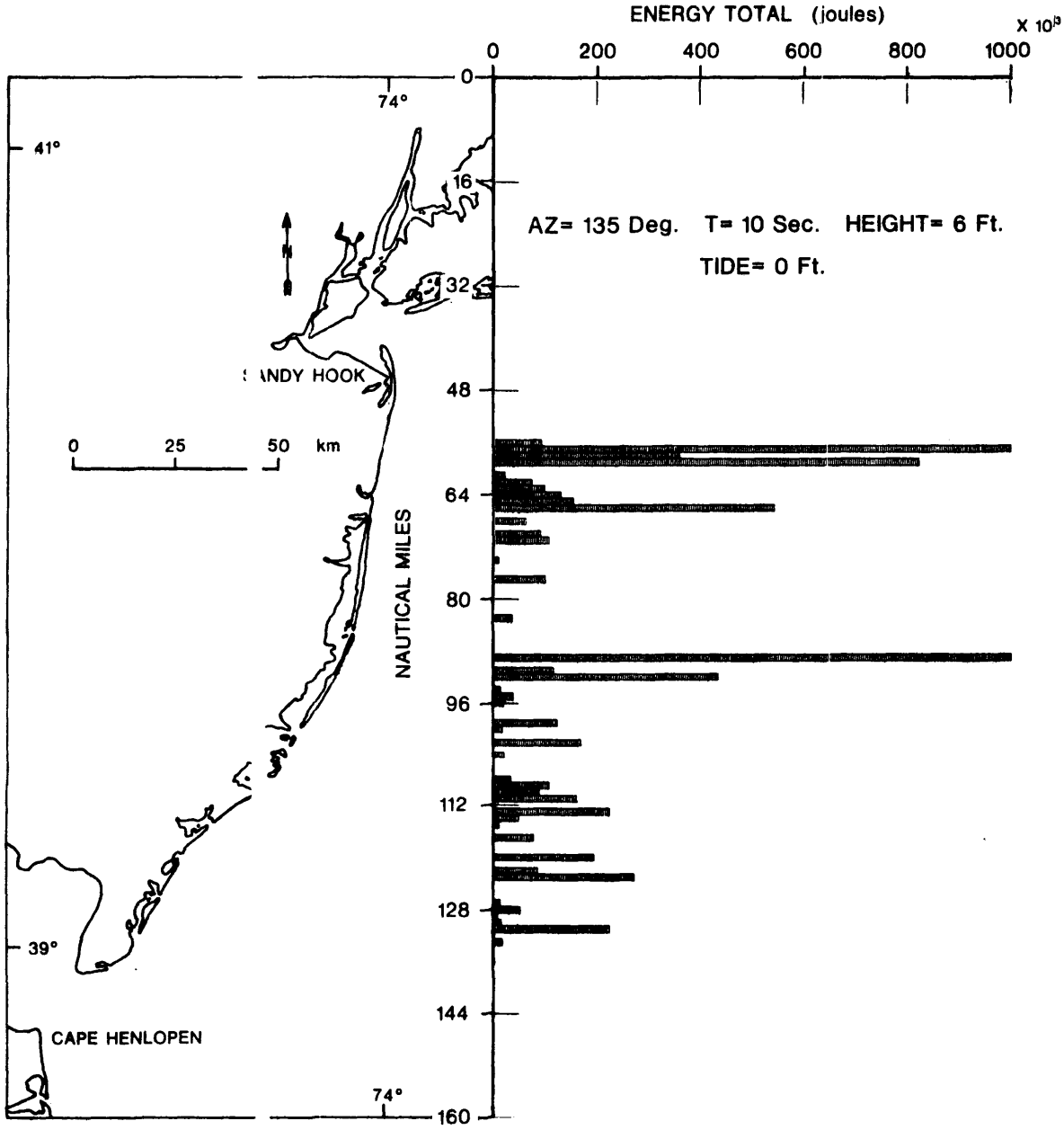

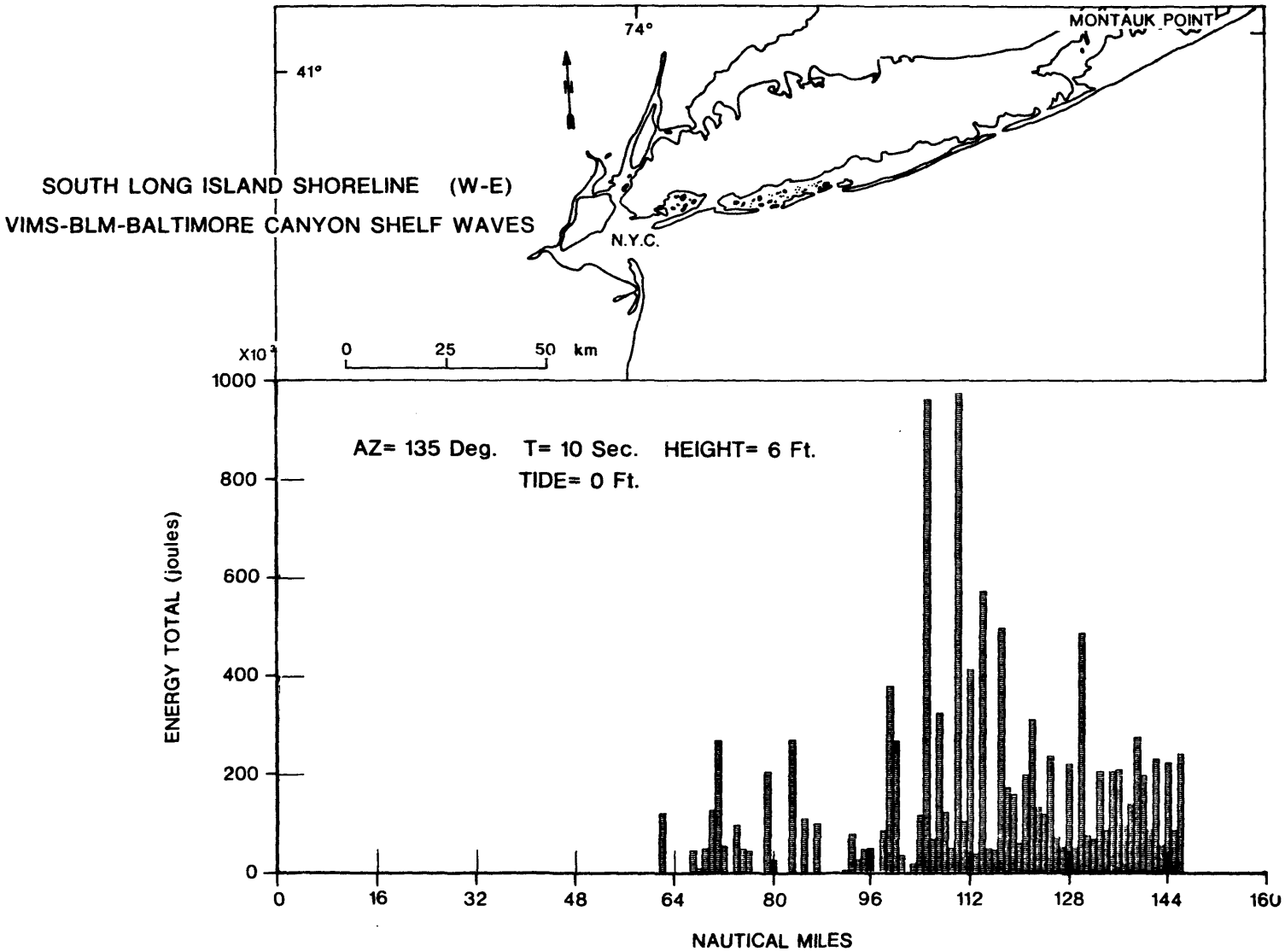
SOUTH LONG ISLAND SHORELINE (W-E)
VIMS-BLM-BALTIMORE CANYON SHELF WAVES
74°
41°
MONTAUK POINT
N.Y.C.
0 25 50 km
X10³
1000
800
600
400
200
0
AZ= 135 Deg. T= 10 Sec. HEIGHT= 6 Ft.
TIDE= 0 Ft.
ENERGY TOTAL (joules)
0 16 32 48 64 80 96 112 128 144 160
NAUTICAL MILES

NEW JERSEY - DELAWARE SHORELINE (N-S)

V MS - BLM - BALTIMORE CANYON SHELF WAVES

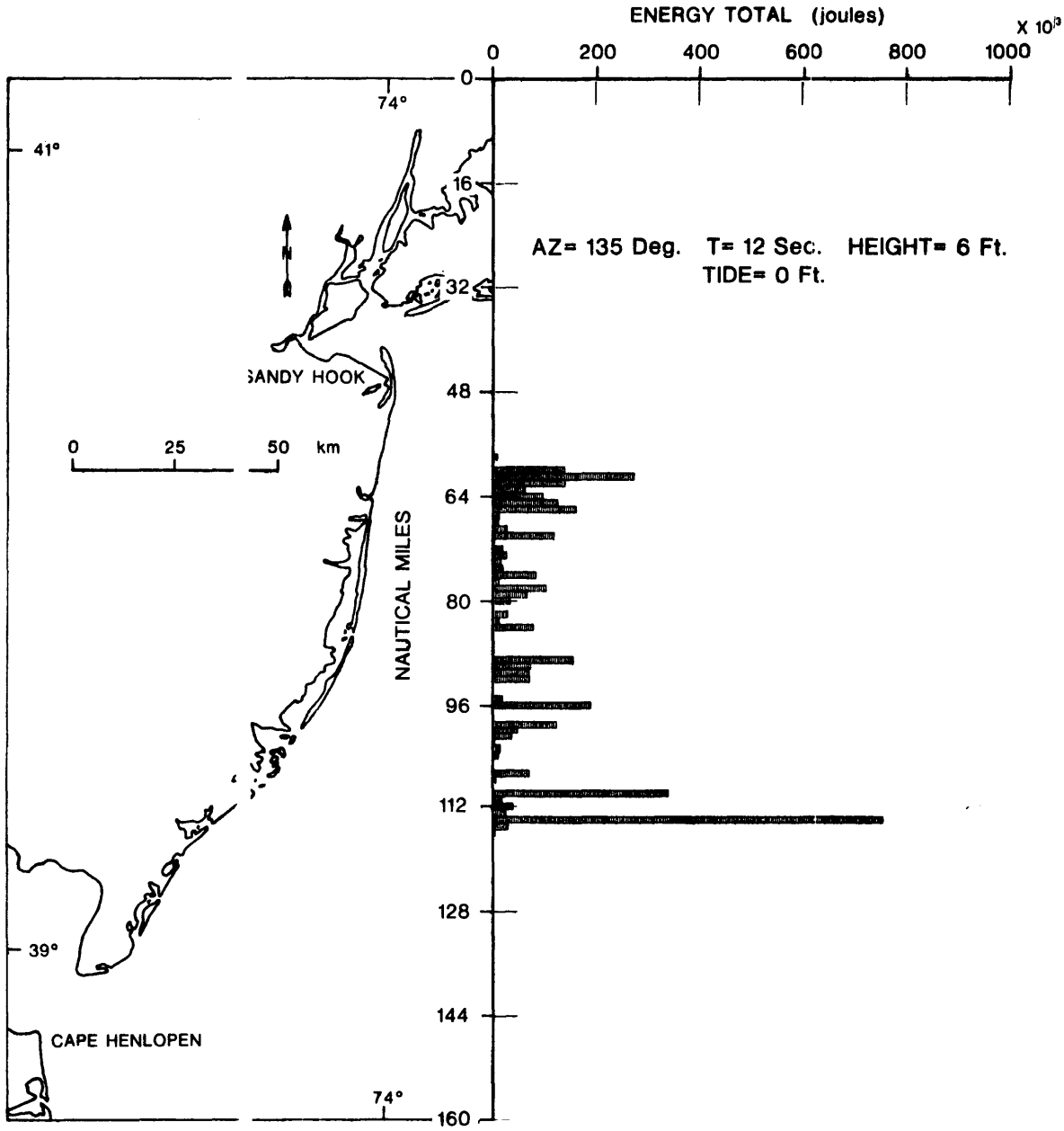

SOUTH LONG ISLAND SHORELINE (W-E)
VIMS-BLM-BALTIMORE CANYON SHELF WAVES

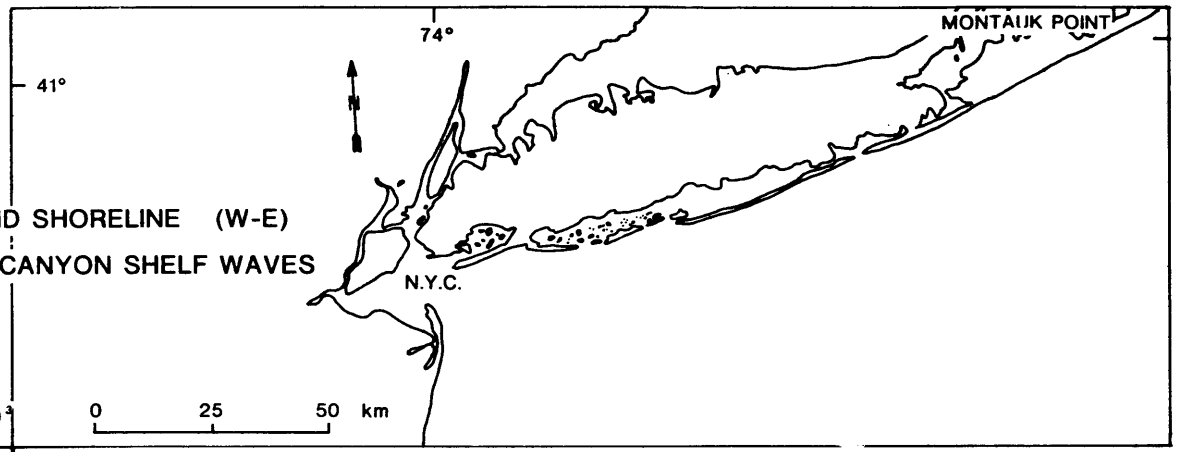

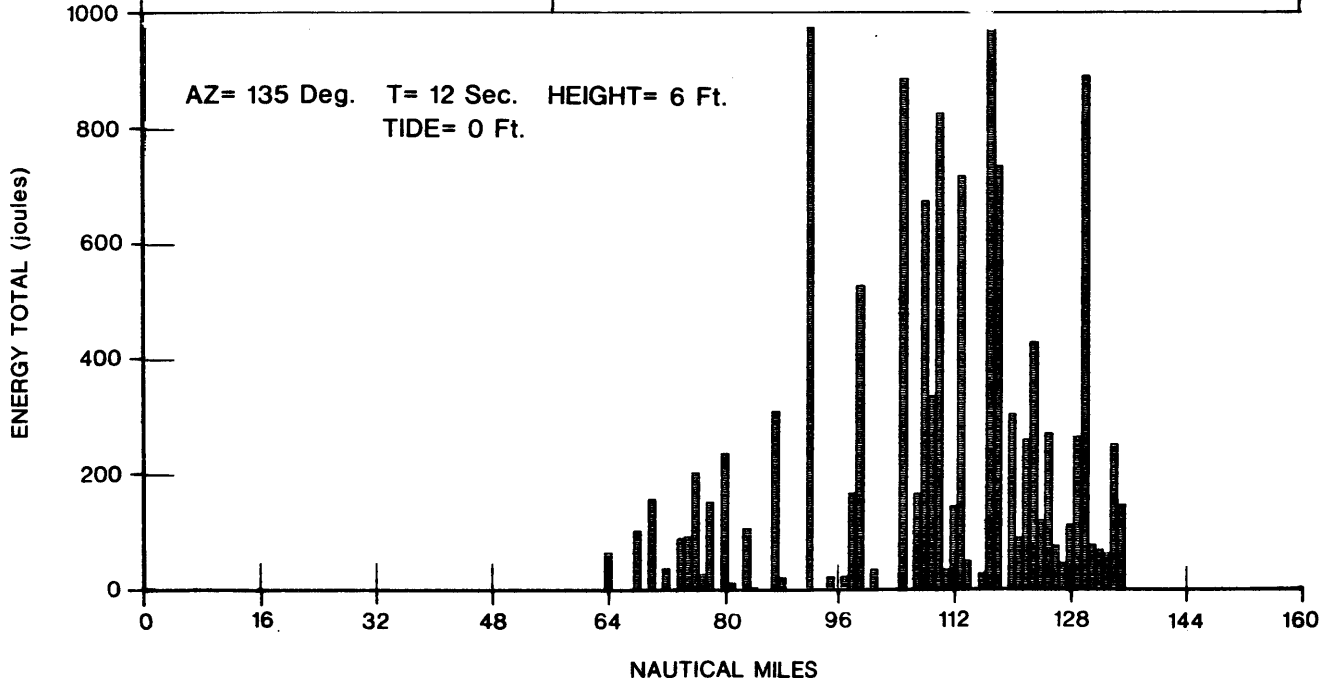

NEW JERSEY - DELAWARE SHORELINE (N-S)
VIMS - BLM - BALTIMORE CANYON SHELF WAVES

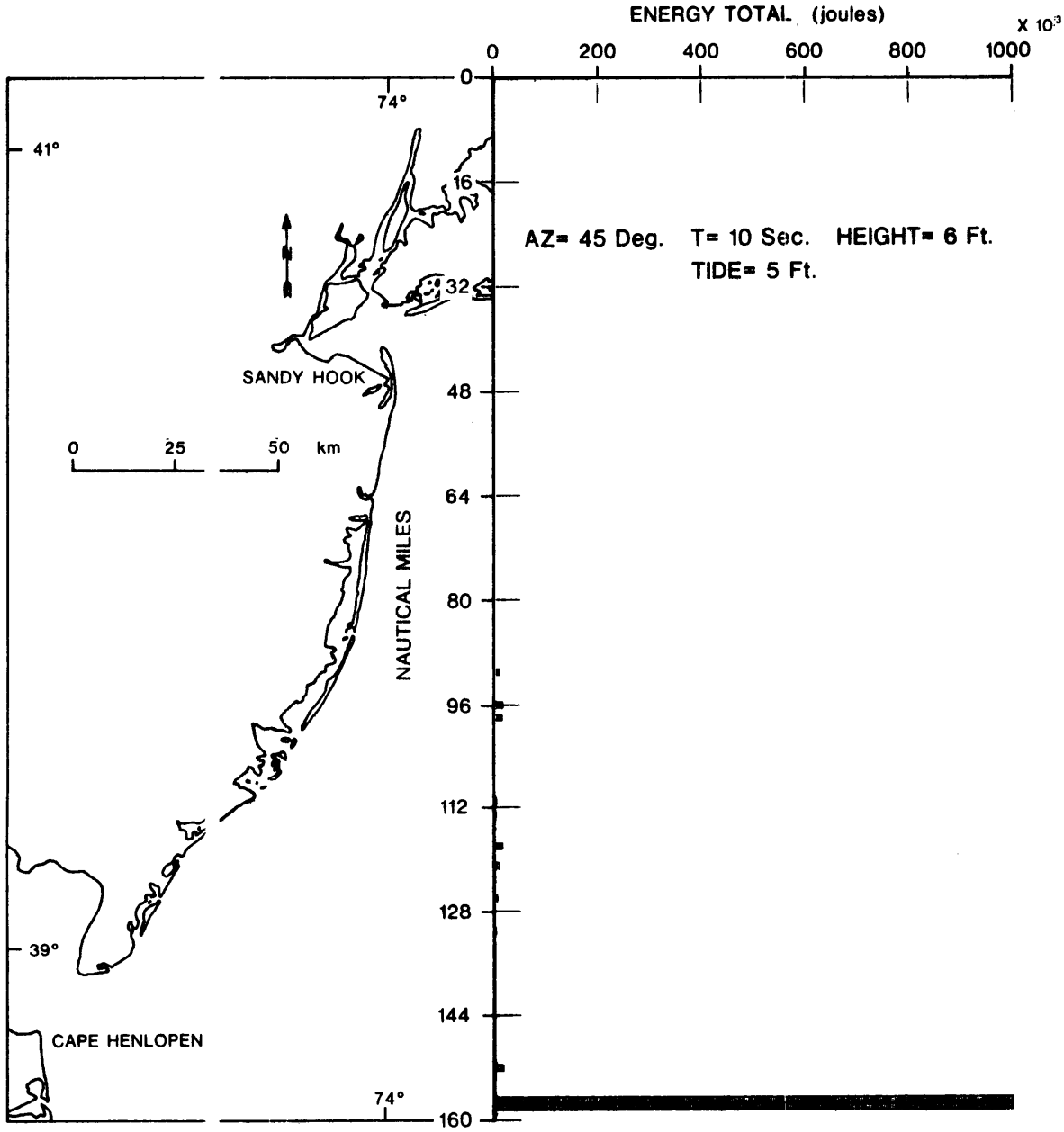

NEW JERSEY - DELAWARE SHORELINE (N-S)
VIMS - BLM - BALTIMORE CANYON SHELF WAVES

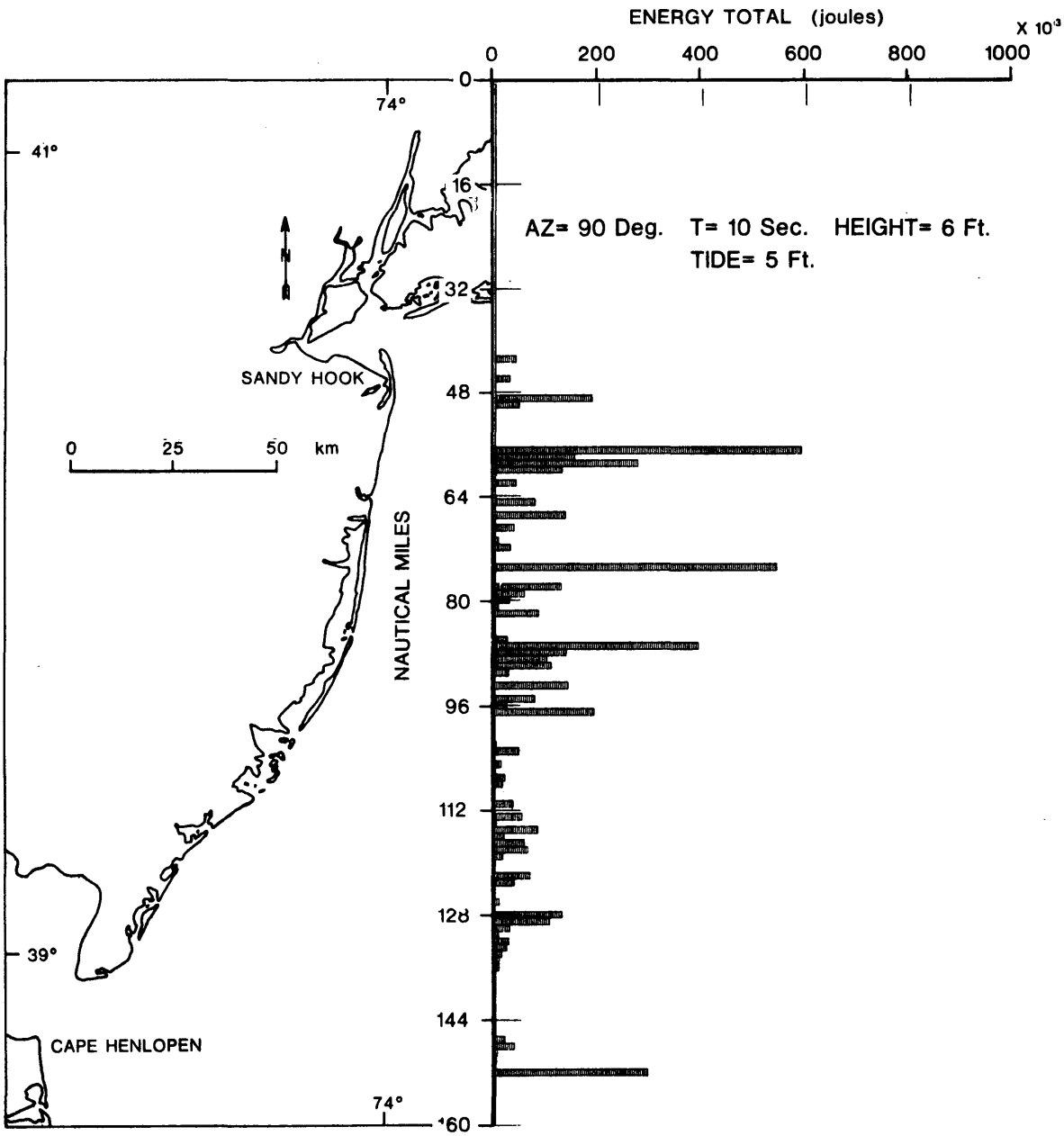

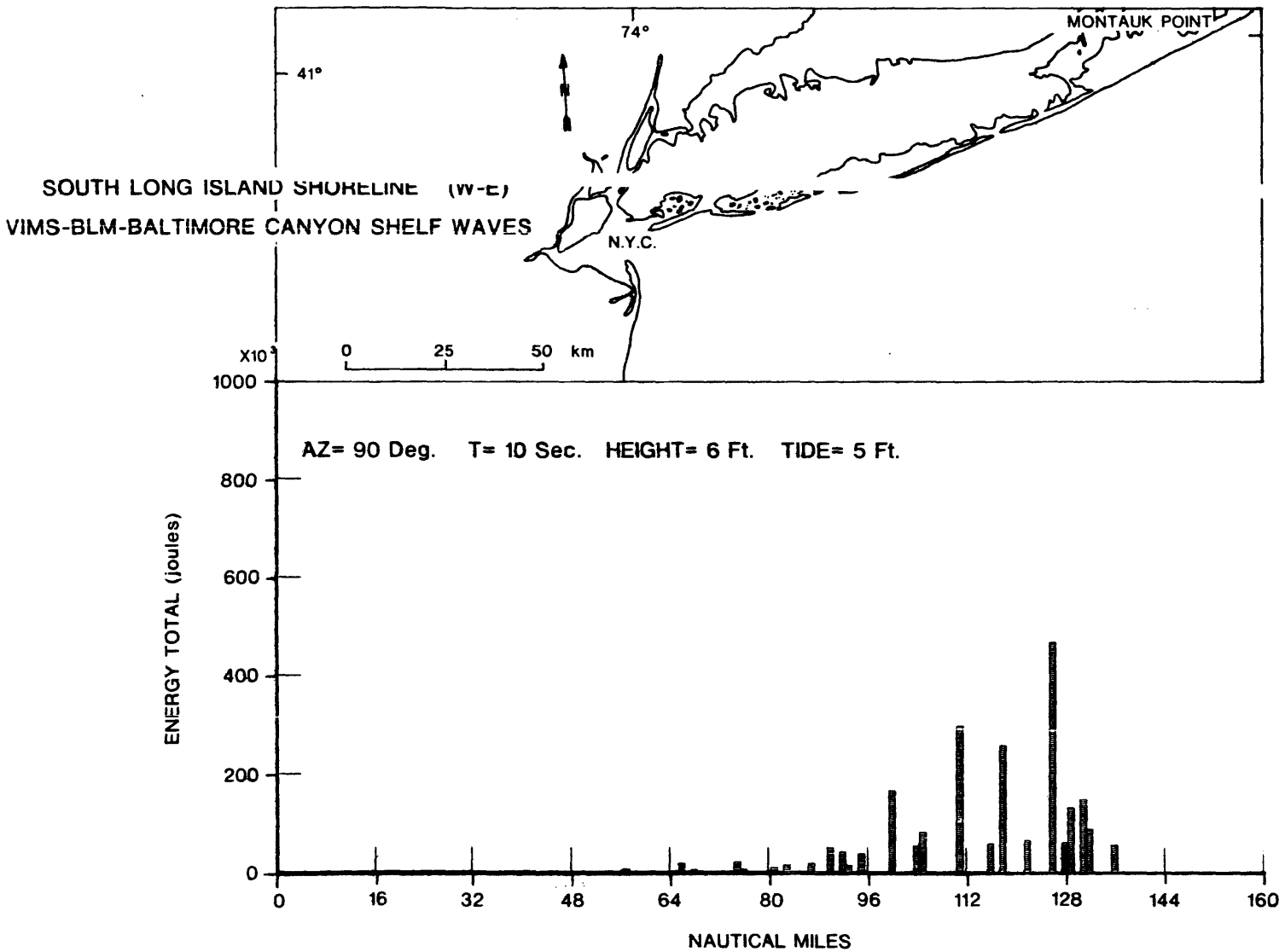
SOUTH LONG ISLAND SHORELINE (W-E)
VIMS-BLM-BALTIMORE CANYON SHELF WAVES
74°
41°
MONTAUK POINT
N.Y.C.
X10³
0 25 50 km
1000
800
600
400
200
0
AZ= 90 Deg. T= 10 Sec. HEIGHT= 6 Ft. TIDE= 5 Ft.
ENERGY TOTAL (joules)
0 16 32 48 64 80 96 112 128 144 160
NAUTICAL MILES

NEW JERSEY - DELAWARE SHORELINE (N-S)
VIMS - BLM - BALTIMORE CANYON SHELF WAVES

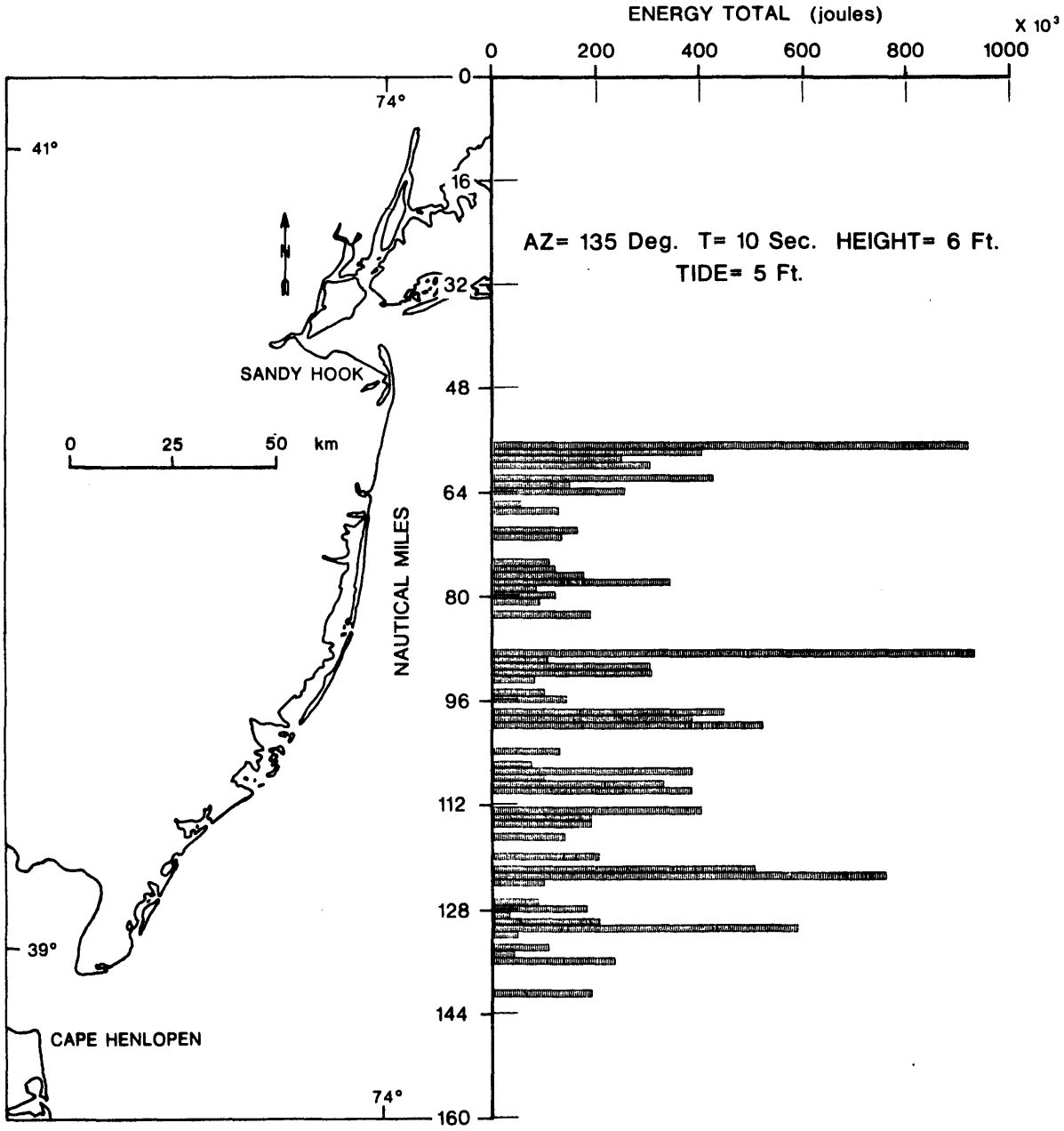

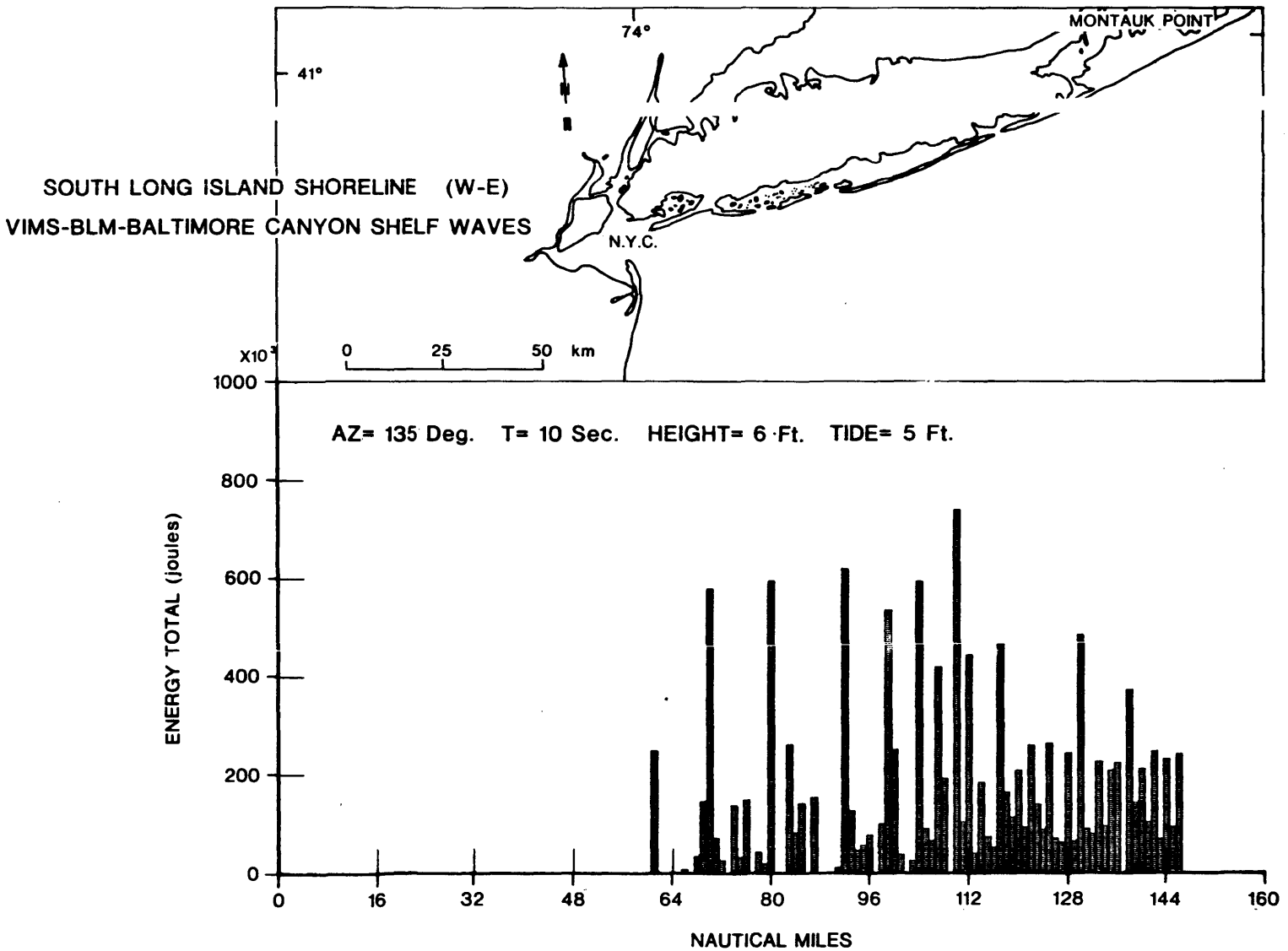
SOUTH LONG ISLAND SHORELINE (W-E)
VIMS-BLM-BALTIMORE CANYON SHELF WAVES
74°
41°
MONTAUK POINT
N.Y.C.
0 25 50 km
AZ= 135 Deg. T= 10 Sec. HEIGHT= 6 Ft. TIDE= 5 Ft.
X10³
1000
800
600
400
200
0
ENERGY TOTAL (joules)
0 16 32 48 64 80 96 112 128 144 160
NAUTICAL MILES